UNIVERSITY OF CALIFORNIA, SAN DIEGO

Functional dissection of homeodomain transcription factors HoxA9 and Meis1 in myeloid leukemia: their epigenetic regulation and their downstream targets

A dissertation submitted in partial satisfaction of the requirements for the degree of

Doctor of Philosophy in

Biomedical Sciences

by

Gang Wang

Committee in Charge:

Professor Mark P. Kamps, Chair
Professor Christopher K. Glass, Co-chair
Professor James T. Kadonaga
Professor Pamela L. Mellon
Professor Bing Ren

2006

The Dissertation of Gang Wang is approved, and it is

acceptable in quality and form for publication on microfilm:

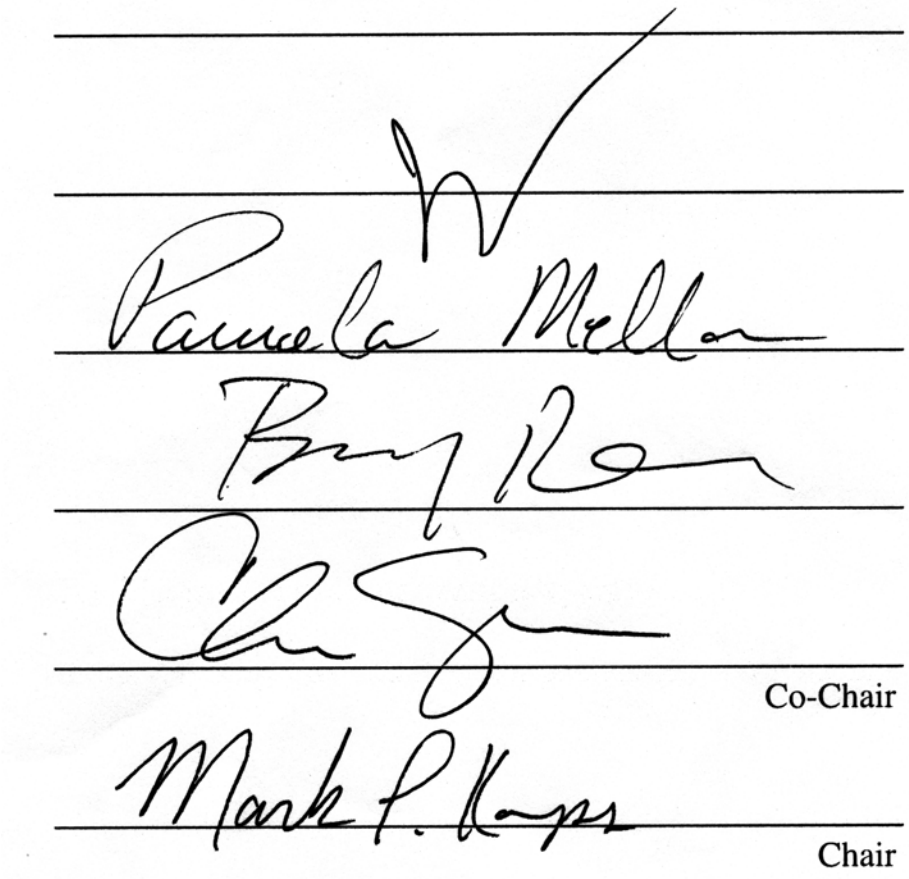

Co-Chair

Chair

University of California, San Diego

2006

DEDICATION

To my mom and dad

who nurture me, love me and support me from the other side of the Pacific Ocean

To my wife Ling Cai

who loves me, cares for me and even sometimes did experiment for me

To Sheng Wang, Sheng-jun Shi and Hao-ran (Xiao-xiao) Shi, my sister's family

EPIGRAPH

"A tree as big as a man's embrace grows from a tiny shoot.

A tower of nine stories begins with a heap of earth.

The journey of a thousand miles starts from where one stands."

by Lao Tzu (Lao Zi), a Chinese philosopher (~600 B.C.)

in "Tao-Te Ching"

TABLE OF CONTENTS

LIST OF FIGURES

Chapter 2

Chapter 3

Chapter 4

Chapter 5

Chapter 6

LIST OF TAB LES

Chapter 2

Chapter 3

Chapter 4

Chapter 5

ACKNOWLEDGEMENTS

I want to give my special thanks to my advisor, Dr. Mark Kamps, for his gift in mentorship, his dedication and patience, his infectious love of science, and his unsurpassed mind of insight and appreciation of data. It has been lucky and truly a privilege for me to have Mark as my thesis mentor. Sincere thanks to Martina Pasillas for her scientific and spiritual supports in the past four years. Many thanks to Dennis Young and Joe Aguilera for their technical supports on flow cytometry and animal radiation. Thanks to Dr. Robert Slany on answers to my questions on MLL fusion proteins. I also want to thank Drs Pierre Chambon and Regine Losson for providing the NSD1 reagents and further collaborating on the NSD1 knockout project. Thanks to Drs Yang Liu, Xianjin Zhou, Junli Luo and Sheng Zhang who gave me the technical guidance on various experiments during my graduate trainings. Thanks to Drs Pin Zhu, Wei Tan and Feng Zhang with whom I found useful scientific discussions.

Chapter 3, in part, is a reprint of the material as it appears in "Meis1 programs transcription of *FLT3* and cancer stem cell character, using a mechanism that requires interaction with Pbx and a novel function of the Meis1 *C*-terminus. Gang G. Wang, Martina P. Pasillas, and Mark P. Kamps." Blood (2005), Volume 106, Number 1, page 254-264. The text of this paper is Copyright © 2005 by The American Society of Hematology. I was the first-author and the primary researcher. I thank my co-authors for permission to use this publication in my dissertation.

Chapter 4, in part, is a reprint of the material as it appears in "Persistent transactivation by Meis1 replaces Hox function in myeloid leukemogenesis models: evidence for co-occupancy of Meis1-Pbx and Hox-Pbx complexes on promoters of

leukemia-associated genes. Gang G. Wang, Martina P. Pasillas, and Mark P. Kamps." Mol. Cel. Biol. (2005), Volume 26, Number 10, page 3902–3916. This text of this paper is Copyright © 2005 reserved by journal "Molecular and Cellular Biology" and the American Society of Microbiology. I was the first-author and the primary researcher. I thank my co-authors for permission to use this publication in my dissertation.

CURRICULUM VITAE

Education

1993-1997	B.Sc. in Biochemistry, Fudan University, School of Life Sciences, China
1997-2000	M.Sc. in Cancer Biology, Shanghai Cancer Institute, Fudan University Medical Center, China
2000-2006	Ph.D. in Biomedical Sciences Ph.D. Program, University of California, San Diego, School of Medicine, USA

Awards and Honors

2000	Union Medical Award, Fudan University Medical Center, China
1997	Admission with examinations waived, Fudan University Graduate School
1994-1996	People's Fellowship, Fudan University School of Life Sciences, China

Professional Experiences

2001-2002	Teaching assistant on "Biochemical Techniques", Department of Biology, University of California at San Diego
1995	Research assistant, Institute of Genetics, School of Life Sciences, Fudan University, China

Peer-review publications

Wang GG, Cai L, Pasillas MP, Kamps MP. Methylation of histone 3, lysine 36 by leukemia translocation protein NUP98-NSD1 caused epigenetic dysregulation of Hox-A locus during hematopoietic transformation. Manuscript in preparation.

Wang GG, Pasillas MP, Kamps MP. Persistent transactivation by Meis1 replaces Hox function in myeloid leukemogenesis models: evidence for co-occupancy of Meis1-Pbx and Hox-Pbx complexes on promoters of leukemia-associated genes. Molecular and Cellular Biologly 2006 May;26(10):3902-16.

Wang GG, Calvo KR, Pasillas MP, Sykes DB, Hacker H, Kamps MP. Quantitative production of macrophages or neutrophils ex vivo using conditional Hoxb8. Nature Methods. 2006 Apr;3(4): 287-93. [Accompanied by editors' comments]

Hacker H, Redecke V, Blagoev B, Kratchmarova I, Hsu LC, Wang GG, Kamps MP, Raz E, Wagner H, Hacker G, Mann M, Karin M. Specificity in Toll-like receptor signalling through distinct effector functions of TRAF3 and TRAF6. Nature. 2006 Jan 12; 439(7073): 204-7.

Wang GG, Pasillas MP, Kamps MP. Meis1 programs transcription of FLT3 and cancer stem cell character, using a mechanism that requires interaction with Pbx and a novel function of the Meis1 C-terminus. Blood. 2005 Jul 1;106(1):254-64 [Accompanied by editors' comments].

Wang G, Zhao Y, Liu X, Wang L, Wu C, Zhang W, Liu W, Zhang P, Cong W, Zhu Y, Zhang L, Chen S, Wan D, Zhao X, Huang W, Gu J. Allelic loss and gain, but not genomic instability, as the major somatic mutation in primary hepatocellular carcinoma. Genes, Chromosomes & Cancer. 2001 Jul;31(3):221-7.

Speech Presentation

Transcriptional activation by Meis1-HOX complex in leukemia: Vp16 domain fused to Meis1 replaces the functions of HOX homeodomain factors during leukemogenesis.
The 47th Annual Meeting of American Society of Hematology (2005) Atlanta, GA.

ABSTRACT OF THE DISSERTATION

Functional dissection of homeodomain transcription factors HoxA9 and Meis1 in myeloid leukemia: their epigenetic regulation and their downstream targets

by

Gang Wang

Doctor of Philosophy in Biomedical Sciences

University of California, San Diego, 2006

Professor Mark P. Kamps, Chair

Professor Christopher K. Glass, Co-chair

Homeodomain-containing transcriptional factors determine patterning and cellular fate during development. Upregulation of homeodomain factors including Hox-A and Meis1 was found in most of acute myeloid leukemias (AML). Hox-A and Meis1 proteins promote hematopoietic progenitor self-renewal, arrest their differentiation and cooperate to induce AML. However their upregulation mechanisms in AML, the molecular basis of

their cooperation, and their downstream leukemogenesis-relevant targets are largely unknown.

Here I report a *Hox-A* gene activation mechanism in AML harboring translocation that fuses Nucleoporin-98 (NUP98) to Nuclear-receptor-binding SET-domain-containing 1 (NSD1). I discovered that AML induced by NUP98-NSD1 was concurrent with upregulation of the *Hox-A* genes and *Meis1*. Mechanistically, NUP98-NSD1 directly bound to the *Hox-A* locus and induced a coordinate epigenetically modifying program via the intrinsic methyltransferase activity of NSD1, recruitment of the histone acetyltransferase CBP/p300, and suppression of the recruitment of Polycomb-group repressor EZH2. Both the NUP98 fusion part and the NSD1 methyltransferase domain were required for leukemogenesis.

To understand Hox-Meis1 cooperation, I established a leukemia stem cell model by coexpression of *HoxA9* plus *Meis1,* which recapitulated the unique AML-initiating character and led to the identification of Meis1-associated leukemia-signature genes. Among them included *CD34, FLT3, Erg1* and etc, the genes found important for stem cell biology and mutated in leukemia. To program leukemogenesis, Meis1 and Hoxa9 required binding to cofactor PBX and to DNA, Meis1 required its C-terminal transactivation domain (CTD), and Hoxa9 required its N-terminal transactivation domain (NTD).

Unexpectedly, I observed that fusing the Vp16 activation domain to Meis1 (Vp16-Meis1) mimicked combined activities of Meis1 plus Hoxa9 and caused leukemia without expression of *Hox* genes. Interestingly, further expression of *HoxA9* or *HoxA7* stimulated transcription of the *Meis1*-related signature genes, and Vp16 activation

domain replaced the functions of the Hoxa9 NTD and the Meis1 CTD. These results favored a model in which Meis-Pbx and Hox-Pbx (or Hox-Pbx-Meis) complexes co-occupy leukemia-relevant promoters and that Meis1 CTD and Hox NTD cooperate in gene activation.

Furthermore, I described a myeloid-linage differentiation system utilizing estrogen-controlled HoxB8 that blocked the differentiation of neutrophil or macrophage-specific progenitors and, upon its inactivation, these progenitors synchronously differentiated into functional mature cells of pre-defined lineages.

Chapter 1

Introduction

1. Hox factors, Meis1 and human acute myeloid leukemia (AML)

The *Hox* related homeobox genes encode homeodomain (HD)-containing transcription factors that determine the anterior-to-posterior patterning and segmental identities during embryogenesis, and control cellular differentiation or/and proliferation of the lineage specific progenitors during hematopoiesis (Pearson et al., 2005; Thorsteinsdottir et al., 1997). Based on the sequence homology of the HD domain, these homeobox factors subdivide into divergent groups that include the Class I Hox factors and the TALE- (*T*hree *a*mino acid *l*oop *e*xtension) class factors. A total of the 39 mammalian Class I *Hox* genes are located in forms of tandem arrays within four evolutionarily conserved chromosomal loci, which are designated as *Hox-A*, *Hox-B*, *Hox-C* and *Hox-D* gene clusters (Burglin, 1997; Pearson et al., 2005). The TALE class homeobox genes comprise *Meis1/Prep1* subfamily and *Pbx* subfamily, both encoding the cofactors that interact with Hox proteins. The dysregulation of these homeobox genes, which at least included a subset of the *Hox* genes (especially *HoxA9* and *HoxA7*) and *Meis1* (*M*yeloid *E*cotrophic *I*nsertion *S*ite *1*), was directly linked to malignant hematopoeisis or leukemia (Lawrence et al., 1999).

Both Hox factors and Meis1 control hematopoiesis by promoting progenitor self-renewal and blocking their differentiation. In normal hematopoiesis, the expression of *HoxA9*, *HoxA7* and *Meis1* is high in CD34+, Sca-1+, lineage-negative human bone marrow subpopulations that are enriched in hematopoietic stem cells (HSCs) and lineage-committed early progenitors, and is rapidly down regulated coincident with transition to the CD34- stage of early progenitor differentiation (Pineault et al., 2002; Sauvageau et al., 1994). The expression of *HoxA9* and *Meis1* in

early progenitors is positively linked to the maintenance of the pool size of HSCs and early progenitors, revealed by gene deletion experiments in mice. Mice harboring null mutation in *HoxA9* had significant reductions in the number of myeloid progenitors, pre-B cell progenitors and HSCs (Lawrence et al., 2005; Lawrence et al., 1997). Similarly, elimination of *Meis1* also resulted in strong reductions in numbers of general myeloid, lymphoid, and multipotent progenitors (Azcoitia et al., 2005; Hisa et al., 2004). Both *Hoxa9*-defiecient HSCs and *Meis1*-defiecient HSCs exhibited dramatic defects in cellular proliferation, the *in vitro* colony-forming potentials and the *in vivo* reconstitution abilities (Hisa et al., 2004; Lawrence et al., 2005). By contrast, retrovirally enforced expression of *Hoxa9* produced a 10-fold increase in the number of long-term repopulating HSCs, which was followed inevitably by the development of myeloid leukemia (Kroon et al., 1998; Thorsteinsdottir et al., 2002).

Multiple lines of evidence directly linked Hox factors and Meis1 to the development of human and murine leukemias. Originally, *Meis1* was discovered as one of two common genes activated by proviral integration in BXH2 murine spontaneous AML models, the second being *Hoxa9* or *Hoxa7* (Moskow et al., 1995). Over 50-80% of human AML and virtually all of the acute lymphoblastic leukemia containing translocations of the *M*ixed *L*ineage *L*eukemia (*MLL*) gene exhibited strong expression of *HoxA7, HoxA9*, *HoxA10* and *Meis1*(Afonja et al., 2000; Ferrando et al., 2003; Lawrence et al., 1999). *HoxA9* was the only expression marker identified as significantly linked to poor prognosis of human AML (Golub et al., 1999). In rare cases of human leukemia, chromosomal translocations occurred on locus encoding Hox factors or their cofactor Pbx1, which either generated a dominant

activating form of Hox factor, such as NUP98-HoxA9, NUP98-HoxA11 or NUP98-HoxA13 in AML with t(7;11)(p15;p15) chromosomal translocation (Borrow et al., 1996; Fujino et al., 2002) and NUP98-HoxC11 or NUP98-HoxC13 in AML with t(11;12)(p15;q13) translocation (Panagopoulos et al., 2003; Taketani et al., 2002), or generated a dominant activating form of Pbx1, i.e., E2a-Pbx1 in pre-B leukemia with (1;19)(q23;p13) translocation (Kamps and Baltimore, 1993). More interestingly, in murine and human AMLs, there is strong cooperation between Hox factors and Meis1 in terms of programming leukemogenesis (Kroon et al., 1998; Thorsteinsdottir et al., 2001), which I will discuss later in the paragraph 4 of this chapter.

2. Epigenetic regulation of *Hox* locus in leukemogenesis

During embryogenesis, the precise regulation of the spatial and temporal expression of *Hox* genes (so called "*Hox* code") is crucial because each of the encoded Hox factors controls the formation of a diversified segmental structure along the anterior-to-posterior axis of animals (Pearson et al., 2005). In *Drosophila,* the mutations within a *Hox* gene or those causing their impropriate expression induced a phenotype termed as homeotic transformation, which is characterized by the alteration of the morphology of one segment into that of another (for example, a four-winged morphology caused by a mutation in *Hox* gene *Ultrabithorax*, transforming the third thoracic segment into an additional second thoracic segment) (Pearson et al., 2005). Intensive knowledge of the upstream transcriptional regulators of *Hox* locus has been obtained from the previous fly genetic screens based on homeotic transformation phenotype, which led to identification of two antagonizing groups,

Trithorax group (TrxG) and Polycomb group (PcG), of the *Hox* locus regulators (Ringrose and Paro, 2004). TrxG group serves as transcriptional activators that maintain the "ON" state of the *Hox* locus, while PcG group as transcriptional repressors that maintain the "OFF" state of the *Hox* locus. The core component of TrxG group proteins, *Drosophila* TRX and its mammalian homologue MLL (also called ALL-1 or HRX), possess histone methyltransferase activity specific for histone 3 at position lysine 4 (H3K4), while the core component of PcG proteins (Ezh2, Eed, Suz12) form a histone methyltransferase complex specifically methylating histone 3 at position lysine 27 (H3K27) (Cao and Zhang, 2004; Milne et al., 2002; Nakamura et al., 2002). Trimethylation of H3K4 was functionally linked to transcriptional activation while trimethylation of H3K27 was linked to transcriptional silencing, which establishes the molecular basis of the regulatory role of TrxG and PcG proteins on the epigenetic regulation of *Hox* gene expression (Bernstein et al., 2005; Pokholok et al., 2005).

The epigenetic regulators of *Hox* genes also contributed to cellular differentiation and proliferation during normal hematopoiesis, and the epigenetic dysregulation leading to the aberrant sustained expression of *Hox* genes was directly linked to leukemia transformation (Hess, 2004; Slany, 2005). For example, the mammalian *TrxG* gene, *MLL*, contributed significantly to the definite hematopoiesis revealed by *MLL* knockout experiments, in which the reduction of the expression of *HoxA9* or *HoxC8* or the skewed distribution pattern of *HoxA7* or *HoxC9* was observed (Ono et al., 2005; Yu et al., 1998). In addition, *MLL* gene was originally identified as the locus mutated and translocated in human leukemia harboring

translocation of chromosomal band 11q23 (Hess, 2004; Slany, 2005). The two major forms of *MLL* mutation, either in the form of 11q23 chromosomal translocation that produced an *MLL* chimeric gene after fusing to one of more than 40 different partners so far identified, or in the form of *MLL* locus partial tandem duplication that generated an elongated version of MLL with duplicated N-terminal sequences (including Ser/Thr rich region, AT hook and DNA methyltransferase-homology domain [CxxC zinc finger motif]), comprised around 5-10% and 10% of all human AML cases respectively. Almost all of the cases containing the *MLL* translocations exhibited the robust expression of *HoxA9*, *HoxA7* and *Meis1* (Armstrong et al., 2002; Ayton and Cleary, 2003; Ferrando et al., 2003; So et al., 2003). One intriguing mechanistic question about the leukemogenic MLL fusion proteins stems from the fact that these fusion proteins retained the functions of directly recruiting the promoters of the endogenous *Hox* genes and activating the *Hox* gene expression, however, they all lost the MLL intrinsic H3K4 methyltransferase SET domain due to chromosomal translocation. This indicated an acquired transacting mechanism responsible for *Hox* gene activation by MLL fusion proteins. Indeed, in the case of MLL fused to CBP/p300 (MLL-CBP (Wang et al., 2005c) or MLL-p300 (Ida et al., 1997)), histone acetylation was an obvious example of acquired *Hox* transactivation mechanisms. More recently, Dr. Yi Zhang and his colleagues found that histone methyltransferase hDOT1L interacted with AF10, and in the case of MLL fused to AF10 (MLL-AF10 (Okada et al., 2005)), trimethylation of histone 3, Lys 79 by hDOT1L was responsible for the aberrant *Hox* gene activation.

Other than *MLL* translocations, other unknown *Hox* gene activation mechanisms in AML may exist, considering the high percentage (>70~80%) of human AML exhibiting *Hox* gene upregulation and considering the potential existence of other to-be-identified *Hox* locus regulators. In Chapter 2, I will describe the first report on mechanistic studies of human AML harboring chromosomal translocation t(5;11)(q35;p15.5), which generated a chimeric gene fusing FG repeat domain (amino acid 1-518) of Nucleoporin 98 (NUP98) to amino acid 1688 to 2596 of a histone methyltransferase NSD1 (*N*uclear receptor-binding *S*ET *d*omain-containing protein *1*) (Jaju et al., 2001). This model led to the identification of a novel *Hox* transactivation mechanism by NUP98-NSD1 in AML.

3. Structural and functional properties of Hox factors and Meis1.

As the master regulators of embryonic patterning formation and cellular fate decision, the Class I Hox homeodomain factors and the TALE-class homeodomian factors are able to recognize the specific genomic elements and modulate the expression of their downstream genes whose identities were largely unknown (Mann and Affolter, 1998; Moens and Selleri, 2006). The DNA binding ability is achieved through the physical interaction between DNA and HD domain, a highly conserved 60 amino-acid-long sequence located near the carboxyl terminus. Although each Hox factor imparted the diversified *in vivo* functional specificity, monomers of Hox factors showed a very similar DNA recognition specificity with poor affinity *in vitro*, indicating that additional mechanisms, such as cofactor interaction, were required to achieve DNA binding with high affinity, complexity and specificity. The TALE class

homeobox genes encode Pbx factors and Meis1/Prep1 family factors that contain a HD domain with an extra three-amino-acid insertion, and these TALE homeobox factors were obligate Hox-interacting cofactors, forming Pbx-Hox or Meis1-Hox heterodimers. Consistent to the physical interaction, a genetic interaction was observed between these genes. *Drosophila* strains harboring mutation in *Pbx* homolog *Extradenticle* (*Exd*) or *Meis1* homolog *Homothorax* (*Hth*) also exhibited homeotic transformation phenotype, and *Pbx* mutants in zebrafish and mouse also recapitulated the *Hox* loss-of-function phenotypes (Kurant et al., 2001; Moens and Selleri, 2006).

Each of these homobox transcription factors recognizes DNA sequence with specificity. *In vitro* affinity binding experiments defined that a Hox monomer was preferentially bound to the consensus sequence TNAT, that Pbx1 bound to TGAT and that Meis1 bound to TGACAG (Knoepfler et al., 1997; Knoepfler et al., 1996). Subtle binding preferences existed for each different Hox factor. For example, as Pbx-Hox heterodimers, Pbx1-HoxA1 preferentially binds consensus sequence *TGAT*TGAT, Pbx1-HoxA5 prefers *TGAT*TAAT and Pbx1-HoxA9 prefers *TGAT*TTAT (Shen et al., 1996). The relevance of these consensus recognition sequences predicted by *in vitro* DNA-protein binding experiments were further validated by the identification of these cognate sites that contributed the proper gene expression *in vivo*. For example, both Pbx-HoxB1 site (Italic, with 5'-Pbx half site ***AGAT*** and 3'-HoxB1 half site *TGAT*) and a more distal Meis1 cognate site (underlined CTGTCA generates TGACAG from reverse orientation) within the *Hoxb2* gene enhancer [GGAGCTGTCAGGGGGCTA***AGAT****TGAT*CGCC] contributed to the proper

expression of *HoxB2* in mouse hinder brain during embrogenesis (Jacobs et al., 1999).

There is also a preference of protein-protein interaction between each member of the Hox, Meis1/Prep1 or Pbx family (Chang et al., 1997; Shen et al., 1996; Shen et al., 1997). First, Pbx and Meis1 tend to form a tight interaction independent of binding their cognate DNA elements. Pbx-Meis1 heterodimerization depended exclusively on the conserved bipartite helical regions, i.e., PBC-A and PBC-B domains in Pbx as well as M1 and M2 domains in Meis1, all of which are located N-terminal to HD domain (Chang et al., 1997; Knoepfler et al., 1997). Pbx-Meis1 heterodimerization was also required for nuclear localization and accumulation of either factor (Rieckhof et al., 1997). Second, Pbx and a subset of Hox factors (paralog group 1 through 10, i.e., Hox-1 to Hox-10) formed stable interactions in the presence of cognate DNA elements, and, without DNA, such interaction became much weaker (Shen et al., 1997). While the HD domain was dispensable for Pbx-Meis1 interaction, Pbx-Hox interaction exclusively depended on the interaction between Pbx HD domain and a conserved tryptophan-containing motif positioned N-terminal to the Hox HD (termed as *P*bx-*i*nteraction *m*otif, PIM), which was supported by biochemical analysis and then X-ray crystallography (Lu and Kamps, 1996; Passner et al., 1999; Piper et al., 1999). The Hox PIM is either IYPWMR for Hox-1 to Hox-8 or ANWL for Hox-9 to Hox-10. Third, Hox paralog groups 9 through 13 interacted with Meis1 in the presence of DNA. Thus, Hox-9 and Hox-10 proteins are unique in interacting with both Pbx and Meis1 factors (Shen et al., 1997).

Although Hox-Pbx, Pbx-Meis1 or Hox-Pbx-Meis1 complexes mediated the assembly of high-order protein complex on gene promoters and such interactions appeared important for the expression of certain downstream targets, it is still unclear how these protein-protein interactions contributed to the transformation in AML.

4. Cooperation between Hox factors and Meis1 in leukemogenesis

An interesting observation in the generation of human and murine AML is that there existed strong cooperation between Hox and Meis1. Originally in spontaneous murine AML, almost all cases harboring transactivation of the *Meis1* locus also contained transactivation mutation at the *Hoxa9* or *Hoxa7* locus (Moskow et al., 1995). In human AML, *Meis1* was found coexpressed with *Hox* genes (especially *HoxA9, HoxA10* or *HoxA7*) (Lawrence et al., 1999; Nakamura et al., 1996). Direct functional evidence supporting such cooperation between Hox factors and Meis1 came from a murine leukemia model induced by bone marrow transplantation experiments, in which bone marrow cells infected with the retrovirus encoding the *Hox* gene alone (*HoxA9* or *HoxB3*) induced leukemia only after a long latency (usually >150~200 days), marrow cells infected with retrovirus encoding the expression of *Meis1* alone never induced any leukemia, however, marrow infected with both retrovirus rapidly induced AML within 50-70 days (Kroon et al., 1998; Thorsteinsdottir et al., 2001).

While HoxA9 and Meis1 can interact physically, it is clear that each impacts at least partly distinct genetic pathways that yield different phenotypes. In our previous studies, we showed that retroviral expression of *HoxA9* alone arrested the

differentiation of cytokine-dependent myeloid progenitors in the absence of coexpressed *Meis1, Meis2,* or *Meis3* (Calvo et al., 2000); however, such progenitors were incapable of initiating leukemia in sub-lethally irradiated mice, suggesting that a second, Meis-dependent genetic response was required to program leukemia initiating properties. Expression of *Meis1* in GM-CSF–dependent HoxA9-immortalized myeloid progenitors induced responsiveness to stem cell factor (SCF) and suppressed the neutrophil-lineage differentiation induced by G-CSF, yet these progenitors as well could not initiate leukemias (Calvo et al., 2001). Thus, while HoxA9 and Meis1 can deregulate facets of progenitor proliferation and differentiation, a relevant cultured cell model that mimicked the cooperation between *Hox* genes and *Meis1* has not been established, and hence, the genetic mechanisms through which Meis1 contributes to leukemia remained unclear and difficult to approach.

5. Scientific questions and general overviews

More and more evidence from recent studies supported that Hox factors and Meis1 are the crucial regulators of leukemogenesis in human AMLs, and understanding the mechanisms of leukemogenesis induced by these factors will bring our understanding of myeloid leukemia transformation to the next level and will help to design the effective therapeutic approaches. Several important scientific questions in the field remain unsolved. First, how was the overexpression of the *Hox* and *Meis1* genes induced at the first place in AMLs? Second, what are the downstream targets regulated by Hox factors and Meis1, and how do these downstream targets contribute to leukemic transformation? Third, what is the molecular and genetic basis of the

cooperation between Hox factors and Meis1 during leukemogenesis? Are Hox-regulated pathways and Meis1-regulated pathways distinct or convergent? Are any of these protein-protein interactions, Hox-Pbx, Pbx-Meis1, or Hox-Meis1, important for leukemogenesis? And what is the nature of transcriptional functions of these factors, i.e., trans-activating or trans-repressing or both, in regulating target gene expression and inducing leukemogenesis? With these questions in mind, I joined the Mark Kamps' lab and began my four-year-long research journey, which were full of joys and pains.

In Chapter 2, I embark on the functional examination of human AML involving translocation of histone methyltransferase NSD1, which generated a fusion protein NUP98-NSD1. I identified the functional link between NUP98-NSD1 and the upregulation of expression of a subset of *Hox-A* genes (*HoxA5* to *HoxA10*) as well as *Meis1*. I found that, after NUP98-NSD1 was recruited to the promoter regions of *HoxA5-A10* genes through the function of a plant homeodomain (PHD) and a Cysteine-Histine rich motif of NSD1, it induced a systematic local histone modification program, which included the induction of histone acetylation and the trimethylation of histone 3, Lys 36 (H3K36) as well as the suppression of the trimethylation of histone 3, Lys 27 (H3K27). This strong *Hox* gene transacting function of NUP98-NSD1 was dependent on the recruitment of CBP/p300 by NUP98 part, on the intrinsic methyltransferase activity of NSD1, and on antagonizing effect on the recruitment of EZH2.

In Chapter 3, I describe the cellular and molecular dissection of Meis1 during leukemogeneis. Cultured leukemia stem cells that induced rapid AML *in vivo* were

established by coexpressing *Meis1* and *HoxA9* (or *Hoxa7*), while progenitors expressing *HoxA9/A7* were not leukemic, thus recapitulating the Meis1-Hox cooperation in a cell model. I then identified a group of the Meis1-associated leukemia signature genes, which included the well-known stem cell genes such as *Cd34, FLT3, Sox4* and *Erg1*. Three functions of Meis1, i.e., interaction to Pbx cofactors, binding to DNA elements and transactivation by its C-terminal domain (CTD), were found to be required for progenitor transformation and the induction of AML when coexpressed *HoxA9*.

In Chapter 4, I examine the nature of the transcriptional activity of Meis1 during leukemia transformation. I discovered that a dominant transacting form of Meis1, Vp16-Meis1 (generated by fusing Vp16 activation domain to Meis1), was able to immortalize the *in vitro* cultured progenitors and induced AML *in vivo* in the absence of expressed *Hox* genes. This observation supported the notion that transcriptional activation is the key leukemogenic function of Meis1 and also provided a cell system to examine the biology of Hox factors. Quite surprisingly, I found that the genes upregulated by HoxA9 or HoxA7 largely covered the Meis1-target genes identified in Chapter 3, suggesting that targeting of a common subset of genes by both Hox and Meis1 as the molecular basis for the Meis1-Hox cooperation in leukemia. Furthermore, I found that Hox-containing complexes and Pbx-Meis1 complexes cooccupied cellular promoters (probably in forms of a Hox-Pbx-Meis1 complex) and transactivated them via transacting functions of both the Hox N-terminal domain and the Meis1 CTD domain.

In Chapter 5, I describe a myeloid cell lineage differentiation system based on the function of Hox factors of arresting progenitor differentiation. Using an estrogen-controlled HoxB8 (ER-Hoxb8), I generated macrophage-specific or neutrphil-specific progenitors, and upon ER-HoxB8 inactivation, these progenitors synchronous differentiated into functionally mature effecter cell types. This ER-Hoxb8 phagocyte maturation system was applicable to fetal liver cells from knockout mice with lethal phenotypes, and combined with small interfering RNA (siRNA) technologies, it represents a rapid analytical tool for studying the differentiation and cell biology of macrophages and neutrophils.

Chapter 6 summarized the major findings and also pointed out the unsolved interesting questions that represent the future directions of the lab.

Chapter 2

Methylation of histone H3 at Lysine 36 by leukemia translocation protein NUP98-NSD1 caused epigenetic deregulation of the *Hox-A* locus during hematopoietic transformation

ABSTRACT

The nuclear receptor-binding SET domain protein 1 (NSD1) and its related proteins (NSD2/MM-SET/WHSC1 and NSD3/WHSC1L1) comprise a novel family of histone methyltransferases (HMT) that were found mutated or dysregulated in myeloid leukemia, multiple myeloma, childhood overgrowth syndrome and solid tumors. However, their functions are largely unknown. *NSD1* was found translocated with nucleoporin *NUP98* in human acute myeloid leukemia (AML) harboring the chromosomal translocation t(5;11)(q35;p15.5). Here we demonstrated that the common translocation product NUP98-NSD1 maintained the expression of two subordinate leukemic pro-oncogenes, the *Hox-A* genes (*HoxA5* to *HoxA10*) and *Meis1*, which caused the transformation of hematopoietic progenitors *in vitro* and the generation of AML in murine marrow transplantation models. Mechanistically, NUP98-NSD1 directly bound to the *HoxA5-A10* locus through function of plant homeodomain PHD^{V}-CH, induced the epigenetic modifications, and transactivated the local genes. The epigenetic changes were achieved through the NSD1 intrinsic HMT domain (SET domain) that methylated the histone H3, lysine 36 (H3K36), recruiting the histone acetyltransferases CBP/p300 that acetylated histones, and suppressing HMT EZH2-mediated trimethylation of histone H3, lysine 27 (H3K27). Point mutations that disrupted the H3K36 methyltrasferase activity, or deletion of the NUP98 FG repeats, abolished the transformation, pinpointing that both the H3K36 HMT activities and the NUP98 fusion part were required for leukemogenesis induced by NUP98-NSD1. It is the first report that linked the H3K36 HMT activities to the *Hox-A* gene upregulation and tumorigenesis.

INTRODUCTION

The mammalian Class I Hox homeodomain transcription factors play a pivotal role in determining body patterning during embryogenesis and regulating cellular differentiation and proliferation during hematopoiesis. These Hox factors, together with their cofactor Meis1 (*M*yeloid *e*cotrophic *i*nsertion *s*ite 1), positively regulate the pool size of hematopoietic stem cells (HSC) and lineage-specific hematopoietic progenitors by promoting cellular proliferation as well as arresting cellular differentiation (Azcoitia et al., 2005; Lawrence et al., 2005; Wang et al., 2005a). The dysregulation of these *Hox* genes and *Meis1* was directly linked to malignant hematopoiesis. In normal hematopoiesis, the expression pattern of the *Hox* genes and *Meis1* is dynamic, present at high levels in marrow subpopulations containing HSCs and early progenitors while quickly downregulated as progenitors differentiate (Sauvageau et al., 1994). The abnormal maintenance or overexpression of each of certain *Hox* genes (especially *HoxA9*, *HoxA7 and HoxA10*) was observed in around 70~80% of human acute myeloid leukemia (AML) cases, which also often evidenced the upregulation of the *Meis1* as well (Afonja et al., 2000; Drabkin et al., 2002; Lawrence et al., 1999). Murine AML models revealed the functional roles of HoxA9 (or HoxA7) and Meis1 in co-programming leukemogenesis (Thorsteinsdottir et al., 2001) and co-activating their downstream genes (Wang et al., 2006), however, it is still not clear how the aberrant upregulation of the *Hox-A* genes and *Meis1* is generally achieved in the first place in human AML.

Epigenetic dysregulation of the *Hox* locus was also directly linked to the development of AML. Around 5~10% of human AMLs harbored the chromosomal

translocation of the *M*ixed *L*ineage *L*eukemia gene (*MLL*), an epigenetic modifier of *Hox* locus (Hess, 2004). MLL positively regulated the proper expression of *Hox* genes by inducing trimethylation of histone 3, Lys 4 (H3K4), a prominent gene activation marker. Chromosomal translocations of *MLL* generated chimeric fusion products, which acquired aberrant transactivation functions that led to the sustained expression of *Hox* genes (Slany, 2005). However, a high percentage (70~80%) of human AML exhibited the *Hox* upregulation pattern, indicating additional regulators other than MLL may also be mutated or activated in AML. In this report, we will describe another *Hox* gene activation mechanism in AML involving translocation of the histone methyltransferase gene *NSD1*.

The *n*uclear receptor-binding *S*ET *D*omain-containing protein 1 (NSD1) and its related genes (NSD2/MMSET/WHSC1 and NSD3/WHSC1L1) comprise a novel family of histone methyltransferases (HMT) that were directly linked to various human diseases including myeloid leukemia (Jaju et al., 2001; Rosati et al., 2002), multiple myeloma (Keats et al., 2005), childhood overgrowth syndrome (Cecconi et al., 2005), and solid cancers (Angrand et al., 2001). Both the NSD1 and NSD3 loci were involved in human AMLs with chromosomal translocation t(5;11)(q35;p15.5) or t(8;11)(p11.2;p15) respectively. Mutation of *NSD1* was found in over 90% of Sotos Syndrome, an overgrowth disorder characterized by childhood overgrowth, facial dysmorphism and mental retardation. NSD proteins contain multiple conserved domains, including a HMT SET domain [*S*u(var)3-9, *E*nhancer of zeste, *T*rithorax], a SAC domain [*S*AC *A*ssociated *C*ysteine-rich region], five PHD fingers [*P*lant *H*omeo*d*omain] and etc, which were also often found in other chromatin modulating

factors such as MLL and Trithorax (Huang et al., 1998). NSD1 is unique, being the only family member that contains nuclear receptor binding motifs. *In vitro* HMT assay indicated that, unlike MLL, NSD1 contained methyltransferase activity specifically targeting histone H3, Lys 36 (H3K36) and much less efficiently, if detectable, targeting histone H4, Lys 20 (H4K20) (Bender et al., 2006; Rayasam et al., 2003). NSD1 is essential for embryonic development, as revealed by mouse knockout experiments in mice that caused an early lethality with a failure to complete gastrulation. However, the mechanistic contribution of NSD family members to leukemia or other diseases is largely unstudied.

About 5% of human AML harbored a translocation between *NSD1* and the nucleoporin-98 gene (*NUP98)*, generating two chimeric fusion genes, *NUP98-NSD1* and *NSD1-NUP98* (Cerveira et al., 2003). In some AML cases, only one transcript, i.e., *NUP98-NSD1*, was detected, indicating *NUP98-NSD1* is the fusion protein that caused AML (Cerveira et al., 2003; La Starza et al., 2004). In leukemia, NUP98 or related gene *NUP214/CA*N was found translocated with at least 17 different translocation partners including *NSD1* and *NSD3* (Nakamura, 2005). All these fusion proteins retained the nucleoporin FG repeats, a domain that activated transcription by recruiting the histone acetyltransferase (HAT) CBP or p300 (Kasper et al., 1999), indicating that directing histone acetylation to the target genes of the fusion partner transcriptional factors serves as the transforming mechanism. Consistently, the translocation of *NSD1* found in leukemia is likely to be gain-of-function instead of loss-of-function, because no obvious leukemia was found in Sotos syndrome patients with one allele of *NSD1* deleted.

Here, we established the leukemic functions of NUP98-NSD1 by *in vitro* hematopoitic progenitor transformation assay and *in vivo* leukemogenic assay. We found that NUP98-NSD1 induced the upregulation of a subset of *Hox-A* genes (*A5, A7, A9, A10*) and *Meis1*. Mechanistically, NUP98-NSD1 was directly bound to *Hox-A* locus and trans-activated the encoded *Hox-A* genes. The fifth PHD finger of NSD1, together with a nearby Cys-His rich region (CH), tethered the fusion protein to the *Hox-A* locus, while the FG repeat domain of NUP98 and the SET domain of NSD1 cooperated to achieve optimal gene activation. Consistently, we detected the recruitment of p300 and increased levels of histone acetylation and H3K36 trimethylation on *HoxA9* and *HoxA7* promoters. NUP98-NSD1 also suppressed the recruitment of HMT EZH2 and trimethylation of H3K27. Point mutations that disrupted H3K36 methyltrasferase activity, or deletion of NUP98 FG repeats, abolished the transformation, pinpointing that both H3K36 methylation and NUP98 fusion part were required for leukemogenesis. This study identified NSD1 as a novel transcriptional modifier of *Hox* locus and its translocation with NUP98 caused *Hox* gene activation and AML transformation.

RESULTS AND DISCUSSIONS

The t(5;11)(q35;p15.5) fusion gene NUP98-NSD1 is sufficient to immortalize cytokine-dependent hematopoietic progenitors *in vitro,* which evidence the upregulation of a subset of *Hox-A* genes, *Meis1* and their downstream target genes.

In order to examine the leukemogenic mechanism involving chromosomal translocation t(5;11)(q35;p15.5), we generated the common chimeric fusion gene *NUP98-NSD1* (Figure 2.1A). Reciprocal fusion gene *NSD1-NUP98* was not expressed in some leukemia cases, and hence was not studied here. *NUP98-NSD1* cDNA was cloned into the murine stem cell virus expression system (Mscv), which was then used to infect murine lineage-negative enriched hematopoietic progenitors followed by cultivation in medium containing stem cell factor (SCF) and Flt3 ligand (FL). The progenitors expressing Flag tagged NUP98-NSD1 proteins (Figure 2.1C, top panel) exhibited sustained proliferation and arrested differentiation *in vitro,* producing immortalized progenitors that sustained cell division over one year. As a control, progenitors infected with empty retrovirus vector showed limited expansion, followed by quick differentiation and maturation within weeks (Figure 2.1B). NUP98-NSD1 exhibited nuclear localization (Figure 2.1E), indicating its function is primarily nuclear. Wright-Giemsa staining showed that cells immortalized by *NUP98-NSD1* were composed mainly of myeloblasts (Figure 2.1D), further supported by flow cytometry (FACS) analysis revealing a typical surface antigen presentation $Cd34^{low}$ $Flt3^{low}$ c-Kit^{+} Mac-I^{+} $B220^{-}$ $Cd19^{-}$ $Thy1.2^{-}$ (Figure 2.1F).

In order to examine the transforming mechanism of NUP98-NSD1, we performed the Affymetrix gene array analysis to compare the gene expression profile of hematopoietic progenitors immortalized by NUP98-NSD1 with those immortalized by other leukemia oncoproteins including MLL fusion protein MLL-ENL, and Meis1 plus HoxA9, HoxA9 alone, and Vp16-Meis1 (Wang et al., 2005a; Wang et al., 2006). Interestingly, progenitors transformed by NUP98-NSD1 were similar to those transformed by MLL-ENL in terms of expression profiling revealed by Affymetrix array analysis (Table 2.1). In both cases, the genes upregulated most included a subset of *Hox-A* genes (*HoxA5, A7, A9, A10*) as well as *Meis1*. As a negative control, none of these endogenous genes were expressed in progenitors immortalized by HoxA9 or Vp16-Meis1 (Wang et al., 2005a; Wang et al., 2006). The previously reported downstream target genes upregulated by HoxA9 and Meis1 (such as *CD34, FLT3, Erg1* and etc) were also expressed in progenitors transformed by NUP98-NSD1, by MLL-ENL, or by exogenously coexpressed HoxA9 plus Meis1. Western blot (Figure 2.1C, middle panel and Figure 2.2D), semi-quatitative reverse-transcription polymerase chain reaction (RT-PCR) (Figure 2.1G) and quantitative real-time PCR (Figure 2.2E) were used to confirm the microarray analysis.

NUP98-NSD1 induces acute myeloid leukemia *in vivo*, which also exhibits the activation of *Hox-A* genes, *Meis1* and their downstream genes.

The immortalization effect in culture by NUP98-NSD1, combined with activation of the *Hox-A* and *Meis1* genes, two potent leukemia oncogenes, indicated that the expression of NUP98-NSD1 is likely to be sufficient to cause leukemia *in*

vivo. Indeed, leukemia developed in the recipient animals injected with bone marrow progenitors infected with retrovirus encoding *NUP98-NSD1* after an average of 126 days (Figure 2.2A). As a negative control, none of the recipients injected with progenitors infected with empty retrovirus developed AML. All recipients injected with progenitor infected with MLL-ENL retrovirus developed leukemia in an average of 53 days. Leukemia induced by NUP98-NSD1 presented with 3 to 12 fold enlarged spleen (Table 2.2 and Supplementary Figure 2.1A), 2 to 10 fold enlarged lymph nodes (Table 2.2), and 3 to 50 fold increased circulating white blood cell counts (Table 2.2). Leukemic cell invasion and expansion in the spleen caused the disruption of normal follicle like histological structure (Supplementary Figure 2.1B-E). Leukemia cells were mostly immature progenitors with surface antigen presentation $Cd34^{variable}$ $Flt3^{variable}$ c-Kit ^{high} Mac-I ^{high} $B220^{-}$ $Cd19^{-}$ $Thy1.2^{-}$ by FACS analysis, supporting the leukemia as typical AML classification (Table 2.2 and Supplementary Figure 2.1F). Northern blot revealed the expression of retrovirus encoded *NUP98-NSD1* in transformed progenitors and derived leukemia cells (Supplementary Figure 2.1G). It is interesting that wildtype NSD1 transcripts were also detected in early Lin- progenitors and progenitors immoratalized by NUP98-NSD1 or MLL-ENL. Southern blot exhibited the same retroviral integration sites in leukemia cells as in parental injected progenitors (Figure 2.2C), confirming injected parental progenitors as origin of leukemia. Like the parental progenitors, the derived leukemia tissue cells retained the overexpression of *Hoxa5, Hoxa7, Hoxa9, Hoxa10, Meis1*, and their downstream target genes *Cd34*, *Flt3* and *Erg1* revealed by real-time PCR and FACS analysis (Figure 2.2E and Supplementary Figure 2.1F). Taken together, like MLL fusion

proteins (Ayton and Cleary, 2003; Zeisig et al., 2004), NUP98-NSD1 transformed hematopoietic progenitors and induced AML likely through the cooperated functions of subordinate protooncogenes, *Hox-A* genes and *Meis1*.

NUP98-NSD1 is directly recruited to the *HoxA9-A7* locus and activates the transcription of these genes.

Functional similarity between NUP98-NSD1 and MLL fusion proteins in transforming progenitors that expressed the *Hox-A* genes and *Meis1* prompted us to question whether or not NUP98-NSD1, like MLL fusion proteins, is also a direct transcriptional activator of Hox genes. Indeed, in a transcriptional activation assay using a luciferase reporter containing *HoxA7* promoter and after comparison to empty vector, the transient transfection of either MLL-ENL or NUP98-NSD1 induced the *HoxA7* promoter reporter up to 6 fold or 5 fold in a dosage-dependent manner in either HEK293 cells (Figure 2.3A) or NIH3T3 fibroblast cells (Figure 2.4D). This indicated that NUP98-NSD1 is a direct transcriptional activator of *Hox-A* genes.

To further confirm the direction activation, we performed the chromatin immunoprecipitation (ChIP) analysis. Previously, twenty ChIP primers were used to survey a region of the *Hox-A* locus covering 3' of *HoxA10* to 5' of *HoxA7* with a resolution of one primer set per 500 base pairs (Figure 2.3B, bottom diagram) (Okada et al., 2005). Cells used for our ChIP analysis were hematopoietic progenitors transformed by *NUP98-NSD1* or by the control gene *MLL-ENL*. Polyclonal antibodies against NUP98 (α-NUP98), but not control IgG antibodies, precipitated the specific genomic fragments of *HoxA7* and *HoxA9* regulatory elements from

progenitors expressing *NUP98-NSD1* (Figure 2.3B, top panel, red line and Figure 2.3C, right panel). As a negative control, the same antibody did not precipitate these fragments from progenitors expressing *MLL-ENL* (Figure 2.3B, top panel, black line and Figure 2.3C, left panel). As an immunoprecipitation control, similar levels of dimethylated H3K4 and no trimethylated H3K9 were detected on *HoxA9-A7* regions in both progenitors (Figure 2.3C and Figure 2.3B, middle and bottom panels). ChIP analysis also indicated the absence of NUP98-NSD1 on promoters of two anterior *Hox-A* genes, *HoxA1* and *HoxA3*, which were not expressed in NUP98-NSD1 transformed progenitors. These same ChIP results were further confirmed using α-Flag antibodies, but not control α-HA antibodies, in progenitors transformed by Flag-tagged version of NUP98-NSD1 (Figure 2.4C and data not shown). Thus, like MLL fusion proteins, NUP98-NSD1 was recruited directly to specific regions of *Hox-A* locus and induced the transactivation of *HoxA5* to *HoxA10*.

Coincident with histone acetylation and H3K36 trimethylation on *Hox-A* locus in transformed hematopoietic progenitors, NUP98-NSD1 retained the intrinsic methyltransferase activity and recruited HAT CBP/p300, while preventing the recruitment of Ezh2 and H3K27 trimethylation.

The next question we ask is what epigenetic changes are induced by NUP98-NSD1 upon direct recruitment to *HoxA5-A10* locus. To address this question, ChIP analysis was repeated in NUP98-NSD1 transformed progenitors by using antibodies against different modified histone epitopes. The control cells used were enriched early hematopoietic progenitors infected by empty vector or those transformed by

coexpressed *HoxA9* plus *Meis1*. *HoxA9* and *Meis1* are downstream effector genes of *NUP98-NSD1*, and their enforced co-expression blocks progenitor differentiation at early stages similar to those by their upstream leukemia oncogenes *MLL* fusion genes or *NUP98-NSD1* (Figure 2.3D) (Ayton and Cleary, 2003; Zeisig et al., 2004). Therefore, the comparison between the progenitors transformed by *NUP98-NSD1* and those by its downstream effectors, *HoxA9* plus *Meis1*, will give the information of epigenetic changes induced by NUP98-NSD1, instead of those changes due to normal differentiation. As shown in Figure 2.3F, in progenitors expressing *NUP98-NSD1* exhibited increased levels of histone actetylation and H3K36 trimethylation along *HoxA9-A7* promoters and coding regions; H3K27 trimethylation exhibited opposite pattern: it was absent on *HoxA9-A7* promoters in progenitors transformed by NUP98-NSD1, but present in two control progenitors; H3K9 trimethylation or H4K20 trimethylation was not detected on *HoxA9-A7* promoters in any progenitor lines.

Increased levels of H3K36 trimethylation are consistent with the intrinsic HMT activity of NSD1. Previous studies of translocation protein NUP98-HoxA9 reported that the FG repeats of NUP98 harbored a transcriptional activation function by recruiting HAT CBP/p300 (Kasper et al., 1999). The same interaction was confirmed for NUP98-NSD1 by co-immunoprecipitation (Co-IP) experiments in 293T cells co-expressing Flag tagged NUP98-NSD1 and HA tagged p300. As shown in Supplementary Figure 2.2, α-Flag antibodies, but not the control α-Myc antibodies, precipitated NUP98-NSD1 together with p300; Similarly, α-HA antibodies, not the α-Myc antibodies, precipitated p300 together with NUP98-NSD1. Previous studies also reported that the H3K27 methyltransferase EZH2-containing

polycomb group complex is directly bound to the *HoxA9* promoter and is responsible for its downregulation (Cao and Zhang, 2004). To examine the recruitment of these histone modifiers on the *HoxA9* promoter, we turned to ChIP analysis. As shown in Figure 2.3E, HAT p300 was detected on the *HoxA9* promoter only in progenitors transformed NUP98-NSD1, but not in progenitors expressing empty vector or those transformed by coexpression of *HoxA9* plus *Meis1*. Interestingly, EZH2 exhibited opposite pattern: it was absent on *HoxA9* promoter in progenitors transformed NUP98-NSD1, but present on *HoxA9* promoter in progenitors transformed NUP98-NSD1 or progenitors expressing empty vector (Figure 2.3E).

Taken together, these results indicate that NUP98-NSD1 induced transactivation epigenetic changes coincident with binding to the *Hox-A* locus by multiple functions: the intrinsic methyltransferase activity of NSD1, recruiting HAT CBP/p300 by NUP98, and antagonizing the recruitment of Ezh2-contaning polycomb group complex.

The fifth PHD finger and Cys-His rich region (CH) of NSD1 tethered the NUP98-NSD1 protein to the *HoxA9* promoter, while both the NUP98 fusion part and the SET domain of NSD1 cooperated for optimal gene activation.

NSD3 is also fused to NUP98 in AML, and the translocation part of NSD3 is very similar to that of NSD1 except that NSD3 lacks the elongated C-terminus of NSD1, indicating that this C-terminus is not essential (Supplementary Figure 2.3). Indeed, a NUP98-NSD1 form with deletion of this tail (ΔC) did not affect any functional assays including binding to the *Hox-A* locus, transactivation of the *HoxA7*

promoter, transforming hematopoietic progenitors *in vitro*, and inducing leukemia *in vivo*, indicating that NUP98-NSD3 contains a similar transforming function to NUP98-NSD1 (Figure 2.4A-E, ΔC form vs WT). In order to address the functional relevance of different domains within NUP98-NSD1 to leukemic transformation, we performed systematic deletion mapping, in which deletion constructs were Flag tagged and mostly made in the context of ΔC form in order to achieve better retroviral titer due to limited viral packaging capacity (Figure 2.4A). When retrovirus encoding these constructs was used to infect hematopoietic progenitors followed by drug resistance selection, we found that all constructs were expressed at similar levels (Figure 2.4B). ChIP analysis performed in drug-resistant early progenitors identified that a post-SET region including the PHD^{V} finger and CH domain is responsible for tethering the NUP98-NSD1 protein to *HoxA9* promoter. Deletion of PHD^{V}-CH domains (Figure 2.4C) abolished the recruitment of NUP98-NSD1 to the *HoxA9* locus to barely undetectable levels. When these constructs were applied to transactivation of the *HoxA7* promoter-luciferase reporter, three regions were identified essential for transactivation, i.e., the *Hox-A* locus targeting region PHD^{V}-CH, the NUP98 part with FG repeats and the SET domain of NSD1 (Figure 2.4D). The PHD^{I-IV} fingers were not required for transactivation of *HoxA7* promoter reporter. Thus, we identified the PHD finger PHDV-CH responsible for targeting the fusion protein to the *Hox-A* locus, and both NUP98 fusion part and the SET domain of NSD1 are required for optimal transactivation of the *HoxA7* promoter probably through each of their intrinsic or recruited histone modification activities.

Deletion of the NSD1 PHD^{V}-CH domain or NUP98 fusion part, or point mutation in the SET domain of NSD1, abolished the leukemia transforming activities.

When the retrovirus encoding these constructs was used in the *in vitro* hemapoietic progenitor transformation assay and *in vivo* leukemogenic assay, deletion of the NSD1 PHD^{V}-CH domain or NUP98 fusion part completely abolished the generation of immortalized progenitors in medium containing SCF and FL (Figure 2.4E) or the induction of AML in irradiated recipient mice (data not shown). Deletion of the SET domain of NSD1 also resulted in the compromised ability of transforming the progenitors *in vitro*. To further address the involvement of H3mK36 methylation during leukemogenesis, five single amino acid substitutions within the SET domain of NSD1 (Figure 2.5A) were made on/near the residues previously reported crucial for efficient HMT activities due to either interfering with the binding of cofactor S-adenosyl-methionine, the methyl group donor, or affecting the enzymatic active site. Three mutations were made on conserved residues, namely N1918Q, H1919T and C1921A, and another mutation made on a non-conserved residue, i.e., C1920A. When applied to *in vitro* hemapoietic progenitor transformation assay, each one of the N1918Q, H1919T and C1921A mutants, but not wildtype or C1920A, failed to generate the immortalized progenitors efficiently (Figure 2.5B), upregulate the *HoxA9* gene expression (Figure 2.5C), induce the increased levels of H3K36 methylation on *HoxA9* locus in hematopoietic progenitors (data not shown), and transactivate the *HoxA7*-promoter luciferase reporter in HEK293 cells (Figure 2.5D). Thus, taken together, both the NUP98 fusion part (probably through the histone

acetylation) and the NSD1 H3K36 methyltransferase activities are required for the NUP98-NSD1-mediated leukemogenesis.

***HoxA9*, a subordinate pro-oncogene, is required for the leukemic transformation induced by NUP98-NSD1.**

The fact that either the deletion of *HoxA9*-locus targeting domain (PHD^{V}-CH), or the mutations that interfered with the transactivation of *Hox-A* genes, abolished the transforming activities of NUP98-NSD1 indicated that Hox-A genes might be essential for the leukemic transformation as well. To examine the role of *HoxA9,* the most prominent subordinate pro-oncogene, in the leukemia transformation induced by NUP98-NSD1, we obtained marrow progenitors from either *HoxA9* knockout (backcrossed to black-6 background over 10 generations that generates a 99.90% black-6 genetic background) and its wildtype littermates, followed by infection with retrovirus encoding *NUP98-NSD1* and transplantation into recipients with wildtype black-6 background (700 Rads, 3 million cells per mouse). While all animals receiving wild-type marrow progenitors infected with NUP98-NSD1 developed AML within 85 days, none of those injected with *HoxA9-/-* marrow progenitors developed AML after 150 days. This indicated that the upregulation of *HoxA9* is required for the efficient survival or expansion of cancer stem cell produced by NUP98-NSD1 *in vivo*.

Wildtype NSD1 is a novel transcriptional regulator of *Hox* locus.

The fact that the *Hox* locus-targeting domain of NUP98-NSD1 identified above also resides in wildtype NSD1 indicates that NSD1 gene families might

represent a novel group of transcriptional regulators of *Hox* locus. Indeed, as shown in Figure 2.6, siRNA specific against *NSD1* in Hela cells, but not the control siRNA, caused the knockdown of endogenous *NSD1* to about 10~15% of normal level, which also concurred with downregulation of specific anterior *Hox-A* genes to different degree, which included *HoxA1* (down by 50%), *HoxA3* (down by 20%) and *HoxA7* (down by 30%). NSD1 knockdown did not dramatically affect posterior *Hox-A* genes, *HoxA9-A11*. Interestingly, siRNA against *MLL* did not affect anterior *Hox-A* genes, but specifically downregulated the expression of *HoxA9* and, to a less degree, *HoxA10*. Consistently, the expression of HoxA1 and HoxB1 was completely lost in the *NSD1*-/- embryos that also failed to complete grastrulation (Rayasam et al., 2003). Thus, like MLL, wildtype NSD1 represents a novel transcriptional modifier of *Hox* locus.

We have established hematopoietic transformation by translocation NUP98-NSD1 in a murine AML model and investigated its mechanisms. (i) We identified the upregulation of *Hox-A* genes and *Meis1* as the downstream pathway of NUP98-NSD1-mediated leukemogenesis, and revealed that NUP98-NSD1 directly bound to *HoxA5-A11* locus, similarly to those MLL translocation proteins. (ii) We demonstrated that NUP98-NSD1 induced dramatic epigenetic transactivation changes along *HoxA5-A11* locus, recruited CBP/p300 and suppressed the recruitment of EZH2-polycomb complex. It is interesting that the C. elegas homolog of NSD1, MES-4, also appeared to antagonize the function of MES-2/MES-3/MES-6, the C. elegas homologs of EZH2 complex, during development (Bender et al., 2006). MES-4 specifically associated with autosomes and functionally differed from SET-2-

related HMT that associated with elongated RNA polymerase II and mediated H3K36-methylation within and at the 3' of the coding regions of active genes (Schaft et al., 2003). (iii) We clearly proved that the H3K36 methyltransferase activity was crucial for hematopoietic transformation by NUP98-NSD1, which provided a novel mechanism of epigenetic *Hox* gene upregulation other than H3K79 methylation in AML harboring translocation MLL-AF10 or CALM-AF10 (Okada et al., 2005; Okada et al., 2006). H3K36 methylation was reported located throughout the actively transcribed gene loci (Bannister et al., 2005; Pokholok et al., 2005), was required for gene activation of plant transcriptional factors *FLOWERING LOCUS C* during the regulation of flowering (Zhao et al., 2005), and suppressed spurious intragenic transcription. (iv) We also identified a *Hox*-locus targeting domain PHD^{V}-CH that located within NSD1. A PHD finger of hNURF was recently identified as a domain that recognizes specific H3mK4 markers, which is important for the hNURF-mediated modulation of *Hox* gene regulation during development (Li et al., 2006; Wysocka et al., 2006). It also prompted a speculation that NSD1 and related proteins represent a novel group of *Hox*-locus regulators that might functionally interact with MLL.

MATERIALS AND METHODS

Plasmid construction and retroviral expression system.

The NUP98-NSD1 fusion gene was generated by ligation of 5'-part of *NUP98* cDNA sequence encoding amino acid 1-518 with *NSD1* sequence encoding amino acid 1166-2596 (Kindly provided by Dr. Pierre Chambon), and then cloned into Mscv-Neo retroviral expression vector. A flag-tagged version was generated by inserting the 3xFlag tag into a unique NsiI site generated by site-directed mutagenesis at the C terminus of *NUP98-NSD1*. Internal deletions were generated after excising cDNA regions flanked by two MfeI sites created by mutagenesis. All constructs were verified by sequencing. Plasmids containing *NUP98*, *MLL-ENL*, *HoxA9*, *Meis1-Ires-HoxA*9, or *Vp16-Meis1* were described previously (Wang et al., 2005a; Wang et al., 2006).

Cell cultures.

293T or HEK293 human embryonic kidney cell lines are cultured with DMEM (Invitrogen cat #11965-092 or MediaTech cat#10-013-CV) containing 4.5g/L glucose (high glucose), 10% fetal bovine serum (FBS) plus 1 % of antibiotics [penicillin, streptomycin and glutamine (PSQ)] in a 37°C humidified incubator with 5% CO_2. To freeze 293 cells, trypsinize cells and collect cells by centrifuge at 500 x g for 5 min. Remove the media and add 1 ml of freezing solution (90% FBS and 10% DMSO) per 10^6 cells. Transfer to a 2 ml cryogenic vial, and place the freezing incubator at -70 °C overnight and transfer to liquid nitrogen on the following day.

Hematopoietic progenitors are usually cultured with medium OptiMEM (Invitrogen Cat#31985-070) or RMPI 1640 (Invitrogen cat# 11875-093)

supplemented with 10% of FBS (Invitrogen, catalog # 16000-044), antibiotics, 30uM beta-mercaptoethanol (1ul pure into 500mls medium) and supporting cytokines in a 37°C humidified incubator with 5% CO_2. To freeze the progenitors, mix the culture medium containing cells 1:1 with freezing solution (80% FBS and 20% DMSO), freeze as described above and store in liquid nitrogen.

***In vitro* hematopoietic progenitor proliferation and immortalization assay.**

Protocols for retroviral infection and culture of primary hematopoietic progenitors in medium containing stem cell factor (SCF) and/or Flt3 ligand (FL, 5~10 ug/mL) were described previously (Wang et al., 2005a; Wang et al., 2006). Briefly, 2~4 x 10^5 of enriched Lin- bone marrow progenitors from Balb/c mice were subjected to two rounds of spinoculation infection using 1 ml of retroviral supernatant with a viral titer of 1~3x10^5/ml, followed by 3~5 days of drug resistance selection (0.8 to 1 mg/ml of G418), and cultured in medium containing SCF and FL. Retroviral titration was obtained by drug resistance colony formation assay using NIH3T3 fibroblast. Proliferation kinetics were evaluated by plating 2~4 x 10^5 drug-resistant Lin- progenitors in a 12-well tissue culture plate (Corning, New York) and splitting every 3 to 4 days in fresh medium, using a protocol that keeps the progenitor number lower than 2 x10^6 per well. Wright-Giemsa staining and fluorescence-activated cell sorter (FACS) analysis were performed as described elsewhere (Wang et al., 2005a; Wang et al., 2006).

Antibodies and immunoblotting.

Twenty microliters of total cellular protein (107 cells per ml) was used for immunoblotting. α-Flag, α-Flt3, and α-Hoxa9 were obtained and used as described

previously (Wang et al., 2005a; Wang et al., 2006). α-NUP98 polyclonal antibodies were a kind gift of Dr. Jan Van Deursen (Mayo Clinic).

Affymetrix microarray analysis.

Total RNA extracted from stably transformed progenitors cultured *in vitro* was examined by using the Affymetrix GeneChip Mouse Genome 430 2.0 array as previously described (Wang et al., 2005a; Wang et al., 2006).

Semiquantitative RT-PCR and real-time qPCR.

Total RNA was extracted from immortalized progenitors, the first-strand total cDNA, used as a template for reverse transcription-PCR (RT-PCR) and quantitative PCR (qPCR), was generated, and RT-PCR or qPCR was performed as previously described (Wang et al., 2005a; Wang et al., 2006).

***In vivo* leukemogenic assay.**

As previously described (Wang et al., 2005a; Wang et al., 2006), the leukemic potential of oncogenes was evaluated in sublethally irradiated syngeneic Balb/c mice (500 rads dosage) followed by tail vein injection with 2 $x10^6$ immortalized progenitors cultured *ex vivo* for 3 weeks or with 5x 10^5 Lin- progenitors that were prestimulated in a cytokine rich medium, infected with retrovirus and subjected to drug resistance selection. For examine the role of *HoxA9*, bone marrow progenitors were extracted from either *HoxA9*-null or wiltype littermate mice (backcrossed into black/6 background over 10 generations, a kind gift of Drs Jeff Lawrence, Corey Largman and Mario Capecchi), followed by retrovirus infection and injection into sublethally irradiated wiltype black/6 mice (700 rads as dosage). Mice exhibiting a leukemia phenotype (scruffy fur, lethargy, paralysis, or splenomegaly) were

sacrificed, and cells isolated from leukemic tissues were subjected to further analysis, including flow cytometry, Wright-Giemsa staining, secondary injection, immunoblotting, retroviral integration site analysis by Southern blotting, and RT-PCR as described before (Wang et al., 2005a; Wang et al., 2006).

Retrovirus genomic integration site analysis.

Genomic DNA was purified, digested, resolved, and transferred to a membrane as previously described (Wang et al., 2005a; Wang et al., 2006). XhoI was used to digest DNA from progenitors infected by retrovirus encoding NUP98-NSD1, and cDNA fragments encoding the amino acid 1890-2596 were used for making probes.

Northern blot.

Total RNA was extracted, resolved and transferred as described before. cDNA fragments encoding the amino acid 1890-2596 were used for making probes.

Luciferase reporter assay.

Transactivation by NUP98-NSD1 was evaluated using a pGL3 luciferase reporter containing a 2.8Kb fragment of *HoxA7* promoter, which was previously used in evaluation of *MLL* fusion proteins (Liu et al., 2004). 100~500 ng of *HoxA7*-promoter reporter was cotransfected with 1ng of pRL-TK into NIH3T3 cell lines with stable expression of either empty retroviral vector, or wildtype or mutant NUP98-NSD1. For luciferase assay done in HEK293 cells, 2ug of Mscv plasmids, either empty or encoding NUP98-NSD1 or MLL-ENL, were cotransfected with 100 ng of *HoxA7*-promoter reporter plus 0.5ng of pRL-TK. At 48~72 hour post transfection, cell lysate was prepared and quantified for firefly and renilla luciferase activity using

a dual luciferase reporter system (Promega) and LMaxII luminometer (Molecular Devices, California). After normalization against renilla luciferase units, transcriptional activation of NUP98-NSD1 was compared to basal firefly luciferase levels in cells expressing empty Mscv vector.

Chromatin immunoprecipitation (ChIP) analysis.

ChIP analysis was performed according to a previously described protocol (Wang et al., 2005a; Wang et al., 2006). The identities of ChIP primers was shown in supplementary Table 2.1. Antibodies α-Flag, α-acetyl-histone H3 and α-dimethylated H3K4 (α-H3K4Me2) were described before. Other antibodies included α-HA (Covance, MMS-101), α-Myc (9E10), α-trimethylated H3K9 (Upstate, cat#07-442), α-trimethylated H3K27 (Upstate, cat#07-449), α-trimethylated H4K20 (Upstate, cat#07-463), α-trimethylated H3K36 (Abcam, cat#9050), α-Pol II (Abcam, 4H8, cat#ab5408), and α-p300 (Santa Cruz Biotech, cat#sc-585, cat#584), and α-Ezh2 (Cell signaling, cat#4905).

Geneneration of GST-fusion proteins.

Expression of recombinant proteins were induced with 1 uM IPTG in ~500 mL cultures of E. coli strain BL21 transformed with pGEX4T fusion construct. The bacteria pellet was solubilized in 10 mL of cold PBS supplemented with 10mM EDTA and protease inhibitor (1mM PMSF plus apropotinin), followed by a 30-sec sonication. After adding up to 1% Triton X100 and incubating for 15 min on ice, the soluble proteins were cleared by centrifugation at 15,000 rpm for 10 min and purified with 400 ul of glutathione Sepharose beads (Pharmacia) and washed three times in

cold PBS or RIPA buffer (20 mM Tris pH 7.5, 500 mM NaCl, 5 mM EDTA, 1% NP-40 and 0.5% sodium deoxycholate) containing a full set of protease inhibitors. Protein concentration was determined by Coomassie staining of SDS–PAGE gels. Matrix-bound fusion proteins were used immediately for in vitro HMT assays or stored at 4 °C.

***In vitro* histone methyltransferase (HMT) assay.**

In vitro HMT reactions were modified on the basis of Upstate protocols, and carried out in a volume of 30~50 µl containing 1xHMT buffer (50 mM Tris pH 8.5, 20 mM KCl, 10 mM $MgCl_2$, 10 mM β-mercaptoethanol, 250 mM sucrose), 10~20 ug of free core histones (mixture of H1, H3, H2B, H2A and H4; Boehringer Mannheim or Upstate) as substrates, and 300 nCi (~0.6 µl) of S-[methyl-^{3}H]- Adenosyl-L-Methionine [Perkin-Elmer, catalog# NET155050UC, 50µCi (1.85MBq) in 100 µl] as methyl donor. I routinely used 10~20 ug of matrix-bound GST fusion proteins to assay for HMT activity. After incubation for 60 min~hours at 37 °C, reactions were stopped by boiling in SDS loading buffer, and proteins were separated by 15% or 18% SDS–PAGE and visualized by Coomassie brilliant blue, and further destained for detection of fusion proteins and free histones. For each fluorography, 50 mL of Fluro-Enhance solution (Research Product International, IL) was added to the destained gel and kept on a shaker in a chemical hood for 1 h. After 1 h, 100 mL of cold MilliQ water was added to the gel. The gel was kept on a shaker for 30 min. The gel was dried between two cellophane films and exposed to Kodak X-ray film overnight to weeks at -80°C.

Figure 2.1. NUP98-NSD1 immortalized myeloid progenitors and maintained the expression of a subset of *Hox-A* genes, *Meis1* and the downstream target genes of HoxA9 plus Meis1.

(A) Depiction of structure of NUP98-NSD1 that was generated by leukemia translocation-caused fusion of the amino acid 1-518 of NUP98 with the amino acid 1166-2596 of NSD1. Major structural domains or motifs were as labeled. NUP98 fusion part contains 37 of FG repeats indicated by bars. The construct was tagged with 3xFlag tag at the C-terminus.

(B) Proliferation kinetics of hematopoietic progenitors after infection of MSCV empty retrovirus (blue) or that encoding NUP98-NSD1 (purple) or MLL-ENL (red). At day 1, 200,000 of drug-resistant Lin-enriched progenitors were plated in the medium containing SCF plus FL. Each construct group included five different infected cultures; Error bars indicated the standard deviation (SD) of progenitor numbers among the group.

(C) Western blot analysis using M2 α-Flag antibody (for the detection of NUP98-NSD1), α-HoxA9 and α-tubulin (for sample loading control) on the total protein extract sample of two control cultures (lane 1-2), three cultures infected with Flag tagged NUP98-NSD1 retrovirus (lane 3-5), and culture infected with MLL-ENL retrovirus.

(D) Nuclear localization of NUP98-NSD1 indicated by DNA straining (Hoescht), signals of GFP tagged at C-terminal of NUP98-NSD1 (GFP), and merged image of NIH3T3 fibroblasts in a transient transfection experiment;

(E) Wright-Giemsa staining revealed cultures immortalized by NUP98-NSD1 composed of mostly immature myeloblasts and occasionally mature neutrophils;

(F) FACS analysis of progenitors infected with NUP98-NSD1 retrovirus four weeks after infection;

(G) RT-PCR confirmed the Affymetrix microarray analysis, revealing the upregulation of a subset of *Hox-A* genes, *Meis1,* and their known downstream targets (*Cd34*, *Flt3, Erg1*) in progenitors immortalized by NUP98-NSD1. The lanes were loaded with PCR products using cDNA template produced from control progenitors expressing empty vector (lane 1) and progenitors transformed by the expression of HoxA9 alone (lane 2), HoxA9 plus Meis1 (lane 3), MLL-ENL (lane 4), NUP98-NSD1 (two cultures as in lane 5 and 6), or Vp16-Meis1 (lane 7). *Gapdh* served as internal template control. As a negative control, progenitors immortalized by Vp16Meis1 did not express *Hox-A* genes, and those immortalized by HoxA9 did not express *Cd34*, *Flt3* and *Erg1*.

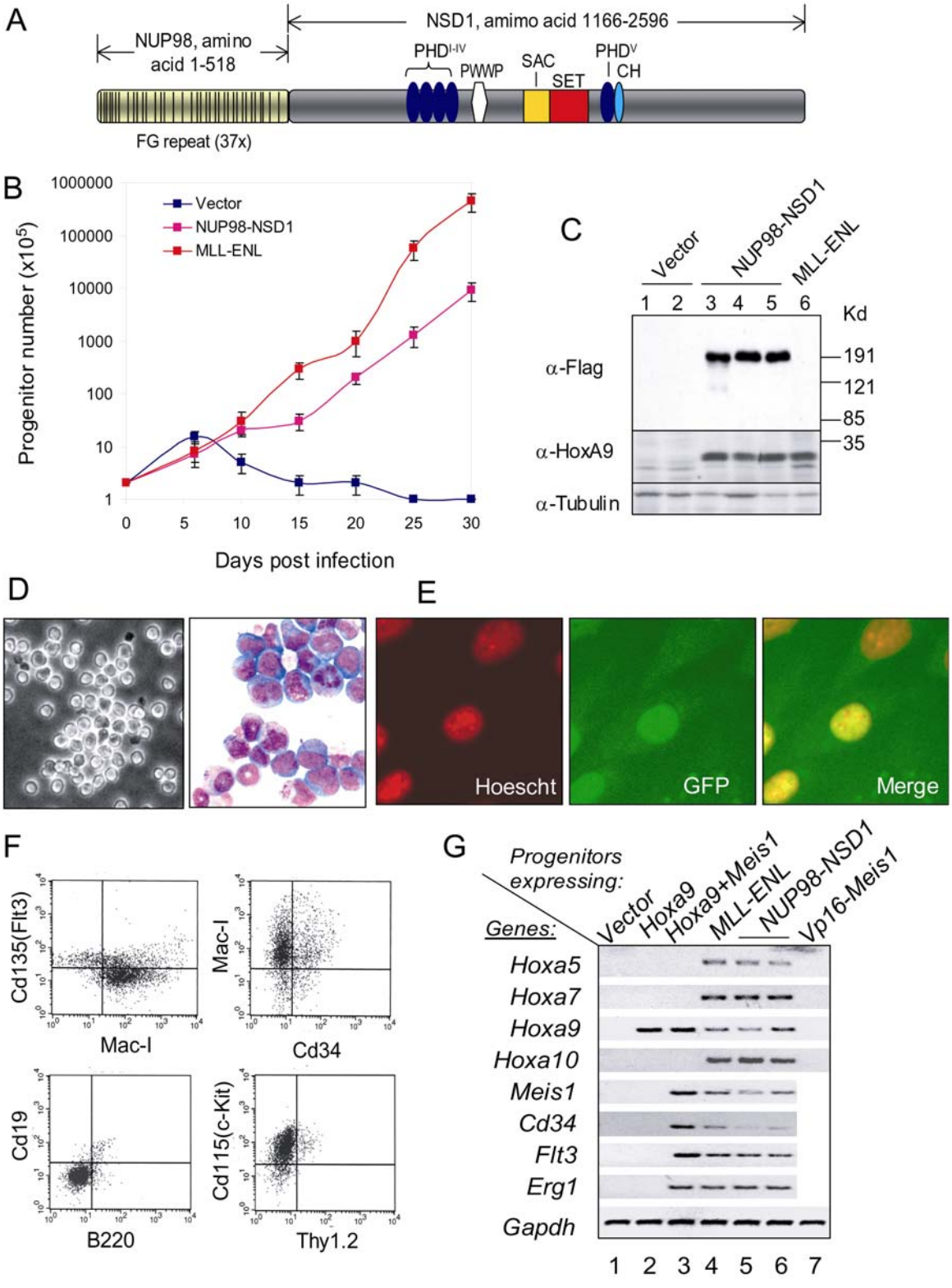
A
NUP98, amino acid 1-518
NSD1, amimo acid 1166-2596
PHD I-IV
PWWP
SAC
SET
PHD V
CH
FG repeat (37x)
B
Progenitor number (x10^5)
Vector
NUP98-NSD1
MLL-ENL
Days post infection
C
Vector
NUP98-NSD1
MLL-ENL
Kd
α-Flag
α-HoxA9
α-Tubulin
191
121
85
35
D
E
Hoescht
GFP
Merge
F
Cd135(Flt3)
Mac-I
Cd34
Cd19
B220
Cd115(c-Kit)
Thy1.2
G
Progenitors expressing:
Genes:
Vector
Hoxa9
Hoxa9+Meis1
MLL-ENL
NUP98-NSD1
Vp16-Meis1
Hoxa5
Hoxa7
Hoxa9
Hoxa10
Meis1
Cd34
Flt3
Erg1
Gapdh

Figure 2.2. NUP98-NSD1 induced AML *in vivo,* which also evidenced the upregulation of *Hox-A* genes, *Meis1* and their downstream target genes.

(A) The kinetics of leukemia induction in the recipient mice after transplantation of marrow progenitors infected with empty retrovirus (blue line), or that encoding NUP98-NSD1 (purple) or MLL-ENL (red). The n number indicates the size of animal group.
(B) Wright-Giemsa cell staining showed the immature progenitors expanded in bone marrow (BM), spleen (SP), lymph nodes (LN) and peripheral circulating blood (BL).
(C) Southern blot analysis of genomic NUP98-NSD1-retrovirus integration sites by using a NSD1 cDNA probe for three parental progenitors (P1, P2, L2) and their derived leukemia cells extracted from bone marrow (M) or spleen (S) of different animals (lane 2-5, 7-8 and 10-12). Arrowheads indicated genomic bands harboring integrated retrovirus, and star indicated the endogenous NSD1 locus.
(D) Western blot analysis of the protein level of Flag tagged NUP98-NSD1, HoxA9 and Flt3 in parental progenitors expressing Flag tagged NUP98-NSD1 (P) and derived leukemic cells extracted from marrow (M), spleen (S), lymph nodes (L) or thymus (T) of AML mice. Stars indicated the nonspecific bands; Progenitors infected with empty vector or that encoding HoxA9 plus Meis1 served as negative and positive controls.
(E) Real-time RT-PCR analysis of the transcript abundance of the endogenous *Hox-A* genes (*HoxA5, A7, A9, A10*), *Meis1, Flt3* and *Erg1* among progenitors immortalized by Hoxa9, Hoxa9 plus Meis1, MLL-ENL, Vp16Meis1 or NUP98-NSD1 and tissue cells from leukemia induced by NUP98-NSD1. 3'-UTR probes were designed for HoxA9 and Meis1 in order to detect their endogenous transcripts.

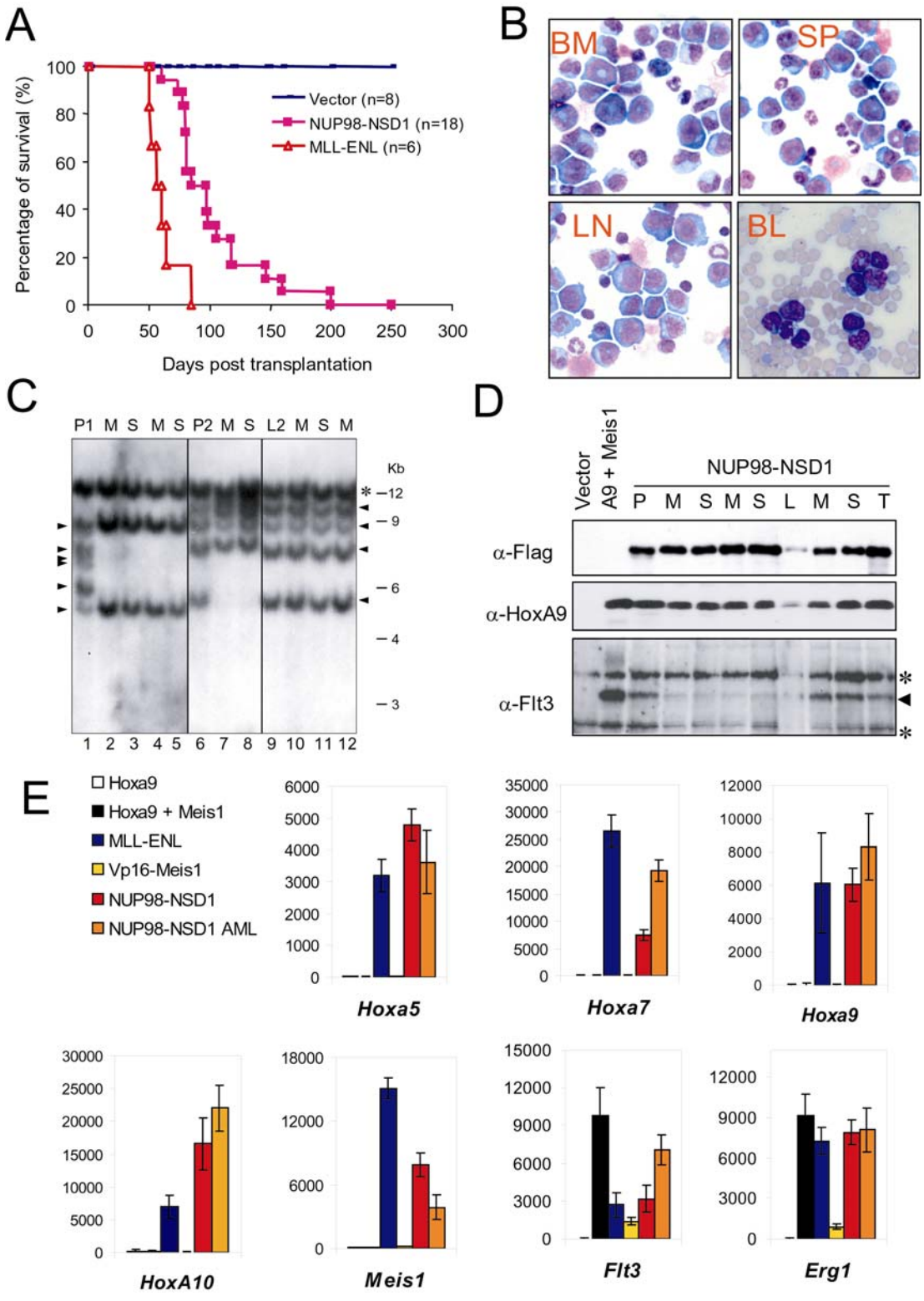
A
Percentage of survival (%)
Days post transplantation
Vector (n=8)
NUP98-NSD1 (n=18)
MLL-ENL (n=6)
B
BM
SP
LN
BL
C
P1 M S M S P2 M S L2 M S M
Kb
12
9
6
4
3
1 2 3 4 5 6 7 8 9 10 11 12
D
Vector
A9 + Meis1
NUP98-NSD1
P M S M S L M S T
α-Flag
α-HoxA9
α-Flt3
E
Hoxa9
Hoxa9 + Meis1
MLL-ENL
Vp16-Meis1
NUP98-NSD1
NUP98-NSD1 AML
Hoxa5
Hoxa7
Hoxa9
HoxA10
Meis1
Flt3
Erg1

Figure 2.3. NUP98-NSD1 was directly recruited to *Hox-A* locus, transactivated the *HoxA7* promoter, and induced H3 acetylation and H3K36 trimethylation as well as prevented H3K27 trimethylation on *HoxA9* promoter, consistent to its functions of recruiting the HAT CBP/p300 and antagonizing the Ezh2 binding.

(A) Transcriptional activation of a luciferase reporter containing a *Hoxa7* promoter fragment 72hrs post transfection of either 0.4ug, 1ug or 2ug of either MLL-ENL or NUP98-NSD1 plasmids in HEK293 cells. Activation fold was normalized against transfection of empty vector. Experiments were repeated three times and bars indicated SD.

(B) Quantitative diagram of the ChIP analysis signals obtained as in Figure 2.3C revealed the NUP98-NSD1 recruitment and histone modification marker levels on the *HoxA10-A7* locus in progenitors transformed by NUP98-Nsd1 (red line) or MLL-ENL (black line). Each circle represents one primer set used for ChIP analysis.

(C) Representative ChIP analysis results revealed by PCR amplification of genomic fragments representing the locus from 3' of *HoxA10* to 5' of *HoxA7* after immuno-precipitation with control antibodies, antibodies against NUP98 (α-NUP98) and antibodies against histone modification markers (α-H3K4-Me^2 or α-H3K9-Me^3) from progenitors transformed by NUP98-NSD1 or MLL-ENL. Nonspecific IgG or α-HA was used as control antibody for ChIP, and 5% of sonicated chromatin DNA used as input control. The position of HoxA9 primer sets was indicated as in Figure 2.3B, bottom panel.

(D) Diagrams showing the differentiation of hematopoietic progenitors arrested by coexpressed *HoxA9* plus *Meis1*, or by their upstream leukemia oncogene *MLL* fusion genes or *NUP98-NSD1*.

(E) ChIP analysis revealed the histone acetylation and methylation status on *Hox-A* locus, using antibodies (Abs) against various histone modification markers as indicated and using as source of sonicated chromatin fragments, either 2 weeks' culture of the Lin- progenitors expressing empty vector, or the progenitors transformed by the expression of *NUP98-NSD1* or the coexpression of *HoxA9* plus *Meis1*. Nonspecific IgG antibodies were used as a negative immuno-precipitation control, and 1% of chromatin DNA used as input control. The letter under each panel represents the primer set used for ChIP analysis as shown in bottom panel of Figure 2.3B.

(F) ChIP analysis revealed the recruitment status of HAT p300 and HMT EZH2 on the *HoxA9* promoter, primer-set position d, in cultures of Lin- progenitors infected with empty retrovirus or NUP98-NSD1 retrovirus, followed by drug resistance selection and culture for one week, as well as in progenitors immortalized by NUP98-NSD1 or by coexpressed *HoxA9* plus *Meis1*.

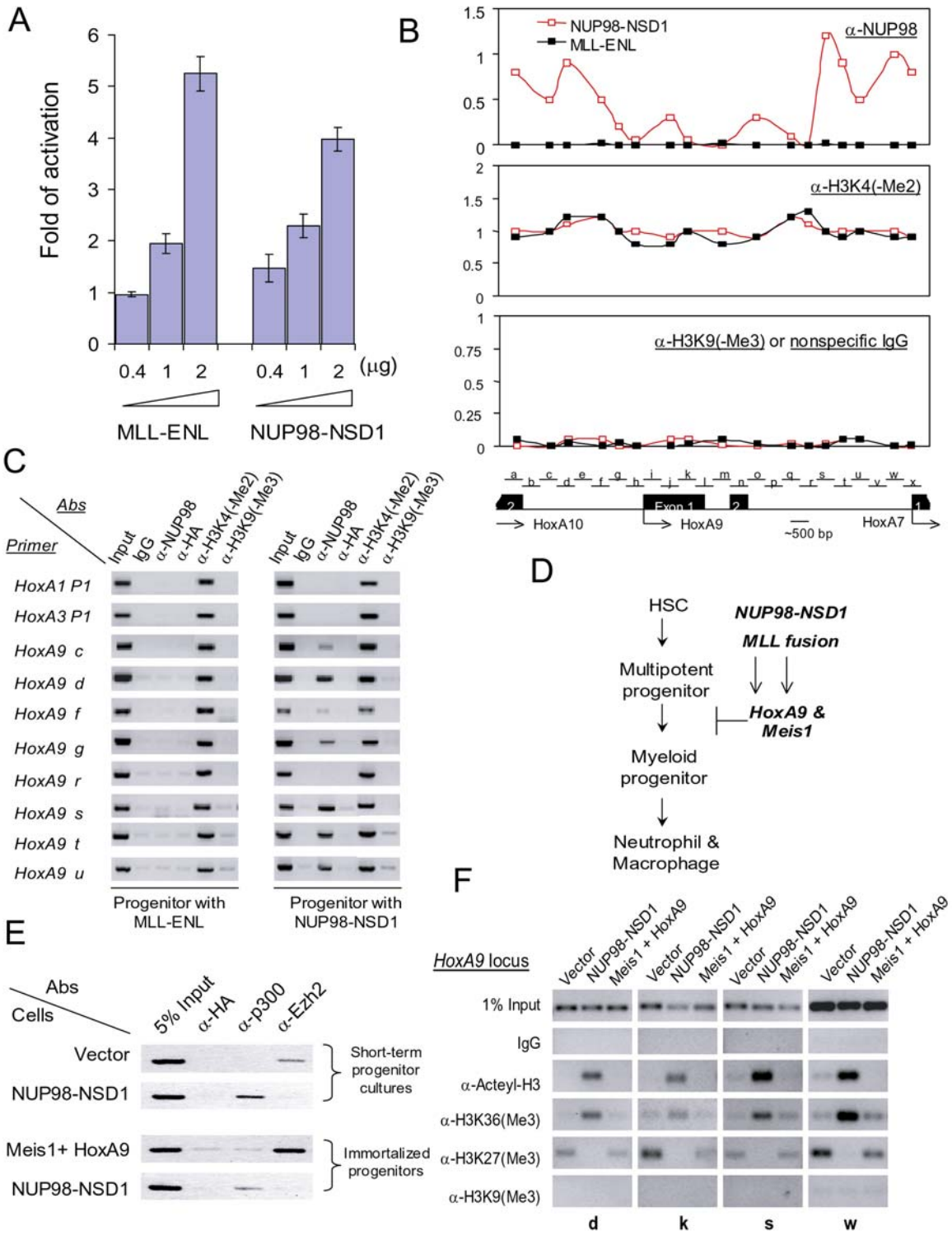
A
Fold of activation
0.4 1 2 0.4 1 2 (μg)
MLL-ENL
NUP98-NSD1
B
NUP98-NSD1
MLL-ENL
α-NUP98
α-H3K4(-Me2)
α-H3K9(-Me3) or nonspecific IgG
HoxA10
HoxA9
~500 bp
HoxA7
C
Abs
Primer
Input
IgG
α-NUP98
α-HA
α-H3K4(-Me2)
α-H3K9(-Me3)
HoxA1 P1
HoxA3 P1
HoxA9 c
HoxA9 d
HoxA9 f
HoxA9 g
HoxA9 r
HoxA9 s
HoxA9 t
HoxA9 u
Progenitor with MLL-ENL
Progenitor with NUP98-NSD1
D
HSC
NUP98-NSD1
MLL fusion
Multipotent progenitor
HoxA9 & Meis1
Myeloid progenitor
Neutrophil & Macrophage
E
Abs
Cells
5% Input
α-HA
α-p300
α-Ezh2
Vector
NUP98-NSD1
Short-term progenitor cultures
Meis1+ HoxA9
NUP98-NSD1
Immortalized progenitors
F
HoxA9 locus
Vector
NUP98-NSD1
Meis1 + HoxA9
1% Input
IgG
α-Acteyl-H3
α-H3K36(Me3)
α-H3K27(Me3)
α-H3K9(Me3)
d
k
s
w

Figure 2.4. The PHD finger PHD^V-CH of NSD1 tethered the NUP98-NSD1 protein to the *HoxA9* promoter, while both the NUP98 fusion part and the SET domain of NSD1 cooperated the optimal *Hox-A* gene activation, which were all required for the efficient leukemic transformation.

(A) Diagrams showing the deletion and point mutation within NUP98-NSD1. All constructs were tagged with a triple Flag tag at C-terminus.

(B) Western blot with M2 α-Flag antibodies showed that all constructs were stably expressed at similar or higher levels than ΔC form in drug-resistance selected hematopoietic progenitors. α-Tubulin was used for the loading control.

(C) ChIP analysis using α-Flag antibodies and primer set d revealed the binding of different NUP98-NSD1 deletion mutants onto the *HoxA9* promoter in drug selected hematopoietic progenitors. 5% of total chromatin, α-HA pulled down chromatin or α-H3K4-Me^2 pulled down chromatin was used as input control, ChIP negative control, or immunoprecipitation control respectively.

(D) Transactivation of a *HoxA7*-promoter luciferase reporter in the stable NIH3H3 cell lines expressing NUP98-NSD1 wildtype or deletion forms. The fold of activation was calculated by the ratio of firefly luciferase scores (*HoxA7* reporter) vs the renilla luciferase scores (internal control), followed by normalization against scores from cells expressing empty vector.

(E) The transforming potentials of wildtype or deletion forms of NUP98-NSD1 to generate the immortalized hematopoietic progenitors in the medium supplemented with SCF and FL. After the retroviral infection and drug-resistance selection, 200,000 progenitors were plated at day 1. The progenitor numbers were counted every 4-5 days, and the number plotted were those obtained at day 10 (open bars), day 25 (light grey), day 40 (dark grey) and day 55 (black). Each construct was evaluated with four different infected cultures. Bars indicated SD.

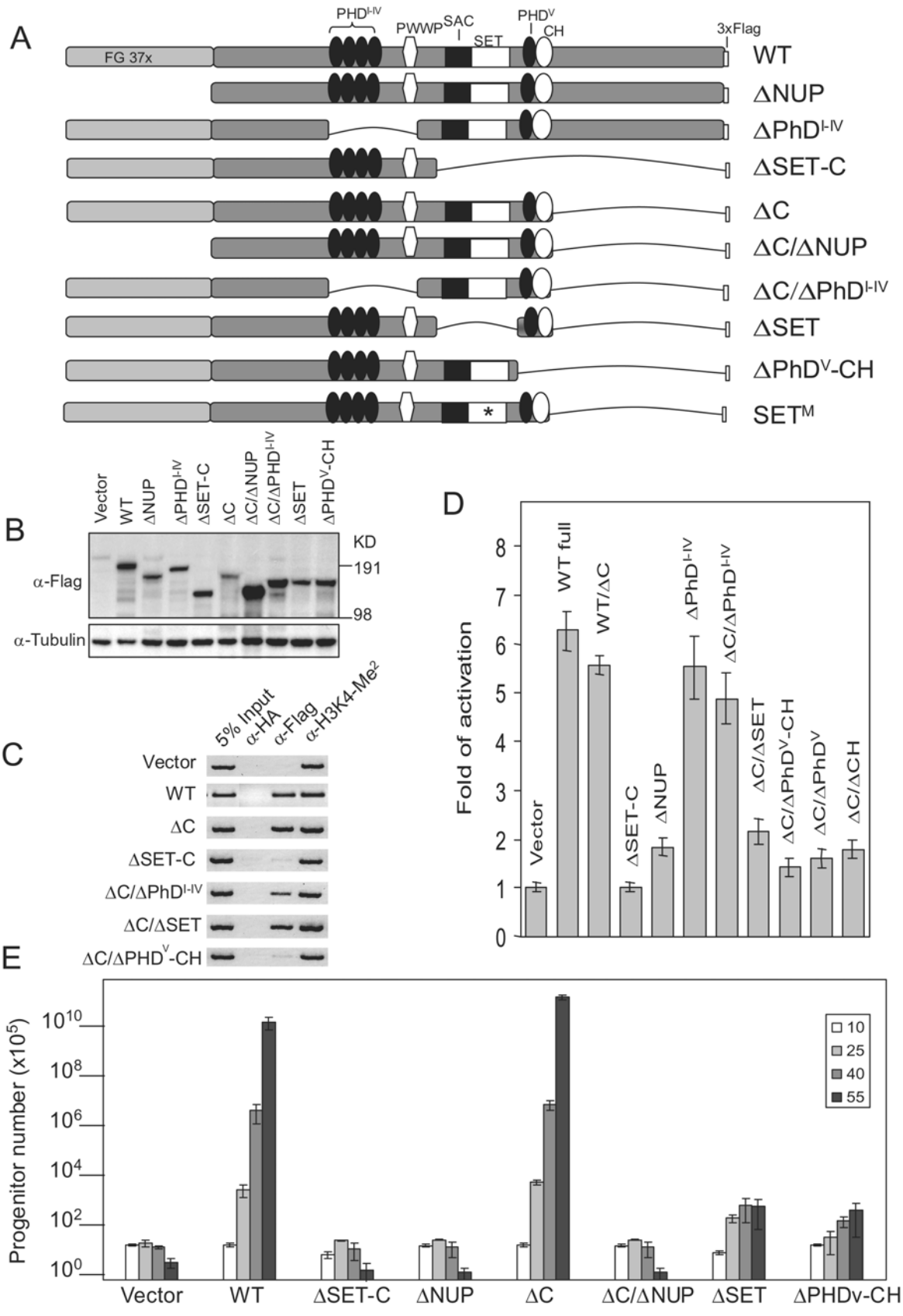
A
PHD I-IV
PWWP
SAC
SET
PHD V
CH
3xFlag
FG 37x
WT
ΔNUP
ΔPhD I-IV
ΔSET-C
ΔC
ΔC/ΔNUP
ΔC/ΔPhD I-IV
ΔSET
ΔPhD V-CH
SET M
B
Vector
WT
ΔNUP
ΔPHD I-IV
ΔSET-C
ΔC
ΔC/ΔNUP
ΔC/ΔPHD I-IV
ΔSET
ΔPHD V-CH
KD
191
98
α-Flag
α-Tubulin
C
5% Input
α-HA
α-Flag
α-H3K4-Me2
Vector
WT
ΔC
ΔSET-C
ΔC/ΔPhD I-IV
ΔC/ΔSET
ΔC/ΔPHD V-CH
D
Fold of activation
Vector
WT full
WT/ΔC
ΔSET-C
ΔNUP
ΔPhD I-IV
ΔC/ΔPhD I-IV
ΔC/ΔSET
ΔC/ΔPhD V-CH
ΔC/ΔPhD V
ΔC/ΔCH
E
Progenitor number (x10^5)
10
25
40
55
Vector
WT
ΔSET-C
ΔNUP
ΔC
ΔC/ΔNUP
ΔSET
ΔPHDv-CH

Figure 2.5. Point mutation within SET domain of NSD1 abolished the in vitro hematopoietic progenitor transformation and transactivation of endogenous *HoxA9* gene and *HoxA7*-promoter reporter.

(A) Point mutations were made in the single amino acid within the crucial region of NSD1.

(B) The effect of the single amino acid mutations in NSD1 SET domain on the transformation of hematopoietic progenitors *in vitro*.

(C) The effect of the single amino acid mutations in NSD1 SET domain on the tranactivation of endogenous *HoxA9* gene in hematopoietic progenitors.

(D) The effect of the single amino acid mutations in NSD1 SET domain on the tranactivation of a *HoxA7*-promoter reporter in HEK293 cells.

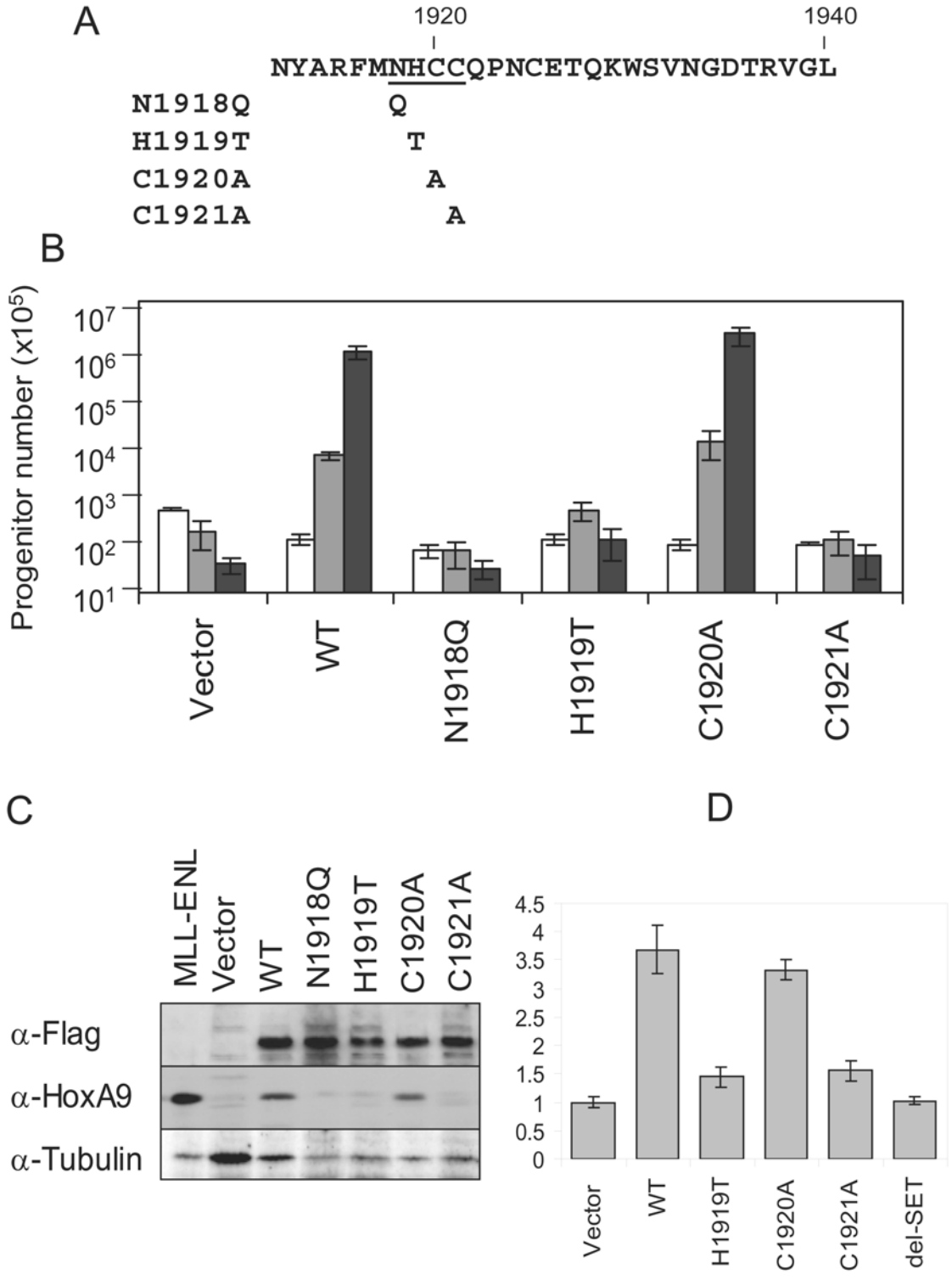
A
1920
1940
NYARFMNHCCQPNCETQKWSVNGDTRVGL
N1918Q
H1919T
C1920A
C1921A
B
Progenitor number (x10^5)
Vector
WT
N1918Q
H1919T
C1920A
C1921A
C
MLL-ENL
Vector
WT
N1918Q
H1919T
C1920A
C1921A
α-Flag
α-HoxA9
α-Tubulin
D
Vector
WT
H1919T
C1920A
C1921A
del-SET

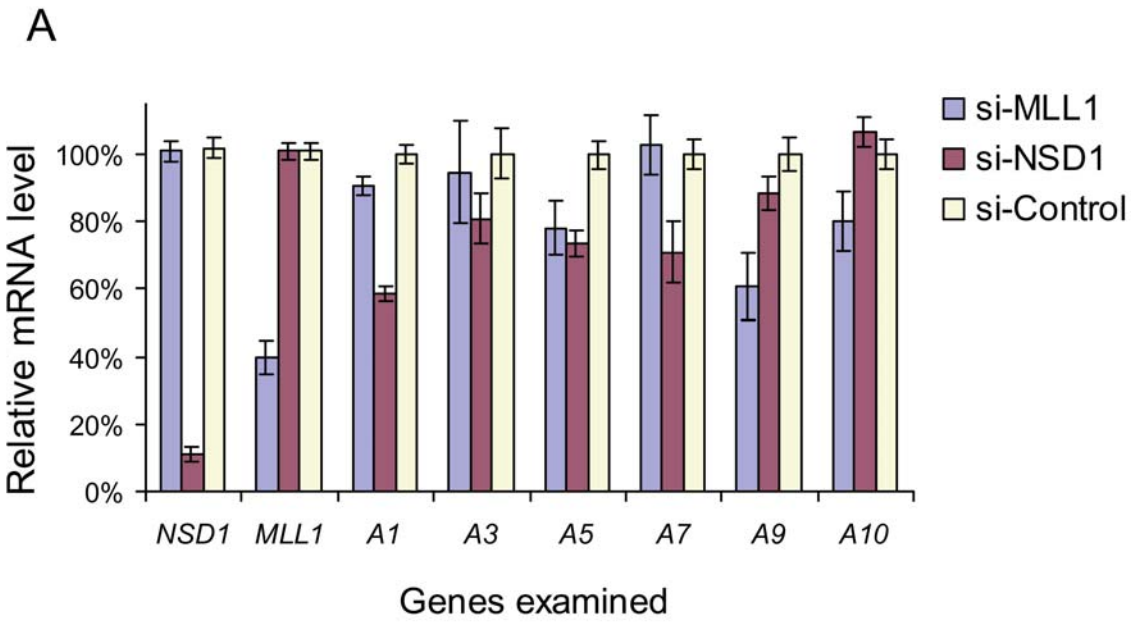

Figure 2.6. The knockdown of endogenous *NSD1* or *MLL1* in Hela cells affected the expression level of specific *Hox-A* genes. Real time RT-PCR analysis of the expression level of the *NSD1*, *MLL1* and *Hox-A* genes in Hela cells 48 hours after transfection of the siRNA against *NSD1*, *MLL1* or nonspecific control luciferase gene.

Table 2.1. The transcript intensities of the *Hox-A* locus genes among the progenitors immortalized by oncoproteins Meis1-plus-HoxA9, NUP98-NSD1, MLL-ENL and NUP98-HoxA9, revealed by Affymetrix array analysis.

Cells / Gene	**Meis1/A9**	**NUP98-NSD1**	**MLL-ENL**	**NUP98-HoxA9**
HoxA4	<40	<40	<40	<40
HoxA5	<40	480	280	730
HoxA7	<40	340	440	370
HoxA9	<40	3700	3600	3700
HoxA10	<40	550	550	250
HoxA11	<40	<40	<40	<40
HoxB3	<40	380	100	230
HoxB5	<40	270	150	120
HoxC6	<40	<40	<40	400
Meis1	<40	550	680	250

Table 2.2. The phenotypes of AML induced by NUP98-NSD1.

Mouse ID	WBC* 103/uL	Myeloid (%)[1]	Lymphoid (%)[2]	Hematocrit (%)	Spleen (mg)	Node (mg)	Thymus (mg)	Latency (days)
1	24.6	84	16	40.8	605	31	50	63
2	137	92	8	38.6	1300	20	66	65
3	160	16	84	18.1	616	18.3	111	65
4	137	77	23	43.1	495	25	27	147
5	113	70	30	42.3	685	51	41	147
6	17.9	76	24	42.9	280	20	32	132
7	112	98	2	30.2	661	40	40	160
8	14.9	51	48	29.3	450	15	30	200

Mouse	FACS of bone marrow (positive%)[3]					FACS of spleen (positive%)				
ID	MacI+	B220+	CD19+	CD34+	Flt3+	MacI+	B220+	CD19+	CD34+	Flt3+
1	82	21	1	37	73	N/D	N/D	N/D	N/D	N/D
2	70	28	2	64	51	69	19	1	65	75
3	62	28	2	82	87	68	24	10	64	80
4	82	12	1	58	41	73	18	10	44	22
5	83	6	1	32	60	84	10	10	16	21
6	60	65	0	70	80	50	44	23	43	40
7	81	4	1	25	30	70	8	8	18	16
8	76	8	1	64	20	64	14	10	55	12

*WBC, white blood cells in circulating peripheral blood (1000 per ul); [1]Percentage of myeloid lineage cells in circulating peripheral blood; [2]Percentage of lymphoid lineage cells in circulating peripheral blood; [3]Flow cytometry analysis of cells extracted from tissue of AML mouse using antigen specific antibodies such as Mac-I, B220, CD19, CD34 or Flt3 (CD115).

Supplementary Table 2.1. Identity of primers used in ChIP analysis of mouse 3' of *HoxA10* to 5' *of HoxA7* locus.

ID	Gene	Amplicon Size	Forward Primer Seq	Reverse Primer Seq
a	A10	509	CTTTGAGTTTCCATATCCCTGC	CCACGCACAGCAGCAATAC
b		465	TCCATTTTATCCTGTCCACCAC	GTGGCCTAGCGGAGGACC
c		517	GGGGAACACTAGGTGGGG	CCTAAATCACCGACCAGTTCTG
d		507	TCCACCTTTCTCTCGACAGCAC	AGCAACAAGGCCAGGATACCAG
e		500	ACTCTCAGTTGCCGCTGTTTC	TCGGGCGACACAGAACCTAG
f		517	GGGTCCTAACTCGGGCTTTG	CACAACACCTCATGCTCAACTG
g		510	TACAACTCATCCAAAAGAAAGCAG	GCAGGAAGAAGAAAGTGGTCAG
h		511	GCTTCCCAGCCCCTCTCTG	CTCCCTCCCTTCCTCTCTTTCC
I	A9	519	AAAGGGGAATGGGAAGGAAGGG	AGGCTCTCTCCACCTCAAACAG
j	A9	481	CACATCTCTGAGGACTGCAAGG	GCAGCTCCACGATCTGGTTTG
k	A9	500	AAACACCGGGCCATTAATAGCG	CGCCTGGGGATGCACGTAG
l	A9	502	CGCCGGACGGCAGGTATATG	GCAGCAGCCTCCTCCCTTTC
m	A9	482	CCCCGCCCCTCTCCTAAG	TTTTGCCAGCAAAGAAAAGAGC
n	A9	536	AGGACGGGAGAGAGGAGAAAGG	GGAGACAGAGGGAGACGGACAG
o		231	CTGCTCTTGGGCTACTGTAGATTTG	ACCTCACCTCAGCCCTCCC
p		508	TGGAACCAGCCGTAGTTGGG	CGAAGGTGGCTTAGCAGTGTAG
q		522	GCCTTAGCAACCGACAAGCC	AGGAACCTACGCTGCCGAG
r		536	CTCCCCAAGGATTCCCCAGG	GGCCGTAGGTGTTCATTCCC
s		522	GACCAGATGAACCCACAGAGAG	AGTAGCCTGAGAATGAATGGGG
t		500	AGGCGGCTAGTGTGTGGGATC	GCTGCTGCCAACCAGTGACTTC
u		502	GGCCTGGTGAAATGACTAGG	CACACACTATTGAGCCCAGAC
v		509	TAAGTAGGGAGCCAACAGTCAG	AAGGCTAGGAGATCAAAGAGGC
w		450	CCCCTCCCTGTTTCACCTCTTC	TGAACCCTTCCCCTAAACGCC
x	A7	513	CAGAGCCTTCACCCGACCTATC	GCGGCCCTGGCAGTTTCTC

Provided by Dr Yuki Okada and Dr. Yi Zhang at UNC/HHMI.

Cell, Vol. 121, 167–178, April 22, 2005. "hDOT1L Links Histone Methylation to Leukemogenesis".

Supplementary Figure 2.1. The phenotypic analysis of AML induced by NUP98-NSD1 in the bone marrow transplantation models.

Panel A: The typical size of spleen in the mice injected with progenitors expressed with empty retroviral vector (top) or in the mice developing AML after injection of progenitors expressed with NUP98-NSD1 retrovirus (bottom).
Panel B to E: H-E tissue staining exhibited that massive invasion and expansion of leukemia cells into spleen occurred in the mice injected with progenitors expressing NUP98-NSD1 (panel D-E), causing the disruption of normal follicle histological structure that was observed in the mice injected with progenitors expressed with empty vector (panel B-C).
Panel F: Facs analysis revealed an aberrant myeloid progenitor expansion stained as $Cd34^{+}$ $Flt3^{+}$ $c\text{-}Kit^{+}$ $MacI^{+}$ $CD19^{-}$ $B220^{-}$ $Thy1.2^{-}$ in the bone marrow extracted from AML induced by progenitors infected with NUP98-NSD1 retrovirus.
Panel G: Northern blot analysis with a probe against NSD1 (upper panel) revealed the expression level of retrovirus-encoded NUP98-NSD1 and endogenously expressed wildtype (wt) NSD1 in the Nalm-6 pre-B cell lines (lane 1), NIH-3T3 fibroblasts (lane 2), two parental progenitors (P1 and P2) infected with NUP98-NSD1 retrovirus (lane 3-4), leukemia cells exacted from bone marrow (B) or spleen (S) of the AML mice injected with P1 or P2 (lane 5-10), and two uninfected cultures of the Lin^{-} enriched bone marrow progenitors (lane 11-12). Bottom panel represents the agarose gel image of RNA samples extracted from the cells above before transfer onto the nitrocellulose membrane. The position of 28S and 18S RNA species as indicated.

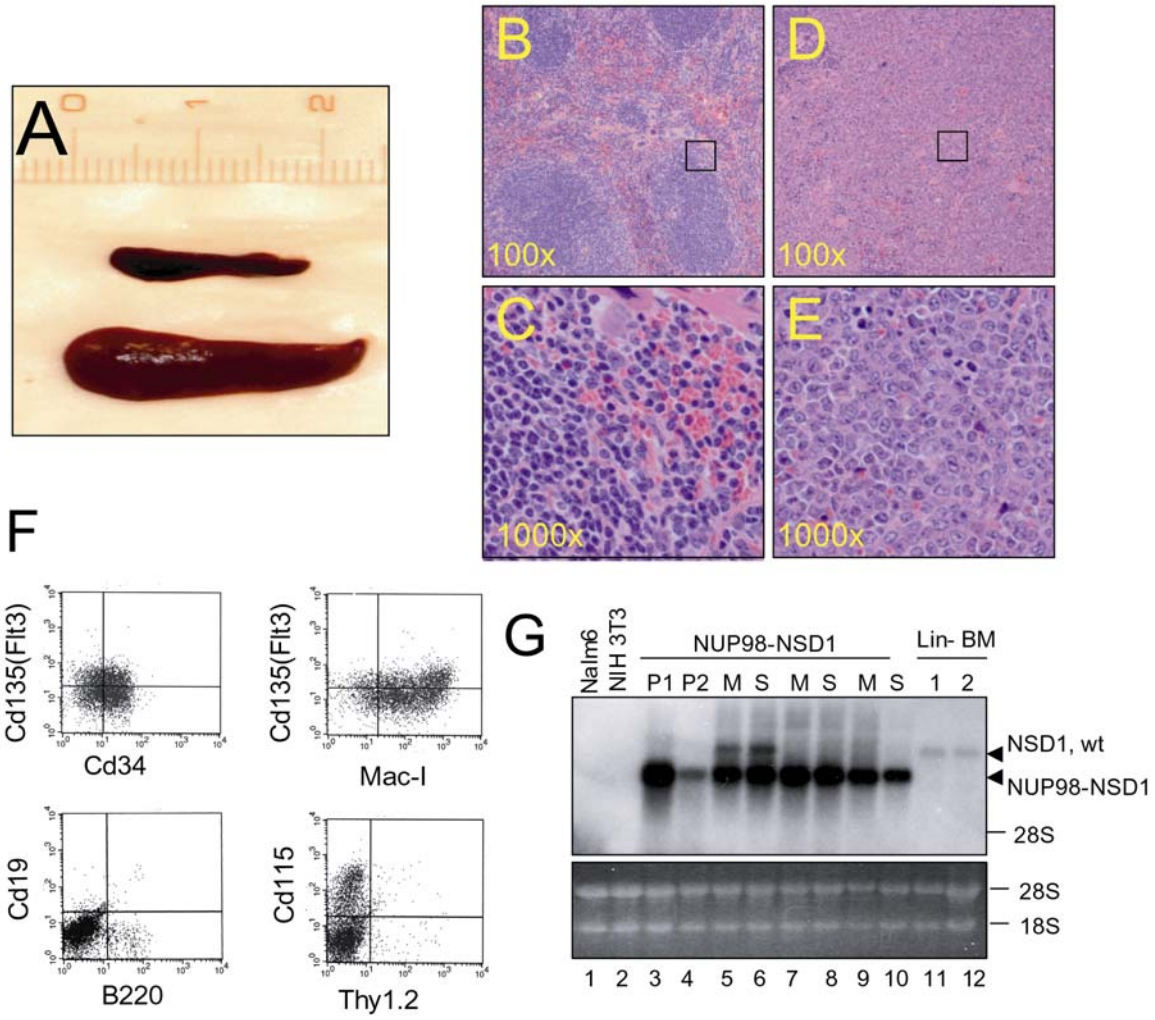
A
B
D
100x
100x
C
E
1000x
1000x
F
Cd135(Flt3)
Cd34
Cd135(Flt3)
Mac-I
Cd19
B220
Cd115
Thy1.2
G
Nalm6
NIH 3T3
NUP98-NSD1
P1 P2 M S M S M S
Lin- BM
1 2
NSD1, wt
NUP98-NSD1
28S
28S
18S
1 2 3 4 5 6 7 8 9 10 11 12

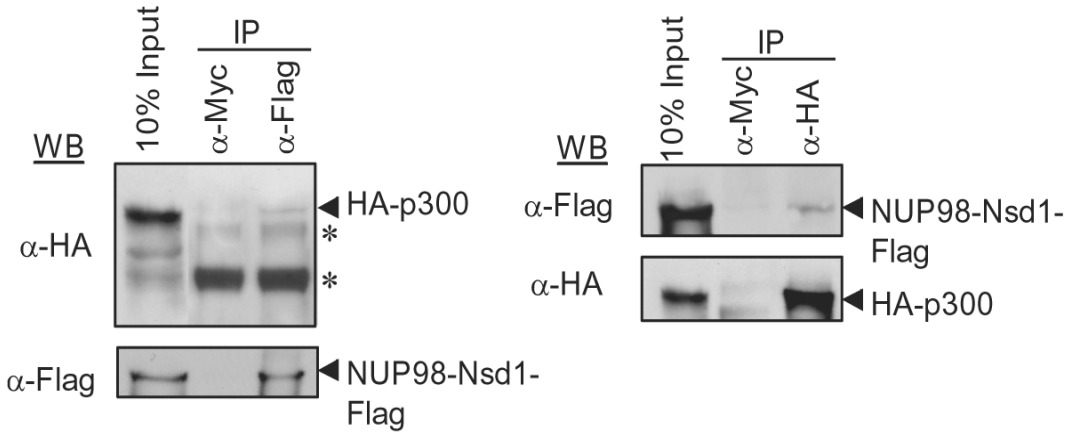

Supplementary Figure 2.2. Coimmunoprecipitation (CoIP) experiments revealed the interaction between Flag tagged NUP98-NSD1 and HA tagged p300 co-expressed in HEK293 cells.

Left panel: α-Flag and α-Myc antibodies were used for IP from total cell extract, followed by western blot using α-HA (upper panel) or α-Flag (bottom). The position of p300 and NUP98-NSD1 was indicated. Stars represent the nonspecific bands cross-reacted to antibody.
Right panel: α-HA and α-Myc antibodies were used for IP from total cell extract, followed by western blot using α-Flag (upper panel) or α-HA (bottom). The position of p300 and NUP98-NSD1 was indicated.

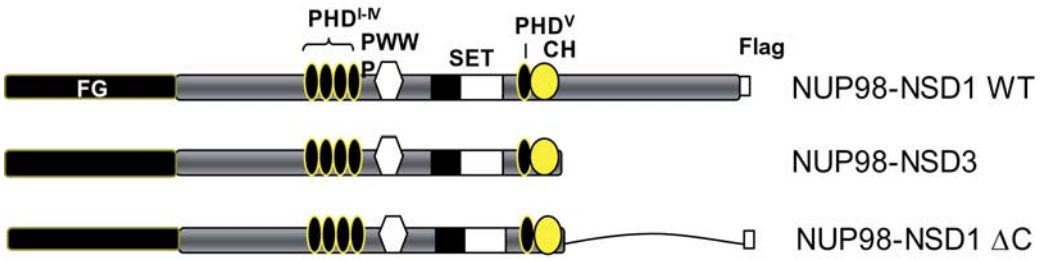

Supplementary Figure 2.3. Structural comparison between NUP98-NSD1 and NUP98-NSD3, both generated by chromosomal translocation in human AML. A Δ-C deletion form of NUP98-NSD1 was generated by deletion of an elongated C-terminus that is found in NSD3.

Chapter 3

Meis1 programs cancer stem cell characters and the transcription of a set of leukemia signature genes, using a mechanism that requires the interaction with Pbx cofactor, DNA binding and a novel function of C-terminal domain

ABSTRACT

Meis1 is a homeodomain transcription factor coexpressed with *HoxA9* in most human acute myeloid leukemias (AMLs). In mouse models of leukemia produced by HoxA9, Meis1 accelerates leukemogenesis. Because HoxA9 immortalizes myeloid progenitors in the absence of *Meis1* expression, the contribution of Meis1 toward leukemia remains unclear. Here, we describe a cultured progenitor model in which Meis1 programs leukemogenicity. Progenitors immortalized by HoxA9 in culture are myeloid-lineage restricted and only infrequently caused leukemia after more than 250 days. Coexpressed *Meis1* programmed rapid AML-initiating character, maintained multipotent progenitor potential, and induced expression of genes associated with short-term hematopoietic stem cells (HSCs), such as *FLT3* and *CD34*, whose expression also characterizes the leukemia-initiating stem cells of human AML. Meis1 leukemogenesis functions required binding to PBX cofactors, binding to DNA, and a conserved function of its *C*-terminal domain (CTD). We hypothesize that Meis1 is required for the homing and survival of leukemic progenitors within their hematopoietic niches, functions mediated by HSC-specific genes such as *CD34* and Fms-like tyrosine kinase 3 (*FLT3*). I also identified two conserved hydrophobic motifs in the Meis1 CTD that are required for upregulation of *FLT3* expression, generation of the FL-responsive immortalized progenitors *in vitro*, and induction of the AML *in vivo*. This is the first example of a transcription factor oncoprotein (Meis1) that establishes expression of a tyrosine kinase oncoprotein (FLT3), and explains their coexpression in human leukemia. This cultured progenitor model will be useful to define the genetic basis of leukemogenesis involving HoxA9 and Meis1.

Meis1 programs transcription of *FLT3* and cancer stem cell character, using a mechanism that requires interaction with Pbx and a novel function of the Meis1 *C*-terminus

Gang G. Wang, Martina P. Pasillas, and Mark P. Kamps

Meis1 is a homeodomain transcription factor coexpressed with Hoxa9 in most human acute myeloid leukemias (AMLs). In mouse models of leukemia produced by Hoxa9, Meis1 accelerates leukemogenesis. Because Hoxa9 immortalizes myeloid progenitors in the absence of Meis1 expression, the contribution of Meis1 toward leukemia remains unclear. Here, we describe a cultured progenitor model in which Meis1 programs leukemogenicity. Progenitors immortalized by Hoxa9 in culture are myeloid-lineage restricted and only infrequently caused leukemia after more than 250 days. Coexpressed Meis1 programmed rapid AML-initiating character, maintained multipotent progenitor potential, and induced expression of genes associated with short-term hematopoietic stem cells (HSCs), such as *FLT3* and *CD34*, whose expression also characterizes the leukemia-initiating stem cells of human AML. Meis1 leukemogenesis functions required binding to Pbx, binding to DNA, and a conserved function of its *C*-terminal tail. We hypothesize that Meis1 is required for the homing and survival of leukemic progenitors within their hematopoietic niches, functions mediated by HSC-specific genes such as *CD34* and Fms-like tyrosine kinase 3 (*FLT3*), respectively. This is the first example of a transcription factor oncoprotein (Meis1) that establishes expression of a tyrosine kinase oncoprotein (FLT3), and explains their coexpression in human leukemia. This cultured progenitor model will be useful to define the genetic basis of leukemogenesis involving Hoxa9 and Meis1. (Blood. 2005;106:254-264)

Introduction

Hoxa9 and Meis1 are homeodomain-containing transcription factors that control progenitor abundance in hematopoiesis and in leukemogenesis. In hematopoiesis, expression of *Hoxa9* and *Meis1* is high in $CD34^+$, Sca-1^+, lineage-negative (Lin^-) bone marrow populations that are enriched in hematopoietic stem cells (HSCs) and in lineage-committed progenitors (LCPs), and is downregulated coincident with transition to the $CD34^-$ stage of early progenitor differentiation.[1,2] Progenitor-specific expression of *Hoxa9* and *Meis1* is linked to positive maintenance of progenitor numbers. Mice harboring null mutation in *Hoxa9* have significant reductions in myeloid and pre–B cell progenitors, and they contain 5- to 10-fold reductions in their numbers of marrow HSCs.[2] Elimination of *Meis1* also results in strong reductions in numbers of myeloid, lymphoid, and multipotent progenitors.[3] By contrast, retroviral expression of Hoxa9 produces a 10-fold increase in the number of long-term repopulating HSCs (LT-HSCs), which is followed, inevitably, by development of myeloid leukemia.[4]

In murine and human leukemias, Hoxa9 and Meis1 function as dominant cooperating oncoproteins, yet the mechanism of cooperativity is unclear. In spontaneous acute myeloid leukemia (AML) arising in BXH2 mice, intracisternal particles activate transcription of *Meis1* in combination with either *Hoxa7* or *Hoxa9*.[5,6] The cooperating nature of *Meis1* and *Hoxa9* in leukemia was verified by using retrovirus to express these genes in primary bone marrow and then using the infected marrow cells to reconstitute the hematopoietic compartment of lethally irradiated mice. In this model, expression of Meis1 alone does not cause leukemia, expression of Hoxa9 eventually causes AML only after a long latency (20 weeks), and coexpression of Hoxa9 plus Meis1 yields rapid AML that emerges within 8 weeks.[7] While Hoxa9 and Meis1 can interact physically,[8] it is clear that each impacts at least partly distinct genetic pathways that yield different phenotypes. Retroviral expression of Hoxa9 alone blocks differentiation of granulocyte-macrophage colony-stimulating factor (GM-CSF)–dependent myeloid progenitors in the absence of coexpressed *Meis1*, *Meis2*, or *Meis3*; however, such progenitors are incapable of initiating leukemia in sublethally irradiated mice, suggesting that a second, Meis-dependent genetic response is required to program leukemia-initiating properties.[9] Expression of Meis1 in GM-CSF–dependent Hoxa9-immortalized myeloid progenitors induces responsiveness to stem cell factor (SCF) and suppresses neutrophil differentiation by G-CSF, yet these progenitor as well cannot initiate leukemia.[10] Thus, while Hoxa9 and Meis1 can deregulate facets of progenitor proliferation and differentiation, there is no cultured cell line model that correlates these properties with accelerated leukemogenesis, and the genetic mechanism through which Meis1 contributes to leukemia remains unclear and difficult to approach.

From the Department of Pathology and Molecular Pathology Program and Biomedical Sciences Graduate Program, School of Medicine, University of California at San Diego, La Jolla, CA.

Submitted December 7, 2004; accepted February 26, 2005. Prepublished online as *Blood* First Edition Paper, March 8, 2005; DOI 10.1182/blood-2004-12-4664.

Supported by Public Health Service grant NIH CA56876 to M.P.K.

The online version of the article contains a data supplement.

An Inside *Blood* analysis of this article appears at the front of this issue.

Reprints: Mark Kamps, Department of Pathology, UCSD Medical School, 9500 Gilman Drive, La Jolla, CA 92093; e-mail: mkamps@ucsd.edu.

The publication costs of this article were defrayed in part by page charge payment. Therefore, and solely to indicate this fact, this article is hereby marked "advertisement" in accordance with 18 U.S.C. section 1734.

Persistent expression of *Hoxa9* and *Meis1* is also proposed to mediate human leukemogenesis. *Hoxa9* and *Meis1* are expressed in more than 80% of human AML,[11,12] as well as in human acute lymphoid leukemias (ALLs) containing *MLL* chromosomal translocations. Evidence that Meis1 cooperates with Hoxa9 in establishing genetic changes underlying human leukemia was suggested by studies of the translocation protein mixed-lineage leukemia–eleven-nineteen leukemia (MLL-ENL). MLL normally controls *Hox* gene expression.[13] Chromosomal translocations produce MLL fusion proteins that have acquired persistent activation function, such as MLL-ENL. Both the human leukemias that express MLL-ENL and the cultured myeloid progenitors that are immortalized by retroviral MLL-ENL[14] exhibit robust expression of *Hoxa9* and *Meis1*, suggesting that MLL-ENL might immortalize progenitors through the functions of subordinate *Hoxa9* genes.[13] Consistent with this hypothesis, myeloid progenitors from *Hoxa9*$^{-/-}$ knockout mice cannot be immortalized by MLL-ENL, demonstrating that the endogenous *Hoxa9* gene mediates an important aspect of progenitor immortalization by MLL-ENL.[15] The human AML oncoprotein Nup98-Hoxa9 encodes a transcriptionally activated version of Hoxa9 and also sustains expression of endogenous *Hoxa9* and *Meis1* genes in cultured progenitors[16] that evoke rapid AML in mice.[17] Thus, human leukemias contain oncogenes that maintain the expression, and hence the transforming functions, of Hoxa9 and Meis1.

FLT3 ligand (FL) is a transmembrane protein produced by stromal cells of the hemopoietic compartment,[18] and plays an important role in the expansion of both normal and leukemic progenitors by activating the tyrosine protein kinase receptor FLT3. FLT3 expression is low in murine LT-HSCs[19] but present in human LT-HSCs,[20] and is up-regulated in short-term HSCs (ST-HSCs) and LCPs and down-regulated in the early stages of LCP differentiation.[19] Knockout mice reveal the importance of the FL-FLT3 interaction in vivo: *Flt3*$^{-/-}$ stem cells are deficient in lymphoid and myeloid reconstituting potential[21] and *FL*$^{-/-}$ mice display 10-fold reductions in common lymphoid progenitors[22] and reduced numbers of myeloid progenitors.[23] Virtually all human AMLs also express FLT3,[24] suggesting that leukemia cells use stromal cytokines to maintain viability and proliferation in the marrow. In AML, FLT3 signaling is activated by receptor mutations, such as FLT3–internal tandem duplication (ITD), in approximately one-third of AML, or by autocrine FL production.[25,26] The mechanism, by which FLT3 transcription is up-regulated transiently in normal hematopoiesis while persistently in leukemia, is undefined.

Here we develop a novel cultured cell model that demonstrates how Meis1 cooperates with Hoxa9 in programming cell phenotype and acute leukemic characteristics. Hoxa9-immortalized progenitors that were myeloid restricted exhibited a low degree of leukemic potential—only 1 of 9 mice acquired AML within 280 days of injection of progenitors immortalized by Hoxa9 alone. Meis1 cooperated with Hoxa9 to immortalize an earlier progenitor resembling the ST-HSCs that induced rapid AML in mice within 3 months, and these AML progenitors expressed *FLT3*, *CD34*, and *Itgb7*. Transcription of these same genes was induced by Meis1 in Hoxa9-immortalized progenitors. We propose that Meis1 endows progenitors with leukemia stem-cell character by activating transcription of genes that permit homing to, and proliferate within, hemopoietic microenvironments that produce FL.

Finally, we develop an assay in which cultivation in FL selects for leukemia-initiating FLT3^{+} progenitors coexpressing exogenous Hoxa9 and Meis1, and use this assay to define the essential biochemical domains of Meis1. In order to cooperate with Hoxa9 to maintain FLT3 expression and initiate AML, Meis1 required binding to Pbx and binding to DNA, as well as a unique function of sequences *C*-terminal to its homeodomain (HD). Together, these results suggest that *FLT3* transcription, expansion of normal ST-HSCs, and expansion of leukemia-initiating progenitors in vivo is regulated by Meis1-Pbx complexes.

Materials and methods

Infection and culture of primary hematopoietic cells

Helper-free retrovirus was prepared by cotransfection of retroviral expression vectors, together with an ecotropic murine leukemia virus (MuLV) packaging vector, into 293T cells, using calcium phosphate coprecipitation. Retroviral titers were calculated by enumerating G418-resistant colonies. $Sca^{+}Lin^{-}$ progenitors were enriched by negative selection against lineage markers (StemCell Technologies, Vancouver, BC, Canada) and cultured in OptiMEM base medium (contains 15% fetal bovine serum, penicillin, streptomycin, and glutamine) that was supplemented with 10 ng/mL of stem cell factor (SCF; from Chinese hamster ovary [CHO] producer cells), 5 ng/mL interleukin-3 (IL-3; Peprotech, Rocky Hill, NJ), and 5 ng/mL interleukin-6 (Peprotech) for 2 days. To examine the impact of Hoxa9 and Meis1 on the proliferation and differentiation of expanded progenitors, 1×10^5 progenitors were subjected to 1 round of spinoculation with 1 mL retrovirus supernatant (provirus titration: 10^5-10^6/mL) in a total volume of 1.25 mL, and plated in OptiMEM base medium (Gibco BRL, Carlsbad, CA) containing 10 ng/mL SCF (SCF media) plus 1 mg/mL G418 (for murine stem-cell virus (MSCV) Neo constructs) or 1 μg/mL puromycin (for MSCVPuro). After drug selection, expression of Hoxa9 and Meis1 was confirmed by Western blotting. Equivalent numbers of G418-resistant progenitors were plated in fresh SCF media for proliferation assays. In some cases, IL-7 (10 ng/mL from J558 cell supernatant) was also added to primary infections. To assess proliferation in FL, 2×10^5 progenitors were spin-infected and plated in OptiMEM base medium containing 5 ng/mL FL (Sigma, St Louis, MO) and 50μM of β-mercaptoethanol. One-half the media was changed every 3 days. Murine recombinant SCF and G-CSF were purchased from Peprotech. Flow cytometry was performed as described.[27] Cultures are initially polyclonal because infection of as few as 2×10^2 progenitors yielded outgrowths. Within 8 weeks of infection, all cultures evaluated (3 of 3) were monoclonal, likely due to the expansion of clones expressing optimal levels of Hoxa9 and Meis1, or of other cellular cofactors.

Leukemogenesis assay

A total of 1 to approximately 2×10^6 retrovirally transduced progenitors were introduced by tail-vein injection into sublethally irradiated (450 rads) 8- to 12-week-old female Balb/c mice as previously described.[28]

Meis1-induced FL responsiveness assay

SCF-dependent Hoxa9-immortalized progenitors were infected with provirus made from Mscv-puromycin vector encoding Flag-Meis1 or from empty vector as a negative control. After 2 days of selection with 2 ng/mL puromycin, 2×10^5 puromycin-resistant progenitors were transferred to media with 5 ng/mL FL as sole cytokine for 48 hours, and the number of live and dead cells were enumerated. Frequency of FL responsiveness is defined as the percentage of live cells in this 48 hour population. Acquisition of Wright-Giemsa stain image was achieved by using Olympus microscope digital camera system (model BX341, Olympus, Melville, NY) at total magnification 500 × (objective lens, 50 ×). The images were modified and assembled with Adobe Photoshop (San Jose, CA).

Electrophoretic mobility shift assay

Radiolabeled oligonucleotides containing a Pbx1-Meis consensus element (PCE: tcacggTGATTGACAGgcgactgctcgg; binding site capitalized) were

subject to electrophoretic mobility shift assay (EMSA) as described,[9] using 5 μL of Pbx1a and Meis1a produced by coupled transcription/translation.

Microarray analysis

Hybridization and quantitation of array signals were performed by the UCSD gene chip core laboratory (UCSD), using the GeneChip Scanner 3000, enabled for high-resolution scanning, coupled with GeneChip operating software (GCOS). Array data were normalized to internal controls, and the overall chip signal intensity was normalized to the mean signal intensity across the group of 6 chips (3 probed with RNA from Hoxa9-immortalized progenitors and 3 with RNA from Hoxa9/Meis1 progenitors). Data were analyzed using "perfect match minus mismatch" algorithms, and signature genes identified based on a minimum 4-fold difference in signal intensity between the averages of each group of 3 samples. Normalization and processing of GCOS data were performed using dCHIP software.

Semiquantitative polymerase chain reaction

cDNA from each sample of total RNA was synthesized using the Superscript reverse transcription kit (Invitrogen, Carlsbad, CA). Polymerase chain reaction (PCR) amplification of genes of interests was performed using primers for products spanning over at least one exon/intron boundary, using appropriate PCR conditions and serial 1:10 dilutions of input cDNA template. cDNA was normalized by PCR amplification of housekeeping gene *G3PDH*.

Description of plasmid construction and protocols followed for Northern and Southern blotting, immunoblotting, and immunoprecipitation are outlined in Supplemental Document S1, available on the *Blood* website; see the supplemental Document link at the top of the online article.

Results

Meis1 cooperates with Hoxa9 to immortalize a distinct target cell that exhibits rapid cell division and an early progenitor phenotype

To derive immortalized progenitors expressing Hoxa9 only or coexpressing Hoxa9 plus Meis1, Sca1$^+$/Lin$^-$-enriched marrow cells were infected with Hoxa9 or Meis1–internal ribosome entry site (IRES)–Hoxa9 retrovirus (Figure 1A) and cultured in medium containing SCF plus IL-7. The efficiency of retroviral transduction was approximately 25%, based on the efficiency of drug-resistant proliferation. Progenitors infected with the "empty" retroviral vector or with virus encoding Meis1 alone failed to become immortalized. The characteristics of SCF-dependent progenitors immortalized by Hoxa9 alone differed from those immortalized by Hoxa9 plus Meis1. Progenitors coexpressing Hoxa9 and Meis1 grew more rapidly (Figure 1B) and formed single layers across the bottom of culture flasks, while those immortalized by Hoxa9 grew as suspended cell clumps and exhibited fewer azurophilic granules (Figure 1C), suggesting that progenitors coexpressing Hoxa9 and Meis1 represented an earlier stage in differentiation. Fluorescence-activated cell-sorting (FACS) analysis confirmed that the 2 progenitor populations were different: progenitors immortalized by Hoxa9 alone were B220$^-$, CD19$^-$, with varying degrees Mac1$^+$ (high in Figure 1D, low in Figure 1F), whereas the vast majority of those immortalized by Hoxa9 plus Meis1 were Lin$^-$ and coexisted with a small population of Mac1^{variable} progenitors (Figure 1D). Retroviral integration analysis demonstrated that by 8 weeks after infection, these cultures became clonal (Figure 1E), suggesting that a dominant clone emerged rapidly. As consistent high levels of Hoxa9 and Meis1 are always observed in these immortalized cultures, it is likely that different retroviral integrations in clones express variable levels of Hoxa9 and Meis1, and that clones with the highest levels emerge. Identical populations were immortalized using medium containing SCF alone. Collectively, these results demonstrated that Hoxa9-immortalized progenitors are committed to myeloid differentiation, but that progenitors immortalized by coexpressed Meis1 plus Hoxa9 are not yet lineage-committed.

Progenitors immortalized by coexpression of Meis1 plus Hoxa9 induced acute myeloid leukemia, while those immortalized by Hoxa9 alone do not

Progenitors immortalized by Hoxa9 or by Hoxa9 plus Meis1 were introduced into sublethally irradiated syngenic recipients to determine their leukemic potential. Those immortalized by Hoxa9 plus

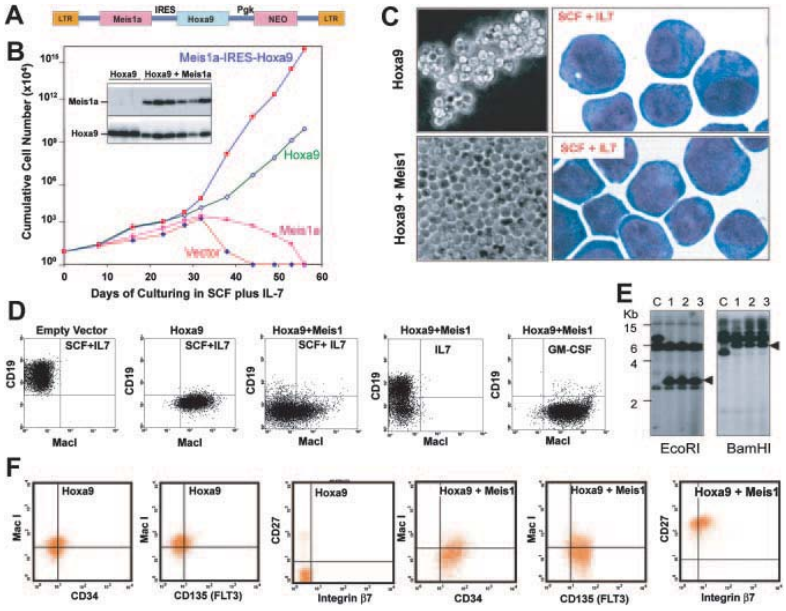

Figure 1. Meis1 coexpression with Hoxa9 immortalizes a distinct hematopoietic progenitor that exhibits multilineage differentiation potential and rapid monolayer proliferation. (A) MSCV retroviral vector used to achieve expression of Hoxa9 and Meis1a. LTR indicates long-term repeat, and NEO, neomycin-resistant gene. (B) Proliferation rates of Lin$^-$ marrow progenitors cultured in SCF and infected with empty MSCV, or MSCV encoding Hoxa9, Meis1, or Meis1 plus Hoxa9. The inserted blot shows expression of Meis1 (top) and Hoxa9 (bottom) by Western blot. (C) Morphology under phase-contrast microscopy (left) or following staining with Wright-Giemsa (right) of progenitors immortalized by Hoxa9 or by Hoxa9 plus Meis1. (D) Flow cytometric analysis of Lin$^-$ progenitors cultured in SCF plus IL-7 for 3 weeks following infection by empty vector (plot 1), Hoxa9 (plot 2), or Hoxa9 plus Meis1 (plots 3-5). Cells depicted in plots 4 and 5 were shifted from SCF into IL-7 or GM-CSF for 5 days prior to FACS analysis. (E) Monoclonality of progenitors immortalized by Hoxa9 and Meis1 depicted in panel D, demonstrated by analysis of retroviral integration using a Hoxa9 cDNA probe. Resolved on the gel are DNA from a different clone as a control (lane C), and from the same Hoxa9 plus Meis1-coexpressing cells grown in SCF, IL-7, or GM-CSF that were analyzed in Panel D (lanes 1-3, respectively). (F) FACS analysis demonstrating up-regulation of CD34, FLT3 (CD135), CD27, and integrin β7 on progenitors expressing Meis1.

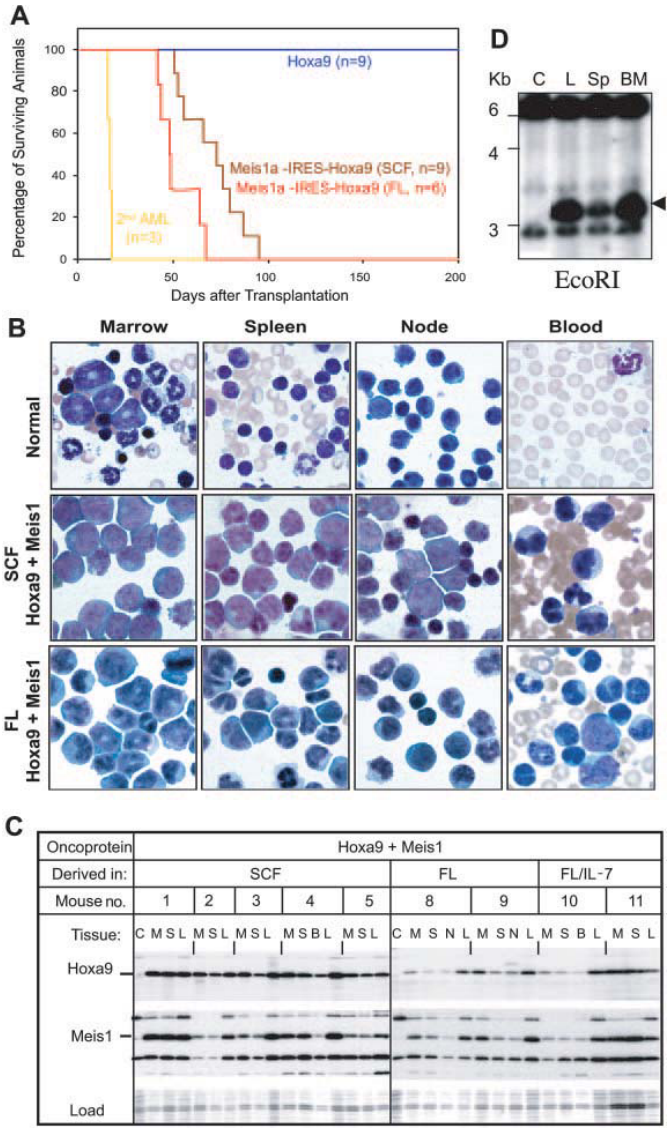

Figure 2. Progenitors immortalized by Hoxa9 plus Meis1 induce overt AML, while those immortalized by Hoxa9 do not. (A) Survival curve for cohorts of sublethally irradiated mice injected with 2 million progenitors immortalized by Hoxa9 or Hoxa9 plus Meis1 and derived in either SCF or FL. Three different Hoxa9-immortalized cell lines (3 mice each) compose the control cohort. Three different Hoxa9/Meis1 cell lines (3 mice each) compose the SCF cohort, and 2 different Hoxa9/Meis1 cell lines (3 mice each) compose the FL cohort. The secondary serial injection was performed using leukemic cells extracted from bone marrow of mice with AML induced by Hoxa9/Meis1 progenitors immortalized in SCF. (B) Comparison of the morphologies of hemopoietic cells in bone marrow, spleen, lymph node, or peripheral blood from normal mice and those bearing AML characterized in panel A. (C) Consistent expression of Hoxa9 and Meis1 in mice with AML induced by Hoxa9 plus Meis1-expressing cell lines, detected by immunoblotting with anti-Hoxa9 or anti-FLAG (for Meis1) antibodies. Cell lysates were derived from marrow (M), spleen (S), blood (B), and leukemic cell lines derived from AML spleen tissue (L). Hoxb8-immortalized progenitors (lane C) served as negative control. (D) Retroviral integration analysis by Southern blot. Genomic DNA was isolated from control cells (lane C), from injected progenitors (L), and from leukemic myeloblasts from the spleen (Sp) or bone marrow (BM) of mice injected with the immortalized progenitors. DNA was digested by *Eco*RI and probed with Hoxa9 cDNA.

Meis1a caused acute leukemia after 72 plus or minus 15 days (Figure 2A), with a characteristic presentation. Bone marrow averaged more than 85% $Mac1^+/B220^-$ blasts, spleens were enlarged 4-fold and contained more than 65% myeloid blasts, and an 18- to 43-fold increase in the levels of circulating myeloid cells was observed (myeloblasts, metamyelocytes, banded and segmented stages; Figure 2B, Table1). Progenitor cell lines immortalized by Hoxa9 exhibited only weak leukemogenicity, with only 1 of 9 mice acquiring AML within 280 days of injection. The length of time that progenitors spent in culture did not alter the outcome of their disease kinetics, with those cultured for 2, 6, or 12 weeks following infection with Meis1-IRES-Hoxa9 retrovirus yielding AML with kinetics that could be superimposed (data not shown). Leukemic cells from all tissue expressed Hoxa9 and Meis1 at an abundance comparable with the parental immortalized cell lines (Figure 2C), indicating that leukemic properties in vivo required the same level of Meis1 and Hoxa9 expression as was required for progenitor immortalization in culture. Injected progenitors contained the same retroviral integration as derivative leukemias (Figure 2D), verifying that leukemias arose from injected cell lines. Transfer of leukemic progenitors to secondary recipients produced AML with much shorter latency (average, 17 days; Figure 2A), suggesting that additional genetic events contribute to leukemias initiated by Hoxa9 plus Meis1. Leukemic blasts from primary or secondary AML were factor dependent. Collectively, these data demonstrate that there is a profound difference in the leukemogenic potential of cultured progenitors immortalized by Hoxa9 versus those immortalized by Hoxa9 plus Meis1.

Clonal progenitors immortalized by Hoxa9 plus Meis1 demonstrate multilineage differentiation potential and express FLT3 and IL-7 receptor

The fact that cultured progenitors immortalized by Hoxa9 plus Meis1 initiated AML, while those immortalized by Hoxa9 did not, led us to question whether each population exhibited differences in

Table 1. Representative characteristics of leukemias induced by populations of progenitors immortalized by Hoxa9

	Peripheral blood cell analysis*					Tissue mass, mg†			FACS analysis, % positive					
									Marrow			Spleen		
Mouse ID	WBC, $10^3/\mu L$	Mye, %	Lym, %	Plat, $10^3/\mu L$	Hemat, %	Spleen	Thy	Node	Macl	B220	Thy1.2	Macl	B220	Thy1.2
Hoxa9 plus Meis1 and SCF or SCF + IL-7														
Scf no. 1.1	91	91	7	370	40	138	14	6	88	3	1	62	6	12
Scf no. 1.2	91	86	13	405	46	450	29	19	94	2	1	73	11	14
Scf no. 2.1	76	97	3	627	35	365	35	14	84	5	1	72	10	9
Scf no. 2.2	68	88	12	331	40	236	27	15	96	4	1	66	16	20
Scf no. 3.1	140	91	9	771	26	350	32	17	72	5	0	74	9	10
Hoxa9 plus Meis1 and FL														
Fl no. 1.1	153	93	6	531	35	400	21	21	85	3	1	66	5	4
Fl no. 2.1	120	79	16	406	27	664	29	12	55	62	1	72	28	7
Fl no. 3.1	105	94	4	461	36	433	27	15	70	30	0	60	8	10
Fl no. 3.2	115	98	2	737	36	421	19	22	95	1	3	70	8	16

WBC indicates white blood cells; Mye, myeloid (principally progenitors in leukemic samples); Lym, B and T lymphocytes; Plat, platelets; Hemat, hematocrit; Thy, thymus; Node, average mass of each poplityl lymph node.

*Average values from 4 normal mice were as follows: WBC, $3 \times 10^3/\mu L$; myeloid progenitors, 25%; platelets, $817 \times 10^3/\mu L$; and hematocrit, 45%.

†Average values from 4 normal mice were as follows: spleen, 106 mg; thymus, 29 mg; and node, <1 mg.

proliferation or differentiation in response to cytokines in the marrow microenvironment that might explain their different behavior in vivo. Both groups of progenitors proliferated well in GM-CSF (Figure 3A-B). While Hoxa9 progenitors differentiated to neutrophils in SCF plus G-CSF or in G-CSF alone, those coexpressing Meis1 proliferated as myeloblasts in SCF plus G-CSF and failed to differentiate in G-CSF alone (Figure 3A-B). Thus, Meis1 suppresses differentiation initiated by G-CSF signaling. Strikingly, progenitors immortalized by Hoxa9 plus Meis1 proliferated in response to FL, as well as to IL-7, while those immortalized by Hoxa9 alone died within 24 hours when cultured in FL or in IL-7, kinetics identical to those obtained when these progenitors were cultured in no cytokine. Proliferation of clonal progenitors coexpressing Hoxa9 plus Meis1 in GM-CSF resulted in outgrowth of $MacI^+$ progenitors, while proliferation in IL-7 produced outgrowths of $CD19^+$ progenitors (Figure 1D). Both the myeloid-shifted and lymphoid-shifted populations contained the same single retroviral integration site as their monoclonal parents (Figure 1E; lane 1 vs lanes 2 and 3). Thus, in SCF, coexpression of Meis1a plus Hoxa9 established an early differentiation block that permitted progenitors to retain both myeloid and lymphoid differentiation potential upon stimulation by appropriate cytokines. This phenotype is similar to the murine ST-HSC, which expresses FLT3 and retains both lymphoid and myeloid reconstitution potential when cultured in SCF.[29]

Distinct responses to FL and IL-7 were attributable to unique expression of the FLT3 and IL-7 receptor in these progenitors (Figure 3C; Northern). Both the cell-surface, glycosylated form of FLT3 (upper

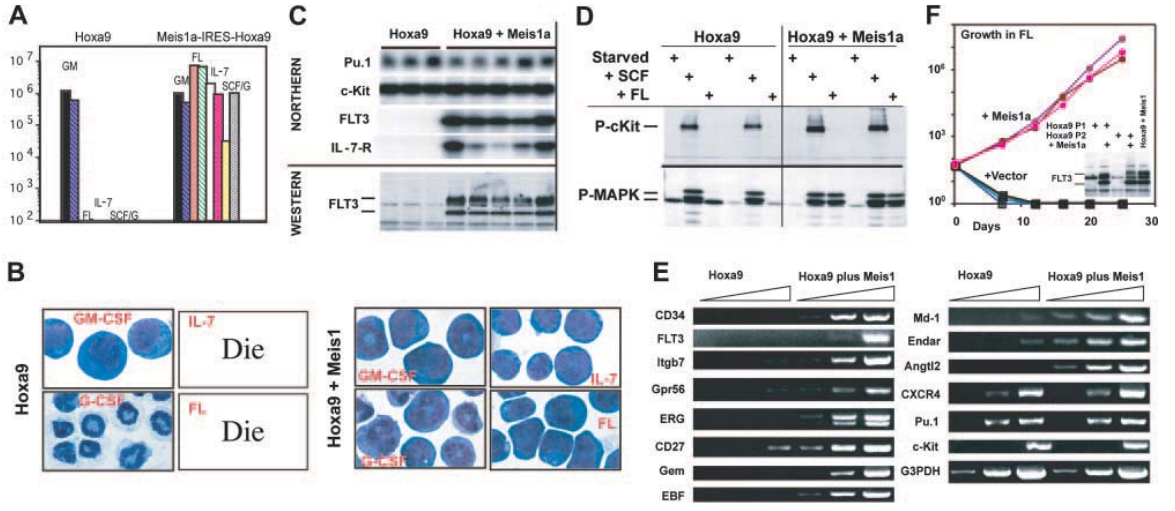

Figure 3. Meis1 induces FLT3 transcription and permits responsiveness to FL. (A-B) Proliferation of 2 progenitor lines immortalized by Hoxa9 and 2 progenitor lines immortalized by coexpressed Hoxa9 and Meis1, cultured in the presence of various cytokines (GM-CSF, FL, IL-7, or SCF plus GCSF). Cells were enumerated 7 days after plating in the indicated cytokines (A), and stained for morphology by Wright-Giemsa (B). (C) Northern blotting demonstrates expression of FLT3 and IL-7-R specifically in progenitors immortalized by coexpressed Hoxa9 plus Meis1, and immunoblotting demonstrates specific production of FLT3 in Hoxa9-immortalized progenitors that coexpress Meis1. (D) Immunoblot demonstrating that FL-induced MAP kinase (MAPK) phosphorylation is restricted to progenitors coexpressing Hoxa9 plus Meis1, while SCF induces receptor phosphorylation and MAP kinase phosphorylation in progenitors immortalized by Hoxa9 alone, as well as those immortalized by Hoxa9 plus Meis1. (E) Confirmation of microarray analysis by semiquantitative PCR, using 1:10 serial dilutions of cDNA as template. (F) Expression of Meis1 in 3 different Hoxa9-immortalized progenitor lines induces expression of FLT3 (inset) and robust proliferation in response to recombinant FL as the sole cytokine.

band) and the internal, unglycosylated form of FLT3 were evident exclusively in progenitors coexpressing Hoxa9 plus Meis1 (Figure 3C; Western). Signaling in response to FL was also found exclusively in progenitors coexpressing Hoxa9 plus Meis1, as reflected by the restricted activation of mitogen-activated protein (MAP) kinase by FL only in these cells (Figure 3D). Consistent with the SCF dependence of all cell lines, the SCF receptor *c-Kit* was expressed in all progenitors at levels unrelated to coexpressed Meis1 (Figure 3C).

Meis1 induces expression of the *FLT3* gene in Hoxa9-immortalized, SCF-dependent progenitors

There are 2 possible mechanisms by which Meis1 could maintain *FLT3* expression in a marrow-derived progenitor. First, Meis1 could activate *FLT3* transcription directly, through binding the *FLT3* promoter, or indirectly, by maintaining expression of other transcriptional activators within an activation cascade. Second, Meis1 could establish an earlier block to progenitor differentiation that prevents a cascade of transcriptional events resulting in down-regulation of the *FLT3* promoter. The second case postulates that Meis1 plays no role in activating *FLT3* transcription. If the first hypothesis were correct, Meis1 might be able to induce *FLT3* expression in Hoxa9-immortalized progenitors. But if the second hypothesis were correct, we would not expect Meis1 to reactivate *FLT3* transcription. Indeed, we found that retroviral expression of Meis1 in Hoxa9-immortalized, SCF-dependent progenitor cultures (5 of 5) induced high levels of FLT3 protein and enabled proliferation in FL as the sole cytokine (Figure 3F). Quantitative PCR analysis confirmed strong activation of FLT3 gene transcription in the Meis1-expressing derivatives. These Meis1-expressing progenitors also initiated rapid AML (70 days after injection in 4 of 4 mice; data not shown). Thus, Meis1 lies within a cascade that activates FLT3 transcription, and this function parallels the ability of Meis1 to produce AML-initiating progenitors. In leukemia, enforced transcription of Meis1 and consequential activation of FLT3 would promote survival of leukemic progenitors in stromal niches that express FL and would maintain responsiveness of myeloid progenitors to mutations that activate autocrine FL production or that activate FLT3 receptor function (eg, FLT3-ITD).

SCF-dependent progenitors immortalized by Hoxa9 plus Meis1 have a stem cell-like genomic signature

Analysis of Affymetrix mouse genome arrays (430 2.0 Array; Santa Clara, CA; display more than 39 000 transcripts, including more than 34 000 for characterized mouse genes) revealed 50 genes exhibiting more than 5-fold difference in expression level among 3 cell lines immortalized by Hoxa9 plus Meis1 versus 3 others immortalized by Hoxa9 alone. This analysis considered genes expressed as low as 1/30 that of *c-Myb* and one-third that of *Bmi-1* (Table 2). Among genes whose expression did not change significantly were those encoding cyclin A2 and cyclin B, which regulate G_1/S and G_2/M progression; those encoding transcription factors Bmi-1 and MLL, which control progenitor self-renewal; and those encoding receptors CD44 and CXC chemokine receptor 4 (CXCR4), which control homing of progenitors to the marrow through their interaction with hyaluronic acid and stromal cell-derived factor 1 (SDF-1).[30] Progenitors immortalized by Hoxa9 alone exhibited significant myeloid character (MPO^{high}, Prtn3^{high}, NB-1^{high}, NE^{high}, Csf2ra^{high}, and TFEC^{high}) and no evidence of nonmyeloid lineage-specific markers. Therefore, these immortalized progenitors are different—both in maturity and leukemic potential—from marrow progenitors freshly transduced with Hoxa9 retrovirus, which contribute to multilineage hematopoiesis and ultimately lead to leukemia. Progenitors immortalized by coexpressed Meis1 expressed fewer myeloid antigens (MPO^{high}, Prtn3^{high}, Csf2ra^{low}, TFEC^{low}, NB-1^{-}, NE^{-}) (genes listed in Table 2) and evidenced lymphoid antigens (MD-1^{high}, EBF^{+}, IL-7Rα^{high}). Strikingly, progenitors immortalized by Hoxa9 plus Meis1 expressed genes in addition to FLT3 that are indicative of ST-HSC (*CD34, CD27*, *ERG1*, *Gpr56*, *CRLR*, and *C1qR1*/*AA4.1*). Therefore, Hoxa9 progenitors represent a more mature myeloid cell, while Hoxa9 plus Meis1 progenitors express myeloid, lymphoid, and early stem-cell antigens. FACS analysis confirmed specific expression of FLT3, CD34, CD27, and integrin β7 (Figure 1F).

Distinct differences in transcription factor gene expression accompanied each overall genomic signature

Transcription factor genes *Tilz1b*, *ERG1*, *PLZF*, *Satb1*, and *RIP140* were expressed uniquely in progenitors immortalized by Hoxa9 plus Meis1, while *Tfec* was expressed uniquely in progenitors immortalized by Hoxa9 alone. Specific gene up-regulation, as detected by microarrays, was measured as more than 50-fold using semiquantitative PCR (Figure 3E).

FL-dependent immortalization represents a novel assay that detects Hoxa9 and Meis1 functions that produce leukemia-initiating progenitors

The exclusive ability of leukemia-initiating Hoxa9/Meis1 progenitors to proliferate in FL suggested they could be selected initially by cultivation of retrovirally infected progenitors in FL. This would represent a powerful assay for mapping physical domains and identifying associated biochemical functions that are required for Meis1 to cooperate with Hoxa9 in leukemogenesis. To test this possibility, Sca^{+}/Lin^{-} progenitors were infected by retrovirus encoding Neo, Hoxa9, Meis1a, or Hoxa9 plus Meis1a, and plated in culture medium supplemented with FL as the sole cytokine (Figure 4A). Cultures infected with retrovirus expressing Neo, Meis1, or Hoxa9 exhibited no proliferation, and evidenced a progressive differentiation and decline in viable cells. By contrast, progenitors infected by retrovirus coexpressing Hoxa9 plus Meis1 expanded as immortalized progenitors that expressed FLT3. Similar to progenitors derived in SCF plus IL-7, those derived in FL were mainly Lin^{-} but did coexpress Mac1 or B220 on subpopulations. Introduction of these FL-dependent immortalized progenitors into mice resulted in myeloid leukemia (Table 1) with kinetics similar to previous experiments using SCF-dependent progenitors (50 days; Figure 2A). Myeloid blasts from AML initiated by FL-dependent progenitors evidenced the same morphology, tissue tropism in vivo, and property of producing elevated levels of circulating progenitors as did the AMLs induced by cognate progenitors immortalized in SCF (Figure 2B; Table 1). Leukemic tissues expressed Hoxa9 and Meis1 (Figure 2C), and leukemias produced by progenitors immortalized in either SCF or in FL expressed FLT3 (Figure 4B). We conclude that the leukemia-initiating target cell immortalized by Hoxa9 plus Meis1 is selected effectively by growth in FL.

Meis1a requires binding to Pbx and DNA, as well as a novel function of its carboxyl terminus to immortalize FL-dependent progenitors and to produce leukemia-initiating progenitors

Next, we used both the FL-dependent and SCF-dependent immortalization assays to identify biochemical functions of Meis1

Table 2. Genomic signature of progenitors immortalized by Hoxa9 versus Hoxa9 plus Meis1

Gene	A9/M	A9	Δ no.	Genebank ID	Comments
Increased expression in Hoxa9 plus Meis1-immortalized progenitors					
Cd34	3600	A	> 50	NM_133654	Adhesion, homing, HSC marker
MD-1	3000	A	> 50	NM_010745	Lymphoid Toll coreceptor
Flt3	2167	A	> 50	NM_010229	Receptor tyrosine kinase, HSC marker
CD45-AP	1045	A	> 50	NM_016933	Activates CD45 tyrosine phosphatase
Itgb7	558	A	> 50	NM_013566	Integrin beta 7, homing
Kcna3	501	A	> 50	A1323624	Voltage gated K channel
Cd27	493	A	> 50	L24495	TNF receptor 7, HSC marker
*Erg1**	465	A	> 50	AB073078	Ets-related gene
Ngn	450	A	> 50	AK002933	Neurogranin
Ednra	373	A	> 50	BC008277	Endothelin receptor A, inhibits migration
IL7R	350	A	> 50	NM_008372	Interleukin 7 receptor
Gpr56	323	A	> 50	NM_018882	G protein coupled receptor, Enriched in HSCs
*CXXC5**	300	A	> 50	AK015150	Cystein methylation, transcription
Oaf	260	A	> 50	BC025514	Out at first, early development
*RIP140**	250	A	> 50	BB764550	Nuclear receptor corepressor
Tspan2	180	A	> 50	AV234585	Tetraspanin 2
CD244	142	A	> 50	NM_018729	NK cell receptor 2B4
Gem	103	A	> 50	U10551	Ras family GTPase, HSC enriched
*Ebf1**	59	A	> 50	NM_007897	Early B-cell factor
*PLZF**	50	A	> 50	AA419994	Promyelocytic leukemia zinc finger
*Meis**	47	A	> 50	NM_010789	Oncogene expressed by retrovirus
CRLR	463	18	26	AF209905	Calcitonin rec.-related, HSC marker
*Satb1**	1300	90	14	NM_009122	Nuclear matrix attachment, DNA-binding
*Tilz1b**	1506	175	9	AF201285	Leucine zipper transcription factor
C1qR1	3025	430	7	AF081789	Complement rec. AA4.1, HSC marker
Tmsb10	3200	500	6	NM_025284	Thymosin beta 10
Increased expression in Hoxa9-immortalized progenitors					
Slfn4	A	1963	> 50	AF099975	Schlafen 4, growth regulatory gene
Tnfsf13	A	977	> 50	NM_023517	TNF superfamily, member 13
TGFRb3	A	623	> 50	BM122301	Transforming growth factor rec.
Rnf128	A	493	> 50	NM_023270	Ring finger protein 128: E3 ligase
ABCa13	A	467	> 50	BB277120	ATP-binding cassette trans. A13
Rhol	A	393	> 50	AF309564	GTPase, cytoskeletal org.
NB-I	A	386	> 50	BC027283	NB-1 glycoprotein
Pde2a	A	230	> 50	BG069616	Phosphodiesterase 2a
TLR4	A	208	> 50	NM_021297	Toll-like receptor 4
B4Ga1T6	95	2070	22	BI685536	Galactosyl transferase
Hsd11b1	97	1122	12	NM_008288	Hydroxysteroid 11 beta dehydro 1
Tsp1	272	2747	10	AV026492	Thrombospondin-1, ECM protein
*Tfec**	317	3200	10	NM_031198	Myeloid Myc-related bHLH TF
Sortilin-1	31	311	10	NM_019972	Trafficking/sorting
ALAS1	437	3770	9	BC022110	Amino levulinic acid synthetase
Clecsf12	167	1500	9	AF262985	C-type lectin superfamily 12
Catns	20	158	8	NM_007615	p120 catenin
Csf2ra	161	1229	8	NM_009970	GM-CSF receptor, alpha chain
Bscl2	80	602	8	BB223872	Fat metabolism
DORA	230	1673	7	NM_030691	Ig superfamily, member 6
Ms4a3	843	5533	7	NM_133246	Hematospecific membrane protein
Akr1cl3	127	782	6	BC021937	Aldol Keto reductase c13
NE	1333	7800	6	NM_015779	Neutrophil elastase
Atip1	73	402	6	AW554551	Inhibits tyrosine kinases
Gda	620	2820	5	AF174583	Guanine deaminase
Gng31g	118	603	5	BB223872	G protein gamma 3 linked
Controls					
Cyclin A2	1180	1470	—	NM_009829	Binds cdk2, G_1/S cell cycle regulation
Cyclin B	670	657	—	X58708	Binds cdk1, G_2/M cell cycle regulation
Mpo	10750	9300	—	NM_010824	Myeloperoxidase
Myb	4900	4800	—	NM_033597	Hematopoietic transcription factor
Bmi-1	257	343	—	M64279	Maintains HSC self-renewal
Mll	96	88	—	AK017541	Histone methyltransferase
Prtn3	7000	8030	—	NM_011178	Myeloblastin, pre-pro-proteinase 3

Hematopoietic stem cell markers are underlined. — indicates no significant change.
*Transcription factor genes.

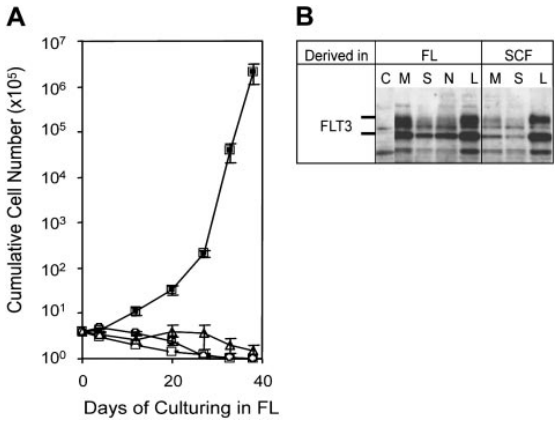

Figure 4. A simple FL-dependent proliferation and immortalization cell system can evaluate cooperation between Meis1 and Hoxa9. (A) Growth curve of progenitors cultured in FL following infection with empty vector (△), Hoxa9 (□), Meis1 (○), or Meis1 plus Hoxa9 (■). Error bar indicates standard deviation of data from 3 repeated experiments. (B) Anti-FLT3 immunoblot demonstrating strong FLT3 expression in representative leukemias arising from Hoxa9/Meis1-immortalized progenitors derived in either SCF or FL. Immunoblots were performed on cell extracts from a control cell line (C), from the bone marrow (M), spleen (S), and lymph nodes (N) of leukemic mice, and from cultured leukemic blasts from splenic tissue (L).

required for expansion of FLT3-expressing, leukemia-initiating progenitors (Diagram of mutations in Figure 5A,C). Each mutant form of Meis1 was tested for its ability to bind Pbx1a in the absence of DNA (Figure 5B), to heterodimerize with Pbx1a on DNA (Figure 5D), to immortalize FL-dependent progenitors (Figure 5F-G), and to cause leukemia in vivo (Figure 5H). Expression of Meis1 mutants and coexpressed Hoxa9 was verified by Western blot using the SCF-dependent progenitors after G418 selection following retroviral infection (Figure 5E). Two regions of Meis1 preceding the homeodomain were dispensable for proliferation in FL: the first 64 residues (Meis1Δ1-64), and residues 202-260, which reside between the M2 motif and the homeodomain (Meis1Δ202-260). Meis1Δ1-64 also retained its ability to cause rapid AML (Figure 5H; Meis1Δ202-260 not tested). Both these deletion mutants preserved the ability of Meis1 to bind DNA and heterodimerize with Pbx (Figure 5B,D).

Meis1 required binding to Pbx and to DNA to cause FL-dependent proliferation and AML. Meis1 required active DNA-binding. Two homeodomain mutations, Meis1-HD^{N51S} or a more dramatic HD mutant, Meis1-HD$^{N51S/RRR53-55AEE}$, did not alter interaction with Pbx in the absence of DNA (Figure 5B, lane 10 vs lane 4) but strongly suppressed DNA binding by Meis1-Pbx heterodimers (Figure 5D, lanes 8-9 vs lane 4) and precluded FL-dependent immortalization. The SCF-dependent progenitors that arose through the function of coexpressed Hoxa9 expressed Meis1^{N51S} efficiently (Figure 5E, lane 11) yet did not produce AML (Figure 5H). Interaction with Pbx was also essential. Deletion of the M1 and M2 motifs, which were previously shown to bind Pbx (Meis1Δ64−202; Figure 5B,D, lane 6), destroyed FL-dependent proliferation and leukemic function despite the fact that this deletion protein was expressed at high levels (Figure 5E, lane 6). The specific requirement for binding Pbx was further investigated by site-direct mutagenesis of the M1 and M2 leucine-zipper–like regions. Changing 3 or 4 residues in either the M1 or M2 helices was generally insufficient to disrupt interaction with Pbx or FL-dependent proliferation (M1ΔLFPLL or M2ΔLLEL; Figure 5D, lane 13; Figure 5G), while combining both M1 and M2 mutations within a single Meis1 protein (M1ΔLFPLL/M2ΔLLEL) or extending the disrupted helical interactions provided by a single M motif (M2ΔLRF/ΔLLEL or M2ΔIQVL/ΔLLEL) completely destroyed interaction with Pbx (Figure 5B,D), destroyed FL-dependent proliferation, and prevented leukemogenesis (Figure 5H) without altering Meis1 expression (Figure 5E, lane 15 vs lane 4).

The Meis1a *C*-terminal domain, composed of 49 residues downstream of the homeodomain, possessed an essential Meis1a leukemogenesis function independent of DNA binding or interaction with Pbx. This region contains 3 reiterated motifs that are highly conserved in Meis1, Meis2, and Meis3, but are not found in Prep1, a less-related family member (Figure 5C). Premature termination mutations were engineered to eliminate 1 (Meis1a^{370T}), 2 (Meis1a^{357T}), or all 3 (Meis1a^{341T}) of these conserved motifs. Meis1a^{370T} retained its ability to immortalize FL-dependent progenitors that caused rapid AML (Figure 5H). By contrast, Meis1a^{357T} and Meis1a^{341T}, despite exhibiting a wild-type ability to heterodimerize with Pbx in the presence of DNA (Figure 5D, lanes 11-12) and in the absence of DNA (Figure 5B, lanes 13-14), were incapable of immortalizing FL-dependent progenitors. Consistent with this observation, SCF-dependent progenitors that were immortalized by coexpressed Hoxa9 expressed Meis1^{341T} efficiently (Figure 5E), yet failed to cause AML (Figure 5H).

Collectively, this mutational analysis demonstrates that Meis1 must bind DNA and interact with Pbx, and that Meis1 uses a yet-undefined function of its conserved *C*-terminus to maintain FLT3 expression and to establish the leukemic phenotype. This analysis also demonstrated an invariant link between the ability to immortalize FL-dependent progenitors and the ability to establish the leukemia-initiating phenotype.

Discussion

Here we present evidence that Meis1 activates expression of the myeloid proto-oncogene *FLT3*, that Meis1 has the general property of up-regulating genes characteristic of ST-HSCs, and that Meis1 confers an AML-initiating phenotype upon nonleukemic Hoxa9-immortalized progenitors. How might Meis1 establish the characteristics of a leukemia-initiating cell? Subpopulations of cancer cells in human leukemia and solid tumors that initiate cancer in xenografted nonobese diabetic–severe combined immunodeficient (NOD-SCID) mice are denoted cancer stem cells. In culture, they are similar to their nontumorigenic counterparts in terms of their proliferation and apoptotic indices; however, they express distinctive surface antigens, such as CD44 in breast cancer[31] or CD34 in both multiple myeloma and in AML.[32] In the case of human AML, only CD34$^+$ normal human progenitors migrate rapidly to bone marrow,[33] and all human progenitors that initiate AML in NOD-SCID mice are restricted to CD34$^+$ blasts.[32] CD34 promotes homing[34] and inhibits differentiation.[35] The behavior of Meis1 is similar to that defined for a cancer stem cell gene because on a cellular level it directs development of AML in vivo, yet it is unnecessary for myeloblast proliferation in culture, and on a genetic level it induces expression of CD34 and FLT3, which are present on human AML-initiating progenitors. Three Meis1 effects we observe in cultured progenitors could establish leukemic stem cell characteristics in vivo—suppressing the differentiation in response to maturation cytokines such as G-CSF, establishing responsiveness to cytokines (FL, IL-7, and CD27 ligand, aka tumor necrosis factor [TNF] superfamily member 7), and promoting interactions within hematopoietic microenvironments through homing and adhesion proteins (CD34, integrin β7, and C1qR1 [AA4.1]).

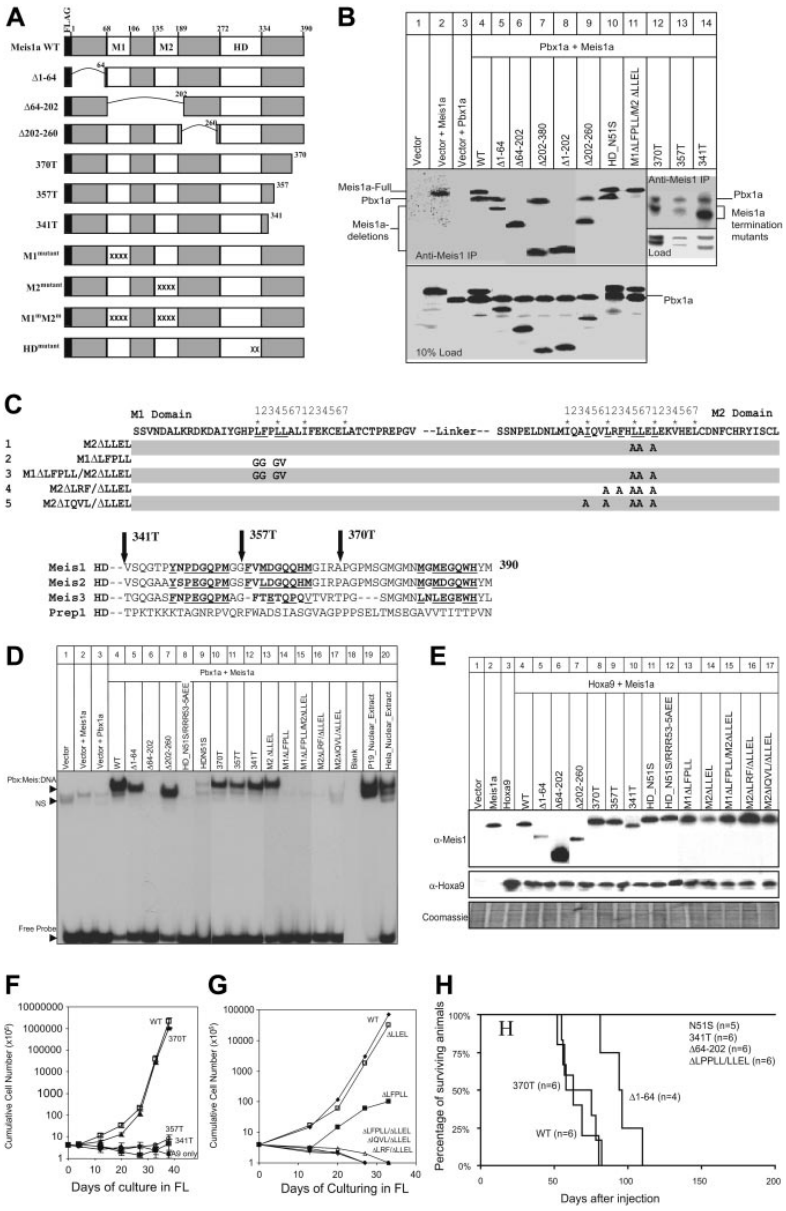

Figure 5. The ability of Meis1 to promote FL-dependent proliferation correlates precisely with its ability to induce leukemogenesis. (A) Location of Meis1 mutations. Point mutations are shown in panel C. (B) Interaction between Meis1a and Pbx1a in the absence of DNA, demonstrated by coimmunoprecipitation. (C) Top panel shows designation of point mutant of Meis1 within the M1 and M2 alpha helices. An asterisk indicates the position of leucine or isoleucine. Bottom panel shows *C*-terminal sequences of Meis1, Meis2, Meis3, and Prep1 that lie downstream of homeodomain. The 3 repeated motifs are underlined. (D) Interaction between Meis1a and Pbx1a on DNA, demonstrated by EMSA. (E) Expression of Meis1 and Hoxa9 in primary Lin$^-$ marrow cells following retroviral infection and selection for G418 resistance. (F) FL-dependent proliferation demonstrating the requirement for *C*-terminal residues upstream of amino acid position 370. (G) FL-dependent proliferation demonstrating the importance of interaction with Pbx. Error bars in panels F and G indicate standard deviation of data from repeated experiments. (H) The ability of Meis1 to cooperate with Hoxa9 to cause AML correlates precisely with its ability to evoke FL-dependent proliferation.

Responsiveness to FL would further augment responsiveness to SCF,[21] although recent studies suggest that human AML blasts capable of providing long-term engraftment in NOD-SCID mice do not express cell-surface c-Kit, reiterating the central importance of FLT3.[36] We have functional data for each of these proposed functions for Meis1 with the exception of engraftment potential.

We propose that while the SCF-dependent cell lines generated by Hoxa9 and Meis1 in culture may not perfectly reflect any particular normal hematopoietic progenitor within freshly isolated marrow, they nevertheless model normal functions of Hoxa9 and Meis1 within native HSCs and LCPs (Table 3). In the mouse, both *FLT3*[19,37] and *CD34*[20] are expressed at low levels in quiescent stem cells, up-regulated in activated ST-HSCs and early LCPs, and down-regulated during differentiation, a transcriptional pattern similar to that of *Meis1*.[1] This temporal coregulation is also consistent with the proposal that transcription of *FLT3* and *CD34* during normal hematopoiesis is also regulated by Meis1 and suggests that *Meis1*$^{-/-}$ mice contain lower numbers of ST-HSCs and LCPs because these cells express lower levels of FLT3 or may interact with their hematopoietic niches less efficiently due to altered expression of adhesion molecules.

An ability of Meis1 to activate transcription of *FLT3* in AML would explain the association of *FLT3* expression with expression of *Hoxa9* and *Meis1* in myeloid and lymphoid leukemias containing MLL translocation[38,39] and would exemplify a novel form of oncoprotein cooperation in which a transcription factor oncoprotein (Meis1) enforces expression of a tyrosine kinase oncoprotein (FLT3-ITD). It would also imply that in human AML, mutations up-regulating *MEIS1* and *HOXA9* transcription precede mutations that activate signaling of the FLT3 receptor,

Table 3. Proposed functions for Hoxa9 and Meis1 in normal HSP and LCP, based on the function of Hoxa9 in immortalized SCF-dependent myeloid progenitor cell lines, and of Meis1 in the Meis1/Hoxa9-immortalized myeloid-lymphoid progenitors that express unique ST-HSC genes

Function in SCF-dependent progenitor cell lines	Proposed function in HSP and LCP in vivo
Hoxa9	
Maintains genetic program specifying self-renewal	Positively regulates self-renewal
Meis1	
Stimulates proliferation	Positively regulates proliferation
Prevents differentiation by G-CSF	Suppresses premature differentiation by lineage-specific cytokines
Induces expression of FLT3, IL-7R, CD27	Positively regulates proliferation/differentiation response by controlling the abundance of receptors for cytokines
Induces expression of CD34, Itgβ7, C1qR1	Regulates homing and migration by controlling the levels of proteins that bind sugars and extracellular matrix proteins

such as FLT3-ITD[25] or autocrine expression of FL.[26,39] From a therapeutic standpoint, the observation that Meis1 activates *FLT3* transcription makes FLT3 an exceptional drug target in AML because it should be expressed on the surface of all Meis1-expressing leukemia-initiating cells.

We hypothesize that the ability of Meis1 to program ST-HSC properties requires additional cooperating factors in immature hematopoietic progenitors, and that maturation cytokines can down-regulate these factors, promoting differentiation of the ST-HSCs within lineage-specific pathways. This is suggested by a number of observations. First, when Meis1 was expressed in Hoxa9 progenitors, only 5% to 30% of each population exhibited FL-dependent proliferation, despite the fact that all progenitor populations expressed high levels of Meis1 on immunoblots (data not shown). This suggests that only a subset of SCF-dependent Hoxa9 progenitors retained transcription of essential cofactor genes. Second, we found that Meis1 has no ability to induce either *FLT3* expression or a leukemic phenotype in Hoxa9-immortalized progenitors cultured in GM-CSF, suggesting that maturation cytokines down-regulate transcription of factors that cooperate with Meis1 (K. R. Calvo, M.P.K., unpublished observations, May 2002). Based on our genomic analysis, cooperating transcription factors could include promyelocytic leukemia zinc finger (PLZF), receptor-interacting protein 140 (Rip140), special AT-rich sequence-binding protein 1 (Satb1), TSC22-related inducible leucine zipper 1b (Tilz1b), and CXXC finger 5 (CXXC5), which are invariantly coexpressed with Meis1. The argument that only a subset of cytokine signaling is compatible with Meis1-mediated leukemogenic function is also supported by the subsets of activated receptors that complement Meis1 function in human AML—FLT3 activation is frequent,[25,26] G-CSFR activation is exceptionally rare,[40] and GM-CSFR activation has never been observed.

The FL- and SCF-dependent progenitor immortalization systems described herein should provide a simple, useful tool for establishing the biochemical and genetic basis of leukemogenesis by Hoxa9 and Meis1, for identifying the important genetic targets required for leukemic stem cell behavior, and for determining the nature of the permissive transcriptional context provided by FL and SCF signaling. It is possible that analysis of oncoprotein domains required for leukemic function within this cell culture system could yield results somewhat different from those based on freshly transduced marrow progenitors in reconstituted irradiated mice, because in mice expression of all mutants of Meis1 or Hoxa9 are retained in LT-HSCs that engraft. Partially active Meis1 or Hoxa9 mutants could produce less aggressive leukemias with slower kinetics or could expand a progenitor pool that becomes susceptible to mutations that cause AML by mechanisms unrelated to the mutant Hoxa9 or Meis1 protein. In our assay, the wild-type functions of Hoxa9 and Meis1 provide the only selection determinants, and mutants with partial transforming function are likely to go undetected. Therefore, the cell culture assay we describe is likely to have a more stringent requirement for retention of transformation-related properties of Hoxa9 and Meis1.

References

1. Pineault N, Helgason CD, Lawrence HJ, Humphries RK. Differential expression of Hox, Meis1, and Pbx1 genes in primitive cells throughout murine hematopoietic ontogeny. Exp Hematol. 2002;30:49-57.
2. Lawrence HJ, Helgason CD, Sauvageau G, et al. Mice bearing a targeted interruption of the homeobox gene HOXA9 have defects in myeloid, erythroid, and lymphoid hematopoiesis. Blood. 1997;89:1922-1930.
3. Hisa T, Spence SE, Rachel RA, et al. Hematopoietic, angiogenic and eye defects in Meis1 mutant animals. Embo J. 2004;23:450-459.
4. Thorsteinsdottir U, Mamo A, Kroon E, et al. Overexpression of the myeloid leukemia-associated Hoxa9 gene in bone marrow cells induces stem cell expansion. Blood. 2002;99:121-129.
5. Moskow JJ, Bullrich F, Huebner K, Daar IO, Buchberg AM. Meis1, a PBX1-related homeobox gene involved in myeloid leukemia in BXH-2 mice. Mol Cell Biol. 1995;15:5434-5443.
6. Nakamura T, Largaespada DA, Shaughnessy JD, Jr., Jenkins NA, Copeland NG. Cooperative activation of Hoxa and Pbx1-related genes in murine myeloid leukaemias. Nat Genet. 1996;12:149-153.
7. Kroon E, Krosl J, Thorsteinsdottir U, Baban S, Buchberg AM, Sauvageau G. Hoxa9 transforms primary bone marrow cells through specific collaboration with Meis1a but not Pbx1b. Embo J. 1998;17:3714-3725.
8. Shen WF, Montgomery JC, Rozenfeld S, et al. AbdB-like Hox proteins stabilize DNA binding by the Meis1 homeodomain proteins. Mol Cell Biol. 1997;17:6448-6458.
9. Calvo KR, Sykes DB, Pasillas M, Kamps MP. Hoxa9 immortalizes a granulocyte-macrophage colony-stimulating factor-dependent promyelocyte capable of biphenotypic differentiation to neutrophils or macrophages, independent of enforced meis expression. Mol Cell Biol. 2000;20:3274-3285.
10. Calvo KR, Knoepfler PS, Sykes DB, Pasillas MP, Kamps MP. Meis1a suppresses differentiation by G-CSF and promotes proliferation by SCF: Potential mechanisms of cooperativity with Hoxa9 in myeloid leukemia. Proc Natl Acad Sci U S A. 2001;98:13120-13125.
11. Kawagoe H, Humphries RK, Blair A, Sutherland HJ, Hogge DE. Expression of HOX genes, HOX cofactors, and MLL in phenotypically and functionally defined subpopulations of leukemic and normal human hematopoietic cells. Leukemia. 1999;13:687-698.
12. Drabkin HA, Parsy C, Ferguson K, et al. Quantitative HOX expression in chromosomally defined subsets of acute myelogenous leukemia. Leukemia. 2002;16:186-195.
13. Imamura T, Morimoto A, Takanashi M, et al. Frequent co-expression of HoxA9 and Meis1 genes in infant acute lymphoblastic leukaemia with MLL rearrangement. Br J Haematol. 2002;119:119-121.
14. Lavau C, Luo RT, Du C, Thirman MJ. Retrovirus-mediated gene transfer of MLL-ELL transforms primary myeloid progenitors and causes acute myeloid leukemias in mice. Proc Natl Acad Sci U S A. 2000;97:10984-10989.
15. Ayton PM, Cleary ML. Transformation of myeloid progenitors by MLL oncoproteins is dependent on Hoxa7 and Hoxa9. Genes Dev. 2003;17:2298-2307.
16. Calvo KR, Sykes DB, Pasillas MP, Kamps MP. Nup98-HoxA9 immortalizes myeloid progenitors, enforces expression of Hoxa9, Hoxa7, and Meis1, and alters cytokine-specific responses in a manner similar to that induced by retroviral co-expression of Hoxa9 and Meis1. Oncogene. 2002;21:4247-4256.
17. Kroon E, Thorsteinsdottir U, Mayotte N, Nakamura T, Sauvageau G. NUP98-HOXA9 expression in hemopoietic stem cells induces chronic and acute myeloid leukemias in mice. EMBO J. 2001;20:350-361.

18. Hannum C, Culpepper J, Campbell D, et al. Ligand for FLT3/FLK2 receptor tyrosine kinase regulates growth of haematopoietic stem cells and is encoded by variant RNAs. Nature. 1994; 368:643-648.
19. Adolfsson J, Borge OJ, Bryder D, et al. Upregulation of Flt3 expression within the bone marrow Lin(-)Sca1(+)c-kit(+) stem cell compartment is accompanied by loss of self-renewal capacity. Immunity. 2001;15:659-669.
20. Sitnicka E, Buza-Vidas N, Larsson S, Nygren JM, Liuba K, Jacobsen SE. Human CD34+ hematopoietic stem cells capable of multilineage engrafting NOD/SCID mice express flt3: distinct flt3 and c-kit expression and response patterns on mouse and candidate human hematopoietic stem cells. Blood. 2003;102:881-886.
21. Mackarehtschian K, Hardin JD, Moore KA, Boast S, Goff SP, Lemischka IR. Targeted disruption of the flk2/flt3 gene leads to deficiencies in primitive hematopoietic progenitors. Immunity. 1995;3:147-161.
22. Sitnicka E, Bryder D, Theilgaard-Monch K, Buza-Vidas N, Adolfsson J, Jacobsen SE. Key role of flt3 ligand in regulation of the common lymphoid progenitor but not in maintenance of the hematopoietic stem cell pool. Immunity. 2002;17:463-472.
23. McKenna HJ, Stocking KL, Miller RE, et al. Mice lacking flt3 ligand have deficient hematopoiesis affecting hematopoietic progenitor cells, dendritic cells, and natural killer cells. Blood. 2000;95: 3489-3497.
24. Griffin JD. FLT3 tyrosine kinase as a target in acute leukemias. Hematol J. 2004;5:S188-S190.
25. Stirewalt DL, Radich JP. The role of FLT3 in haematopoietic malignancies. Nat Rev Cancer. 2003;3:650-665.
26. Zheng R, Levis M, Piloto O, et al. FLT3 ligand causes autocrine signaling in acute myeloid leukemia cells. Blood. 2004;103:267-274.
27. Sykes DB, Kamps MP. Estrogen-dependent E2a/Pbx1 myeloid cell lines exhibit conditional differentiation that can be arrested by other leukemic oncoproteins. Blood. 2001;98:2308-2318.
28. Sykes DB, Kamps MP. E2a/Pbx1 induces the rapid proliferation of stem cell factor-dependent murine pro-T cells that cause acute T-lymphoid or myeloid leukemias in mice. Mol Cell Biol. 2004; 24:1256-1269.
29. Borge OJ, Adolfsson J, Jacobsen AM. Lymphoid-restricted development from multipotent candidate murine stem cells: distinct and complimentary functions of the c-kit and flt3-ligands. Blood. 1999;94:3781-3790.
30. Avigdor A, Goichberg P, Shivtiel S, et al. CD44 and hyaluronic acid cooperate with SDF-1 in the trafficking of human CD34+ stem/progenitor cells to bone marrow. Blood. 2004;103:2981-2989.
31. Al-Hajj M, Wicha MS, Benito-Hernandez A, Morrison SJ, Clarke MF. Prospective identification of tumorigenic breast cancer cells. Proc Natl Acad Sci U S A. 2003;100:3983-3988.
32. Blair A, Hogge DE, Sutherland HJ. Most acute myeloid leukemia progenitor cells with long-term proliferative ability in vitro and in vivo have the phenotype CD34(+)/CD71(-)/HLA-DR. Blood. 1998;92:4325-4335.
33. Kollet O, Spiegel A, Peled A, et al. Rapid and efficient homing of human CD34(+)CD38(-/low)CXCR4(+) stem and progenitor cells to the bone marrow and spleen of NOD/SCID and NOD/SCID/B2m(null) mice. Blood. 2001;97:3283-3291.
34. Healy L, May G, Gale K, Grosveld F, Greaves M, Enver T. The stem cell antigen CD34 functions as a regulator of hemopoietic cell adhesion. Proc Natl Acad Sci U S A. 1995;92:12240-12244.
35. Fackler MJ, Krause DS, Smith OM, Civin CI, May WS. Full-length but not truncated CD34 inhibits hematopoietic cell differentiation of M1 cells. Blood. 1995;85:3040-3047.
36. Blair A, Sutherland HJ. Primitive acute myeloid leukemia cells with long-term proliferative ability in vitro and in vivo lack surface expression of c-kit (CD117). Exp Hematol. 2000;28:660-671.
37. Christensen JL, Weissman IL. Flk-2 is a marker in hematopoietic stem cell differentiation: a simple method to isolate long-term stem cells. Proc Natl Acad Sci U S A. 2001;98:14541-14546.
38. Tsutsumi S, Taketani T, Nishimura K, et al. Two distinct gene expression signatures in pediatric acute lymphoblastic leukemia with MLL rearrangements. Cancer Res. 2003;63:4882-4887.
39. Armstrong SA, Staunton JE, Silverman LB, et al. MLL translocations specify a distinct gene expression profile that distinguishes a unique leukemia. Nat Genet. 2002;30:41-47.
40. Forbes LV, Gale RE, Pizzey A, Pouwels K, Nathwani A, Linch DC. An activating mutation in the transmembrane domain of the granulocyte colony-stimulating factor receptor in patients with acute myeloid leukemia. Oncogene. 2002;21:5981-5989.

Mutational analysis revealed that two conserved hydrophobic motifs within the Meis1 CTD are required for the upregulation of *FLT3* expression, the generation of FL-responsive immortalized progenitors *in vitro*, and the induction of AML *in vivo*.

The mutational analysis of Meis1a described above in Figure 3.5 indicates that the leukemogenic functions of Meis1 depend on the integrity of the CTD domain. However, little is known about the functions of this domain. The blast database search using the amino acid sequences of the Meis1a CTD domain identified few homologues except the close Meis1 family members, Meis2 and Meis3 (Figure 3.6A). Although Prep1/pKnox1, a closely related Meis1/Prep family member, has been reported functionally redundant to Meis1 proteins in aspects such as the contribution to the nuclear accumulation of PBX (Berthelsen et al., 1999), PBX interaction (Ferretti et al., 1999) and the embryonic development (Ferretti et al., 2005; Ferretti et al., 2006), the overexpression of Prep1 in hematopoietic progenitors is incapable of accelerating the HoxA9-initiated leukemia (Thorsteinsdottir et al., 2001) or inducing the upregulation of *FLT3* expression (Figure 3.6B). This indicates that Meis1 proteins harbored a unique activity of programming leukemogenesis. Interestingly, Prep1 protein shows the high similarity to Meis1 proteins at the PBX interaction domains (M1 and M2) and the homeodomain (Berthelsen et al., 1998; Burglin, 1997), yet its C-terminal domain has no sequence similarity to Meis1 proteins (Figure 3.6A), suggesting that the Meis1 CTD may impart the unique leukemia transforming functions. In order to identify the potentially crucial motifs within the Meis1 CTD domain, I performed the systematic mutational analysis by the substitution of the

amino acids as shown in Figure 3.6C. Retrovirus encoding both Meis1 (wildtype or mutant) and *HoxA9* (containing bicistronic cassette Meis1-Ires-HoxA9) was used to infect hematopoietic progenitors, and the drug resistant progenitors are then cultured in the medium containing SCF. While HoxA9 alone is able to promote the progenitor proliferation in response to SCF independent of Meis1 proteins (Figure 3.6F), the transcription of endogenous *FLT3* gene is only induced with coexpressed functional Meis1 (Figure 3.6E, lane 2 vs lane 1). The endogenous *FLT3* expression is usually detected and maintained from around 7 days post retroviral infection of wiltype Meis1 and HoxA9 (data not shown). However, point mutation made on two conserved motifs [MGGFV and WHYM (as underlined in Figure 3.6A)] dramatically interfered with the induction of *FLT3* expression (Figure 3.6D and Figure 3.6E, top panel) at any time points of culture and the generation of FL-responsive progenitors when transferred to medium containing FL as the sole supporting cytokine (Figure 3.6G). A single amino acid substitution (F358A and W387A), but not dramatic mutations on other regions, also had dramatic effect on upregulation of the *FLT3* expression, indicating the specificity of these two motifs. Similar levels of HoxA9 and Meis1 were expressed in these progenitors (Figure 3.6E, middle and bottom panels). Deletion of the motif WHYM (370T) or the mutation on motif MGGFV (ΔFVM) had only moderate or undetectable interfering effect on the generation of FL-responsive immortalized progenitors *in vitro* (Figure 3.5F and Figure 3.6G) or the induction of AML *in vivo* (Figure 3.5H), and the combined mutation (as 370T/ΔFVM) completely abolished these two functions.

Taken together, I identified two conserved hydrophobic motifs within the Meis1 CTD domain that were required for the upregulation of FLT3 and the induction of AML. A recent report indicated that the Meis1 CTD domain, but not the Prep CTD domain, harbored the strong transcriptional activation activities that are regulated by the cellular signals (Huang et al., 2005). I hypothesize that these motifs provide the interaction surface for some unknown Meis1 cofactors whose functions are required for transcriptional activation and leukemia transformation.

Figure 3.6. Mutational analysis revealed that two conserved hydrophobic motifs within the Meis1 CTD are required for the upregulation of *FLT3* expression, the generation of FL-responsive immortalized progenitors *in vitro*, and the induction of AML *in vivo*.

(A) The sequence alignment of the CTD domains of Meis1, Meis2, Meis3 and Prep1.

(B) The ability of Prep1 and Meis1, with the coexpresed HoxA9, to upregulate the *FLT3* expression in drug-resistance selected hematopoietic progenitors after two weeks' culture in the medium containing SCF. Lanes are loaded with the total protein extraction sample from progenitors coexpressing Flag tagged Prep1 and HoxA9 (lane 1) or those coexpressing Flag tagged Meis1 and HoxA9 (lane 2).

(C) The diagram showing the location of mutations made on the residues within the Meis1 CTD domain. The identity of each point mutation was shown on the left, the position of premature termination mutations shown on the top, the residues mutated shown as underlined and the substitution shown in each line.

(D) Quantitative graph of the FLT3 protein levels in hematopoietic progenitors coexpressed with Meis1 [either wildtype (WT) or mutant as shown in the y-axis] and HoxA9 after two weeks' culture in the medium containing SCF. The x-axis showed the intensity of FLT3 protein band detected by western blot as in Figure 3.6E, top panel.

(E) Western blot revealed the protein level of FLT3, HoxA9 and Meis1 (Flag tagged) in hematopoietic progenitors after retroviral infection, drug resistant selection and two weeks' culture in the medium containing SCF. Retrovirus used encodes HoxA9 alone (lane 1) or a bicistronic cassette containing both Meis1 and HoxA9 (lane 2-14).

(F) The growth kinetics of hematopoietic progenitors in the medium containing SCF. 200,000 of drug-resistance selected progenitors were plated at day 0 (open bars), and the total progenitor number at day 10 (gray bars) and at day 20 (black bars) are plotted.

(G) The growth kinetics of hematopoietic progenitors in the medium containing FL as the sole supporting cytokine. 200,000 of progenitors collected at day 10 shown in Figure 3.6F were transferred into the medium containing FL as the sole supporting cytokine at day 0 (open bars), and the total progenitor number at day 6 (gray bars) and at day 10 (black bars) are plotted.

(H) The leukemia induction kinetics of mice injected with the drug-resistance selected hematopoietic progenitors that were expressed with coexpressed Meis1, WT or mutant, and HoxA9.

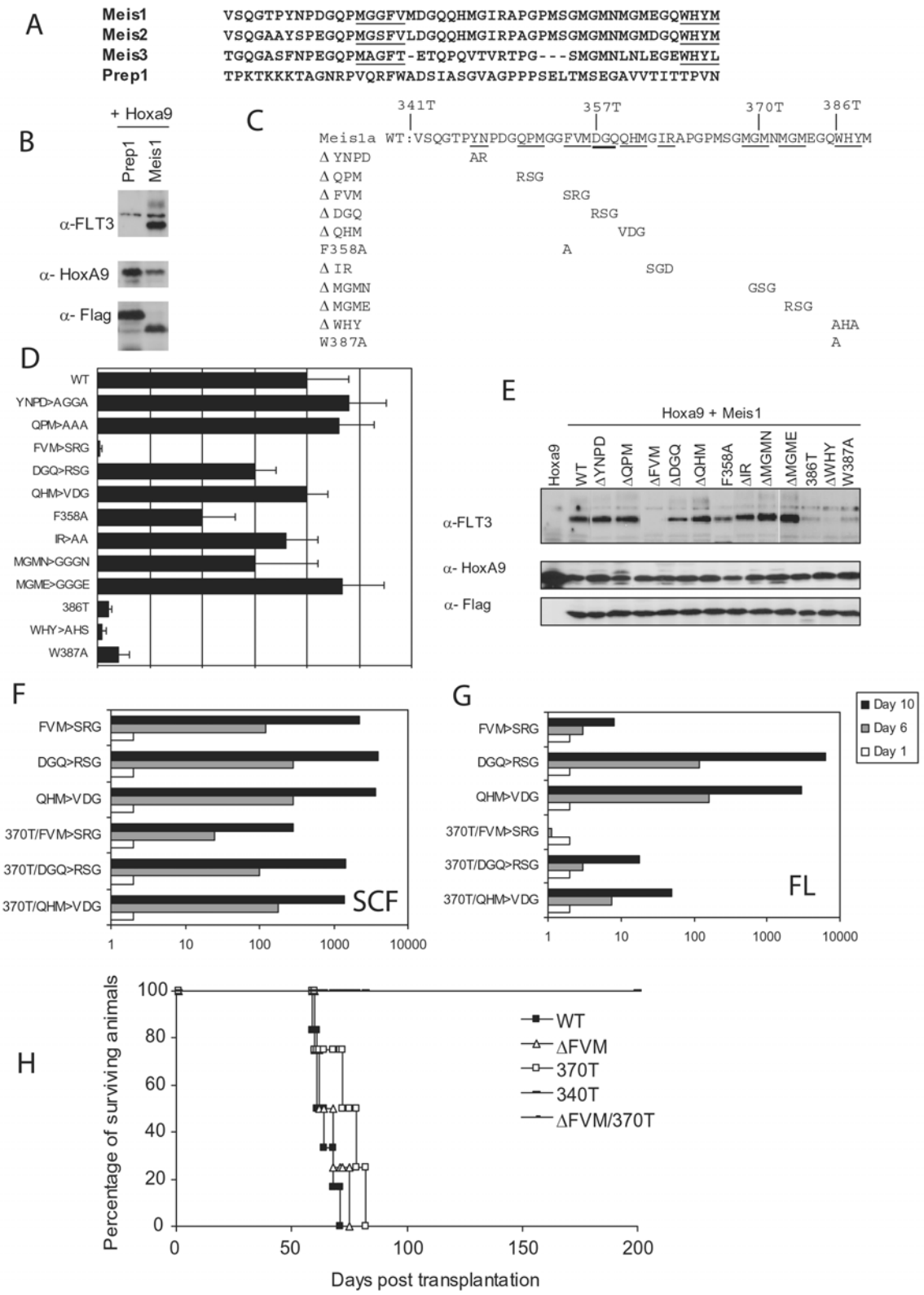
A
Meis1 VSQGTPYNPDGQPMGGFVMDGQQHMGIRAPGPMSGMGMNMGMEGQWHYM
Meis2 VSQGAAYSPEGQPMGSFVLDGQQHMGIRPAGPMSGMGMNMGMDGQWHYM
Meis3 TGQGASFNPEGQPMAGFT-ETQPQVTVRTPG---SMGMNLNLEGEWHYL
Prep1 TPKTKKKTAGNRPVQRFWADSIASGVAGPPPSELTMSEGAVVTITTPVN
B
+ Hoxa9
Prep1
Meis1
α-FLT3
α- HoxA9
α- Flag
C
341T
357T
370T
386T
Meis1a WT:VSQGTPYNPDGQPMGGFVMDGQQHMGIRAPGPMSGMGMNMGMEGQWHYM
Δ YNPD AR
Δ QPM RSG
Δ FVM SRG
Δ DGQ RSG
Δ QHM VDG
F358A A
Δ IR SGD
Δ MGMN GSG
Δ MGME RSG
Δ WHY AHA
W387A A
D
WT
YNPD>AGGA
QPM>AAA
FVM>SRG
DGQ>RSG
QHM>VDG
F358A
IR>AA
MGMN>GGGN
MGME>GGGE
386T
WHY>AHS
W387A
E
Hoxa9 + Meis1
Hoxa9
WT
ΔYNPD
ΔQPM
ΔFVM
ΔDGQ
ΔQHM
F358A
ΔIR
ΔMGMN
ΔMGME
386T
ΔWHY
W387A
α-FLT3
α- HoxA9
α- Flag
F
FVM>SRG
DGQ>RSG
QHM>VDG
370T/FVM>SRG
370T/DGQ>RSG
370T/QHM>VDG
SCF
1
10
100
1000
10000
G
Day 10
Day 6
Day 1
FVM>SRG
DGQ>RSG
QHM>VDG
370T/FVM>SRG
370T/DGQ>RSG
370T/QHM>VDG
FL
1
10
100
1000
10000
H
Percentage of surviving animals
100
80
60
40
20
0
0
50
100
150
200
Days post transplantation
WT
ΔFVM
370T
340T
ΔFVM/370T

ACKNOWLEDGEMENT

The first part of this chapter is composed of the paper published as: "Meis1 programs transcription of *FLT3* and cancer stem cell character, using a mechanism that requires interaction with Pbx and a novel function of the Meis1 *C*-terminus". Gang G. Wang, Martina P. Pasillas, and Mark P. Kamps. Blood (2005), Volume 106, Number 1, page 254-264. The text of this paper is Copyright © 2005 by The American Society of Hematology. I was the first-author and the primary researcher, and the coauthors listed in this publication aided in and/or supervised the research which formed the basis of this chapter. My contributions included performing most primary work in tissue culture, mouse leukemia models, DNA expression construct production, and molecular and biochemical analysis of Meis1 proteins, actively participating in experimental design, analyzing the primary data, and preparing the manuscript. Coauthor Martina Pasillas gave technical support in mouse model, western blot, northern and southern blot, and Facs analysis. The correspondence author Mark Kamps supervised and designed the research, and prepared the final version of the manuscript. I thank my co-authors for permission to use this publication in my dissertation.

Chapter 4

The formation of Hox-Meis1-PBX transcriptional activation complexes on cis-elements of the leukemia-associated downstream target genes underlines the molecular basis of their cooperation during leukemogenesis.

ABSTRACT

Homeobox transcription factors *Meis1* and *HoxA9* cooperate to cause AML, and coexpression of *Meis1* is required for the production of AML-initiating progenitors, which also transcribe a group of hematopoietic stem cell genes, including *Cd34* and *Flt3* (defined as *Meis1*-related leukemic signature genes). Here, I use dominant *trans*-activating (Vp16 fusion) or *trans*-repressing (*engrailed* fusion) forms of Meis1 to define its biochemical functions that contribute to leukemogenesis. Surprisingly, Vp16-Meis1 functioned as an autonomous oncoprotein that mimicked combined activities of Meis1 plus HoxA9, immortalizing early progenitors, inducing low-level expression of *Meis1*-related signature genes, and causing leukemia without coexpression of the exogenous or endogenous *Hox* genes. The absence of endogenous *Hox* gene expression in Vp16Meis1 immortalized progenitors allowed us to investigate how Hox alters gene expression and cell biology in early hematopoietic progenitors. Strikingly, expression of *HoxA9* or *HoxA7* stimulated both leukemic aggressiveness and transcription of *Meis1*-related signature genes in Vp16-Meis1 progenitors. Interestingly, while the HoxA9 N-terminal domain (NTD) is essential for cooperative transformation with wild-type Meis1, it was dispensable in Vp16-Meis1 progenitors. The fact that a transactivation domain fused to Meis1 replaces the essential functions of the Meis1 CTD and Hoxa9 NTD suggests that Meis-Pbx and Hox-Pbx (or Hox-Pbx-Meis) complexes co-occupy cellular promoters that drive leukemogenesis and that Meis1 CTD and Hox NTD cooperate in gene activation. ChIP analysis confirmed the co-occupancy of HoxA9, Meis1 and PBX on the *Flt3* promoter. Furthermore, the inter-molecular swapping of the Meis1 CTD and HoxA9 NTD domains does not interfere with their transforming activities *in vitro* and *in vivo*.

MOLECULAR AND CELLULAR BIOLOGY, May 2006, p. 3902–3916 Vol. 26, No. 10
0270-7306/06/$08.00+0 doi:10.1128/MCB.26.10.3902–3916.2006

Persistent Transactivation by Meis1 Replaces Hox Function in Myeloid Leukemogenesis Models: Evidence for Co-Occupancy of Meis1-Pbx and Hox-Pbx Complexes on Promoters of Leukemia-Associated Genes

Gang G. Wang,[1,2]* Martina P. Pasillas,[1] and Mark P. Kamps[1]

Department of Pathology and Molecular Pathology Graduate Program, University of California at San Diego School of Medicine, 9500 Gilman Drive, La Jolla, California 92093,[1] *and Biomedical Sciences Graduate Program, University of California at San Diego School of Medicine, 9500 Gilman Drive, La Jolla, California 92093*[2]

Received 16 September 2005/Returned for modification 16 November 2005/Accepted 21 February 2006

Homeobox transcription factors Meis1 and Hoxa9 promote hematopoietic progenitor self-renewal and cooperate to cause acute myeloid leukemia (AML). While Hoxa9 alone blocks the differentiation of nonleukemogenic myeloid cell-committed progenitors, coexpression with *Meis1* is required for the production of AML-initiating progenitors, which also transcribe a group of hematopoietic stem cell genes, including *Cd34* and *Flt3* (defined as *Meis1*-related leukemic signature genes). Here, we use dominant *trans*-activating (Vp16 fusion) or *trans*-repressing (*engrailed* fusion) forms of Meis1 to define its biochemical functions that contribute to leukemogenesis. Surprisingly, Vp16-Meis1 (but not *engrailed*-Meis1) functioned as an autonomous oncoprotein that mimicked combined activities of Meis1 plus Hoxa9, immortalizing early progenitors, inducing low-level expression of *Meis1*-related signature genes, and causing leukemia without coexpression of exogenous or endogenous *Hox* genes. Vp16-Meis1-mediated transformation required the Meis1 function of binding to Pbx and DNA but not its C-terminal domain (CTD). The absence of endogenous *Hox* gene expression in Vp16-Meis1-immortalized progenitors allowed us to investigate how Hox alters gene expression and cell biology in early hematopoietic progenitors. Strikingly, expression of *Hoxa9* or *Hoxa7* stimulated both leukemic aggressiveness and transcription of *Meis1*-related signature genes in Vp16-Meis1 progenitors. Interestingly, while the Hoxa9 N-terminal domain (NTD) is essential for cooperative transformation with wild-type Meis1, it was dispensable in Vp16-Meis1 progenitors. The fact that a dominant transactivation domain fused to Meis1 replaces the essential functions of both the Meis1 CTD and Hoxa9 NTD suggests that Meis-Pbx and Hox-Pbx (or Hox-Pbx-Meis) complexes co-occupy cellular promoters that drive leukemogenesis and that Meis1 CTD and Hox NTD cooperate in gene activation. Chromatin immunoprecipitation confirmed co-occupancy of Hoxa9 and Meis1 on the *Flt3* promoter.

Meis1 (*m*yeloid *e*cotrophic *i*nsertion *s*ite *1*) encodes a homeodomain (HD) transcription factor that positively regulates the expansion and pool size of hematopoietic stem cells (HSCs) and is commandeered in leukemic transformation. Meis1 belongs to the three-amino-acid loop extension family of HD proteins that includes Pbx, which heterodimerizes with Meis1 (9). While *Pbx* genes are broadly expressed in hematopoiesis, *Meis1* expression is high in Sca-I$^+$ Lin$^-$ HSCs but down-regulated during transition to Lin$^+$ lineages (4, 15, 37). A positive role of Meis1 in HSC expansion is suggested in *Meis1*$^{-/-}$ mice, which exhibit severe reduction in the number and colony-forming potential of HSCs (4, 15). Hoxa9, which is also expressed specifically in progenitors and required for the expansion and repopulating abilities of HSCs (29, 37, 47), binds both Meis1 and Pbx, suggesting that combinations of Meis-Pbx, Hox-Pbx, and Hox-Pbx-Meis complexes, such as those that regulate *Hoxb1* and *Hoxb2* expression (16, 21), may also target promoters that control HSC expansion.

The functions of Meis, Pbx, and Hox proteins are usurped in leukemogenesis. Originally, *Meis1* was discovered as one of two genes activated by proviral integration in BXH2 murine acute myeloid leukemia (AML), the second being *Hoxa9* or *Hoxa7* (32, 33). Over 50% of human AML and virtually all acute lymphoblastic leukemias containing translocations of the mixed lineage leukemia (MLL) gene exhibit strong expression of MEIS1, HOXA9, and HOXA7 (2, 17, 30). In murine AML models, Meis1 dramatically accelerates leukemia initiated by Hoxa9, Hoxb6, or Hoxb3 (reduces latency from ~200 days to ~60 days) yet exhibits no independent ability to cause disease by itself (13, 28, 46). Dominant activating forms of the MEIS1-interacting protein PBX1 [E2A-PBX1, produced by the t(1;19) translocation in human pre-B leukemia (24)] and HOXA9 [NUP98-HOXA9, produced by the t(7;11) of human AML (8)] also induce AML in mouse models, suggesting that activation of the same subset of Meis1-Pbx-Hox target genes may underlie leukemic transformation.

Hox and Meis1 have distinct roles in progenitor immortalization and in regulating gene expression. Hoxa9 blocks differentiation of cultured myeloid progenitors that do not express endogenous *Meis1/2/3* and do not cause leukemia when transplanted into syngeneic recipients (7, 47, 49). Coexpression of *Meis1* plus *Hoxa9* in cultured progenitors immortalizes an earlier myeloid progenitor that induces AML in syngeneic recipients. The leukemia stem cell (LSC) phenotype induced by

* Corresponding author. Mailing address: Leichtag 249B, UCSD Medical School, 9500 Gilman Dr., La Jolla, CA 92093. Phone: (858) 534-5822. Fax: (858) 534-4715. E-mail: gawang@ucsd.edu.

Meis1 is paralleled expression of a set of leukemia-associated genes, including *Cd34*, *Flt3*, and *Erg*, which have been therefore defined as *Meis1*-related leukemic signature genes, and we hypothesized that these *Meis1* signature genes are important for LSCs to survive and expand in marrow stem cell niches (49). Whether the expression of *Meis1*-related signature genes requires Hoxa9 function is unknown, but it is now strongly implicated by our results presented below.

Equally unclear is the type of transcriptional activity that Meis1-Pbx complexes use to induce the LSC phenotype. Whereas Pbx can mediate repression through its recruitment of corepressors such as histone deacetylases and mSin3, Meis1 contains a C-terminal domain (CTD) that can promote transactivation in response to cell signals such as those induced by protein kinase A (16, 40). By interacting with both Hox and non-Hox factors (e.g., MyoD [6] and Oct1 [38]), Meis1-Pbx complexes contribute to both gene activation (e.g., of *Myogenin* [6], *Hoxb1* [16], *Hoxb2* [21], and *Pax6* [51]) and gene repression (e.g., of *CYBB* [5]). It is not clear whether activation, repression, or both functions mediate the role of Meis1 in leukemia.

Here, we ask whether activation or repression by Meis1 plays the more important role in myeloid leukemogenesis by fusing Meis1 to a dominant activation domain of Vp16 or a dominant repression domain of *engrailed*. This same strategy was used to identify transcriptional functions of the *Drosophila melanogaster Meis1* homologue, *Homothorax*, that contribute to embryonic development (18). Strikingly, in the absence of coexpressed *Hoxa9*, Vp16-Meis1 alone was able to immortalize early hematopoietic progenitors in culture that caused myeloid leukemia in syngeneic mice. Neither the immortalized progenitors nor the leukemia cells derived from them expressed endogenous *Hox* genes. The transforming ability of Vp16-Meis1 required interaction with Pbx and binding to DNA but not the function of the Meis1 CTD, which is required for cooperative leukemogenesis by wild-type Meis1 with Hoxa9. Vp16-Meis1 progenitors expressed low to moderate levels of the same *Meis1*-related leukemic signature genes (e.g., *Flt3*, *Cd34*, *Erg*, and *Msi2h*). Surprisingly, retroviral expression of *Hoxa9* or *Hoxa7* in Vp16-Meis1-expressing progenitors strongly up-regulated these *Meis1*-associated signature genes, promoted cell division, and reduced disease latency to less than 30 days. This is the first evidence that Hox proteins contribute to transcriptional activation of *Meis1*-related signature genes. Hoxa7, which also cooperates with Meis1 to induce AML, induced the same cellular and genetic changes as Hoxa9. Strikingly, the N-terminal domain (NTD) of Hoxa9 (residues 1 to 138), which is essential for its transforming properties with Meis1, was unnecessary for promoting proliferation and transcription of *Meis1* signature genes (such as *Flt3*) in Vp16-Meis1 progenitors. Taken together, these results indicate that transactivation represents the key function of Meis1 that contributes to leukemogenesis and that Meis, Hox, and Pbx proteins form a common regulatory complex that activates transcription through mechanisms dependent on the Hoxa9 NTD and the Meis1 CTD, functions that can be replaced by the Vp16 domain fused onto Meis1. Consistent with this hypothesis, chromatin immunoprecipitation (ChIP) revealed that Hoxa9 and Meis1 were both recruited to the *Flt3* promoter.

MATERIALS AND METHODS

Plasmid construction and retroviral expression system. The murine stem cell virus (MSCV) retroviral expression system for Meis1 and Nup98-Hoxa9 was described previously (8, 49). The NCBI accession numbers designating the nucleotide and protein sequences of the murine *Meis1a* isoform used are U33629 and AAA85508, respectively. Vp16-Meis1 and en-Meis1 were created by inserting sequences encoding the Vp16 activation domain or the *engrailed* repression domain into an MluI site made by mutating the first two codons of Meis1. Vp16-Meis1 mutants were generated as described elsewhere for Meis1 (49). Flag-Hoxa7 was generated by inserting the Flag tag at the N terminus of Hoxa7, and the bicistronic MSCV vector used for coexpression of Meis1 and Hoxa7 was constructed with Flag-Meis1 upstream of the internal ribosomal entry site (IRES) and Flag-Hoxa7 downstream of the IRES (49). Internal deletions in Hoxa9 were generated by excising cDNA regions flanked by two MluI sites created by site-directed mutagenesis in the MSCV-Neo vector encoding tagged Hoxa9 (7). Plasmids containing the Vp16 activation domain or *engrailed* repression domain were kindly provided by Adi Salzberg (18), and MLL-ENL was provided by Robert Slany. All constructs were verified by sequencing.

Infection and culture of hematopoietic progenitors. Protocols for retroviral infection and culture of primary hematopoietic progenitors in granulocyte-macrophage colony-stimulating factor (GM-CSF), stem cell factor (SCF), or Flt3 ligand (FL) were described previously (7, 49). Briefly, 2×10^5 to 4×10^5 of enriched Sca^+ Lin^- bone marrow progenitors from BALB/c mice were subjected to a single round of spinoculation-infection using 1 ml of retroviral supernatant (2×10^5 to 4×10^5/ml), followed by 3 days of drug resistance selection (0.6 to 1 mg/ml of G418 for MSCV-Neo or 1 μg/ml of puromycin for MSCV-Puro [drug selection is optional]), and cultured in medium containing either GM-SCF, SCF, or FL. Proliferation kinetics were evaluated by plating 2×10^5 to 4×10^5 drug-resistant Lin^- progenitors in a 12-well tissue culture plate (Corning, New York) and splitting every 3 to 4 days in fresh medium, using a protocol that keeps the progenitor number lower than 2×10^6 per well. For coexpression of Meis1 with Hoxa9 mutants, equal amounts of retrovirus encoding Flag-Meis1 (MSCV-Puro) and Hoxa9 (MSCV-Neo) were combined and used for infection, followed by dual drug selection and cultivation in SCF or FL. Wright-Giemsa staining and fluorescence-activated cell sorter (FACS) analysis were performed as described elsewhere (49).

Antibodies and immunoblotting. Ten microliters of total cellular protein (10^7 cells per ml) was used for immunoblotting. Anti-Flag, anti-Flt3, and anti-Hoxa9 were obtained and used as described previously (49). Anti-Pbx was obtained from Santa Cruz Biotechnology (C-20; sc-888).

Luciferase reporter assays. Cooperative transactivation by Vp16-Meis1 and Pbx1a was evaluated using 7xPRS-pGL3, a pGL3 luciferase derivative driven by seven tandem repeats of the *P*bx1-Meis1-*r*esponsive *s*equence (PRS), TGATT GAT, which was first identified as an E2a-PBX1 binding site (27) and later demonstrated to be recognized by Meis1 plus Pbx1 (26). One microgram of 7xPRS-pGL3 was cotransfected with 1 μg of MSCV–Vp16-Meis1, 0.5 μg of pcDNA3-Pbx1a, and 0.2 μg of pRL-TK (internal control that expresses *Renilla* luciferase persistently) into 293T cells. At 48 h after transfection, cell lysate was prepared and quantified for firefly and *Renilla* luciferase activity using a dual luciferase reporter system (Promega) and LMaxII luminometer (Molecular Devices, California). Luciferase measurements were calculated as firefly luciferase units versus *Renilla* luciferase units. Transcriptional activation was compared to basal luciferase levels in cells cotransfected with 7xPRS-pGL3, empty MSCV, and Pbx1a.

Semiquantitative RT-PCR and real-time qPCR. Total RNA was extracted (49) from immortalized progenitors 6 to 8 weeks post-retroviral infection, when normal progenitors are no longer present and when immortalized progenitors exhibit stable proliferation, stable expression of surface markers, and little to no differentiation. First-strand total cDNA, used as a template for reverse transcription-PCR (RT-PCR) and quantitative PCR (qPCR), was generated with the SuperScript reverse transcription system (Invitrogen) by using 4 μg of total RNA and 50 ng of random hexamers. Real-time qPCR was performed using 4 μl of 1:10-diluted cDNA as a template, 400 nM of primers, and SYBR Green PCR master mix (Applied Biosystems) in a 15-μl reaction volume and an Mx3000P real-time PCR system (Stratagene). The housekeeping gene *Gapdh* was used as control for mass of cDNA. The specificity and relative signal intensity of real-time qPCR amplifications were analyzed according to the manufacturer's specifications (Stratagene). Primers covered at least one intron-exon boundary. Semiquantitative RT-PCR was performed as described elsewhere (49). The sequences of primers used for each murine gene were as follows: for *Gapdh*, 5′-ATGAC ATCAAGAAGGTGGTGAAG and 5′-TCCTTGGAGGCCATGTAGG; for *Hoxa9*, 5′-TGGTTCTCCTCCAGTTGATAG and 5′-AGAAACTCCTTCTCCA

GTTCC; for *Hoxa7*, 5′-CGGGCTTATACAATGTCAACAG and 5′-AAATGG AATTCCTTCTCCAGTTC; for *Hoxa5*, 5′-GCAAGCTGCACATTAGTCAC and 5′-GCATGAGCTATTTCGATCCT; for *Hoxa10*, 5′-GGAAGGAGCGAG TCCTAGA and 5′-TTCACTTGTCTGTCCGTGAG; for *Flt3*, 5′-AAATCCCA GAAGGAGTTTGG and 5′-CGCATAGAAGGAGATGTTGTC; for *Erg*, 5′-G ACCACAAATGAGCGCAGAG and 5′-CTTTGGACTGAGGGGTGAGG; for *Cd34*, 5′-ACAGCAGTAAGACCACACCAGC and 5′-AGACACTAGCAC CAGCATCAGC; for *Il7r*, 5′-CTGACCTGAAAGTCGTTTATCGC and 5′-CA TCCTCCTTGATTCTTGGGTTC; and for *Msi2h*, 5′-ACGATTGACCCAAAA GTTGC and 5′-ACAAAGCCAAACCCTCTGTG.

In vivo leukemogenesis assay. The leukemic potential of oncogenes was evaluated in sublethally irradiated syngeneic BALB/c mice (450-rad dosage) followed by tail vein injection with 2×10^6 immortalized progenitors cultured ex vivo for 4 to 8 weeks (49) or with 5×10^5 ScaI$^+$ Lin$^-$ progenitors that were prestimulated in a cytokine cocktail containing murine SCF (1:100 dilution of culture supernatant of SCF-secreting cell lines), 10 ng/ml of murine interleukin-3 (IL-3; PeproTech Inc., New Jersey), 10 ng/ml of IL-6 (PeproTech), IL-7 (1:100 dilution of culture supernatant of IL-7-secreting cell lines), and 5 ng/ml FL (Sigma); infected with retrovirus; subjected to drug resistance selection for 2 days; and cultured for 2 more days in nonselection medium containing the same cytokine cocktail. SCF- or IL-7-containing supernatant from cytokine-secreting cell lines (SCF-secreting CHO cells and IL-7-secreting J558 cells) was harvested every 24 h as 50 ml of total medium from 15-cm plates of highly confluent cells (45). Mice exhibiting a leukemia phenotype (scruffy fur, lethargy, paralysis, or splenomegaly) were sacrificed, and cells isolated from leukemic tissues were subjected to further analysis, including flow cytometry, Wright-Giemsa staining, secondary injection, immunoblotting, retroviral integration site analysis by Southern blotting, and RT-PCR (45).

Affymetrix microarray analysis. Total RNA from 5×10^7 to 10×10^7 progenitors cultured in SCF was purified using a Maxi RNA isolation kit (QIAGEN). Gene expression profiling was examined by using the Affymetrix GeneChip Mouse Genome 430 2.0 array probed with total RNA (MicroArray Core Facility, UCSD-VA Medical Center). After normalization of overall signal intensities among different hybridization experiments, levels of gene expression were calculated using d-CHIP software, taking into consideration both the perfect match (PM) and mismatch (MM) values for all 11 sets of oligonucleotide probes representing each gene (49). At signal intensities of less than 50, the PM versus MM ratio approached unity; therefore, any signal below 50 units was designated background. Because computation analysis methods will include false positives selected due to high-level expression indicated by only one or a few of the 11 pairs of diagnostic oligonucleotides, all d-CHIP results were confirmed by visual inspection of normalized chip raw data, and a subset of genes was confirmed by semiquantitative or real-time PCR.

Two approaches were used to characterize leukemogenesis genes in Vp16-Meis1 progenitors: (i) identification of genes up-regulated threefold or greater in Vp16-Meis1 progenitors by comparison to nonleukemic Hoxa9 progenitors, and (ii) identification of genes up-regulated threefold or greater by Hoxa9 in Vp16-Meis1 progenitors. Among 39,000 genes represented on the array, only 24 genes were up-regulated >3-fold in three of the Vp16-Meis1 progenitor lines by comparison to five of the Hoxa9 progenitor lines, and only 77 genes (which included 22 of those 24 genes induced by Vp16-Meis1) were up-regulated >3-fold by expression of Hoxa9 in each of the Vp16-Meis1 progenitor lines, demonstrating that in both cases, the transcriptional impact of the oncoprotein is specific and limited. Among those 24 genes induced by Vp16-Meis1 were 16 of the original 25 genes we reported as *Meis1*-related signature genes that were expressed specifically in leukemogenic Hoxa9-plus-Meis1 progenitors but not in Hoxa9 progenitors (i.e., *Cd34*, *Flt3*, *Il7r*, *Crlr*, *Erg*, *Gpr56*, *Tilz1b*, *Nrip1*/*RIP140*, *C1qr1*, *Tmsb10*, *Kcna3*, *Ngn*, *Ptprcap*/*CD45AP*, *Satb1*, *Ngn*, and *Ly86*/*MD-1*) (see Table 3, below). The other nine of the original *Meis1* signature genes, expressed at extremely low levels in our original analysis of Hoxa9-plus-Meis1 progenitors, have been eliminated as candidate leukemogenesis genes based on their inconsistent activation in additional cell lines immortalized by Hoxa9 plus Meis1, lack of their expression in Vp16-Meis1 progenitors, and lack of activation by Hoxa9 (*Tspan2*, *CD244*, *Gem*, *PLZF*, *Cd27*, *Itgb7*, *Oaf*, *CXXC5*, and *Ebf*). The eight new genes activated by Vp16Meis1 (*Msi2h*, *Sox4*, *Dbx4*, *P2x*, *Bcl2*, and *Sesn3*, plus two unknown expressed sequence tags) were also expressed at significantly higher levels in Hoxa9-plus-Meis1 progenitors than in Hoxa9 progenitors and were added to the genes shown below in Table 3. The remaining 54 genes that were activated by Hoxa9 in Vp16-Meis1 progenitors (except c-*kit*, listed below in Table 3) were not expressed in Hoxa9 progenitors or Hoxa9-plus-Meis1 progenitors; therefore, they may be artificial targets of Hoxa9 in the context of Vp16-fused Meis1 or they may be real targets under different cellular contexts that were mimicked/activated by Vp16-Meis1. However, their activation is physiologically irrelevant to leukemogenesis by Hoxa9 plus Meis1 (they are not included in Table 3; information is available upon request).

Retrovirus integration site analysis. Genomic DNA was purified, digested, resolved, and transferred to a membrane as previously described (49). EcoRI or BamHI was used to digest DNA from progenitors infected by retrovirus encoding Vp16-Meis1 or Meis1-IRES-Hoxa7, respectively, and cDNA fragments encoding the Vp16 activation domain and Hoxa7 were used for making probes.

EMSA. Heterodimerization of Hoxa9 with either Pbx1 or Meis1 on DNA was examined by electrophoretic mobility shift assay (EMSA), as described previously (7, 43).

ChIP analysis. ChIP analysis was performed according to a modified protocol based on ChIP protocols of Upstate Biotechnology (New York) and Active Motif (California). Briefly, 2×10^7 to 3×10^7 myeloid progenitors were collected and subjected to DNA-protein cross-linking in 10 ml of phosphate-buffered saline plus 1% formaldehyde for 10 to 15 min at room temperature, followed by a 5-minute treatment in 5 ml of 0.125 M glycine (supplemented with 1× Complete protease inhibitor cocktail [PIC; Roche]) to stop the cross-linking reaction. After washing with cold phosphate-buffered saline–1× PIC, the cell pellet was suspended in 200 μl of sodium dodecyl sulfate lysis buffer (Upstate; 1× PIC added), incubated on ice for 15 min, and then subjected to three repeats of 12- to 13-second sonication (Sonifier 450 [VMR Scientific]). Sheared DNA was 400 bp to 1.5 kbp. The sheared sample was centrifuged at 14,000 rpm for 15 min at 4°C, and the supernatant was diluted 1:10 with ChIP dilution buffer (Upstate; 1× PIC added). The chromatin was immuno-precleared with 60 μl salmon sperm DNA-protein A-agarose (Upstate) per 2 ml chromatin, followed by a 1-h rotation (4°C) and removal of the agarose by 2 min of centrifugation at 1,500 rpm. Five hundred microliters of chromatin was used for overnight immunoprecipitation by control antibody (immunoglobulin G [IgG]) or specific antibody with rotation at 4°C. Sixty microliters of protein A-agarose was added to each tube followed by rotation for 2 h and sequential washing with low-salt wash buffer, high-salt wash buffer, LiCl wash buffer, and Tris-EDTA buffer as described elsewhere (Upstate; 1× PIC added to all buffers). Chromatin was eluted twice with 100 μl of freshly made 1% sodium dodecyl sulfate plus 0.1 M $NaHCO_3$ with 15 min of vigorous shaking on a vortex mixer. A 200-μl aliquot of eluted chromatin-protein was subjected to reverse cross-linking, removal of RNA (by addition of 8 μl of 5 M NaCl and 1 μl of RNase A [10 μg/μl] and incubation at 65°C for 6 to 16 h), and then removal of protein (by subsequent addition of 4 μl of 0.5 M EDTA, 8 μl of 1 M Tris-HCl [pH 6.5], and 1 μl of 20-mg/ml protease K, with incubation at 45°C for 1 to 2 h). DNA was recovered using a QIAQuick spin column and suspended in 100 μl of elution buffer (QIAGEN). PCR amplification was performed using 1 U of Platinum *Taq* polymerase (Invitrogen) and 2 to 4 μl of eluted DNA.

Antibodies for ChIP (amount added per 500 μl of chromatin) included M2 anti-Flag (8 μg; Sigma), anti-Hoxa9 HD (10 μg), anti-Meis1 HD (10 μg), anti-Meis1 N terminal (10 μg; gift of Mark Featherstone), anti-acetyl-histone H3 (1 μg; Upstate 06-599) and anti-dimethylated histone H3 Lys4 (anti-H3K4Me2 [1 μg]; Upstate 07-030).

The murine *Flt3* genomic structure was deduced using information provided by the UCSC Genome Browser (http://genome.ucsc.edu), and the putative transcription start site was defined using in silico mapping of common 5′ expressed sequence tag sequences onto the genomic sequence. The ChIP primers used to amplify regions of the *Flt3* locus were P3 (5′-GGACAAATGGCTCAGGAGGG and 5′-CATCTGGTAGATCTGCATTGTGG), P4 (5′-CTAGATGTGGCTCT GGGAACC and 5′-AGACAGATAGACAGAGTGCCAGC), P5 (5′-AGTCA GAAGGGACTGGCTCC and 5′-GAGTGCTGCTTAGCAGATTACC), and P6 (5′-CCTCAGAAGTGAACTCAGTTTCC and 5′-CTGCATCCAGACCAT GAAGG).

RESULTS

Hoxa7 mimics Hoxa9 in its independent and Meis1-dependent leukemic properties. *Hoxa7* is also coactivated with *Meis1* in BXH-2 murine AML (32); however, its leukemic functions have not been described in experimental models. Therefore, *Hoxa7* was cloned into the MSCV retroviral vector, and its independent and Meis1-dependent transforming functions were assessed. Like Hoxa9, Hoxa7 immortalized GM-CSF-dependent (Fig. 1A and E) or SCF-dependent (Fig. 1B) progenitors in the absence of coexpressed *Meis1*. Like Hoxa9-immortalized progenitors, Hoxa7-immortalized progenitors were 100% MacI$^+$ (data not shown), differentiated into mature

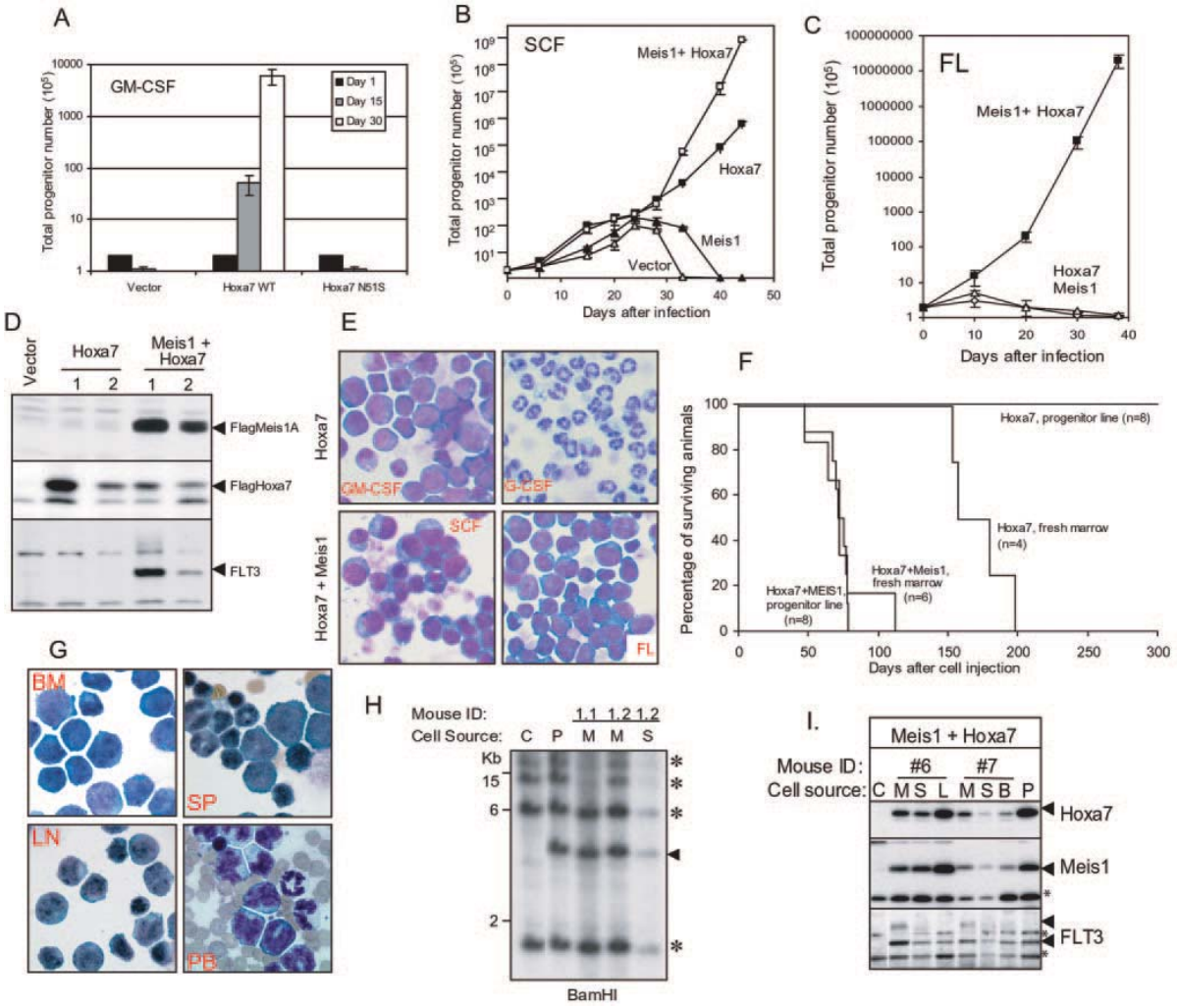

FIG. 1. Hoxa7 mimics Hoxa9 in terms of its independent and Meis1-dependent transforming functions. (A) Growth kinetics of GM-CSF-dependent marrow progenitors infected with MSCV retrovirus encoding vector only, wild-type (WT) *Hoxa7*, or a DNA-binding-defective *Hoxa7* (N51S), followed by drug selection. Error bars indicate the standard deviations among three repeated experiments. (B and C) Growth kinetics of primary marrow progenitors infected with retrovirus encoding vector only, *Meis1*, *Hoxa7*, or *Meis1* plus *Hoxa7*, followed by culture in SCF (B) or in FL (C). (D) Immunoblot analysis of Hoxa7, Meis1, and Flt3 in cultures shown in panel B. (E) Wright-Giemsa stain of GM-CSF-dependent progenitors immortalized by Hoxa7 in GM-CSF or when shifted to G-CSF and those immortalized by Meis1 plus Hoxa7 in SCF or FL. (F) Survival curves of mice injected with two progenitor lines immortalized by *Hoxa7* in SCF (four for each), progenitors immortalized by coexpressed *Meis1* and *Hoxa7* (four for one line in SCF and four for one line in FL), and Sca^+ Lin^- marrow progenitors freshly transduced with retrovirus encoding *Hoxa7* (four mice) or *Meis1* plus *Hoxa7* (six mice). (G) Representative Wright-Giemsa stains of tissue samples from mice bearing AML induced by Meis1 plus Hoxa7. BM, bone marrow; SP, spleen; LN, lymph node; PB, peripheral blood. (H) Southern blot of retroviral integration sites, using BamHI-digested genomic DNA from control Hoxa9-immortalized progenitors (C), injected parental progenitors immortalized by Meis1 plus Hoxa7 (P), and leukemic cells extracted from bone marrow (M) or spleen (S). The arrowhead indicates a band that represents the proviral Hoxa7 integration site. Stars indicate nonspecific bands. ID, identification. (I) Immunoblot analysis of expression of retrovirus-encoded genes, Flag-tagged Hoxa7 and Meis1, and Flt3 in control Hoxa9-immortalized progenitors (C); in parental progenitors immortalized by Meis1 plus Hoxa7 that were injected into mice (P); in leukemia cells from bone marrow (M), spleen (S), and lymph node (L); and in purified white blood cells (B). The arrowhead indicates a specific band, and the star indicates a nonspecific band.

neutrophils when shifted into medium containing G-CSF (Fig. 1E), and did not cause leukemia when injected into sublethally irradiated mice (Fig. 1F). Similar to the effect of coexpressing *Meis1* with *Hoxa9*, coexpression of *Meis1* with *Hoxa7* immortalized a distinct SCF-dependent progenitor (Fig. 1B and E) that expressed Flt3 (Fig. 1C and D), proliferated more rapidly (Fig. 1B), underwent self-renewal in FL (Fig. 1C and E) or IL-7, GM-CSF, or SCF plus G-CSF (data not shown), and induced myeloblastic leukemia (Fig. 1F and G) ($Mac\text{-}I^+$ $B220^-$ $Cd19^-$) that exhibited the same pathophysiology as that

TABLE 1. Phenotypes of leukemias induced by coexpressed *Hoxa7* and *Meis1*[c]

Cell type injected	Latency (days)	Organ wt (mg)		WBC count (1,000/μl)[b]	Leukemia FACS[a]	
		Spleen	Node		MacI$^+$	B220$^+$
Hoxa7 + *Meis1* (progenitor line)	70 ± 10	500 ± 100	26 ± 5	85 ± 17	78 ± 16	25 ± 6
Hoxa7 + *Meis1* (fresh marrow)	74 ± 21	637 ± 200	31 ± 6	92 ± 12	80 ± 18	18 ± 9

[a] FACS results (percentage) of leukemia cells from spleen and bone marrow.
[b] WBC, white blood cells in peripheral blood.
[c] Values are averages ± standard deviations.

induced by *Hoxa9* plus *Meis1* (Table 1). Leukemic cells contained the same retroviral integration sites as injected progenitors (Fig. 1H) and expressed retroviral Flag-Hoxa7 and Flag-Meis1 and endogenous Flt3 (Fig. 1I), confirming that they arose from injected cells.

In contrast to the use of stably immortalized progenitors to initiate leukemia, we also reconstituted mice with Sca$^+$ Lin$^-$-enriched marrow progenitors following an immediate infection with *Hoxa7* or *Hoxa7* plus *Meis1* retrovirus. Mice transduced with *Hoxa7*-infected progenitors developed myeloid leukemia after a long latency (170 days), while those transduced with *Hoxa7* plus *Meis1* acquired AML rapidly (74 days) (Fig. 1F) with leukemic myeloblasts that evidenced the same phenotypes as those resulting from injections of immortalized progenitor lines (Table 1). Therefore, Hoxa7 behaved the same as Hoxa9, as both immortalized a nonleukemic myeloid progenitor when expressed without *Meis1* and immortalized an Flt3$^+$, leukemia-initiating progenitor when coexpressed with *Meis1* (49).

Vp16-Meis1 immortalizes hematopoietic progenitors in the absence of coexpressed *Hox* genes. To identify the transcriptional function of Meis1 that is important for cooperation with Hoxa9 and Hoxa7 in establishing the leukemic stem cell phenotype, dominant transactivating or transrepressing forms of Meis1 were produced by fusing it to the activation domain of herpes simplex viral protein Vp16 or to the repression domain of *Drosophila engrailed* (en) (Fig. 2A). Sca1$^+$ Lin$^-$-enriched marrow progenitors were infected with retrovirus encoding empty vector, Meis1, Vp16-Meis1, or en-Meis1 and cultured in medium containing SCF or FL as the sole cytokine. With either cytokine, expression of Vp16-Meis1 itself was able to immortalize progenitors, while cultures infected with Meis1 or en-Meis1 retrovirus followed the same decline in progenitors as uninfected cultures (Fig. 2B). Vp16-Meis1 had no effect on NIH 3T3 fibroblasts, indicating that the differentiation arrest phenotype was not accompanied by a cell proliferation phenotype, as is the case with E2A-PBX1, a transcriptionally activated form of the MEIS1 partner PBX1 (25). To test whether immortalization by Vp16-Meis1 might be mediated by expression of endogenous *Hox* genes, the expression of *Hoxa5*, *Hoxa7*, *Hoxa9*, and *Hoxa10* was measured by semiquantitative RT-PCR (Fig. 2C) and quantitative real-time PCR (data not shown, except for Hoxa9 in Fig. 4D, below). None of these four *Hox* genes was expressed in two of the Vp16-Meis1-immortalized progenitors, while they were all expressed strongly in progenitors immortalized by the *Hox* locus transactivators MLL-ENL (50) or Nup98-Hoxa9 (8). A global view of *Hox* gene expression assessed by using Affymetrix mouse gene arrays demonstrated no expression of any of 31 *Hox* genes present on the array chip (*Hoxa1* to *-5*, *-a7*, *-a10*, *-a11*, *-a13*, *-b1*, *-b3* to *-9*, *-b13*, *-c4* to *-6*, *-c8*, *-c9*, *-c13*, *-d1*, *-d3*, *-d4*, or *-d10* to *-13*) among five independent Vp16-Meis1 progenitor lines (19), while each of two Nup98-Hoxa9-immortalized progenitor lines exhibited strong expression of eight *Hox* genes (*Hoxa5*, *-a7*, *-a9*, *-a10*, *-c4* to *-6*, and *-c8*). Therefore, *Hox* genes are not expressed in Vp16-Meis1 progenitors. Affymetrix arrays also revealed strong expression of Pbx1a, weak expression of Pbx2a, and no expression of Pbx1b, Pbx2b, or Pbx3 in Vp16-Meis1 progenitors (Fig. 2E). Pbx1a expression was verified by Western blotting (Fig. 2D). Vp16-Meis1 progenitors were cytokine dependent, proliferating as progenitors in SCF or FL, and a subset (5 to 25%) proliferated as undifferentiated progenitors in IL-7, GM-CSF, or G-CSF (Fig. 2F and G), a behavior similar to progenitors coexpressing *Hoxa9* plus *Meis1* (49). Thus, Vp16-Meis1 mimics the combined activities of Hoxa9 plus Meis1, immortalizing progenitors capable of responding to both lymphoid and myeloid cytokines. The ability of a dominant activating form of Meis1 to replace the immortalizing function of Hox proteins raises the possibility that Meis1 binds the same promoters as Hoxa9 and Hoxa7 and that the histone acetyltransferase (HAT) activity recruited by Vp16 (31) replaces an intrinsic Hox-dependent activation function.

Vp16-Meis1-mediated immortalization requires binding to Pbx and to DNA but not the function of the Meis1 CTD, an essential domain for cooperation of wild-type Meis1 with Hoxa9. The immortalization potential of Vp16-Meis1 corresponded to its ability to induce cooperative transactivation with Pbx1. A mutation that eliminated the entire M1-M2 Pbx interaction domain (Δ64-202), a five-residue neutral mutation in the M2 domain (M2$^{\Delta LRF/LELL}$) that disrupts heterodimerization with Pbx1 (49), or an HD mutation (HD$^{N51S/\Delta RRR}$) that virtually eliminates binding of Meis1-Pbx1 heterodimers to DNA (Fig. 3A) each reduced activation of a reporter construct driven by Pbx1-Meis1 binding motifs to levels 20% or less of those induced by wild-type Vp16-Meis1 (Fig. 3C), and each of these mutants was incapable of immortalizing progenitors in either SCF or FL (Fig. 3B). By contrast, an N-terminal deletion preceding the Pbx interaction domain (Δ1-64), a three-residue neutral mutation in M2 (M2$^{\Delta LELL}$), and an internal deletion between the M2 domain and HD (Δ202-260), all of which retained active Pbx-Meis1 heterodimerization potential on DNA (49), maintained more robust activation of the reporter construct and immortalized FL-responsive progenitors actively (Fig. 3B and C). The Meis1 CTD, which is essential for the ability of wild-type Meis1 to immortalize Flt3$^+$ progenitors in cooperation with Hoxa9, was dispensable for transactivation by Vp16-Meis1 and was also unnecessary for Vp16-Meis1-mediated immortalization of Flt3$^+$ progenitors. Immunoblot analysis confirmed expression of all

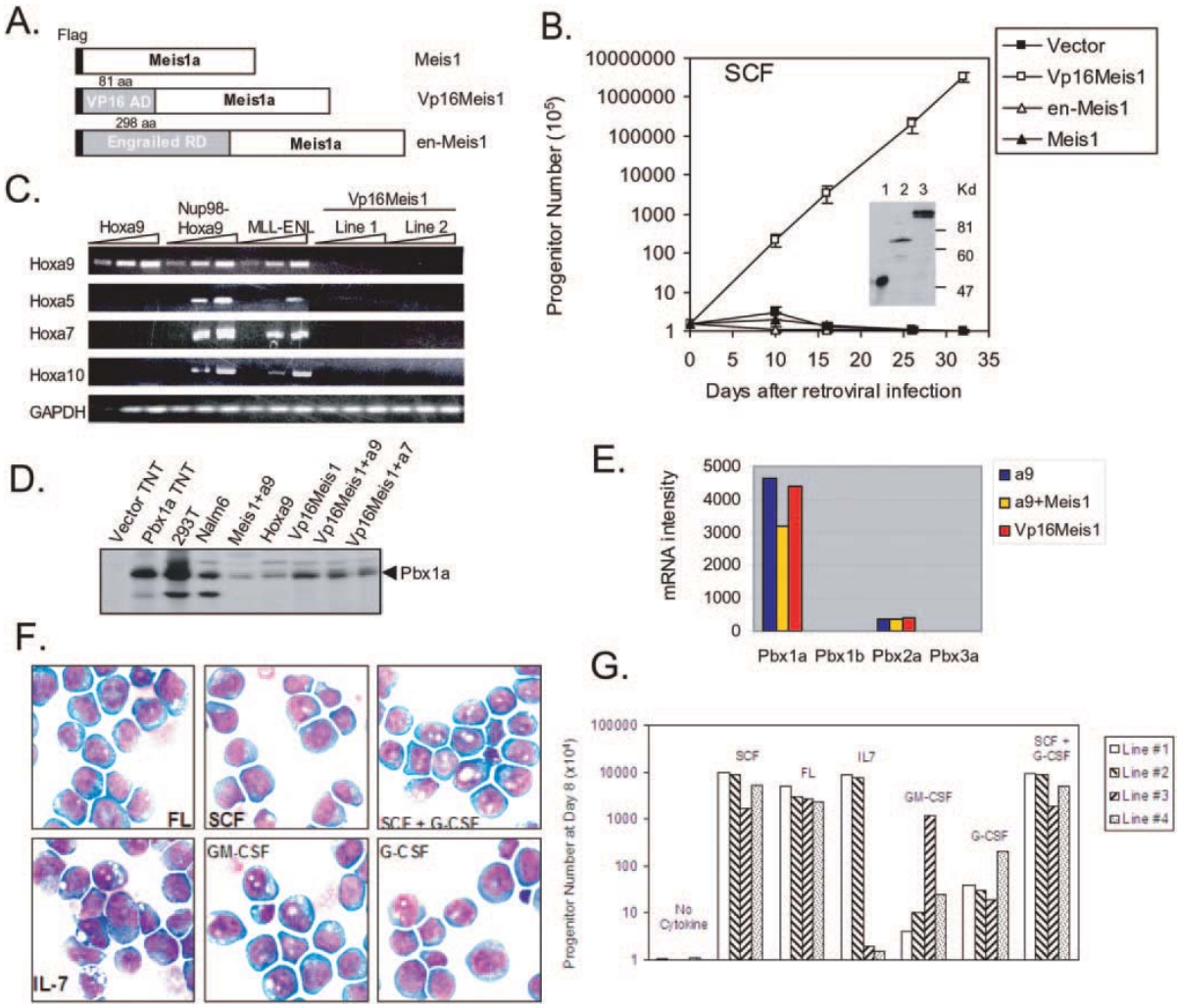

FIG. 2. Vp16-Meis1 immortalizes early hematopoietic progenitors in the absence of coexpressed *Hox* genes. (A) Depiction of Flag-tagged Meis1, Vp16-Meis1, and en-Meis1. (B) Proliferation kinetics of progenitors cultured in SCF, after infection with retrovirus encoding Vp16-Meis1, Meis1, or en-Meis1 followed by 3-day puromycin resistance selection. A total of 200,000 puromycin-resistant progenitors were plated at day 0, and culture medium was changed every 3 days. Error bars indicate standard deviations from three repeat experiments. The inserted panel indicates Western blot analysis of Meis1 (lane 1), Vp16-Meis1 (lane 2), and en-Meis1 (lane 3) expressed in NIH 3T3 fibroblasts with anti-Flag antibody. (C) Semiquantitative RT-PCR demonstrating that Vp16-Meis1 progenitors do not express *Hoxa5*, *Hoxa7*, *Hoxa9*, or *Hoxa10*, while progenitors immortalized by Nup98-Hoxa9 or MLL-ENL express these *Hox* genes. RNA was prepared from immortalized progenitor cultures 5 to 7 weeks after retroviral infection, when progenitor phenotypes were stabilized. *Gapdh* served as the cDNA internal control. Triangles indicate a 1:10 serial dilution of cDNA template from right to left. (D) Western blot analysis of Pbx1a protein levels in progenitors immortalized by Hoxa9 alone or with coexpressed Meis1 and by Vp16-Meis1 in the absence or presence of coexpressed Hoxa9/a7; positive and negative controls were 1 μl of in vitro transcription-translation (TNT) reaction mixture added with Pbx1a or empty expression vector. (E) mRNA expression level of Pbx isoforms quantified by Affymetrix arrays in progenitors immortalized by Hoxa9, Hoxa9 plus Meis1, or Vp16-Meis1. (F and G) Vp16-Meis1 progenitors proliferate in SCF or FL as the sole supporting cytokine. All four tested lines proliferated well in SCF or FL, two lines proliferated well in IL-7, and 5 to 20% of each cell line proliferated slowly in G-CSF or GM-CSF. The morphology of immortalized progenitors following Wright-Giemsa stain is illustrated in panel F, and their relative expansion in various cytokines is quantified in panel G.

retrovirus-encoded Vp16-Meis1 proteins in infected progenitors subjected to drug selection (Fig. 3D). The fact that the Vp16 transactivation domain can replace the function of the Meis1 CTD in immortalization of FL-responsive progenitors (16) supports the notion that gene activation is the essential biochemical function performed by the Meis1 CTD in establishing leukemia with Hoxa9.

Vp16-Meis1 induces basal transcription of *Meis1*-related signature genes. Previously, we demonstrated that the AML-initiating progenitors produced by coexpressed *Meis1* plus

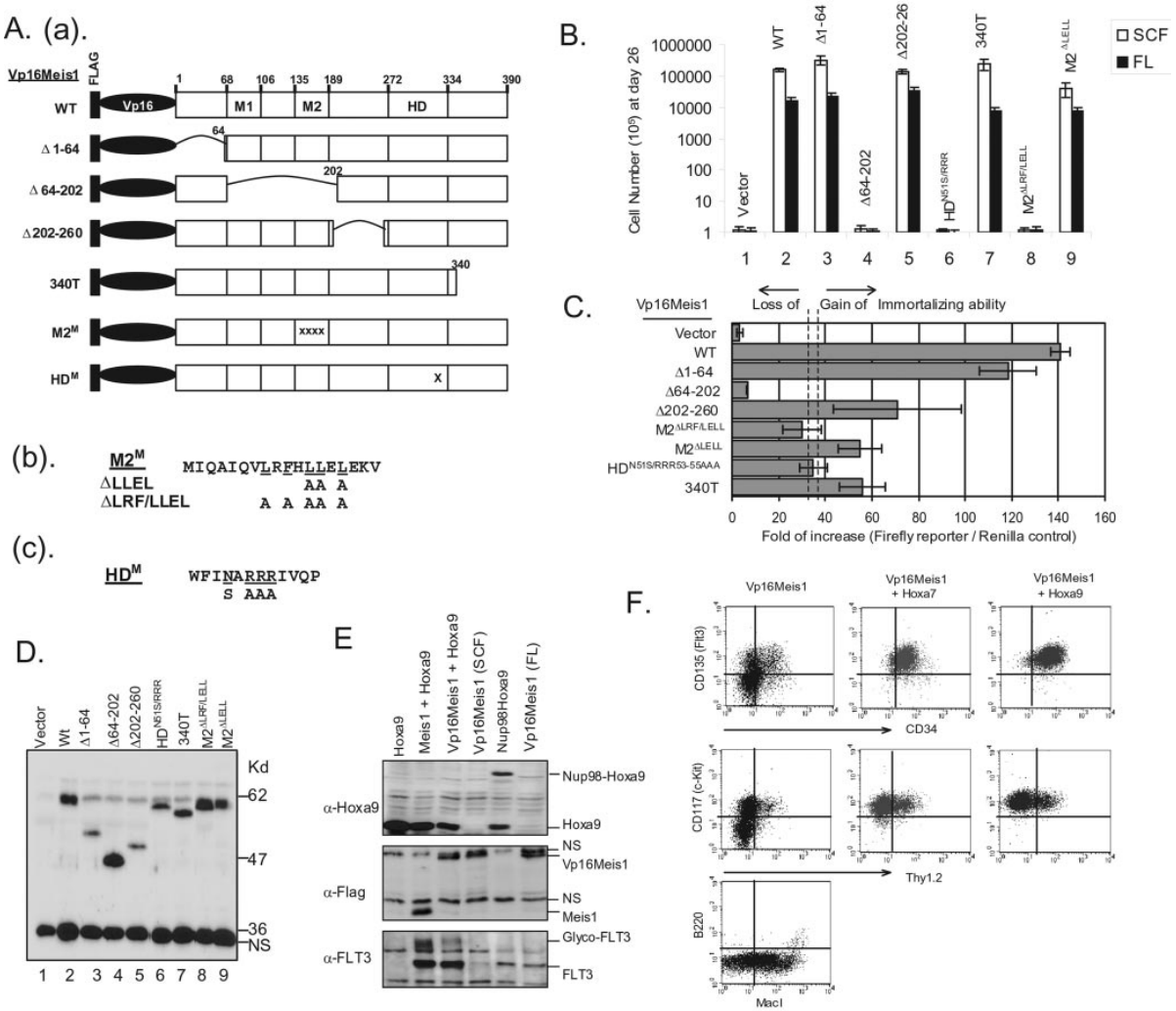

FIG. 3. Vp16 replaces the essential function of the Meis1 CTD and circumvents Hox cofactor dependence. (A) Depiction of Vp16-Meis1 wild-type and mutant constructs (a) and point mutations in M2 or in the HD (b and c). (B) Mutational analysis of domains required for immortalization by Vp16-Meis1 in SCF or FL. Plotted are the cumulative progenitor numbers after 26 days of culture following plating of 200,000 retrovirus-infected and puromycin-resistant Lin^- progenitors. Error bars indicate standard deviations from three duplicate cultures. (C) Transactivation of a Pbx-Meis-responsive luciferase reporter (7xPRS-luc) by Vp16-Meis1 wild type and mutants in the presence of Pbx1a in 293T cells: increase of normalized luciferase activity. Error bars represent the standard deviations from two duplicate experiments. (D) Immunoblot using anti-Flag antibody to examine retroviral expression of Vp16-Meis1, 1 week after infection of Lin^- progenitors followed by drug resistance selection shown in panel B (SCF). NS, nonspecific band. (E) Immunoblot demonstrating that Vp16-Meis1 activates a low level of *Flt3* expression in the absence of Hoxa9 (lanes 4 and 6), which is augmented by subsequent coexpression of *Hoxa9* (lane 3). (F) Typical presentation of FACS analysis of Vp16-Meis1-immortalized progenitors without (left panels) and with sequential retroviral infection of Hoxa7 or Hoxa9 (middle and right panels). Vp16-Meis1-immortalized progenitors (6 weeks after initial Vp16-Meis1 infection) were used for a sequential Hox infection, and cells were subjected to FACS analysis after cultivation for another 4 weeks.

Hoxa9 exhibited a genetic signature that includes stem cell-specific genes (i.e., *Meis1*-related signature genes, such as *Cd34*, *Flt3*, *Erg*, *Msi2h*, etc.) which were not expressed in non-leukemic progenitors immortalized by Hoxa9 alone (49). Because Vp16-Meis1 progenitors expressed *Flt3*, we evaluated the expression of other *Meis1*-related signature genes using FACS, immunoblotting, and microarray analysis. FACS demonstrated that Vp16-Meis1-immortalized progenitors were $Cd34^{low}$ $Flt3^{low}$ c-$Kit^{low/medium}$ $MacI^{variable}$ $B220^-$ $Cd19^-$ $Cd27^-$ $Thy1.2^{-/low}$ (Fig. 3F), a profile similar to that of progenitors immortalized by Meis1 plus Hoxa9 (49), with the major difference being a lower level of *Cd34* and *Flt3*. Immunoblot analysis confirmed a low level of Flt3 protein in Vp16-Meis1 progenitors (Fig. 3E). Analysis of Affymetrix gene expression arrays revealed that many of the previously identified *Meis1* signature genes were expressed at low to moderate levels

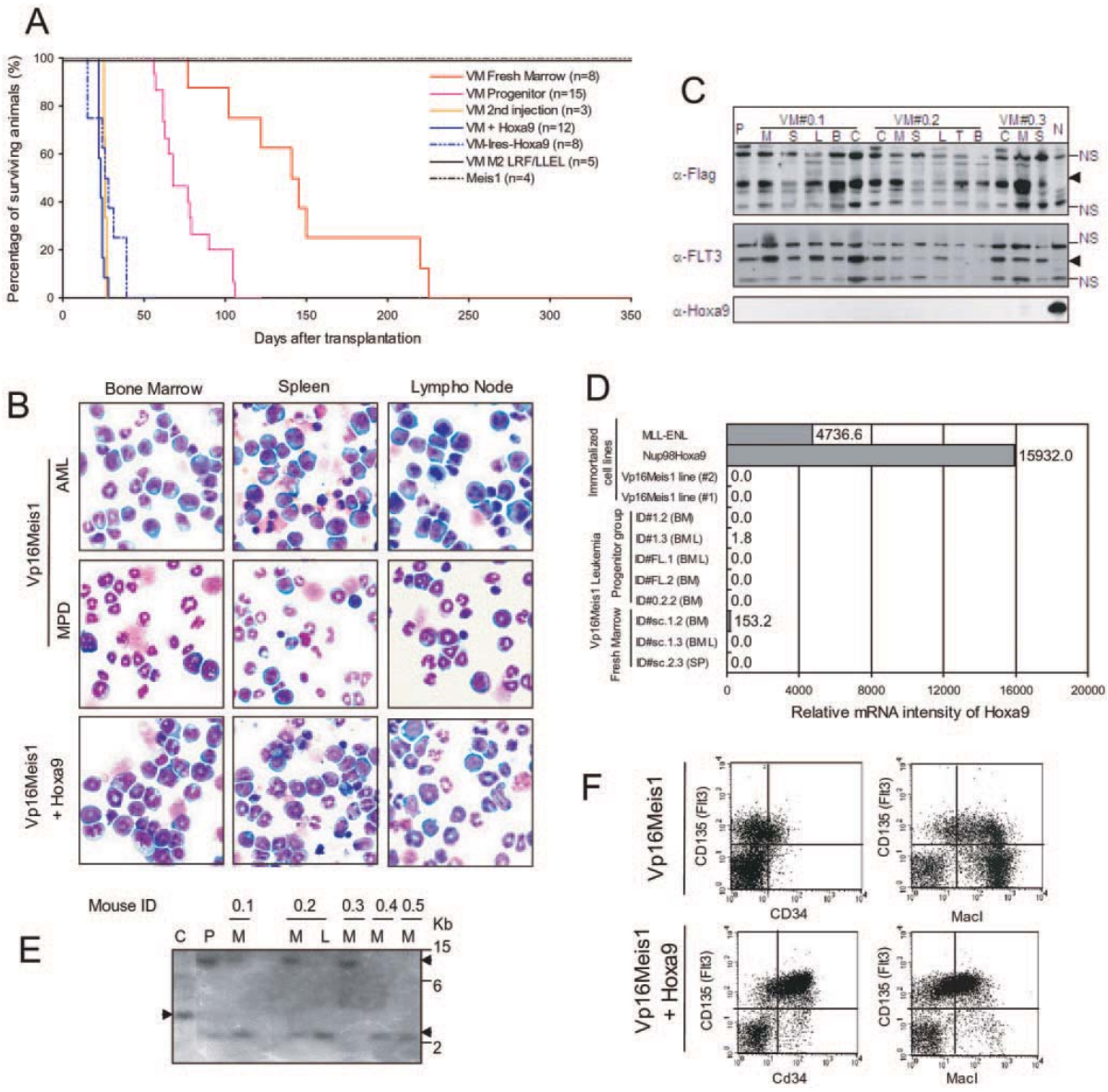

FIG. 4. Vp16-Meis1 causes AML and MPD by a mechanism independent of Hoxa7 or Hoxa9. (A) Survival curves for mice injected with Lin$^-$ marrow progenitors 48 h following infection with retrovirus expressing Vp16-Meis1 (VM, fresh marrow), a VM mutant defective in binding Pbx (M2 LRF/LELL), or Meis1, mice injected with progenitor cell lines immortalized by VM (VM progenitor) or by VM plus Hoxa9 (VM-Ires-Hoxa9), or mice injected with VM progenitors expressing retroviral Hoxa9 (VM+Hoxa9). The second injection was performed using bone marrow cells freshly extracted from a VM leukemic mouse. The *n* value indicates the cohort size (injected mice). (B) Wright-Giemsa stains of cells extracted from tissues of mice with AML or MPD induced by Vp16-Meis1 or by Vp16-Meis1 plus Hoxa9. (C) Western blot analysis of Vp16-Meis1, Flt3, and Hox in tissues from mice with leukemia caused by Vp16-Meis1. Arrowheads indicate specific bands. NS, nonspecific bands; N, Hoxa9 progenitors as a control; P, injected parental VM progenitors; M, marrow; S, spleen; L, lymph nodes; B, peripheral blood white cells; T, thymus; C, cell lines derived from marrow leukemic progenitors. (D) Real-time qPCR analysis of Hoxa9 mRNA levels in immortalized cell lines and in leukemias induced by Vp16-Meis1. Cell lines were the same as those used in Fig. 2C. Samples of leukemia induced by Vp16-Meis1 were derived from the experiment shown in panel A from either the fresh marrow group or the progenitor group. The amplicon of Hoxa9 targets sequences encoding the N-terminal domain, which does not exist in Nup98-Hoxa9. Values to the right of the bars represent relative values of Hoxa9 transcript intensity, after verification of PCR specificity, threshold setup, relative transcript intensity calculated from the cycle threshold value, and normalization against *Gapdh*. BM, bone marrow; SP, spleen; BML, leukemic cell lines from bone marrow. (E) Southern blot analysis of Vp16-Meis1-retrovirus integration sites among leukemia tissues, as indicated by arrowheads. C, a different VM progenitor line as a negative control; P, injected parental progenitors; M, bone marrow; L, lymph node. (F) FACS analysis of leukemia induced by Vp16-Meis1 alone or with coexpressed Hoxa9.

TABLE 2. Phenotypic characterization of Vp16-Meis1-induced leukemia in mice[a]

Parameter	Vp16-Meis1		Vp16-Meis1 + Hoxa9	Control (avg)
	Fresh marrow	Progenitor line		
No. of mice examined	7	11	5	4
Disease latency (days)	134 ± 49	74 ± 18	24 ± 5	NA
Organ wt (mg)				
Spleen	625 ± 213	723 ± 338	396 ± 219	106
Lymph node	58 ± 28	51 ± 39	15 ± 8	<1
Thymus	40 ± 18	51 ± 29	54 ± 27	29
Peripheral blood cell analysis				
WBC[b] (10^3/ml)	100 ± 36	58 ± 47	ND	3
Granulocytes (%)	74 ± 6	68 ± 30	ND	25
Lymphocytes (%)	23 ± 9	31 ± 27	ND	67
Platelets (10^3/ml)	370 ± 136	216 ± 105	ND	817
Hematocrit (%)	34 ± 7	40 ± 10	ND	45
FACS analysis of marrow leukemia cells (%)				
Mac-I	73 ± 15	84 ± 14	56 ± 33	NA
B220	2 ± 1	0 ± 0	10 ± 9	NA
Thy1.2	2 ± 1	1 ± 1	15 ± 10	NA
Cd135 (Flt3)	56 ± 31	28 ± 23	55 ± 33	NA
Scored as AML[c]	4	6	5	NA
Scored as MPD[c]	3	5	0	NA

[a] Values are averages ± standard derivations unless otherwise indicated. ND, not determined; NA, not applicable.
[b] WBC, white blood cells.
[c] According to the French-American-British classification, in which counts of immature myeloblasts in marrow are ≥30% for AML and ≤30% for MPD.

(see Fig. 5D and E and Table 3, below). The additional genes (identified as described in Materials and Methods), *Msi2h*, *Sox4*, *Dbx4*, *P2rx3*, *Bcl2*, and *Sesn3*, which were expressed in Vp16-Meis1 progenitors, were also found expressed at significantly higher levels in Hoxa9-plus-Meis1 progenitors than in Hoxa9 progenitors and have been added to the list of *Meis1*-related signature genes (see Table 3, below). The expression of *Cd34*, *Flt3*, *Erg*, *Msi2h*, *Il7r*, *Grp56*, and *Tizl1b* was further confirmed by semiquantitative RT-PCR (data not shown) and real-time PCR (see Fig. 5E).

Vp16-Meis1 induces AML and MPD in vivo. Activation of *Meis1*-related signature genes suggested that Vp16-Meis1 progenitors would initiate leukemia. Indeed, AML arose in each of 12 mice injected with three different Vp16-Meis1-immortalized progenitor lines (2×10^6 cells per mouse), as well as in each of 8 mice injected with Lin^- marrow progenitors freshly infected with Vp16-Meis1 retrovirus (5×10^5 cells per mouse) with a latency of 74 and 134 days, respectively (Fig. 4A and Table 2). Mice injected with progenitors transduced with a Pbx interaction-defective mutant, $M2^{\Delta LRF/LELL}$, did not develop leukemia over 370 days. Leukemia cells were factor dependent, expressed retroviral Vp16-Meis1 (Fig. 4C), and contained the same retroviral integration sites as those within the oligoclonal parental progenitors (Fig. 4E), indicating that they arose from injected cells. FACS analysis demonstrated that the majority of leukemic cells were myeloid ($Mac\text{-}I^+$ $B220^-$ $Cd19^-$ $Thy1.2^-$ $c\text{-}Kit^+$) (Fig. 4F and Table 2). Mice exhibited two forms of disease. The first (10 of 18 examined animals) was AML, in which 30 to 95% of leukemic cells stained as immature myeloblasts. The second (in 8 out of 18) was a myeloproliferative disease (MPD) in which 70 to 90% of leukemia cells exhibited significant neutrophil maturation (Table 2 and Fig. 4B). In both diseases, mice presented with 3- to 12-fold enlarged spleens, 10- to 50-fold enlarged lymph nodes, and 4- to 40-fold increases in circulating myeloid cells (Table 2). Comparable amounts of Vp16-Meis1 protein were present in myeloid cells from both diseases (data not shown), discounting the possibility of a reactive granulocytosis. Over 50% of leukemic progenitors expressed *Flt3* (FACS in Fig. 4F and Table 2 and immunoblot in Fig. 4C). Thus, Vp16-Meis1 causes myeloid leukemia with 100% penetrance, and leukemic myeloblasts retain a low level of *Flt3* and *Cd34* expression, similar to the parental cells.

Secondary recipients of leukemic marrow acquired leukemia with a much shorter latency, averaging 26 days (Fig. 4A), indicating that additional genetic change accelerates leukemogenesis initiated by Vp16-Meis1. Because *Hoxa9* and *Hoxa7* are coactivated with *Meis1* in BXH2 mouse AML, we evaluated whether *Hoxa9* or *Hoxa7* might be activated as a cooperating event during progression of Vp16-Meis-induced leukemia. Immunoblot analysis using a polyclonal antibody against the homeodomain of Hoxa9, which also detects Hoxa7 less efficiently, revealed no apparent up-regulation of these two proteins in 10 independent leukemias, regardless of whether AML arose from progenitor lines or from freshly infected marrow (Fig. 4C). This result was confirmed by real-time qPCR (Fig. 4D): in seven of eight leukemias examined (three from the fresh marrow group and the other five leukemias from the progenitor group [as in Fig. 4A]), *Hoxa5*, *Hoxa7*, *Hoxa9*, and *Hoxa10* transcripts were absent or were present at levels lower than 0.01% of that expressed in progenitors immortalized by Nup98-Hoxa9 or MLL-ENL (results for Hoxa9 are exemplified in Fig. 4D). A single exception, exhibiting a very low level of *Hoxa9* (~3% of the Hoxa9 level expressed in MLL-ENL progenitors) (sample sc1.2), also expressed *Hoxa5*, *Hoxa7*, and *Hoxa10* at levels 1 to 5% of that expressed in progenitors immortalized by MLL-ENL. Thus, the large majority of myeloid leukemias induced by Vp16-Meis1 did not acquire activation of endogenous *Hoxa7* or *Hoxa9* genes as secondary cooperating events.

Expression of *Hoxa9* or *Hoxa7* in Vp16-Meis1 progenitors induces further activation of *Meis1* signature genes, stimulates proliferation, and accelerates disease progression to the level of bona fide AML myeloblasts. An important unresolved question concerning the mechanism of cooperativity by *Hox* plus *Meis1* is whether Hoxa7 or Hoxa9 assists Meis1 in the activation of *Meis1*-related signature genes or Meis1 functions independent of coexpressed Hox proteins. Because Vp16-Meis1 progenitors expressed low levels of *Meis1*-related signature genes and expressed no endogenous *Hox* genes, they represented a good cell model to test whether Hoxa9 or Hoxa7 could further activate expression of *Meis1*-related signature genes. Strikingly, retroviral expression of *Hoxa9* or *Hoxa7* in Vp16-Meis1 progenitors induced strong proliferation (Fig. 5B), strong up-regulation of Flt3 and Cd34 proteins (Fig. 3F and 5A), and 3- to 20-fold activation of other *Meis1* signature genes (Table 3 and Fig. 5D). The reliability of the Affymetrix array analysis was verified using semiquantitative RT-PCR (data not shown) and real-time qPCR (Fig. 5E). Six newly

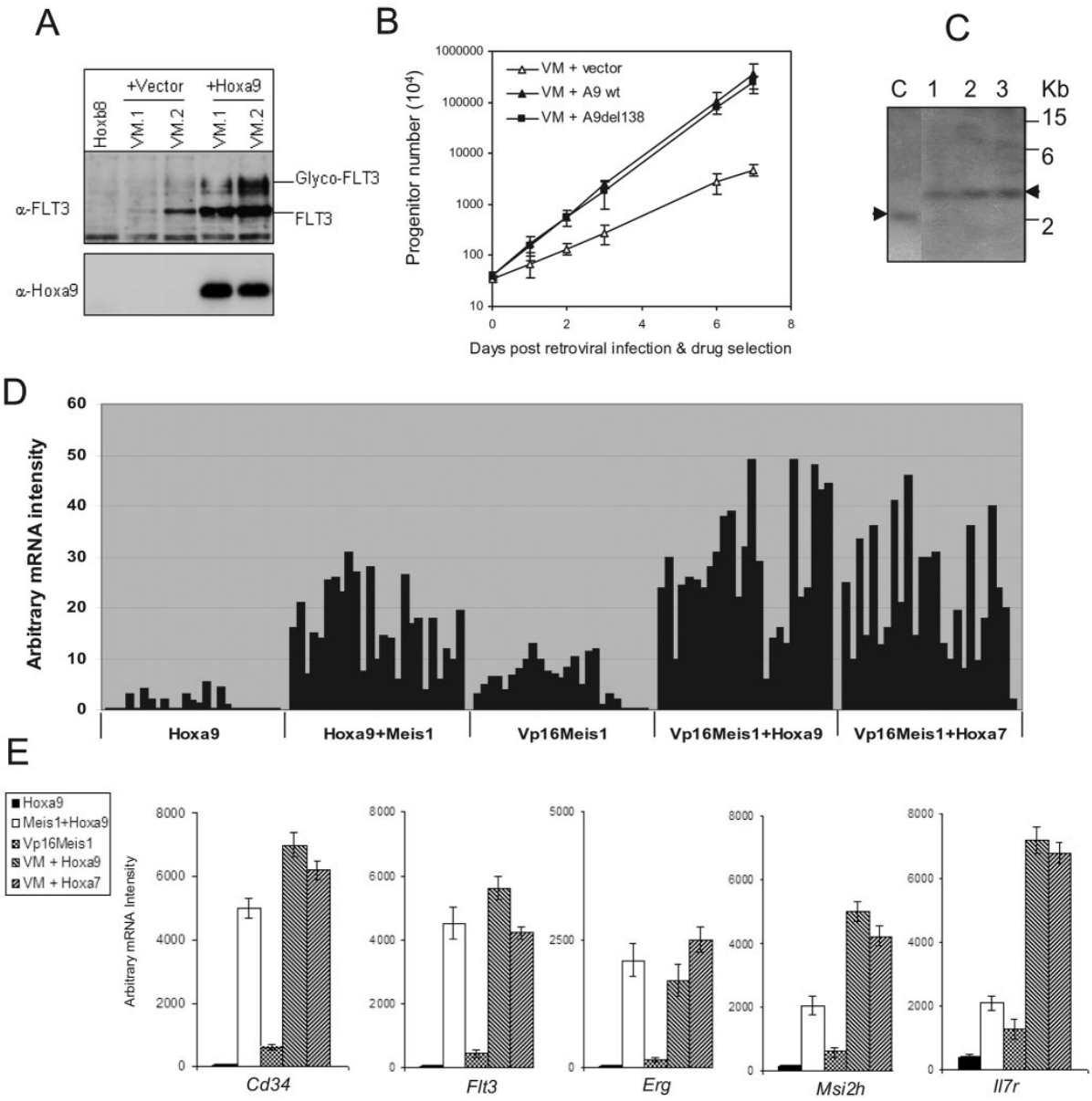

FIG. 5. Both Hoxa9 and Hoxa7 activate expression of *Meis1*-related signature genes in Vp16-Meis1 progenitors. (A) Immunoblot analysis of Flt3 in two Vp16-Meis1 progenitor lines (VM.1 and VM.2) before and after coexpression of *Hoxa9*, analyzed subsequently by Affymetrix gene arrays. (B) Proliferation rates of Vp16-Meis1 progenitors after infection with MSCV-neo retrovirus encoding empty vector (open triangles), wild-type Hoxa9 (filled triangles), or Hoxa9 Δ1-138 (A9del38; filled squares). Three different lines of Vp16-Meis1 progenitors were used for infection, and 400,000 G418-selected progenitors were plated in SCF-containing medium at day zero. Error bars represent standard deviations. (C) Southern blot analysis of Vp16-Meis1-retrovirus integration sites demonstrated the clonality of Vp16-Meis1 progenitors before (lane 1) and after expression of Hoxa9 (lane 2) or Hoxa7 (lane 3). Lane C, control progenitor line containing a different retroviral integration site. (D) Overall expression pattern of the 25 *Meis1*-related signature gene listed in Table 3, quantified using Affymetrix gene arrays in progenitors immortalized by Hoxa9 alone or with coexpressed Meis1 or by Vp16-Meis1 alone or superinfected with Hoxa9/a7 retrovirus. The *y* axis indicates relative mRNA intensity. (E) Comparison of expression levels of five representative *Meis1*-related signature genes shown in panel D and Table 3 among different progenitors, using real-time PCR. The template was first-strand cDNA produced by reverse transcription using pooled mRNA purified from two progenitor lines. Error bars represent the standard deviations from two repeated experiments.

TABLE 3. Gene expression profiling analysis of progenitors expressing Vp16-Meis1 or coexpressing Hox

Activation group and gene[b]	Gene description	GenBank accession no.	Transcript level score[a]				
			a9 (n = 5)	M+a9 (n = 5)	VM (n = 3)	VM+a9 (n = 3)	VM+a7 (n = 3)
Weak to moderate activation by Vp16-Meis1, further activation by Hox							
Cd34	Cd34 antigen	NM_133654	137	3,270	610	4,890	5,040
Flt3	Fms-like tyrosine kinase 3	NM_010229	<50	4,142	995	5,940	1,992
Il7r	Interleukin-7 receptor	NM_008372	<50	692	680	1,000	3,350
Crlr	Calcitonin receptor-like receptor	AF209905	<50	690	193	1,305	1,785
Msi2h	Musashi homologue 2; RNA-binding protein	BB418489	<50	756	145	3,875	1,425
Erg	v-Est-related gene	XM_622815	<50	884	70	625	1,775
Sox4	SRY box containing gene 4	NM_009238	536	1,376	1,050	2,795	1,310
Gpr56	G-protein-coupled receptor 56	AK141886	<40	126	50	575	990
Tilz1b	TSC22-related inducible leucine zipper 1b	AF201285	370	1,964	1,250	6,375	5,905
Ptprcap	CD45-associated protein	NM_016933	<50	1,160	520	1,400	2,035
Satb1	Special AT-rich sequence-binding protein	NM_009122	154	1,512	582	1,525	1,010
Ly86	MD1; lymphoid toll receptor	NM_010745	<50	1,350	513	1,900	2,300
Ngn/RC3	Neurogranin, protein kinase C substrate	AK002933	276	2,896	1,658	9,715	6,185
C1qR1	Complement subcomponent 1q, receptor 1	AK150385	630	3,030	1,308	4,900	2,875
Tmsb10	Thymosin beta-10	BB096368	1,080	6,320	1,718	6,350	3,175
Dbx4	DEAD (Asp-Glu-Ala-Asp) box 4	AK014844	<50	1,968	50	4,450	115
Ednra	Endothelin receptor type A	AK135555	<50	588	50	2,370	1,195
P2rx3	Purinergic receptor P2X, 3; ion channel	BC023089	<50	496	50	2,150	1,000
Kcna3	Potassium voltage-gated channel 3	AI323624	84	660	210	590	400
Wbscr15	Transmembrane adaptor protein	AF257136	170	1,374	258	1,075	1,500
Unknown	Unknown	AV365503	<50	402	395	4,875	920
Unknown	Unknown	BG071655	<50	418	113	550	405
Activation by Vp16-Meis1, no superactivation by Hox							
Nrip1	RIP140; Nuclear receptor-interacting protein	BB764550	60	310	255	283	500
Bcl2	B-cell leukemia/lymphoma 2; antiapoptosis	BI664467	514	2,660	1,415	1,400	1,925
Sesn3	Sestin 3	AK017464	70	836	605	825	370
Activation by Hox only							
c-*kit*	Stem cell factor receptor	X65997	2,350	2,390	831	3,850	2,675
Control							
Gapdh	Glyceraldehyde-3-phosphate dehydrogenase	BC083080	12,890	14,016	11,021	13,123	14,125
Actb	β-Actin	AK147787	13,530	15,168	13,200	14,125	16,450

[a] Score generated by the microarray scan program. M, Meis1; VM, Vp16-Meis1; a9, Hoxa9; a7, Hoxa7. The value of n represents the number of different immortalized progenitor lines (all cultured in SCF) that were used for analysis.

[b] Genes shown in bold have been implicated in the literature as either HSC markers or enriched in stem cell populations.

identified genes (*Msi2h*, *Sox4*, *Dbx4*, and *P2rx3*, plus two unknown genes) were activated by Hoxa9 in Vp16-Meis1 progenitors and expressed at much higher levels in Hoxa9-plus-Meis1 progenitors than in Hoxa9 progenitors, and they have been added to our list of *Meis1* signature genes (Table 3).

Vp16-Meis1 progenitors expressing *Hoxa9* or *Hoxa7* contained the same Vp16-Meis1 retroviral integration site as parental progenitors (Fig. 5C), ruling out the possibility that these dramatic transcriptional changes arose from selective expansion of an unrelated $Cd34^+$ $Flt3^+$ stem cell subpopulation that might still exist in cultures. Expression of Hoxa9 in Vp16-Meis1 progenitors reduced AML latency to an average of 24 days (Fig. 4A) and generated AML that was more similar to the myeloblastic phenotype (Fig. 4B, bottom panels), comprised of Lin^- and $MacI^+$ $B220^-$ subpopulations with high levels of Flt3 and Cd34 (Fig. 4F, bottom panels). This suggests that Hoxa9 and Hoxa7 participate in gene coactivation with Meis1.

The Hoxa9 N-terminal domain, which is essential for all transforming functions of Hoxa9, is dispensable for activating Flt3 expression and transforming properties in Vp16-Meis1-expressing progenitors, suggesting that it performs an activation function replaced by Vp16 on promoters co-occupied by Vp16-Meis1 and Hoxa9. The fact that fusion of Vp16 to Meis1 replaces Hox function, combined with the fact that both Meis1/Vp16-Meis1 and Hoxa9/a7 activate transcription of the same *Meis1*-related signature genes, favors a model in which Meis1, Hox, and Pbx directly bind these signature gene promoters that mediate leukemogenesis. If this model were correct, then Hoxa9 transactivation domains that are essential for activation of the *Meis1* signature genes in the context of wild-type Meis1 might be dispensable in the context of Vp16-Meis1. Indeed,

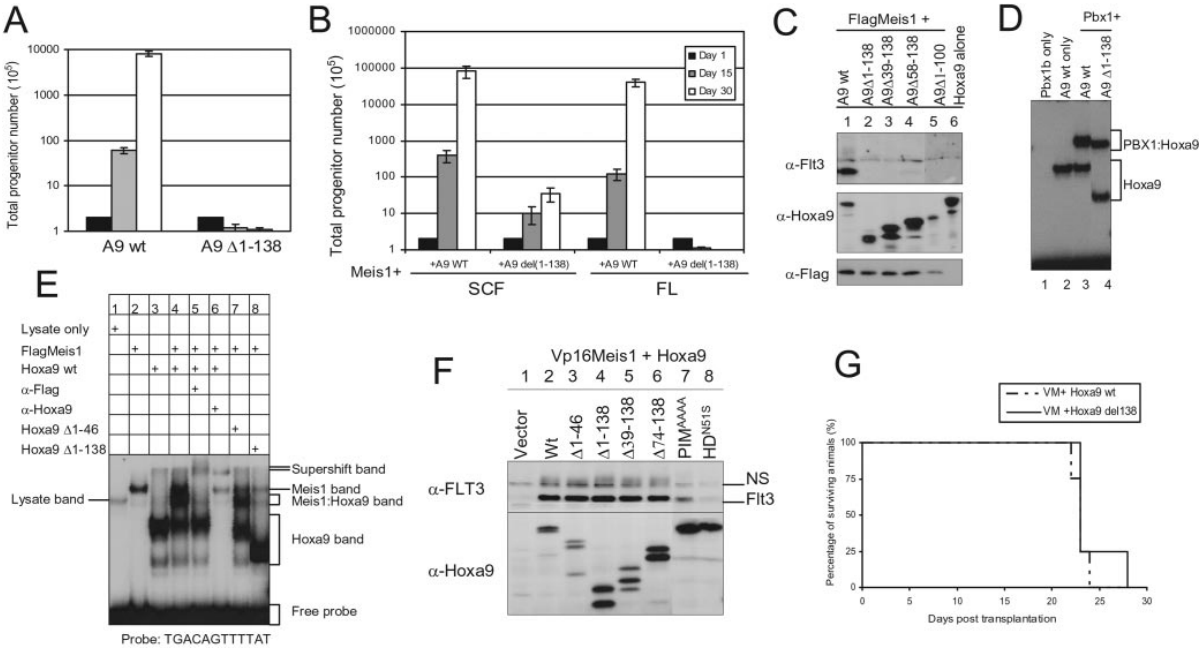

FIG. 6. The N-terminal residues 1 to 138 of Hoxa9 are dispensable for activation of *Flt3* and transformation in Vp16-Meis1-expressing progenitors but are required for Hoxa9-mediated immortalization and Meis1-cooperating functions in terms of *Flt3* activation and transformation. (A) Growth kinetics of primary bone marrow progenitors infected with retrovirus encoding either wild-type (WT) Hoxa9 or Hoxa9Δ1-138, followed by selection for 3 days in G418. The number of progenitors cultured in GM-CSF was counted on days 1 (solid bars), 15 (gray bars), and 30 (open bars) after drug selection. Error bars represent standard deviations of three duplicates. (B) Growth kinetics of primary ScaI$^+$ Lin$^-$-enriched progenitors infected with a 1:1 mixture of retrovirus encoding Meis1 and that encoding Hoxa9 (WT or Δ138), followed by dual drug resistance selection and cultivation in SCF or FL. Duplicate cultures were evaluated, and error bars indicate standard deviations. (C) Expression of Flt3, Hoxa9, and Flag-Meis1, 2 weeks after coinfection (as for panel B, with SCF and dual selection) of ScaI$^+$ Lin$^-$-enriched marrow progenitors with retrovirus encoding Flag-Meis1 and Hoxa9. (D) Heterodimer formation between Pbx1 and Hoxa9 examined by EMSA on the DNA element TGATTTAT. The identity of proteins added to the binding reaction mixture is indicated above each lane. (E) Interaction between Meis1a and wild-type or mutant Hoxa9 examined by EMSA to the DNA probe TGACAGTTTTAT. Recombinant proteins produced by coupled transcription-translation were lysate only (lane 1), Flag-Meis1 (lane 2), Hoxa9 (lane 3), and Flag-Meis1 plus Hoxa9 (lanes 4 to 8). Antibody against Flag-Meis1 (lane 5) or Hoxa9 (lane 6) was added to supershift protein-DNA complexes. (F) Expression levels of Flt3 and Hoxa9 in Vp16-Meis1 progenitors 3 weeks after retroviral expression of wild-type or mutant forms of Hoxa9 followed by drug selection in SCF-containing medium. (G) Survival curves of mice intravenously injected with 1×10^6 Vp16-Meis1 progenitors superinfected with retrovirus encoding Hoxa9 WT ($n = 4$) or Δ138 ($n = 4$).

the Hoxa9 NTD (residues 1 to 138), which has been reported to contain a transactivation domain and Meis1 interaction motif (41), which is essential for immortalization by Hoxa9 alone in GM-CSF (Fig. 6A) or in SCF (not shown), is essential for immortalization of SCF- or FL-dependent progenitors with Meis1 (Fig. 6B), and is essential for Meis1-dependent production of Flt3 in infected ScaI$^+$ Lin$^-$ marrow progenitors (Fig. 6C, lanes 2 to 5 versus lane 1), was dispensable for Hoxa9-induced proliferation (Fig. 5B), for Flt3 up-regulation (Fig. 6F, lane 4 versus lane 2) in Vp16-Meis1 progenitors, or for increasing the aggressiveness of leukemias produced by Vp16-Meis1 progenitors (Fig. 6G). By contrast, the DNA binding and Pbx interaction mutants Hoxa9-HD^{N51S} and Hoxa9-PIM^{AAAA} (7) exhibited no activation or minimal activation (25% of wild type) of *Flt3* transcription (Fig. 6F, lanes 7 and 8 versus lane 2). Hoxa9Δ1-138 retained its ability to interact with Pbx1 on DNA (Fig. 6D, lane 3 versus lane 4) and lost its heterodimerization abilities with Meis1 on DNA (Fig. 6E, lane 4 versus lane 8). The fact that the NTD of Hoxa9 is dispensable for Hoxa9 transforming functions in Vp16-Meis1 progenitors suggests that its transactivation function is replaced by the persistent transactivation function of a Vp16-Meis1 complex bound to an adjacent DNA element.

Hoxa9 and Meis1 directly bind the *Flt3* proximal promoter and 5′ enhancer regions. ChIP was used to examine whether Hoxa9 and Meis1 bind the promoter of *Flt3*, the prototypic *Meis1* signature gene whose transcription is further augmented by either Hoxa9 or Hoxa7. Primers were designed to randomly cover 10-kb upstream *Flt3* promoter/enhancer sequences (Fig. 7A). ChIP demonstrated that Hoxa9 was recruited to the proximal promoter (P3) and 5′ enhancer regions (P5 and P6) in progenitors expressing either *Hoxa9* alone or coexpressing *Meis1* plus *Hoxa9* (Fig. 7B) and that Meis1 (Flag tagged; anti-Flag used for ChIP) was recruited to loci P3, P5, and P6 only in progenitors immortalized by *Hoxa9* plus *Meis1*. The same ChIP results were observed using antibodies against the N terminus or homeodomain of Meis1 (data not shown). Interestingly, recruitment of Meis1 was accompanied by acet-

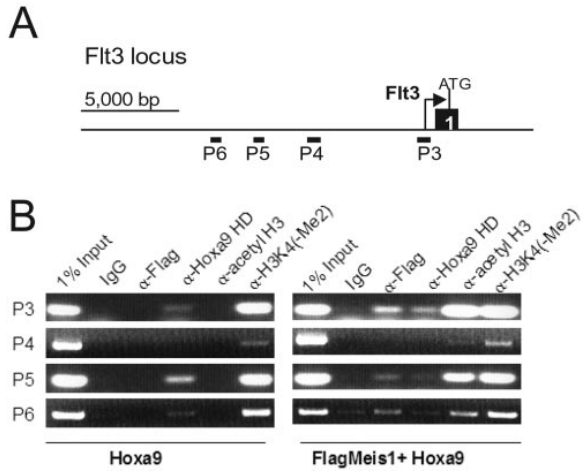

FIG. 7. Meis1 and Hoxa9 bind to the *Flt3* proximal and distal promoter regions. (A) Schematic of the murine *Flt3* locus. Black boxes represent exons, and the arrowhead represents the putative transcription start site. Black bars P3 to -6 designate positions of the amplicons used in ChIP analysis; ATG indicates the position of the initiation methionine. (B) ChIP analysis examining the recruitment of Hoxa9 and Flag-Meis1 and the status of histone modification on *Flt3* promoters (loci P3 to P6) in myeloid progenitors immortalized by Hoxa9 alone or by both Hoxa9 and Flag-Meis1. Lanes were loaded with products of PCR amplification using template prepared from either 1% sheared chromatin (input control) or immunoprecipitated chromatin using nonspecific antibodies (IgG) or specific antibodies against the Flag tag, the homoedomain of Hoxa9, acetylated histone H3, or dimethylated histone 3 Lys 4 (H3K4).

ylation of histone H3 along *Flt3* promoter and enhancer regions, while both cell lines exhibited dimethylation of histone H3 Lys 4 (H3K4) within the same regions. All signals were specific, based on the cell type specificity and precipitation control results using nonspecific IgG. These results indicate that Meis1 may induce histone acetylation prior to activation of *Flt3* transcription.

DISCUSSION

Here we demonstrated that in the absence of coexpressed *Hox* genes, a dominant activating form of Meis1 (Vp16-Meis1) sustains self-renewal of undifferentiated hematopoietic progenitors that exhibit leukemic potential in vivo, functions that are not possessed by either wild-type Meis1 or the dominant repressive form of Meis1, en-Meis1. We then demonstrated that Vp16-Meis1 mimics the combined functions of Hoxa9 and Meis1 in terms of activating expression of *Meis1*-related signature genes, albeit at low levels, which are characteristically expressed in leukemic progenitors immortalized by Hoxa9 plus Meis1 but not in nonleukemic progenitors immortalized by Hoxa9 alone. Next, we demonstrated that Hoxa9 and Hoxa7 further augment transcription of most of these *Meis1* signature genes (*Hox*/*Meis1* signature genes, as a more proper definition), indicating that their transcription is driven by the combined functions of Meis1 and Hoxa7/a9 functions in AML. The mechanism of cooperativity is implicated as promoter co-occupancy by Hoxa7/a9 and Pbx1/2-Meis1 complexes, based on the result that fusion of the Vp16 domain to Meis1 replaced both the essential function of the Hoxa9 NTD and the Meis1 CTD and was verified as such for the *Flt3* promoter, using ChIP analysis. Collectively, our data support a model in which a subset of leukemogenesis-related promoters are directly bound and activated by complexes containing Hoxa7/a9, Meis1, and Pbx1/2.

Four transcriptional principles related to Meis1 and its interacting cofactors in hematopoietic progenitors are suggested by our analysis. First, the fact that Vp16-Meis1–Pbx complexes enforce self-renewal of leukemic stem cells in vivo suggests that Meis1-Pbx complexes regulate progenitor expansion during normal hematopoiesis by activating target gene transcription. Second, the fact that Hoxa7 and Hoxa9 augment expression of *Meis1* signature genes in Vp16-Meis1 progenitors suggests that Hox proteins actively participate in transactivation of *Meis1*-related signature genes in normal hematopoiesis. Prior to this report, there was no evidence that Hoxa7 or Hoxa9 controlled expression of Meis1 target genes in leukemia. Third, the mutational analysis of Hoxa9 and Meis1 domains critical for their functions in Vp16-Meis1 progenitors suggests a model in which all three homeodomain proteins—Pbx1/2, Meis1, and Hoxa7/a9—cooperate on single promoters critical for establishing the leukemogenic stem cell phenotype (Fig. 8). Specifically, the Meis1 CTD and the Hoxa9 NTD may recruit cofactors harboring HAT activity (Fig. 8), functions replaced by the Vp16 domain in Vp16-Meis1. Fourth, the ability of the C-terminal half of Hoxa9 to activate transcription of *Flt3* in Vp16-Meis1 progenitors in a manner as robust as that

FIG. 8. Model of Pbx, Meis (Vp16-Meis1), and Hox complexes binding to a subset of promoters required for expression of leukemogenesis. Numbers near the arrowheads indicate the following transcriptional activities: 1, a signal-induced transactivation mediated by the Meis1 CTD; 2, Hoxa9-NTD-mediated transactivation; 3, transactivation function mediated by the Hoxa9 C-terminal half, residues 139 to 271; 4, transactivation by the Vp16 domain fused onto Meis1, by recruiting HAT. The Vp16 domain replaces the function mediated by the Meis1 CTD and Hoxa9 NTD, suggesting that the Meis1 CTD and Hoxa9 CTD might recruit cofactors containing HAT activity and the Hoxa9 C-terminal half might utilize a different transactivation mechanism, such as recruiting factors harboring chromatin remodeling factor. AD, activation domain; RD, repression domain.

of wild-type *Hoxa9* suggests that this region possesses an additional transcriptional function which might be, for example, recruiting histone methyltransferase or chromatin remodeling factors (Fig. 8) that complements those provided by the Meis1 CTD and Hoxa9 NTD. The biochemical activities responsible for the N-terminal and C-terminal transactivating functions of Hoxa9 remain to be determined. This hypothesis, which is based on the genetic and cellular properties of leukemic progenitors, is consistent with physical interaction studies, which also found Meis1, Hoxa9, and Pbx2 in single nuclear complexes in myeloid cells (44), and reporter studies, which delineated cooperating functions of Meis1, Pbx1, and Hoxa1 proteins on regulation of the *Hoxb1/b2* enhancer (16, 21).

We also demonstrated that Hoxa7 is functionally redundant with Hoxa9 in terms of its Meis1-independent ability to arrest differentiation of nonleukemic progenitors and its Meis1-dependent function of targeting SCF- or FL-dependent leukemia-initiating progenitors that express *Flt3*. *Hoxa7* was originally identified as a locus coactivated with *Meis1* in BHX2 mouse leukemia (32) and activated in leukemia induced by large-scale retroviral insertional mutagenesis (23). *Hoxa7* was also suggested to be a crucial downstream mediator of MLL fusion oncoproteins (3, 50). Our results imply that Hoxa7, like Hoxa9, controls HSC expansion in cooperation with Meis1 and is likely to form interacting complexes. While Hoxa7 does not bind Meis1 in gel shift analysis (43), our data (as suggested by Hoxa9Δ1-138) suggest that it interacts with Pbx-Meis1 complexes via Pbx on target promoters as others have hypothesized previously (21). The promoter co-occupancy model would also account for leukemic cooperativity between Meis1 and Hoxb6/b3, which are also not predicted to bind Meis1 directly. We predict that coexpression of *Meis1* and *Hoxb6/b3* in SCF-dependent immortalized progenitors would also result in transcriptional activation of *Flt3* and other *Meis1* signature genes.

The *Hox/Meis1*-related signature genes that are coactivated by Meis1 plus Hox are involved in normal HSC biology and implicated in leukemogenesis. *Cd34* and *Flt3* are prominent HSC markers (1). Flt3 catalytic function is activated by mutations in over one-third of human AML, and we propose that *Flt3* expression permits expansion of LSCs in response to FL in stem cell niches. *Gpr56* (20), *Msi2h* (34), *Erg* (48), *C1qR1* (10, 48), and *Wbscr5* (48) are enriched in HSC or other tissue-type stem cells. The *Msi2h*-related gene *Msi1* is crucial for maintenance of neuronal stem cells (39). The *Ets*-related transcription factor *Erg* is fused to TLS/FUS and EWS in leukemia and Ewing sarcoma, respectively (14, 35). *Il7r* is important for lymphoid progenitor expansion, and *Gpr56* is overexpressed in brain tumors and mutated in a genetic disorder involving brain cortical malformation (36, 42). It is possible that up-regulation of the *Grb2*-interacting adaptor *Wbscr5*/*LAB* (22) contributes to specific signaling pathways in HSCs. Understanding functions of these genes will cast additional light on how they contribute to the LSC phenotype.

Previous studies reported over 200 genes regulated by Hoxa9 in leukemia cell lines or in $CD34^+$ HSCs (11, 12), but with the exception of *Erg*, these genes do not include the *Hox/Meis1*-activated signature genes examined herein. It is possible that studies using leukemia cell lines do not identify these signature genes because such genes are already expressed at high basal levels in the control parental progenitors. Alternatively, these *Hox/Meis1* signature genes may not be activated by introduction of exogenous *Hoxa9* if progenitors do not express essential cofactors, such as *Meis1*. Indeed, Hoxa9 alone does not activate any of the signature genes, as exhibited by Hoxa9-immortalized progenitors. When exogenous Hoxa9 is expressed in normal $CD34^+$ HSCs, the expression of endogenous *Hox* and *Meis1* may preclude significant further activation of these *Hox/Meis1* signature genes. The heterogeneity of this population may also dilute the strong response of responsive subsets that express required cofactors. By contrast, because Vp16Meis1 progenitors lack *Hox* gene expression, they may be particularly sensitive to transcriptional regulatory mechanisms induced by *Hox* and, because they are uniform populations, the impact of *Hox* genes is maximized. Thus, Vp16-Meis1 progenitors may represent a unique tool for determining both the specificity and biochemical mechanisms of *Hoxa7* and *Hoxa9* gene activation in AML.

ACKNOWLEDGMENTS

This work is supported by Public Health Service grant NIH CA56876 awarded to M.P.K.

We thank Dennis Young for assistance with FACS analysis and Joe Aguilera for assistance with mouse radiation (UCSD Cancer Center Shared Resources). We give special thanks to Mark Featherstone, Corey Largman, Robert Slany, and Adi Salzberg for providing reagents for work related to this paper.

REFERENCES

1. **Adolfsson, J., R. Mansson, N. Buza-Vidas, A. Hultquist, K. Liuba, C. T. Jensen, D. Bryder, L. Yang, O. J. Borge, L. A. Thoren, K. Anderson, E. Sitnicka, Y. Sasaki, M. Sigvardsson, and S. E. Jacobsen.** 2005. Identification of $Flt3^+$ lympho-myeloid stem cells lacking erythro-megakaryocytic potential a revised road map for adult blood lineage commitment. Cell **121:**295–306.
2. **Afonja, O., J. E. Smith, Jr., D. M. Cheng, A. S. Goldenberg, E. Amorosi, T. Shimamoto, S. Nakamura, K. Ohyashiki, J. Ohyashiki, K. Toyama, and K. Takeshita.** 2000. MEIS1 and HOXA7 genes in human acute myeloid leukemia. Leuk. Res. **24:**849–855.
3. **Ayton, P. M., and M. L. Cleary.** 2003. Transformation of myeloid progenitors by MLL oncoproteins is dependent on Hoxa7 and Hoxa9. Genes Dev. **17:**2298–2307.
4. **Azcoitia, V., M. Aracil, A. C. Martinez, and M. Torres.** 2005. The homeodomain protein Meis1 is essential for definitive hematopoiesis and vascular patterning in the mouse embryo. Dev. Biol. **280:**307–320.
5. **Bei, L., Y. Lu, and E. A. Eklund.** 2005. HOXA9 activates transcription of the gene encoding gp91Phox during myeloid differentiation. J. Biol. Chem. **280:** 12359–12370.
6. **Berkes, C. A., D. A. Bergstrom, B. H. Penn, K. J. Seaver, P. S. Knoepfler, and S. J. Tapscott.** 2004. Pbx marks genes for activation by MyoD indicating a role for a homeodomain protein in establishing myogenic potential. Mol. Cell **14:**465–477.
7. **Calvo, K. R., D. B. Sykes, M. Pasillas, and M. P. Kamps.** 2000. Hoxa9 immortalizes a granulocyte-macrophage colony-stimulating factor-dependent promyelocyte capable of biphenotypic differentiation to neutrophils or macrophages, independent of enforced Meis expression. Mol. Cell. Biol. **20:**3274–3285.
8. **Calvo, K. R., D. B. Sykes, M. P. Pasillas, and M. P. Kamps.** 2002. Nup98-HoxA9 immortalizes myeloid progenitors, enforces expression of Hoxa9, Hoxa7, and Meis1, and alters cytokine-specific responses in a manner similar to that induced by retroviral co-expression of Hoxa9 and Meis1. Oncogene **21:**4247–4256.
9. **Chang, C. P., Y. Jacobs, T. Nakamura, N. A. Jenkins, N. G. Copeland, and M. L. Cleary.** 1997. Meis proteins are major in vivo DNA binding partners for wild-type but not chimeric Pbx proteins. Mol. Cell. Biol. **17:**5679–5687.
10. **Danet, G. H., J. L. Luongo, G. Butler, M. M. Lu, A. J. Tenner, M. C. Simon, and D. A. Bonnet.** 2002. C1qRp defines a new human stem cell population with hematopoietic and hepatic potential. Proc. Natl. Acad. Sci. USA **99:** 10441–10445.
11. **Dorsam, S. T., C. M. Ferrell, G. P. Dorsam, M. K. Derynck, U. Vijapurkar, D. Khodabakhsh, B. Pau, H. Bernstein, C. M. Haqq, C. Largman, and H. J. Lawrence.** 2004. The transcriptome of the leukemogenic homeoprotein HOXA9 in human hematopoietic cells. Blood **103:**1676–1684.
12. **Ferrell, C. M., S. T. Dorsam, H. Ohta, R. K. Humphries, M. K. Derynck, C. Haqq, C. Largman, and H. J. Lawrence.** 2005. Activation of stem-cell specific

genes by HOXA9 and HOXA10 homeodomain proteins in CD34$^+$ human cord blood cells. Stem Cells **23:**644–655.

13. **Fischbach, N. A., S. Rozenfeld, W. Shen, S. Fong, D. Chrobak, D. Ginzinger, S. C. Kogan, A. Radhakrishnan, M. M. Le Beau, C. Largman, and H. J. Lawrence.** 2005. HOXB6 overexpression in murine bone marrow immortalizes a myelomonocytic precursor in vitro and causes hematopoietic stem cell expansion and acute myeloid leukemia in vivo. Blood **105:**1456–1466.
14. **Giovannini, M., J. A. Biegel, M. Serra, J. Y. Wang, Y. H. Wei, L. Nycum, B. S. Emanuel, and G. A. Evans.** 1994. EWS-erg and EWS-Fli1 fusion transcripts in Ewing's sarcoma and primitive neuroectodermal tumors with variant translocations. J. Clin. Investig. **94:**489–496.
15. **Hisa, T., S. E. Spence, R. A. Rachel, M. Fujita, T. Nakamura, J. M. Ward, D. E. Devor-Henneman, Y. Saiki, H. Kutsuna, L. Tessarollo, N. A. Jenkins, and N. G. Copeland.** 2004. Hematopoietic, angiogenic and eye defects in Meis1 mutant animals. EMBO J. **23:**450–459.
16. **Huang, H., M. Rastegar, C. Bodner, S. L. Goh, I. Rambaldi, and M. Featherstone.** 2005. MEIS C termini harbor transcriptional activation domains that respond to cell signaling. J. Biol. Chem. **280:**10119–10127.
17. **Imamura, T., A. Morimoto, M. Takanashi, S. Hibi, T. Sugimoto, E. Ishii, and S. Imashuku.** 2002. Frequent co-expression of HoxA9 and Meis1 genes in infant acute lymphoblastic leukaemia with MLL rearrangement. Br. J. Haematol. **119:**119–121.
18. **Inbal, A., N. Halachmi, C. Dibner, D. Frank, and A. Salzberg.** 2001. Genetic evidence for the transcriptional-activating function of Homothorax during adult fly development. Development **128:**3405–3413.
19. **Irizarry, R. A., B. Hobbs, F. Collin, Y. D. Beazer-Barclay, K. J. Antonellis, U. Scherf, and T. P. Speed.** 2003. Exploration, normalization, and summaries of high density oligonucleotide array probe level data. Biostatistics **4:**249–264.
20. **Ivanova, N. B., J. T. Dimos, C. Schaniel, J. A. Hackney, K. A. Moore, and I. R. Lemischka.** 2002. A stem cell molecular signature. Science **298:**601–604.
21. **Jacobs, Y., C. A. Schnabel, and M. L. Cleary.** 1999. Trimeric association of Hox and TALE homeodomain proteins mediates Hoxb2 hindbrain enhancer activity. Mol. Cell. Biol. **19:**5134–5142.
22. **Janssen, E., M. Zhu, W. Zhang, and S. Koonpaew.** 2003. LAB: a new membrane-associated adaptor molecule in B cell activation. Nat. Immunol. **4:**117–123.
23. **Joosten, M., Y. Vankan-Berkhoudt, M. Tas, M. Lunghi, Y. Jenniskens, E. Parganas, P. J. Valk, B. Lowenberg, E. van den Akker, and R. Delwel.** 2002. Large-scale identification of novel potential disease loci in mouse leukemia applying an improved strategy for cloning common virus integration sites. Oncogene **21:**7247–7255.
24. **Kamps, M. P., C. Murre, X. H. Sun, and D. Baltimore.** 1990. A new homeobox gene contributes the DNA binding domain of the t(1;19) translocation protein in pre-B ALL. Cell **60:**547–555.
25. **Kamps, M. P., D. D. Wright, and Q. Lu.** 1996. DNA-binding by oncoprotein E2a-Pbx1 is important for blocking differentiation but dispensable for fibroblast transformation. Oncogene **12:**19–30.
26. **Knoepfler, P. S., K. R. Calvo, H. Chen, S. E. Antonarakis, and M. P. Kamps.** 1997. Meis1 and pKnox1 bind DNA cooperatively with Pbx1 utilizing an interaction surface disrupted in oncoprotein E2a-Pbx1. Proc. Natl. Acad. Sci. USA **94:**14553–14558.
27. **Knoepfler, P. S., and M. P. Kamps.** 1997. The highest affinity DNA element bound by Pbx complexes in t(1;19) leukemic cells fails to mediate cooperative DNA-binding or cooperative transactivation by E2a-Pbx1 and class I Hox proteins: evidence for selective targetting of E2a-Pbx1 to a subset of Pbx-recognition elements. Oncogene **14:**2521–2531.
28. **Kroon, E., J. Krosl, U. Thorsteinsdottir, S. Baban, A. M. Buchberg, and G. Sauvageau.** 1998. Hoxa9 transforms primary bone marrow cells through specific collaboration with Meis1a but not Pbx1b. EMBO J. **17:**3714–3725.
29. **Lawrence, H. J., J. Christensen, S. Fong, Y. L. Hu, I. Weissman, G. Sauvageau, R. K. Humphries, and C. Largman.** 2005. Loss of expression of the HOXA-9 homeobox gene impairs the proliferation and repopulating ability of hematopoietic stem cells. Blood **106:**3988–3994.
30. **Lawrence, H. J., S. Rozenfeld, C. Cruz, K. Matsukuma, A. Kwong, L. Komuves, A. M. Buchberg, and C. Largman.** 1999. Frequent co-expression of the HOXA9 and MEIS1 homeobox genes in human myeloid leukemias. Leukemia **13:**1993–1999.
31. **Memedula, S., and A. S. Belmont.** 2003. Sequential recruitment of HAT and SWI/SNF components to condensed chromatin by VP16. Curr. Biol. **13:**241–246.
32. **Moskow, J. J., F. Bullrich, K. Huebner, I. O. Daar, and A. M. Buchberg.** 1995. Meis1, a PBX1-related homeobox gene involved in myeloid leukemia in BXH-2 mice. Mol. Cell. Biol. **15:**5434–5443.
33. **Nakamura, T., D. A. Largaespada, J. D. Shaughnessy, Jr., N. A. Jenkins, and N. G. Copeland.** 1996. Cooperative activation of Hoxa and Pbx1-related genes in murine myeloid leukaemias. Nat. Genet. **12:**149–153.
34. **Okano, H., T. Imai, and M. Okabe.** 2002. Musashi: a translational regulator of cell fate. J. Cell Sci. **115:**1355–1359.
35. **Pereira, D. S., C. Dorrell, C. Y. Ito, O. I. Gan, B. Murdoch, V. N. Rao, J. P. Zou, E. S. Reddy, and J. E. Dick.** 1998. Retroviral transduction of TLS-ERG initiates a leukemogenic program in normal human hematopoietic cells. Proc. Natl. Acad. Sci. USA **95:**8239–8244.
36. **Piao, X., R. S. Hill, A. Bodell, B. S. Chang, L. Basel-Vanagaite, R. Straussberg, W. B. Dobyns, B. Qasrawi, R. M. Winter, A. M. Innes, T. Voit, M. E. Ross, J. L. Michaud, J. C. Descarie, A. J. Barkovich, and C. A. Walsh.** 2004. G protein-coupled receptor-dependent development of human frontal cortex. Science **303:**2033–2036.
37. **Pineault, N., C. D. Helgason, H. J. Lawrence, and R. K. Humphries.** 2002. Differential expression of Hox, Meis1, and Pbx1 genes in primitive cells throughout murine hematopoietic ontogeny. Exp. Hematol. **30:**49–57.
38. **Rave-Harel, N., M. L. Givens, S. B. Nelson, H. A. Duong, D. Coss, M. E. Clark, S. B. Hall, M. P. Kamps, and P. L. Mellon.** 2004. TALE homeodomain proteins regulate gonadotropin-releasing hormone gene expression independently and via interactions with Oct-1. J. Biol. Chem. **279:**30287–30297.
39. **Sakakibara, S., Y. Nakamura, T. Yoshida, S. Shibata, M. Koike, H. Takano, S. Ueda, Y. Uchiyama, T. Noda, and H. Okano.** 2002. RNA-binding protein Musashi family: roles for CNS stem cells and a subpopulation of ependymal cells revealed by targeted disruption and antisense ablation. Proc. Natl. Acad. Sci. USA **99:**15194–15199.
40. **Saleh, M., I. Rambaldi, X. J. Yang, and M. S. Featherstone.** 2000. Cell signaling switches HOX-PBX complexes from repressors to activators of transcription mediated by histone deacetylases and histone acetyltransferases. Mol. Cell. Biol. **20:**8623–8633.
41. **Schnabel, C. A., Y. Jacobs, and M. L. Cleary.** 2000. HoxA9-mediated immortalization of myeloid progenitors requires functional interactions with TALE cofactors Pbx and Meis. Oncogene **19:**608–616.
42. **Shashidhar, S., G. Lorente, U. Nagavarapu, A. Nelson, J. Kuo, J. Cummins, K. Nikolich, R. Urfer, and E. D. Foehr.** 2005. GPR56 is a GPCR that is overexpressed in gliomas and functions in tumor cell adhesion. Oncogene **24:**1673–1682.
43. **Shen, W. F., J. C. Montgomery, S. Rozenfeld, J. J. Moskow, H. J. Lawrence, A. M. Buchberg, and C. Largman.** 1997. AbdB-like Hox proteins stabilize DNA binding by the Meis1 homeodomain proteins. Mol. Cell. Biol. **17:**6448–6458.
44. **Shen, W. F., S. Rozenfeld, A. Kwong, L. G. Kömüves, H. J. Lawrence, and C. Largman.** 1999. HOXA9 forms triple complexes with PBX2 and MEIS1 in myeloid cells. Mol. Cell. Biol. **19:**3051–3061.
45. **Sykes, D. B., and M. P. Kamps.** 2004. E2a/Pbx1 induces the rapid proliferation of stem cell factor-dependent murine pro-T cells that cause acute T-lymphoid or myeloid leukemias in mice. Mol. Cell. Biol. **24:**1256–1269.
46. **Thorsteinsdottir, U., E. Kroon, L. Jerome, F. Blasi, and G. Sauvageau.** 2001. Defining roles for HOX and MEIS1 genes in induction of acute myeloid leukemia. Mol. Cell. Biol. **21:**224–234.
47. **Thorsteinsdottir, U., A. Mamo, E. Kroon, L. Jerome, J. Bijl, H. J. Lawrence, K. Humphries, and G. Sauvageau.** 2002. Overexpression of the myeloid leukemia-associated Hoxa9 gene in bone marrow cells induces stem cell expansion. Blood **99:**121–129.
48. **Wagner, W., A. Ansorge, U. Wirkner, V. Eckstein, C. Schwager, J. Blake, K. Miesala, J. Selig, R. Saffrich, W. Ansorge, and A. D. Ho.** 2004. Molecular evidence for stem cell function of the slow-dividing fraction among human hematopoietic progenitor cells by genome-wide analysis. Blood **104:**675–686.
49. **Wang, G. G., M. P. Pasillas, and M. P. Kamps.** 2005. Meis1 programs transcription of FLT3 and cancer stem cell character, using a mechanism that requires interaction with Pbx and a novel function of the Meis1 C-terminus. Blood **106:**254–264.
50. **Zeisig, B. B., T. Milne, M. P. Garcia-Cuellar, S. Schreiner, M. E. Martin, U. Fuchs, A. Borkhardt, S. K. Chanda, J. Walker, R. Soden, J. L. Hess, and R. K. Slany.** 2004. Hoxa9 and Meis1 are key targets for MLL-ENL-mediated cellular immortalization. Mol. Cell. Biol. **24:**617–628.
51. **Zhang, X., A. Friedman, S. Heaney, P. Purcell, and R. L. Maas.** 2002. Meis homeoproteins directly regulate Pax6 during vertebrate lens morphogenesis. Genes Dev. **16:**2097–2107.

Intermolecular swapping of the Meis1 CTD and the HoxA9 NTD domains does not interfere with their transforming potentials *in vitro* and *in vivo*, providing further evidence for the "Hox-Pbx-Meis1 common complexes" model of leukemogenesis.

The "Hox-Pbx-Meis1 common complex" model for AML proposed as above is based on the fact that a transcriptional activation domain fused on Meis1 is able to replace the functions of both the Meis1 CTD domain and the HoxA9 NTD domain, the fact that HoxA9 (HoxA7) regulates the same group of leukemia signature genes as Meis1 does in AML-initiating progenitors, and the fact that Meis1, Pbx and HoxA9 all bind to the *FLT3* cis-element regions. In a further survey of the Hox-Meis1 target gene *Sox4*, we observed a conserved Pbx-Hox complex recognition site together with a nearby Meis1 site (Figure 4.9A), indicating that *Sox4*, as *FLT3,* is also a direct downstream target of HoxA9 and Meis1. The observation that the Meis1 CTD domain is replaceable by Vp16 activation domain indicated that this domain is structurally independent, which prompts us to test whether or not the Meis1 CTD and the HoxA9 NTD, two domains harboring the transcriptional activation activities, are swappable (Figure 4.9B). In the light that the Meis1 CTD and the HoxA9 NTD domains recruit unknown essential transcriptional cofactors, the rationale for the swapping experiment is that the recruited cofactors would be still around and functional (even if the locations of recruiting domains are changed) if Meis1 and HoxA9 bind to the same promoters, and the scenario would be wrong if the Meis1 and HoxA9 bind to distinct promoters. Indeed, after the dual expression but not the single expression in the hematopoietic progenitors, the swapping of the Meis1 CTD

and HoxA9 NTD domains recapitulated the transforming functions of the corresponding wildtype forms, producing the immortalized progenitors in the medium containing FL as the sole cytokine and inducing AML in the murine marrow transplantation models (Figure 4.9C). The FLT3+-progenitor immortalization caused by coexpression of the swapped forms is slightly less efficient than the wildtype forms, and the AML induced by coexpression of the swapped forms required a longer latency than the wildtype forms (95 days vs 60 days), indicating that the domain-swapped forms are indeed sufficient for the leukemia transformation although somewhat less potent than wildtype ones due to the apparent reasons. Thus, this domain swapping experiment provides the evidence for the co-occupancy of Meis1 and HoxA9 proteins on at least a subset of downstream target promoters whose activation is sufficient enough for the hematopoietic transformation.

Figure 4.9. Swapped protein forms generated by intermolecular exchange of the Meis1 CTD and the HoxA9 NTD domains recapitulate the wildtype proteins in terms of their transforming potentials *in vitro* and *in vivo*, providing further evidence for the "Hox-Pbx-Meis1 common complexes model" of leukemogenesis.

(A) The sequence analysis of *Sox4* promoter region (~600 base pairs before the transcription initiation site) revealed a conserved Pbx-Hox (red-blue) recognition site with a nearby Meis1 recognition site (green).

(B) The diagram showing the structure of HoxA9 and Meis1 proteins before and after the swapping of the Meis1 CTD and HoxA9 NTD domains.

(C) The abilities of single and dual expression of either wildtype or swapped forms of HoxA9 and Meis1 in hematopoietic progenitors to program the generation of FLT3+-immoratalized progenitors *in vitro* (top panel) and the induction of AML *in vivo* (bottom panel). For the *in vitro* assay, 200,000 drug resistant selected hematopoietic progenitors were plated in the medium containing FL as the sole supporting cytokine at day 0 (white bars) and the progenitors at day 8 (yellow), day 16 (green) and day 24 (black) were numerated and plotted. Three cultures were assayed for each group and the SD were plotted as the error bars. For the *in vivo* assays, 2 millions of cells were injected into the sub-lethally irradiated mice. Each group contains 5 mice and the average of AML latency was shown in the bottom panel.

A

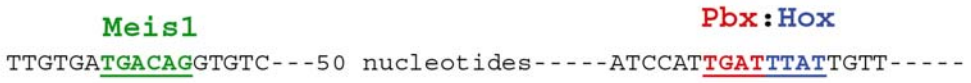
Meis1
Pbx:Hox
TTGTGATGACAGGTGTC---50 nucleotides-----ATCCATTGATTTATTGTT-----

B

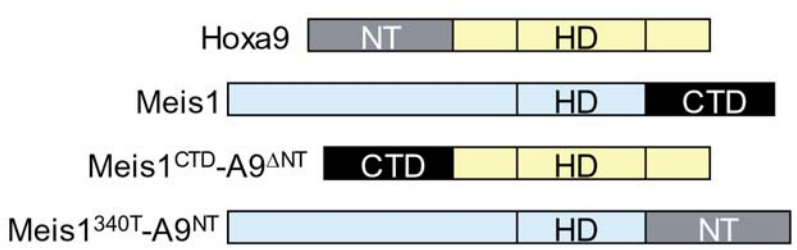
Hoxa9
NT
HD
Meis1
HD
CTD
Meis1CTD-A9ΔNT
CTD
HD
Meis1340T-A9NT
HD
NT

C

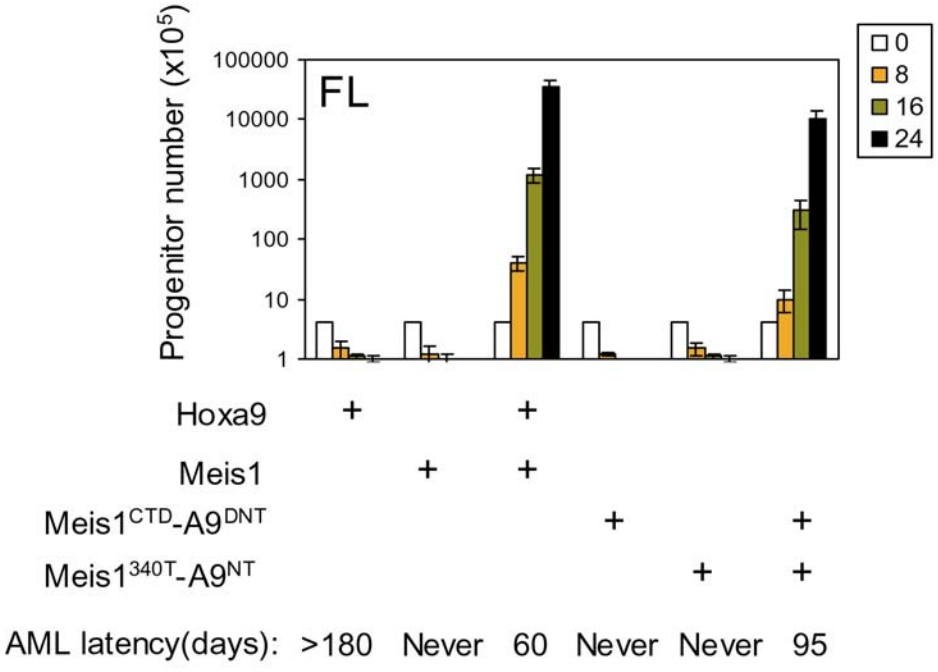
Progenitor number (x10^5)
100000
10000
1000
100
10
1
FL
0
8
16
24
Hoxa9 + +
Meis1 + +
Meis1CTD-A9DNT + +
Meis1340T-A9NT + +
AML latency(days): >180 Never 60 Never Never 95

ACKNOWLEDGEMENT

The main body of Chapter IV is in a reprint of the material as it appears in "Persistent transactivation by Meis1 replaces Hox function in myeloid leukemogenesis models: evidence for co-occupancy of Meis1-Pbx and Hox-Pbx complexes on promoters of leukemia-associated genes." Mol. Cel. Biol. (2005), Volume 26, Number 10, page 3902–3916. This text of this paper is Copyright © 2005 reserved by journal "Molecular and Cellular Biology" and the American Society of Microbiology. I was the first-author and the primary researcher, and the coauthors listed in this publication aided in and/or supervised the research which formed the basis of this chapter. My contributions included performing most primary work in tissue culture, mouse leukemia models, DNA expression construct production, and molecular and biochemical analysis, actively participating in experimental design, analyzing the primary data, and preparing the manuscript. Coauthor Martina Pasillas gave technical support in mouse model, western blot, northern and southern blot, and Facs analysis. The correspondence author Mark Kamps supervised and designed the research, and prepared the final version of the manuscript. I thank my co-authors for permission to use this publication in my dissertation.

Chapter 5

Quantitative production of macrophages or neutrophils ex vivo using conditional Hoxb8 --- the generation of committed progenitors that model the normal differentiation, innate immune function, and inflammatory response

ABSTRACT

The differentiation mechanisms and inflammatory functions of neutrophils and macrophages are pursued by genetic and biochemical approaches that require costly breeding and time-consuming purification to obtain phagocytes for functional analysis. Because Hox oncoproteins enforce self-renewal of factor-dependent myeloid progenitors, we queried whether estrogen-regulated Hoxb8 (Hoxb8-ER) could immortalize macrophage or neutrophil progenitors that would execute normal differentiation and normal innate immune function upon Hoxb8-ER inactivation. Here we describe methods to derive unlimited quantities of murine macrophages or neutrophils by immortalizing their respective progenitors with Hoxb8-ER using different cytokines to target expansion of different committed progenitors. Hoxb8-ER neutrophils and macrophages are functionally superior to those produced by many other ex vivo differentiation models, possess strong inflammatory responses, and can be derived easily from day-13 fetal liver for mice exhibiting embryonic lethal phenotypes. Using knockout or siRNA technologies, this Hoxb8-ER phagocyte maturation system represents a rapid analytical tool for studying macrophage and neutrophil biology.

INTRODUCTION

Phagocytic cells and inflammation play critical roles in immunologic regulation as well as in the pathology of chronic inflammatory diseases (e.g. multiple sclerosis, liver cirrhosis, arthritis, atherosclerosis, diabetes, vascular diseases, and inflammatory bowel disease) and acute inflammatory disease (e.g. toxic shock syndrome). Inflammation biology has also been linked to complex diseases such as the proliferation and metastasis of cancer (Karin and Greten, 2005) and the development of obesity (Weisberg et al., 2003). Elucidating the molecular mechanisms by which a phagocyte responds to chemokines and cytokines, activates a pro-inflammatory cascade, modulates lymphocyte expansion and function, and effects microbial killing will ultimately reveal mechanisms of chronic inflammation, while identifying the genetic pathways that control phagocyte differentiation are important for understanding myeloid leukemogenesis. While the function of innate immune proteins is studied by knockout technologies that reveal their importance in phagocyte functions, there is no simple protocol to generate large numbers of neutrophils or monocytes from these mutant mice in order to characterize the impact of a genetic mutation on their differentiation, signal transduction, or effecter functions.

Class I Hox homeodomain transcription factors promote the expansion of hemopoietic progenitors, and their expression is deregulated in both human and murine myeloid leukemia. The abundance of Hoxa9 and Hoxa7 is high in CD34+, Sca-1+, lineage-negative (Lin-) bone marrow populations that are enriched in hematopoietic stem cells (HSC) and in lineage-committed progenitors (LCP) and both are down-regulated coincident with transition to the CD34– stage of early progenitor

differentiation(Lawrence et al., 1997; Pineault et al., 2002). *Hoxa9*$^{-/-}$ mice have 5- to 10-fold fewer marrow HSC and significant reductions in myeloid and pre-B cell progenitors(Lawrence et al., 1997), while retroviral expression of Hoxa9 produces a 10-fold increase in the number of long-term repopulating HSC (LT-HSC)(Thorsteinsdottir et al., 2002). Enforced production of Hoxb8 or Hoxa9 blocks differentiation of SCF- or GM-CSF-dependent myeloid progenitors(Calvo et al., 2000; Fischbach et al., 2005; Knoepfler et al., 2001; Owens and Hawley, 2002).

Based on the ability of Hox proteins to arrest myeloid differentiation and permit infinite progenitor expansion, we asked whether factor-dependent hematopoietic progenitors immortalized by estrogen receptor fusions (conditional forms) of Hoxb8 or Hoxa9 could yield cell models of normal neutrophil- or macrophage-restricted differentiation. By testing combinations of progenitor isolation protocols, cytokines used for pre-stimulation and long-term culture, and oncoprotein identity, we derived a simple and reliable protocol to derive macrophage-committed progenitor lines and a second protocol to derive neutrophil -committed progenitor lines.

Based on immunologic, functional, and genetic criteria, the macrophages and neutrophils produced from these lines model normal exit from the cell cycle, and acquisition of phagocytic and inflammatory functions. In response to Toll receptor agonists, macrophages derived from Hoxb8-ER progenitors up-regulated components of NF-□B signaling and downstream effectors genes such as *Il1*, *Il6*, *Ptgs2* and *Tgm2*. The ability of Hoxb8-ER to drive progenitor expansion and permit their subsequent differentiation to neutrophils or macrophages makes this model system an

ideal tool to study myeloid differentiation and the cell biology and inflammatory functions of macrophages and neutrophils.

RESULTS

Hoxb8-ER and Hoxa9-ER exhibit estrogen-stimulated function.

We fused the estrogen-binding domain of the estrogen receptor (ER) to the N-terminus of Hoxb8 and Hoxa9, added N-terminal epitope tags to facilitate subsequent identification, and expressed the fusion cDNA's using an MSCV retroviral expression vector (Fig. 5.1a). We measured estrogen-regulated transcriptional function of Hoxb8-ER and Hoxa9-ER by virtue of their ability to cooperate with activated forms of Pbx to activate transcription of a luciferase reporter driven by TGAT-TTAT Pbx-Hox motifs. Using this assay, Hoxa9-ER and Hoxb8-ER exhibited β-estradiol (estrogen)-dependent transcriptional activation of 10- and 3-fold, respectively, with half-maximal activation occurring at 10nM (Fig. 5.1b).

Hoxb8-ER immortalizes neutrophil or macrophage progenitors.

In the presence of 1uM estrogen, infection of primary marrow progenitors cultured in interleukin 3 (IL-3), stem cell factor (SCF), or granulocyte-macrophage colony-stimulating factor (GM-CSF) with retrovirus expressing *Hoxb8-ER* or *Hoxa9-ER* produced immortalized, factor-dependent, progenitors (Fig. 5.1c; ER fusion proteins identified by Western blotting in insert), which ceased proliferation (Fig. 5.1d) and exhibited terminal morphologic differentiation upon estrogen withdrawal (Fig. 5.2a). Progenitors were not immortalized when infections were performed in the presence of granulocyte colony stimulating factor (G-CSF) or macrophage colony stimulating factor (M-CSF). By testing different progenitor isolation protocols, cell

culture conditions, and ER-Hox fusion oncoproteins, we derived conditions for derivation of cell lines demonstrating quantitative neutrophil differentiation or quantitative macrophage differentiation. By employing negative selection (removing MacI+, B220+, Thy1.2+ cells) of total bone marrow progenitors followed by a 2-day pre-expansion in SCF, IL-3, and IL-6, and immortalization with *Hoxb8-ER* retrovirus in medium containing SCF as the only cytokine, immortalized progenitors differentiated into 98-99% neutrophils following estrogen withdrawal (1-2% mast cells with an occasional eosinophilic granulocyte; 4 of 4 clones; Fig 5.2a). We define progenitors derived in this manner as "SCF Hoxb8-ER progenitors". SCF-dependent Hoxb8-ER progenitors have proliferated over 9 months, maintaining both a normal 40-XX karyotype (19 of 20 chromosome spreads) and quantitative neutrophil differentiation. By contrast, when we purify total marrow progenitors by centrifugation onto Ficoll (no negative selection for MacI+ committed myeloid progenitors) and immortalize with *Hoxb8-ER* retrovirus in medium containing GM-CSF as the only cytokine the progenitors are committed to macrophage differentiation at levels >99% (Fig 5.2a; 10 of 10 clones). We define progenitors derived in this manner as "GM-CSF Hoxb8-ER progenitors". These progenitors have proliferated over two years (over 850 generations), maintaining a normal 40-XX karyotype (in 17 of 20 chromosome spreads; Sup. Fig. 5.1) and quantitative macrophage differentiation. Therefore, Hoxb8-ER progenitors do not become aneuploid as a requirement for immortalization, they do not become aneuploid at a substantial rate over long durations of passage, and they maintain stable commitment to lineage-restricted differentiation pathways.

We characterized neutrophil or macrophage progenitors immortalized by Hoxb8-ER for surface antigens and enzyme activities characteristic of neutrophils or macrophages. Neutrophils produced by differentiation of SCF-dependent Hoxb8-ER progenitors up-regulated NADPH oxidase (Fig. 5.2a), the neutrophil surface antigen Gr-1 and the myeloid integrin Mac1, and down-regulated the macrophage marker F4/80 (Fig. 5.2b). By contrast, macrophages produced by differentiation of GM-CSF-dependent Hoxb8-ER macrophage progenitors exhibited activation of macrophage nonspecific esterase (Fig. 5.2a), up-regulation of F4/80 and Mac1, and down-regulation of Gr-1 (Fig. 5.2b).

Contrasting the behavior of Hoxb8-ER, Hoxa9-ER and Hoxa7-ER progenitors exhibited principally biphenotypic neutrophil and macrophage differentiation regardless of the cytokine used during their derivation (Sup. Table 5.1). We continued characterization of Hoxb8-ER-immortalized progenitors because they did not require cloning to select progenitors that differentiated into pure populations of neutrophils or macrophages, and because a simple change in experimental protocol allowed for derivation of either macrophage- or neutrophil-committed progenitors.

Genomic arrays demonstrate normal specific differentiation.

We interrogated Affymetrix genome arrays (430 2.0 Array; over 34,000 mouse genes) with RNA from SCF Hoxb8-ER progenitors undergoing neutrophil differentiation and from GM-CSF Hoxb8-ER progenitors undergoing macrophage differentiation (Table 5.1; Comprehensive analysis in Sup. Tables 5.2, 5.3, 5.4) and compared expression of 130 macrophage-specific, neutrophil-specific, or general

myeloid genes (Fig. 5.3). *Il8rb*, *Ltf, Lrg1*, *CD177*, *Cnlp*, and *Lcn2* and other neutrophil marker genes were up-regulated selectively during differentiation of SCF Hoxb8-ER neutrophil progenitors while *Mmp12*, *Cd68*, *Msr1*, *Msr2*, *Mgl2*, *Itgax* (CD11c), *Clec4n*, and other macrophage-specific marker genes were up-regulated selectively with differentiation of GM-CSF Hoxb8-ER macrophage progenitors (Table 5.1 and Sup. Table 5.2). The monocytic lineage markers *Irf8*, *Emr1 (F4/80)*, and *Tfec* were expressed at high levels in undifferentiated GM-CSF Hoxb8-ER progenitors, demonstrating their commitment to macrophage differentiation (Table 5.1). Other common myeloid differentiation marker genes were up-regulated during maturation of both progenitor cell types (*Fpr1*, *Fpr-rs2*, *Mrc1*, *Tlr2*, *Mmp8*, *Itgam*, *Fgr*, *Lgmn*), while common promyelocytic genes, including *Mpo*, *Prt3*, *Ela2*, and *Cnn3* were strongly down-regulated (Table 5.1). Dynamic regulation of neutrophil, macrophage, and general myeloid markers demonstrates that both the SCF-derived and GM-CSF-derived Hoxb8-ER progenitors execute normal differentiation programs. Changes in gene expression predicted by Affymetrix arrays were verified for the macrophage scavenger receptor (Msr1) and the transcription factors Rel-B and Jun using immunoblotting, for CD11c using FACS analysis, and for *Gfi-1*, *Myb*, *Nolc1*, *Ela2*, and *Fos* and by Northern blotting for; (Sup. Fig. 5.2).

GM-CSF Hoxb8-ER macrophage progenitors were positioned at a later stage of myeloid differentiation than were SCF Hoxb8-ER neutrophil progenitors. They exhibited high basal levels of a subset of late differentiation genes, such as *Lyzs*, *Gsn*, *CD14*, *Lilrb4*, *Pira1*, *Pira6*, *Pilrb1*, *Gp49b1*, and *Gpnmb* that were not expressed in SCF Hoxb8-ER neutrophil progenitors (blue signals in Fig. 5.3), but were strongly

up-regulated SCF Hoxb8-ER neutrophil progenitors during their subsequent differentiation (red signals in Fig. 5.3). SCF Hoxb8-ER neutrophil progenitors expressed the stem cell genes *Cd34*, *Flt3*, *Crlrc*, *C1qr1*, *Sox4*, *Hmgn1*, *Hmga2*, *Meis1*, *Erg*, and *Nrip1*, which were not expressed in GM-CSF Hoxb8-ER macrophage progenitors and were shut off during differentiation of SCF Hoxb8-ER neutrophil progenitors (Table 5.1). The more committed differentiation stage of GM-CSF Hoxb8-ER progenitors was mirrored by their lower expansion potential--inactivation of Hoxb8-ER in GM-CSF-dependent progenitors resulted in cell cycle arrest following only a 4-fold expansion while inactivation of Hoxb8-ER in SCF Hoxb8-ER neutrophil progenitors was followed by a 90-fold expansion.

Regardless of their striking difference in expansion potential, promyelocytic genes, cell cycle genes, and genes encoding cell cycle regulators were down-regulated coincident with up-regulation of differentiation genes in both progenitor types (Sup. Fig. 5.3). Cell cycle genes (e.g. *CycB1*, *Mcm2*), as well as Myc target genes (e.g. *Nolc1*, *Shmt2*) fell in parallel with expression of *Myc*, *Myb*, *Ruvbl1*, and *Ruvbl2* (yellow tracings). Expression of the Myb targets, *ELA2*, *Ctsg*, *Prtn3*, and *Mpo* fell in parallel with *Myb* (brown tracings). Synchronous expression of terminal differentiation genes *Fpr1*, *Fpr-rs2*, *Clec7A*, *Mrc1*, and *Fgr* (green tracings) paralleled the leucine zipper transcription factors genes *Atf3*, *JunB*, *Fos*, and *Jund1* (purple tracings). This suggests that a broad program of cell cycle gene down-regulation and differentiation gene up-regulation (Supplement Table 5.2) is driven by down-regulation of *Myc* and *Myb* and up-regulation of bZIP transcription factors (Kharbanda et al., 1991; Krishnaraju et al., 1998; Liebermann and Hoffman, 1994).

Genes controlling divergent aspects of neutrophil and macrophage biology were regulated normally in this cell differentiation model (Table 5.1, Sup. Tables 5.2, 5.3). Maturing phagocytes up-regulated genes encoding proteins involved in adhesion (*Itgax*, *Itgam*, *Gpnmb*, *Bst1*), migration (*Cd74*, *Ccr1*, *Ccr5*), phagocytosis (*Sirpb1*, *Clec4b*, *Clec4a3*), activation (*Clec2i*), pathogen pattern recognition (*Mgl2*, *Clec4d*, *Mrc1*, *Clec7a*, *Fpr1*, *Fpr-r2*, *Bst1*), recognition of necrotic cell debris (*Msr1*, *Msr2*, *Cd68*), T-cell activation (*Il18* and genes encoding MHC2 class II complex antigens E alpha, A beta 1, A alpha, E alpha, Ebeta1, DM loci alpha and beta2), MHC class I recognition (*Pira1*, *Pilra*, *Pira6*, *Pilrb1*, *Pirb5*), migration (*Cxcl2*, *Ccr2*), bacterial killing (*Ngp*, *Camp*), opsinophagocytosis (*C3*, *C3ar1*), proteolysis and MHC class II peptide generation (*Lgmn*, *Mmp9*), protease inhibition (*Stfa1*, *Stfa2l1*, *StfA3*, *Timp2*, *Expi1*), nitric oxide biosynthesis (*Arg2*, *Pdi4*), metal ion transport (*Slc11a1*, *Ltf*), and receptor signaling via tyrosine kinases (*Hck*, *Fgr*).

SCF Hoxb8-ER progenitors mimic the GMP stem cell.

While expression of promyelocytic genes (e.g. *Mpo* and *Prt3*) established SCF Hoxb8-ER progenitors as myeloid, their expression of multipotent stem cell genes *Flt3*, *CD34*, *Meis1*, *Hmgn1*, coupled with their negligible basal expression of any terminal differentiation gene and their low level of differentiation to mast cells and eosinophils (<2%), suggested they might retain the ability to execute alternative differentiation fates in response to other lineage-specific cytokines. To test this hypothesis, we allowed SCF Hoxb8-ER progenitors to differentiate in SCF medium supplemented with G-CSF, IL-5, M-CSF, GM-CSF, or erythropoietin (Fig. 5.4).

Inclusion of G-CSF augmented chromatin condensation and increased expansion from 70- to 120-fold. Inclusion of IL-5 induced eosinophilic granules in one third of maturing granulocytes (enlarged example in inset). Inclusion of GM-CSF increased expansion to 830-fold, and produced 16% macrophages. Southern blots demonstrated the same unique retroviral integration site in macrophages derived from differentiation in GM-CSF as for neutrophils derived by differentiation in SCF, proving the multipotent nature of this progenitor (not shown). M-CSF did not alter expansion, but induced 6% of progenitors to mature as macrophages. Erythropoietin had no impact on neutrophil-committed differentiation. Thus, SCF Hoxb8-ER progenitors are similar to granulocyte-macrophage progenitors (GMP), which retain the ability to differentiate into eosinophils, neutrophils or macrophages.

Hoxb8-ER macrophages exhibit robust inflammatory responses.

The inflammatory response of Hoxb8-ER macrophages was evaluated by measuring gene activation in response to lipopolysaccaride (LPS), an activator of toll-like receptor 4 (TLR4) and bacterial lipoprotein (BLP), an activator of toll-like receptor 2 (TLR2). LPS activated strong transcription of the genes encoding members of the NF-κB, Stat, Jun, and Egr transcription factors (Sup. Fig. 5.4), as well as over 50 involved in inflammation (Sup. Table 5.4), including coactivators of T-cell migration and proliferation (Tnfsf9, Il12b, Il23), monocyte chemokines (Ccl2, Ccl3, Ccl5, Ccl7) and pleotropic cytokines (Ifnb, Tnfa, IL6, IL1a, IL1b, LIF).

Hoxb8-ER immortalizes d13 fetal liver progenitors.

A useful application of the Hoxb8-ER system would be immortalization of progenitors from mice carrying transgenic or knockout alleles designed to address immunologic and inflammatory functions, particularly those from mice that are difficult to breed or have poor survival. To address this issue, we tested whether macrophages produced by maturation of Hoxb8-ER GM-CSF progenitors from *Traf3*$^{-/-}$ mice would exhibit a signaling defect that could be corrected by expression of wild-type *Traf3* in trans. TRAF3 is essential for induction of type I IFNs and the anti-inflammatory cytokine IL-10, but is dispensable for induction of pro-inflammatory cytokines (Hacker et al., 2006). *Traf3*$^{-/-}$ mice die shortly after birth from hypoglycemia and a runting disease that prevents the generation of significant numbers of macrophages from *Traf3*$^{-/-}$ mice. We infected *Traf3*$^{-/-}$ d13 fetal liver progenitors with Hoxb8-ER retrovirus and observed progenitor immortalization. To reconstitute Traf3, we expressed HA-tagged Traf3 by infection with an MSCV-based retroviral vector (Fig. 5.5a). *HA-TRAF3* expression persisted in differentiated monocytes produced by estrogen withdrawal (Fig. 5.5b). We stimulated both the differentiated HoxB8-ER *Traf3*$^{-/-}$ monocytes and their siblings expressing HA-TRAF3 with CpG-DNA (TLR9 agonist) and measured IFN and IL-10 production by bioassay and ELISA, respectively. While the *Traf3*$^{-/-}$ macrophages produced no IFN or IL-10, robust expression was detected in wild-type cells and in *Traf3*$^{-/-}$ macrophages reconstituted with HA-TRAF3 (Fig. 5.5c). Thus, Hoxb8-ER-immortalized d13 fetal liver progenitors can be prepared from knockout mice whose lethal genetic phenotype would preclude extensive ex vivo studies. Then function encoded by the genetic knockout can be reconstituted in Hoxb8-ER progenitors, and

the abundant source of phagocytes generated by the system provides a convenient means to study functional properties of the knockout protein in mature phagocytes.

DISCUSSION

Here we describe a rapid and convenient method to produce unlimited macrophages or neutrophils from mice surviving past embryonic d13, a method that overcomes the significant time, cost and animal mortality involved in using mice as a source of mature phagocytes. Macrophage differentiation of Hoxb8-ER GM-CSF progenitors is at least as good as that produced by TPA treatment of HL60 cells, IL6 treatment of M1 AML cells, or M-CSF treatment of Hoxa9 progenitors. While each of these other models of macrophage differentiation is accompanied by up-regulation of *Egr1*, *Egr2*, *Atf3*, *Fos*, *Jun*, *RelB* and down-regulation of *Myb*, and *Myc* transcription (Kharbanda et al., 1991; Krishnaraju et al., 1998; Liebermann and Hoffman, 1994), they also yield heterogeneous morphologies accompanied by significant apoptosis, likely due to an incomplete differentiation program that is counteracted by the presence of active oncoproteins. The functional maturation of neutrophils derived from Hoxb8-ER SCF progenitors is stronger than that produced by G-CSF-induced differentiation of either 32D progenitors or Hoxa9 progenitors. 32D progenitors fail to up-regulate secondary granule genes such as *Lfn*, and Hoxa9 progenitors fail to down-regulate *Myb* and the promyelocytic genes, *Ela2* and *Mpo*, and fail to up-regulate the secondary granule gene *Lfn*. The incomplete transcriptional modeling of these inducible cell lines is likely due to the persistent oncoprotein activity during differentiation induction, which contrasts the complete inactivation in oncoprotein-ER fusions. ATRA-induced differentiation of GM-CSF-dependent EPRO promyelocytes (Gaines et al., 2005) yields results comparable to those observed in with Hoxb8-ER, and interestingly also inactivates the intrinsic

oncoprotein (a dominant-negative retinoic acid receptor α), using supra-physiologic levels of ATRA.

Other conditional oncoproteins described to date have not evidenced reproducible derivation of lineage-specific progenitors that execute normal differentiation. Avian v-Myb-ER immortalizes primary chicken monocyte progenitors that differentiated, unexpectedly, into multinucleated giant cells similar bone-marrow-derived osteoclasts (Engelke et al., 1997). Their expansion in the presence of estrogen is also limited to 10^7. Mll-Enl-ER (tamoxifen-regulated) immortalizes a biphenotypic progenitor that requires 14 days to exit the cell cycle following removal of tamoxifen and to differentiate into neutrophils and monocytes (Zeisig et al., 2004). Terminal differentiation of progenitors immortalized by E2a-ER-Pbx1 is variable (5 to 12 days), and while derivation of neutrophil-committed progenitors is common using the Δ1 E2a-Pbx1 mutant, derivation of macrophage-committed progenitors is rare (Sykes and Kamps, 2001), an observation somewhat akin to the behavior of Hoxa9-ER in our current study, which yielded mostly biphenotypic progenitors, a lower number of neutrophil-committed progenitors, and rare monocyte-committed progenitors. Therefore, oncoprotein-specific functions dictate the expansion potential, differentiation stage, and differentiation fate of immortalized progenitors. Hoxb8-ER has the advantage of targeting or programming progenitors so that its subsequent inactivation results in their predictable neutrophil or macrophage differentiation.

Hoxb8-ER is unique in being able to target two different types of progenitors, one producing macrophages and another producing neutrophils under defined cell

culture conditions. These properties will be useful for investigations into the differentiation, signaling, and effecter mechanisms of phagocytes, and having an infinite supply of cells will permits functional analysis by classical biochemistry or molecular biology approaches. One clear application of this system is understanding how Hox oncoproteins maintain the undifferentiated state in human myeloid leukemia, a goal that can now be approached by determining the biochemical link between Hox activity and maintaining transcription of other proto-oncogenes involved in cancer and stem cell expansion, such as *Myb* (Chen et al., 2002; Lipsick and Wang, 1999; Lyon and Watson, 1995; White and Weston, 2000), *Myc* (Kumar et al., 2003), *Ruvbl1* (Wood et al., 2000), *Gfi1* (Hock et al., 2003), and *Hmgb3* (Nemeth et al., 2005). A second application is in understanding transcriptional mechanisms governing terminal phagocyte differentiation, such as those controlling activation of *Lfn*, the pattern recognition gene *Fpr*, or the antimicrobial gene *Camp*. This field has lacks easily-derived model systems (Gaines et al., 2005). A third application is in identifying new genes controlling phagocyte differentiation, an example of which may be 30-fold up-regulation of the duel-specific phosphatase *Dusp1* (cell cycle regulation (Li et al., 2003)) and strong down-regulation of the tyrosine phosphatase *Ptpn1*.

The accuracy of Hoxb8-ER progenitors in modeling normal differentiation suggests it should be possible to derive hematopoietic progenitors modeling erythroid, megakaryocytic, or lymphoid differentiation, or even epithelial progenitors modeling breast ductal formation or colonic microvillar differentiation using conditional oncogenes that are native to tumors within these progenitors coulpled

with cytokines that drive their normal expansion. Such models of tissue differentiation would be useful tools in understanding the biochemistry and genetics of how oncogenes enforce the stem cell phenotype, as well as in understanding the functions of differentiated cell types that are difficult to culture from native sources.

MATERIALS AND METHODS

Construction of tagged, estrogen receptor fusions of Hoxb8 and Hoxa9.

A murine stem cell provirus (Mscv) expressing Hoxb8-ER or Hoxa9-ER was generated by inserting estrogen-binding domain (ERBD) of estrogen receptor (ER) at an N-terminal MluI restriction site engineered into epitope-tagged murine Hoxb8 or Hoxa9 proteins. Tagged Hoxb8 was generated by PCR using the 5' primers (FLAG tag: g **gaa ttc** gcc acc ATG *GAC TAC AAG GAC GAC GAT GAC AAA GGA* **ACG CGT** GGA AGC TCT TAT TTC GTC AAC TCA C; HA tag: g gaa ttc gcc acc ATG GGA *TAC CCA TAC GAT GTT CCG GAT TAC GCT* **ACG CGT** GGA AGC TCT TAT TTC GTC AAC TCA C) and the common 3' primer: ccg **ctc gag** tta **CTA** CTT CTT GTC ACC CTT CTG CG. Underlined sequences complement the 5' sense strand sequences for amino acid positions 2 to 7 and the 3' antisense strand sequences encoding the last 7 amino acids. Sequences encoding the Flag (DYKDDDDKG) or HA (YPYDVPDYA) tags are in italics. There is a unique *EcoRI* site (bold lower case) followed by canonical *Kozac* sequence (gcc acc) preceding the initiating ATG (first capitalized codon), and a unique *XhoI* site (bold lower case) after the stop codon (bold upper case). Following sequences encoding the tag (italics), there is a unique in-frame *MluI* site in each 5' PCR primer (bold upper case) as well as an additional GGA codon encoding glycine which could facilitate flexibility between the tag and Hox protein domains. This is an important consideration, because we have demonstrated that the N-terminal domain of Hox proteins is critical for their immortalizing function. In preparation for cloning, the PCR product was digested by *EcoRI* and *XhoI*, and ligated into the pMscvNeo proviral vector (Clontech). To

generate ER fusions of Hoxb8, in-frame sequences encoding the estrogen-binding domain of the human estrogen receptor (residues 282 to 595; ERBD) containing a Gly400Val mutation were produced by PCR using primers containing in-frame *Mlu*I sequences at their 5' ends followed by digestion with MluI and ligation into the MluI site of each tagged Hoxb8 construct. The Gly400Val mutant ER was used because this point mutation renders the receptor insensitive to the low levels of estrogen found in fetal bovine serum (FBS) as well as to the estrogenic effects of other compounds, such as phenol red.

To generate conditional Hoxa9 proteins, codons encoding amino acids 4 to 5 of Hoxa9 were mutated into an *MluI* site in pGEM3zf-EE-Hoxa9, and the same fragment encoding the mutant human ERBD described above was ligated into the Hoxa9 *MluI* site. The EE-ER-Hoxa9 coding sequence was excised by *EcoRI* and inserted into pMscvPuro (Clontech). All plasmids were sequenced over their cloning junctions to verify integrity.

Luciferase reporter assay.

Estradiol-responsiveness was evaluated by measuring the ability of Hox-ER and an activated form of E2a-Pbx1 (or Vp16-Pbx1) to induce coopertiave activation of a luciferase reporter gene driven by tandem repeats of TGAT-TTAT motifs in Nalm6 (for Hoxa9-ER) or 293T (for Hoxb8-ER) cells cultured in medium supplemented with a wide range of concentration of □-estradiol (10^{-11} M to 10^{-5} M). Transcription activation was calculated as the value of relative light units for firefly luciferase versus that for a control renilla luciferase construct that was cotransfected in all samples.

Cell culture.

Myeloid progenitor lines were maintained in a 37°C humidified incubator with 5% CO_2. Progenitors were frozen as described below, and stored in liquid nitrogen.

Affymetrix array analysis.

Gene expression profiling analysis was performed and analyzed using affymetrix mouse total genome array. Hybridization and quantitation of array signals were performed by the UCSD gene chip core laboratory, using the GeneChip Scanner 3000, enabled for high-resolution scanning, coupled with GeneChip operating software (GCOS). Array data was normalized to internal controls, and the overall chip signal intensity was normalized to the mean signal intensity across a group of 12 chips used to evaluate RNA levels in Hoxb8-ER progenitors undergoing neutrophil or macrophage differentiation, and in Hoxb8-ER macrophages stimulated with LPS or BLP. Data was analyzed using "perfect match minus mismatch" algorithms, and signature genes identified exhibited a minimum 5-fold difference in signal intensity between the averages of each groups of three samples. Normalization and processing of GCOS data was performed using dCHIP software. All data is normalized to a basal level of "1", which was selected as a moderately low level of expression.

General Methods.

Spectral karyotype analysis (Yang et al., 2003) and Northern blots (Sykes and Kamps, 2003) were performed as described. For Western blotting, antibodies to Hoxa9, Flag, HA, RelB, Jun, RelA, and Msr1 were used as described previously (Calvo et al., 2000; Park et al., 2005; Sykes and Kamps, 2001; Wang et al., 2005b).

Flow cytometric analysis (FACS), Wright-Giemsa staining, the nitroblue tetrazolium reduction assay (NBT), and the nonspecific esterase assay (NSE): was performed as described previously (Sykes and Kamps, 2001).

Derivation of SCF-dependent neutrophil progenitors using negative selection of progenitors followed by cytokine pre-stimulation and cultivation in SCF.

Bone marrow was harvested from the femur and tibia of female Balb/c mice, and lineage-negative progenitors obtained by negative selection using an antibody cocktail reactive against MacI, B220, and Thy1.2 followed by removal of lin+ cells on a magnetic column (Stemcell Technologies, Vancouver, BC, Canada). Progenitors were pre-stimulated for 48 hours in Iscoves modified Dulbecco medium (IMDM) containing 15% FBS, 1% PSE, 50 ng/mL stem cell factor (SCF), 25 ng/mL IL-3, and 25 ng/mL IL-6. 25,000 marrow progenitors were infected with 1 mL *ER-Hoxb8* retrovirus by spinoculation (2,500*g*, 2 hours, 22°C) in the presence of lipofectamine (1:1000, Gibco BRL), as described in Methods Supplement 5. Infected progenitors were cultured in OptiMem medium containing 10% FBS, 1% PSE, 10ng/ml SCF, 30uM beta mercaptoethanol (1ul into 500 mls medium), and 1 uM β-estradiol (Sigma). An infection efficiency of 10% was approximated based on comparison of the initial rates of progenitor outgrowth in the presence or absence of G418 selection. Immortalized myeloid progenitors were enriched by the serial passage of non-adherent cells every 3 days into new 12-well tissue culture plates. Immortalized progenitors predominated cultures infected by Hox-ER retroviruses by day 14 (cell generation time 18-20 hours), while control cultures evidenced reduce proliferation and stopped dividing by day 21. If GM-CSF is substituted for SCF during selection of

immortalized progenitors in this protocol, clones yielding bi-phenotypic differentiation to neutrophils and macrophages arise.

Derivation of macrophage-committed progenitors immortalized by Hoxb8-ER or of biphenotypic, neutrophil, or macrophage progenitors immortalized by Hoxa9-ER.

Bone marrow was isolated from the femurs of mice following ammonium sulfate lysis of red cells and centrifugation onto a cushion of Ficoll-Paque (Pharmacia, Piscataway, NJ). Ficoll-purified progenitors can be used directly or pre-stimulated 48 hours in 50 ng/mL SCF, 25 ng/mL IL3, and 25 ng/mL IL6. 100,000 Ficoll-purified mononuclear cells were subjected to spinoculation with one ml of Hoxb8-ER retrovirus. Infected progenitors were cultured in "Myeloid Cell Medium" (RPMI 1640 with 10% FBS, 1%Pen-Strep-Glut (PSQ, Gibco BRL, Rockville, MD), 1% GM-CSF-conditioned media from B16 melanoma expressing the GM-CSF cDNA (approximately 10 ng/mL GM-CSF) and 1 uM β-estradiol (Sigma)). Estrogen was kept as 1,000x (1mM) or 10,000x (10mM) stocks in 100% ethanol and stored at -20°C. An infection efficiency of 10% was approximated based on comparison of rates of progenitor outgrowth in the presence of G418, which selects for the co-expressed neomycine phosphotransferase gene encoded by MSCV. Immortalized myeloid progenitors were selected by removal of non-adherent progenitor cells every 3 days to a new well in a 6-well culture plate. This protocol was continued over 3 weeks to produce immortalized macrophage progenitor lines. Selection for G418 resistance permitted derivation of immortalized progenitors in 10 to 14 days. Differentiation to macrophages was performed in the same base medium.

Derivation of neutrophil, macrophage, and biphenotypic progenitors, using Hoxa9-ER or Hoxa7.

These progenitors were derived using the same culture system as described for GM-CSF Hoxb8-ER macrophage progenitors. Derivation of progenitors committed exclusively to neutrophil or monocyte differentiation required cloning, which was performed using 96 well microtiter plates.

Institutional committee approval for animal use.

The experimental protocols were approved by the UCSD animal subjects committee.

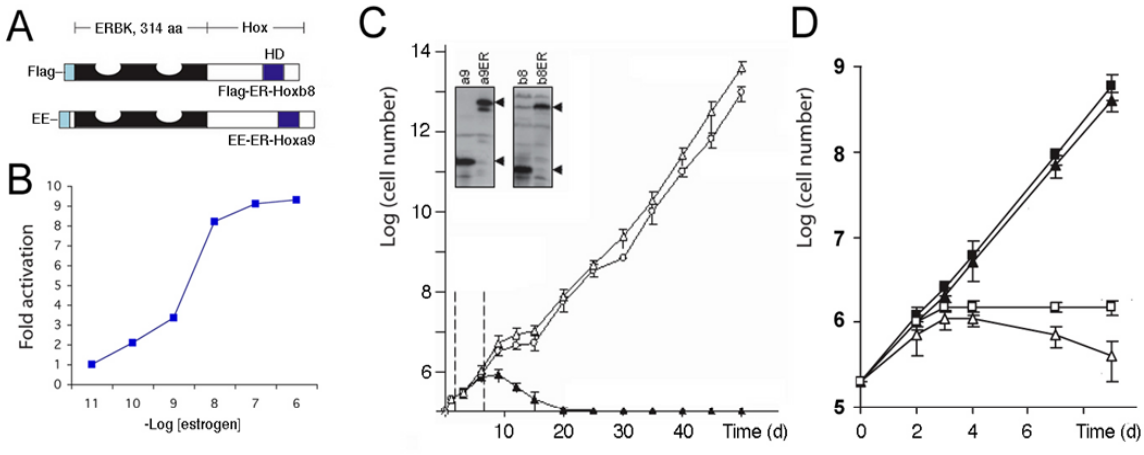

Figure 5.1. Hoxb8-ER and Hoxa9-ER functions conditionally at the biochemical and cellular levels. (**a**) Estrogen-binding domain (ERBD) of the estrogen receptor fused to Hoxa9 or Hoxb8. Epitope tags are indicated at left. HD represents the homeodomain. (**b**) Concentration-dependent transcriptional activity of Hoxa9-ER, measured as co-activation through TGAT-TTAT motifs in cooperation with E2a-Pbx1 in 293T cells. Hoxb8-ER yielded a similar concentration-dependent activation curve. (**c**) Immortalization kinetics of GM-CSF-dependent progenitors following infection by Hoxa9-ER or Hoxb8-ER. Retroviral infection was performed at day 0, and dashed lines signify duration of selection in G418. Inserted panel represents a Western blot using anti-Hoxa9 (left) and anti-Flag antibodies (right) on G418-selected, immortalized progenitors. Immortalization kinetics and doubling times were somewhat faster for progenitors derived in SCF. (**d**) Proliferation of GM-CSF-dependent progenitors immortalized by Hoxa9-ER or Hoxb8-ER following withdrawal of estrogen (day zero).

Figure 5.2. Hoxb8-ER SCF progenitors execute neutrophil differentiation while Hoxb8-ER GM-CSF progenitors execute macrophage differentiation. (**a**) Morphologic changes of Hoxb8-ER SCF neutrophil progenitors (left six photos) and Hoxb8-ER GM-CSF macrophage progenitors (right six photos) following 6 days of cell culture in the absence of estrogen. Identical magnifications were used within the context of the phase contrast, Wright-Giemsa, and differentiation marker pictures (**b**) FACS analysis of neutrophil and macrophage surface markers present on Hoxb8-ER progenitors in the presences of estrogen (blue tracings) or following the removal of estrogen for 6 days (red tracing). Analyzed are Gr-1 (neutrophil differentiation antigen), F4/80 (macrophage differentiation antigen) and Mac1 (general myeloid differentiation antigen).

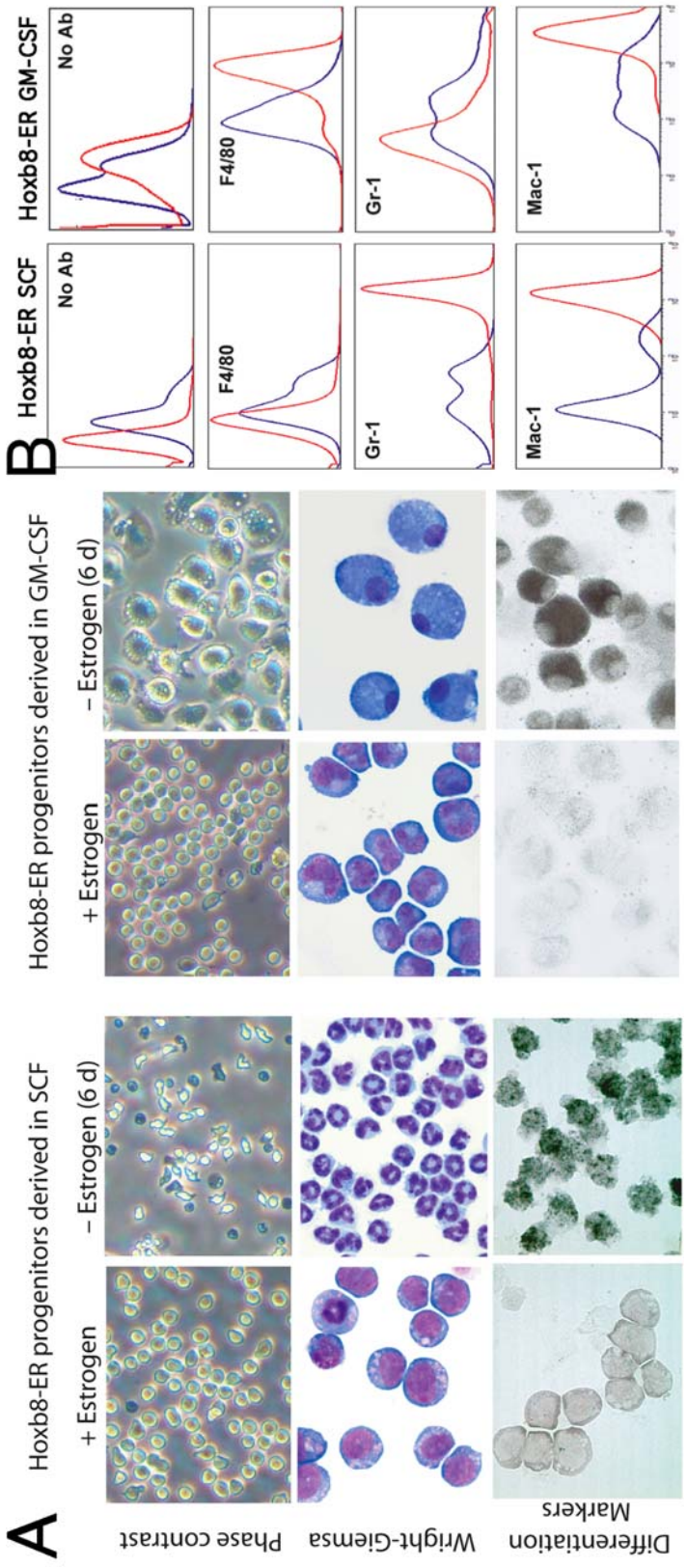
A
Hoxb8-ER progenitors derived in SCF
+ Estrogen
– Estrogen (6 d)
Hoxb8-ER progenitors derived in GM-CSF
+ Estrogen
– Estrogen (6 d)
Phase contrast
Wright-Giemsa
Differentiation Markers
B
Hoxb8-ER SCF
Hoxb8-ER GM-CSF
No Ab
F4/80
Gr-1
Mac-1

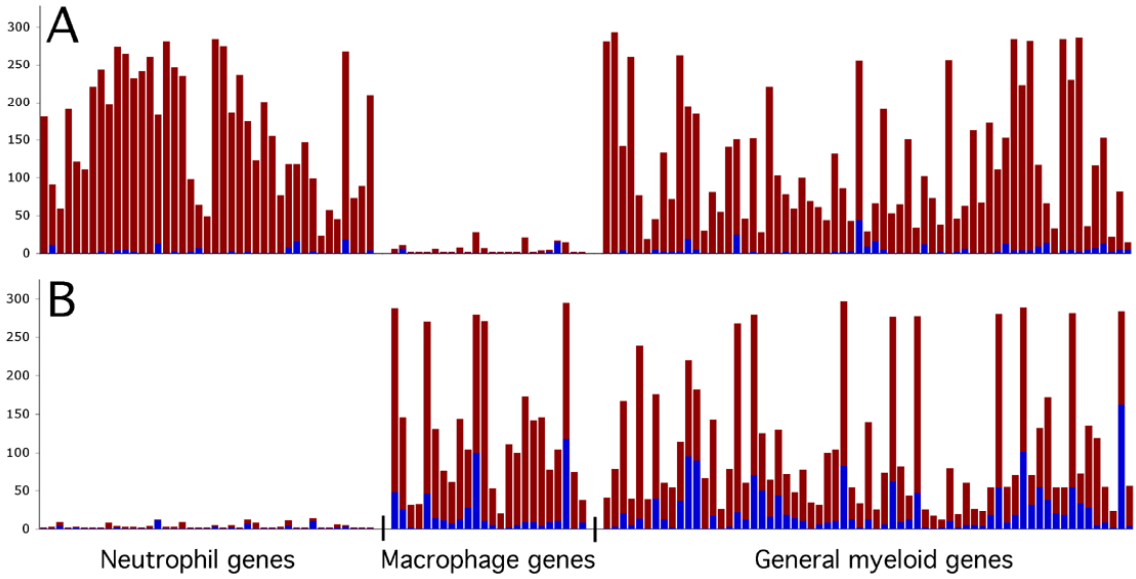

Figure 5.3. Lineage-specific gene expression in Hoxb8-ER SCF neutrophil progenitors and Hoxb8-ER GM-CSF macrophage progenitors. Affymetrix gene arrays were used to quantify the expression levels of 130 myeloid genes in a Hoxb8-ER SCF neutrophil cell line (**a**) and a Hoxb8-ER GM-CSF macrophage cell line (**b**) in the presence of estrogen (blue) and at 6 days of differentiation following estrogen withdrawal (red). Genes illustrated are subdivided among those exhibiting neutrophil-restricted, macrophage-restricted, and general myeloid expression. Genes plotted are underscored in Sup. Tables 5.2, 5.3. The Y-axis plots the relative abundance of RNA, with blue designating basal levels in undifferentiated progenitors and red designating levels in differentiated cells following 6 days of estrogen withdrawal.

Figure 5.4. Hoxb8-ER SCF progenitors behave as GMP, retaining an ability to differentiate into eosinophils and macrophages. Hoxb8-ER SCF progenitors were permitted to differentiate in SCF medium supplemented with the lineage-specific cytokines GCSF, IL5, MCSF, and GM-CSF, as indicated above the photographs. Cells were photographed 6 days after differentiation was initiated by removal of estrogen. In the column demarcated "SCF+IL5", a developing eosinophil is magnified at lower left. All photographs within the "Visible" and "Wright-Giemsa" series are presented at identical magnifications. Proportions of mature cell types within cell cultures following 6 days of differentiation are indicated below each column.

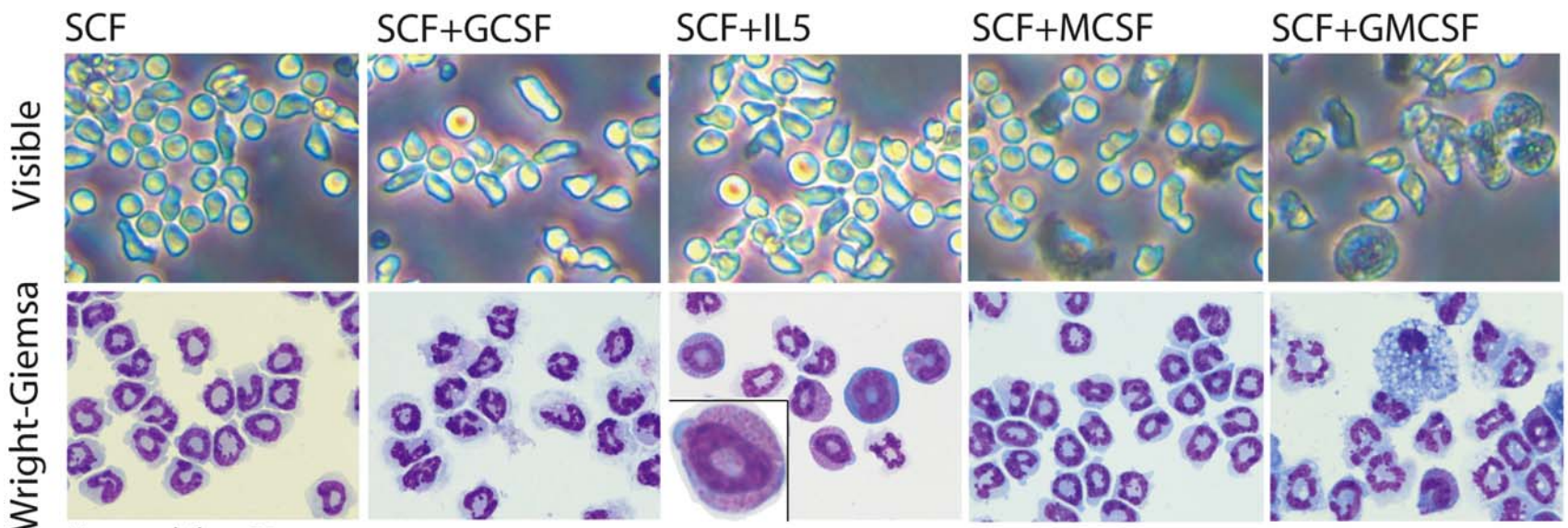

	SCF	SCF+GCSF	SCF+IL5	SCF+MCSF	SCF+GMCSF
Neutrophil	99	100	68	94	81
Eosinophil	0	0	32	0	3
Macrophage	0	0	0	6	16 (100% after 10 d)
Expansion	x70	x120	x110	x75	x840

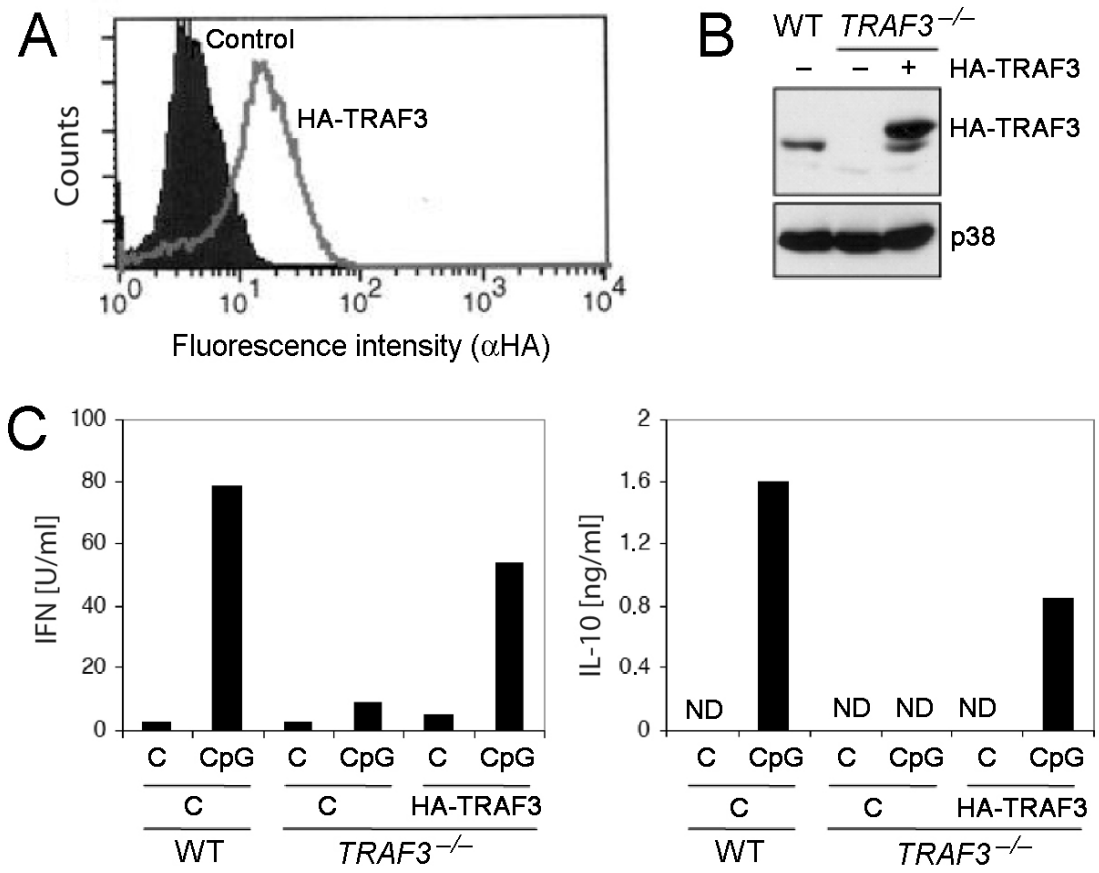

Figure 5.5. Re-expression of TRAF3 restores the signaling defect in CpG-induced transactivation of *IFN* and *IL-10* genes in *Traf3*$^{-/-}$ macrophages produced by Hoxb8-ER. Wild-type (wt) and *Traf3*$^{-/-}$ HoxB8-ER-immortalized macrophage progenitor cells (cultured in GM-CSF) were transduced with MSCV-Puro retroviral vectors encoding HA-tagged TRAF3 or a control empty vector and selected with puromycin. (a) TRAF3 expression was measured by intracellular staining with anti-HA antibodies using flow cytometry, and is presented as fluorescence intensity vs. cell number. (b) HA-TRAF3 expression in *Traf3*$^{-/-}$ progenitors transduced with control vector or the HA-TRAF3 expression vector following differentiated for 6 days in the absence of estrogen. Cell lysates were analyzed by immunoblotting, using antibodies to HA and p38. (c) Differentiated Hoxb8-ER macrophages were stimulated with CpG-DNA and analyzed for IFN and IL-10 production by bioassay and ELISA, respectively. ND = not detectable. This figure was published previously as supplemental data(Hacker et al., 2006).

Supplementary Figure 5.1. SKY karyotype analysis of Hoxb8-ER macrophage progenitors cultured 2.5 years. The karyotype of 20 cells were analyzed and the frequency of cells plotted as a function of their chromosome number. 17 exhibit the normal 40, XX karyotype and 3 exhibited abnormal karyotypes listed adjacent to their histogram bars. A typical analysis is inseted at left.

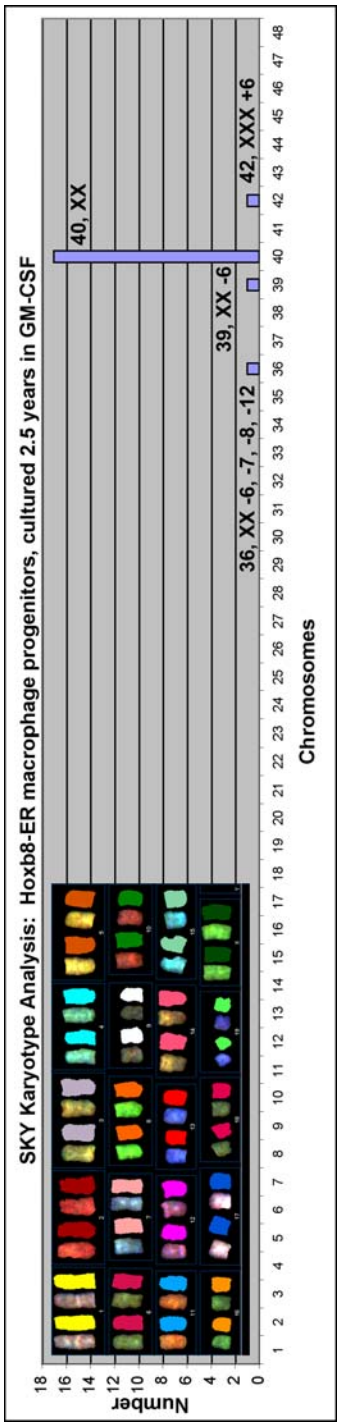
SKY Karyotype Analysis: Hoxb8-ER macrophage progenitors, cultured 2.5 years in GM-CSF
Number
Chromosomes
40, XX
39, XX -6
36, XX -6, -7, -8, -12
42, XXX +6

Supplementary Figure 5.2. **Verification of changes observed on Affymetrix arrays**. (**a**) Immunoblot analysis of the macrophage scavenger receptor (Msr1) and the transcription factors RelB, Jun, and RelA three and six days following removal of estrogen from Hoxb8-ER GM-CSF macrophage progenitors. (**b**) FACS analysis for CD11c in Hoxb8-ER GM-CSF progenitors in the presence of estrogen and 4 days after withdrawal of estrogen. (**c**) Northern blot verification of transcriptional down-regulation of *Gfi1*, *Myb*, *Nolc1,* and *Ela2*, and up-regulation of *Fos*.

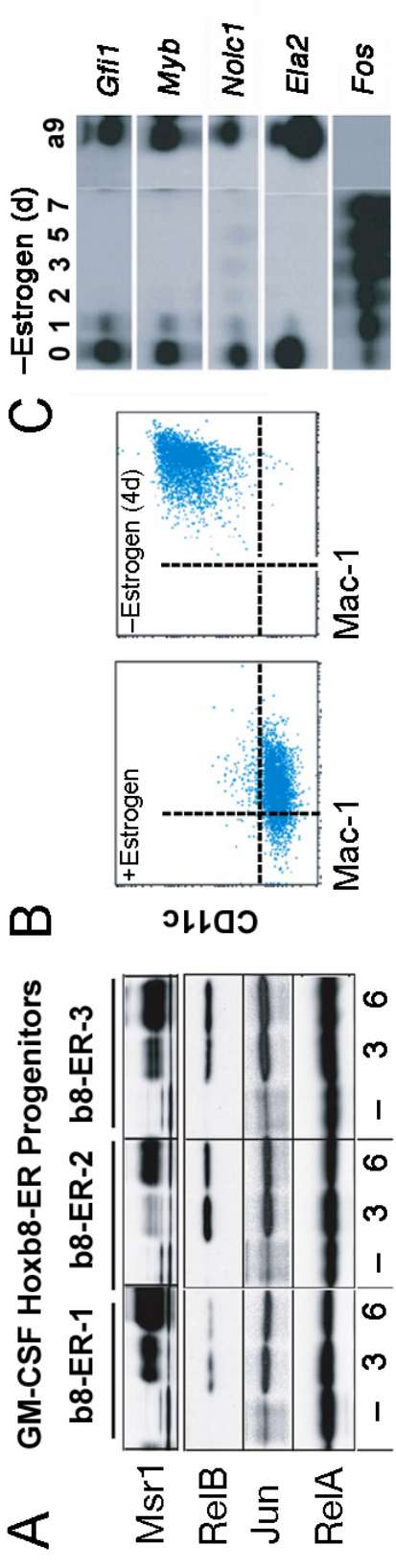
A
GM-CSF Hoxb8-ER Progenitors
b8-ER-1
b8-ER-2
b8-ER-3
– 3 6 – 3 6 – 3 6
Msr1
RelB
Jun
RelA
B
CD11c
+Estrogen
Mac-1
–Estrogen (4d)
Mac-1
C
–Estrogen (d)
0 1 2 3 5 7 a9
Gfi1
Myb
Nolc1
Ela2
Fos

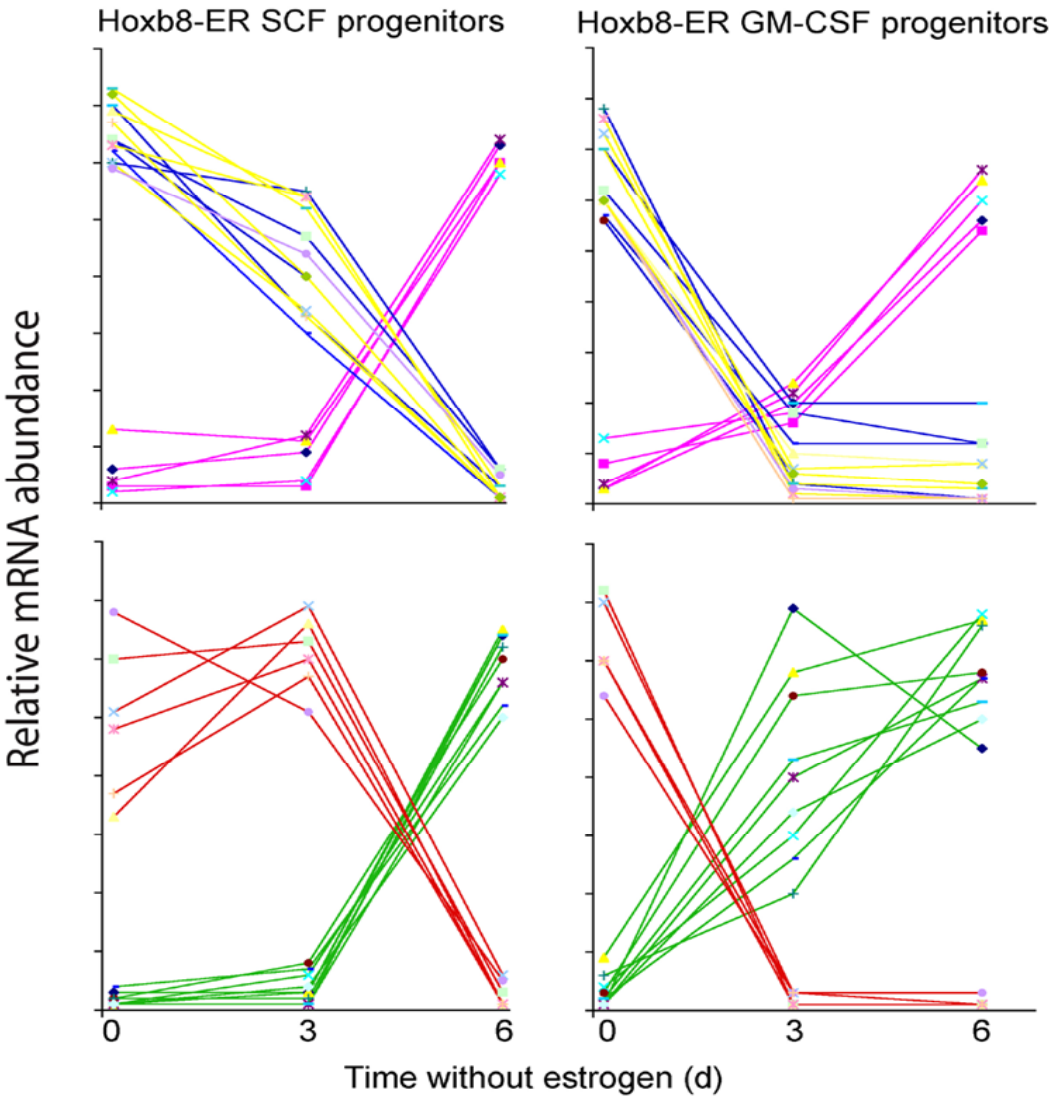

Supplementary Figure 5.3. A concerted program of phagocytic differentiation follows inactivation of Hoxb8-ER in both neutrophil and macrophage progenitors. Down-regulation kinetics of *Myb*, *Myc*, *Hmgb3*, *Ruvbl1* and *Ruvbl2* (blue tracing) mirrors down-regulation of the cell cycle genes *CycB1*, *Shmt2*, *Mcm2*, *Nola1*, *Nol5*, *Nola5*, and *Nolc1* (yellow tracings) in both Hoxb8-ER SCF neutrophil progenitors and Hoxb8-ER GM-CSF macrophage progenitors, and precedes up-regulation of the transcription factor genes *Atf3*, *JunB*, *Fos*, *Jund1*, and *Btg2* (purple tracings; top panels). Down-regulation of the promyelocytic genes *Ctsg*, *Prtn3*, *Cys7*, *Mpo*, *Plac8*, and *Ms4a3* (brown tracings) conincides with up-regulation of the terminal differentiation genes *Fpr1*, *Fpr-rs2*, *Clec7a*, *Mrc1*, *Fgr*, *Atp6vOd2*, *Dusp1*, *Vti1b*, and *Sirpb1* (green tracings; bottom panals). The X-axis designates days following estrogen withdrawal, and the Y-axis designates relative expression level of mRNA measured by Affymetrix arrays.

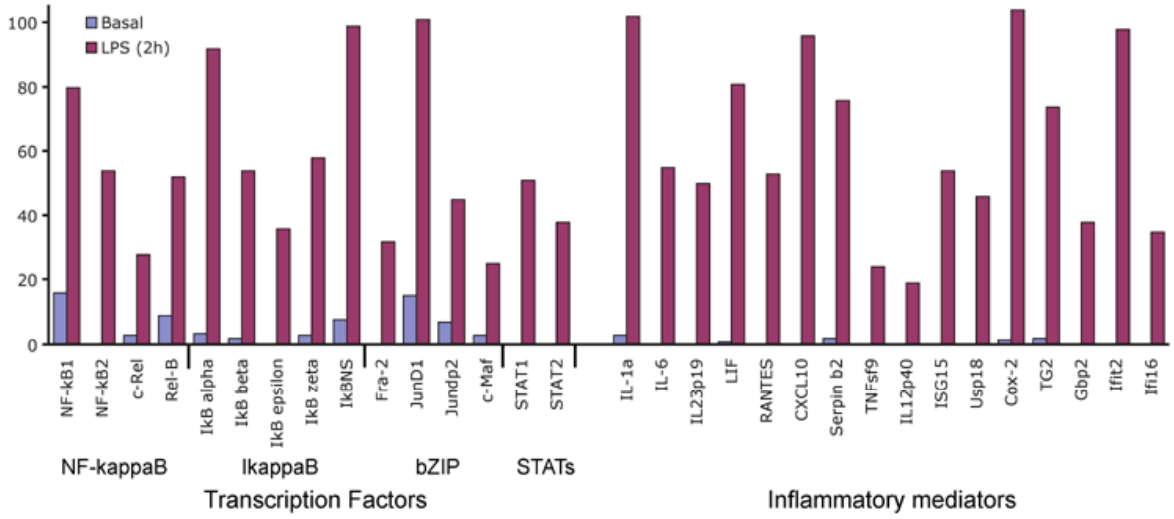

Supplementary Figure 5.4. Inflammatory signaling pathways are preserved in macrophages derived from Hoxb8-ER GM-CSF progenitors. LPS induces rapid activation of genes encoding family members of NF-κB, IκB, bZip, Stat transcription factors, and inflammatory mediators in macrophages produced by withdrawal of estrogen from Hoxb8-ER GM-CSF progenitors for 6 days. Basal levels of mRNA in unstimulated progenitors is represented in blue, and levels induced following 2 h stimulation with LPS are in red.

Table 5.1. Expression of genes encoding transcription factors, cell cycle regulators, and proteins involved in myeloid innate immunity, assessed during neutrophil differentiation of SCF Hoxb8-ER progenitors and during macrophage differentiation of GM-CSF Hoxb8-ER progenitors. "Neutrophil" denotes SCF Hoxb8-ER neutrophil progenitor cells. "Macrophage" denotes the GM-CSF Hoxb8-ER macrophage progenitor cells. "Prog" denotes undifferentiated progenitors. "Diff" denotes mature neutrophils or monocytes resulting from estrogen withdrawal for 6 days. Hybridization and quantitation of array signals were performed as described in Methods.

Gene	Comment	SCF HoxB8-ER Neut Prog		GM Hoxb8-ER Mac Prog		Genbank
		Prog	Diff	Prog	Diff	
Housekeeping control						
Actb	Beta actin, cytoplasmic	266	321	262	311	M12481
Myeloid lineage control genes						
Fcgr2b	Fc fragment of IgG, low affinity IIb	32	34	34	52	BM224327
Fcgr3	Fc receptor, IgG, low affinity III	38	38	32	58	NM_010188
Ccr2	chemokine (C-C motif) receptor 2. Receptor for MCP1	138	62	84	192	U47035
Fcer1g	Fc receptor, IgE, high affinity I, gamma polypeptide	32	30	44	103	NM_010185
Cd33	CD33 antigen, SIGLEC-3	23	30	26	17	NM_021293
Neutrophil genes up-regulated						
IL8rb	IL8 receptor beta. Neutrophil chemokine receptor	<1	180	<1	<1	NM_009909
Ltf	Lactoferrin	<1	190	<1	<1	NM_008522
Lrg1	Leucine-rich alpha-2-glycoprotein, granulocyte marker, unknown function	<1	120	2	1	NM_029796
CD177	CD177, Neutrophil marker of unknown function	<1	110	<1	<1	BC027283
Cnlp	Cathelin, anti-bacterial peptide	<1	440	<1	<1	NM_009921
Lcn2	Lipocalin 2. Neutrophil granual protein. Function unknown	3	240	3	5	X14607
Itgb2l	Integrin beta 2-like. Neutrophil granual protein released on activation	<1	240	<1	<1	NM_008405
Mmp9	Neutrophil gelatinase, Gelatinase B	<1	196	2	14	NM_013599
Pglyrp1	Peptidoglycan recognition protein 1. In traps. Hydrolyzes peptidoglycan	4	380	8	9	NM_009402
Stfa1	Stefin A1. Cystein proteinase inhibitor. Aka Cathepsin, Stefin 3, Cystatin A	10	520	2	10	AW146083
Arg1	Arginase 1, inflammation modulation. Hydrolysis of L-arginine into ornithine	<1	330	<1	<1	NM_007482
Ceacam1	CEA-related cell adhesion molecule 1. Binds SHP1 and SHP2.	3	183	4	6	BC016891
Ceacam10	CEA-related cell adhesion molecule 10.	<1	235	<1	1	NM_007675
Olfm4	Olfactomedian 4. Secreted neutrophil glycoprotein. Aka pDP4	<1	320	8	6	AV290148
Monocyte genes up-regulated						
Mmp12	Matrix metalloproteinase 12, Macrophage elastase	<1	8	36	196	NM_008605
Cd68	Macrosialin, Class D scavenger receptor	6	5	26	120	BC021637
Msr1	Macrophage scavenger receptor 1	<1	<1	3	30	NM_031195
Msr2	Macrophage scavenger receptor 2	<1	<1	<1	32	BC016551
Mgl2	Macrophage galactose N-acetyl-galactosamine specific lectin 2	<1	7	12	132	AW494220
Itgax	Integrin alpha X, Dendritic marker, Cd11c	<1	5	14	117	NM_021334
Clec4n	C-type lectin domain family 4, member n. Clecsf10. Dectin2	<1	<1	72	360	NM_020001
Clec2i	C-type lectin domain family 2, member I. Dcl1, Dendritic cell receptor	<1	<1	11	66	NM_025422
Clec4b	C-type lectin domain family 4, member b. DCAR, activating immunoreceptor	<1	<1	7	54	NM_027218
CD74	CD74 antigen. Macrophage migration inhibitory factor receptor	<1	6	11	292	BC003476
Ccl17	chemokine (C-C motif) ligand 17. Binds CCR4. T cell chemokine	<1	<1	5	48	NM_011332
Ccl22	chemokine (C-C motif) ligand 22. Binds CCR4. T cell chemokine	<1	<1	<1	17	BC012658
C11orf34	Chomrosome 11 open reading fram 34. Plet1, Unknown function	<1	<1	4	116	BC022950
Macrophage commitment genes expressed specifically in GM-CSF Hoxb8 progenitors						
Emr1	Egf-like module containing, mucin-like, hormone receptor-like 1, F4/80	<1	1	10	26	U66888
IRF-8	Interferon regulatory factor 8, ICSBP	4	<1	18	16	NM_008320
TFEC	Transcription factor EC. Microphthalmia-TFE (MiT) subfamily	1	3	101	20	NM_031198
General myeloid genes upregulated						
Fpr1	Formyl peptide receptor 1	<1	280	<1	40	NM_013521
Fpr-rs2	Formyl peptide receptor, related sequence 2	1	392	4	104	NM_008039
Clec7A	C-type lectin domain family 7, member A. Clecsf12, Dectin1, fungal recognition	4	138	20	147	NM_020008
CD300lf	CD300 antigen like family member F, Pigr3, CLIM1, Polymeric Ig Receptor III	<1	260	5	35	BM230330
Mrc1	Mannose receptor, C type 1. Binds bacterial C-terminal mannose	<1	76	13	226	NM_008625
Tlr2	Toll-like receptor 2	<1	28	10	25	NM_011905
Cd14	Cd14 antigen. TLR coreceptor	5	40	40	136	NM_009841
Mmp8	Matrix metalloproteinase 8	5	520	74	154	NM_008611
Itgam	Integrin alpha M, CD11b/CD18, Mac1	2	131	12	48	NM_008401
Fgr	Gardner-Rasheed feline sarcoma viral oncogene homologue. Tyrosine kinase.	2	70	2	52	NM_010208
Lgmn	Legumain. Specific protease. Activates cathepsins B, H, L	<1	29	1	65	NM_011175
Ptpns1	SHP substrate 1. Adhesion receptor coupled to SHP-2.	6	63	17	128	
Sirpb1	Signal regulatory protein b1. Binds DAP12. Activates MAP kinase, phagocytosis	<1	140	3	76	AI662854
Vti1b	Vesicle transport via interaction w/ tSNAREs 1B. Impt in LPS cytokine secretion	<1	54	<1	26	AV002218
Dusp1	Duel specificity phosphatase 1. Ptpn16. Downregulates inflammatory activation	7	109	5	114	NM_013642

(Table 5.1, continued)

Myeloid genes expressed at higher basal levels in GM-CSF Hoxb8-ER progenitors, and upregulated in SCF Hoxb8-ER neutrophil progenitors						
Lyz	Lysozyme	19	350	190	250	AW208566
Gsn	Gelsolin. Involved in podosome formation	5	180	90	92	NM_010354
Cd14	CD14 antigen. TLR coreceptor	5	40	40	136	NM_009841
Lilrb4	Leukocyte immunoglobulin-like receptor, subfamily B, member 4. Inhibitory Rec.	2	150	70	210	U05264
Pira1	Paired-Ig-like activating receptor A1, binds FcRgamma	<1	27	50	75	NM_011087
Pira6	Paired-Ig-like activating receptor A6, binds FcRgamma	<1	102	44	86	NM_011093
Pilrb1	Paired-Ig-like type II activating receptor beta	2	76	18	53	NM_133209
Gpnmb	Glycoprotein nmb. Osteoactivin, DCHIL. Transmembrane, adhesion, binds RGD	4	104	108	266	NM_053110
S100a8	Mrp8; pro-inflammatory, activates endothelial cells, high in neutrophils	6	312	140	258	NM_013650
S100a9	Mrp14; pro-inflammatory, activates endothelial cells, high in neutrophils	4	368	42	48	NM_009114
Ctss	Cathepsin S	7	217	108	457	NM_021281
Csf2ra	Colony stimulating factor 2 receptor, alpha, low-affinity (GM-CSF-receptor)	9	108	54	78	NM_009970
Myeloid transcription factor genes up-regulated						
Fos	FBJ murine osteosarcoma viral oncogene homolog, bZIP transcription factor	8	116	12	256	NM_010234
Jun	v-jun sarcoma virus 17 oncogene homolog, bZIP transcription factor	2	40	2	13	BC002081
Atf3	Activating transcription factor 3, jun-related bZIP transcription factor	<1	32	3	56	NM_007498
Jund1	Jun proto-oncogene related gene d1, bZIP transcription factor	9	168	22	100	NM_010592
JunB	jun B proto-oncogene, bZIP transcription factor	16	80	8	54	NM_008416
Cebpb	CCAAT/enhancer binding protein (C/EBP), beta, up in myeloid differentiation	14	102	82	136	NM_009883
Btg2	B-cell translocation gene 2. Anti-proliferative. Downregulates cyclin D1	3	52	12	200	BG965405
Mxd1	MAX dimerization protein 1, Mad	4	88	7	15	BB036846
Stem cell receptor and transcription factor genes expressed exclusively in SCF Hoxb8-ER progenitors						
Cd34	CD34 antigen. Early hemopoietic stem cells, adhesion	128	7	<1	<1	NM_133654
Flt3	Fms-related tyrosine kinase 3, early hemopoietic stem cells	23	<1	<1	<1	NM_010229
Crlrc	Calcitonin receptor-like receptor	40	1	<1	<1	AF209905
Gpr56	G-protein coupled recptor 56	48	<1	<1	<1	AK141886
Ptprcap	CD45-associated protein	21	<1	<1	<1	NM_016933
Kcna1	Potassium voltage-gated channel, shaker-related subfamily, member 3	14	<1	<1	<1	AI323624
C1qr1	Complement component 1, q subcomponent, receptor 1. AA4.1, Ly68	39	1	<1	<1	AF209905
Msi2	Musashi homolog 2	28	1	<1	<1	BB418489
Sox4	SRY-box containing gene 4, HMG protein, oncoprotein	32	<1	<1	<1	NM_009238
Hmgn1	High-mobility group nucleosome binding domain 1. In embryogenesis/stem cells	94	6	<1	<1	NM_008251
Hmga2	High mobility group AT-hook 2	87	2	<1	<1	NM_010441
Meis1	Meis1, myeloid ecotropic viral integration site 1 homolog, hemopoietic stem cells	17	<1	<1	<1	NM_010789
Erg	Ets-related gene	16	1	<1	<1	AV329219
Nrip1	Nucelar receptor interacting protein 1, RIP140	22	<1	<1	<1	BB764550
Promyelocyte genes down-regulated in both SCF Hoxb8-ER and GM-CSF Hoxb8-ER progenitors						
Mpo	Myeloperoxidase. In azurophilic (primary) granuals	340	4	240	<1	NM_010824
Prtn3	Proteinase 3. Serine proteinase Myeloblastin. In azurophilic (primary) granuals	294	4	400	2	U97073
Ela2	Elastase 2. Neutrophil elastase, serine proteinase	20	<1	300	<1	NM_015779
Cnn3	Calponin 3, acidic. Actin-binding protein	136	3	46	<1	BB724741
Nedd4	Neural precursor cell expressed, developmentally down-regulated gene 4.	110	12	9	<1	NM_010890
Plac8	Placenta-specific 8. Unknown function	240	4	180	1	AF263458
Ms4a3	Membrane-spanning 4-domains, subfamily A, member 3, HTm4.	56	3	144	3	NM_133246
Transcription factor genes down-regulated in both SCF Hoxb8-ER and GM-CSF Hoxb8-ER progenitors						
Myc	v-myc myelocytomatosis viral oncogene homolog	88	<1	37	3	BC006728
Ruvbl1	RuvB-like protein 1. Pontin52 helicase. Binds TBP, Myc, E2F, b-catenin	30	<1	14	4	NM_019685
Ruvbl2	RuvB-like protein 2, Reptin52 helicase. Transcription regulation	43	3	29	6	NM_011304
Myb	v-myb myeloblastosis viral oncogene homolog, transcript variant 1	78	3	52	<1	NM_010848
Mybl2	B-Myb. Regulates cell cycle via p107, maintains ES cell stem-likeness	8	<1	14	<1	NM_008652
Rbbp4	Retinoblastoma binding protein 4	62	<1	36	10	BF011461
Tsc22d1	TSC22 domain family, member 1. Tgfb1i4, HLH transcription factor	49	1	96	9	AU016382
Hmgb3	High mobility group box 3, Hmg4. In hemopoietic stem cells. Inhibits dif.	72	4	12	2	NM_008253
Nsbp1	Nucleosome binding protein 1. Transactivation function, embryonic expression	21	3	18	2	NM_016710
Cell division genes down-regulated						
CycB1	Cyclin B1, binds cdk1/cdc2, G2/M progression	40	<1	18	3	X58708
Shmt2	Serine hydroxymethyl transferase 2. Nucleotide biosynthesis	21	<1	37	4	BM222403
Rrm2	Ribonucleotide reductase M2. Nucleotide biosynthesis	46	<1	52	4	NM_009104
Mcm2	Minichromosome maintenance deficient 2-DNA replication licensing helicase	84	2	38	<1	NM_008564
Cdc6	Cell division cycle 6, loads MCM7, licensing factor. DNA replication	40	7	12	<1	NM_011799
Cdt1	DNA replication factor. Licensing factor. Loads mcm2-7. Oncoprotein in 3T3	27	8	60	8	AF477481
Nola1	Nucleolar protein family A, member 1, snRNP. RNA maturation	32	10	30	<1	NM_026578
Nol5	Nucleolar protein 5, Nop5/Nop58. RNA maturation	44	<1	24	<1	BB729616
Rnu50	RNA, U50 small nuclear. mU50, snoRNA. RNA maturation	42	4	23	<1	AK012825
Nol5a	Nucleolar protein 5A. NOP56. RNA maturation, ribosome Biogenesis	66	6	28	1	BM249243
Nolc1	Nucleolar and coiled body phosphoprotein 1. RNA maturation, ribosome genesis	22	<1	24	2	BM236574
Set	SET translocation. PP2A inhibitor. High in cancer/regenerating cells.	104	15	72	6	BF134272

Supplementary Table 5.1. **Ratios of neutrophils and monocytes produced by differentiation of cloned progenitors immortalized by Hoxa9-ER, following estrogen withdrawal**. Among 23 clones of GM-CSF-dependent Hoxa9-ER progenitors, four exhibited strict neutrophil differentiation, one exhibited exclusive macrophage differentiation, and 18 exhibited biphenotypic differentiation that favored production of neutrophils over macrophages.

Clone ID#	% Neutrophils	% Monocyte
1	78	22
2	67	33
3	72	28
4	85	15
5	94	6
6	98	2
7	41	59
8	46	54
9	82	18
10	79	21
11	84	16
12	100	0
13	90	10
14	94	6
15	95	5
16	100	0
17	100	0
18	43	57
19	100	0
20	91	9
21	6	94
22	87	13
23	0	100

Supplementary Table 5.2. Gene down-regulation in SCF Hoxb8-ER neutrophil progenitors and in GM-CSF Hoxb8-ER macrophage progenitors during terminal differentiation.

		SCF Hoxb8-ER Neut Prog		GM-CSF Hoxb8-ER Mac Prog		
Gene	**Comment**	**0**	**6d**	**0**	**6d**	**Genbank**
Cell cycle genes						
Ccnb1	cyclin B1, binds cdk1/cdc2, G2/M progression	40	<1	18	130	X58708
Cenph	Centromere autoantigen H	14	2	8	<1	NM_021886
Wee1	Wee 1 homolog, Inhibits cdk1	10	<1	12	2	BC006852
Ard1	N-acetyltransferase ARD1 homolog	20	5	14	3	NM_019870
Cdc20	CDC20 cell division cycle 20 homolog.	42	20	60	12	BB041150
Cdk4	cyclin D dependent kinase 4, c-Myc target gene	25	6	13	4	NM_009870
Ccnd2	cyclin D2	46	1	8	7	NM_009829
Nucleotide biosynthesis						
Apex1	Apurinicapyrimidinic endonuclease. DNA repair enzyme	32	6	30	3	AV263745
Shmt2	Serine hydroxymethyltransferase 2	21	<1	37	4	BM222403
Ppat	Phosphoribosyl pyrophosphate amidotransferase	33	2	8	<1	BG064988
Rrm2	Ribonucleotide reductase M2	46	<1	52	4	NM_009104
Dtymk	Deoxythymidylate kinase	52	10	27	3	NM_023136
Prps1	Phosphoribosyl pyrophosphate synthetase 1	28	2	12	3	NM_021463
Gart	Phosphoribosylglycinamide formyltransferase	19	6	40	10	NM_010256
Impdh2	Inosine 5'-phosphate dehydrogenase 2	106	3	40	4	NM_011830
DNA replication						
Mcm2	Minichromosome maintenance deficient 2- licensing helicase	84	2	38	<1	NM_008564
Srm	Spermidine synthase	48	2	52	2	NM_009272
Dut	Deoxyuridine triphosphatase, eliminates dUTP	38	9	17	<1	AF091101
Hells	Helicase, lymphoid specific	18	10	17	<1	NM_008234
Cdc6	Cell division cycle 6 homologue. Loads MCM7. Licensing factor	40	6	12	<1	NM_011799
Ris2	Retroviral integration site 2. Cdt1. Loads mcm2-7. Oncoprotein	27	8	60	8	AF477481
Mcm3	Mini chromosome maintenance deficient 3	24	4	19	3	BF606890
Mcm5	Mini chromosome maintenance deficient 5-replication licensing helicase	42	3	27	4	NM_008566
Mcm6	Mini chromosome maintenance deficient 6-replication licensing helicase	90	4	50	7	NM_008567
Mcm7	Mini chromosome maintenance deficient 7-replication licensing helicase	134	20	100	15	BB464359
Rpa2	Replication protein A2	30	1	19	4	AK011530
Prim1	DNA primase, p49 subunit	24	6	14	3	NM_008921
Smu1	Suppressor of mec-8 and unc-52 homolog. DNA replication	26	3	20	12	NM_021535
Ribosome biogenesis, RNA maturation						
Nola1	Nucleolar protein family A, member 1	32	10	30	<1	NM_026578
Nol5	Nucleolar protein 5, Nop5	44	<1	24	<1	BB729616
Rnu50	mU50, snoRNA	42	4	23	<1	AK012825
Nol5a	Nucleolar protein 5A. Nucleolar protein 56	66	6	28	70	BM249243
Nolc1	Nucleolar and coiled body phosphoprotein 1	22	<1	24	2	BM236574
Pa2g4	Proliferation-associated PA2G4	44	3	46	5	NM_011119
Lyar	Ly1 antibody reactive clone. Zinc-finger nucleolar protein.	54	10	24	4	NM_025281
Rnu22	RNA, U22 small nucleolar	50	6	40	7	BQ177137
Hnrnpa1	heterogeneous nuclear ribonucleoprotein A1	92	10	90	24	AK007802
Sfrs1	splicing factor, arginine/serine-rich 1 (ASF/SF2)	32	3	30	7	NM_173374
SF3a	splicing factor 3a	30	2	10	4	BC009141
Wdr12	WD repeat domain 12. Required for ribosome biogenesis, proliferation	32	1	13	2	NM_021312

(Supplementary Table 5.2, continued)

Differentiation-related genes (not transcription factors)						
Ela2	Elastase 2. Neutrophil	20	<1	156	<1	NM_015779
Mpo	Myeloperoxidase	320	3	176	3	NM_010824
Prtn3	Proteinase 3, myeloblastin, serine proteinase, in azurophilic granuals	294	4	188	<1	U97073
Ctsg	Cathepsin G, granual protein, serine proteinase	400	20	194	2	NM_007800
Cst7	Cystatin F (leukocystatin). hematopoietic-specific	82	8	82	<1	NM_009977
Cnn3	Calponin 3, acidic. Actin-binding protein	136	3	54	<1	BB724741
Ms4a3	Membrane-spanning 4-domains subfamily A, member 3, , HTm4	50	4	154	1	NM_133246
Plac8	Placental 8, onzin	240	4	180	1	AF263458
Igfbp4	Insulin-like growth factor binding protein 4	32	3	34	2	BC019836
Slc16a1	monocarboxylate transporter	66	5	41	4	NM_009196
Ppid	Peptidylprolyl isomerase D. Cyclophilin D	48	8	28	3	BC011499
Slc19a1	solute carrier family 19 (sodium/hydrogen exchanger), member 1	26	2	32	4	AI323572
F13a1	Coagulation factor XIII, A1 subunit	112	20	170	25	NM_028784
Fkbp4	FK506 binding protein 4. FKBP52	34	4	31	5	NM_010219
Icam2	Intercellular adhesion molecule 2	26	6	17	4	NM_010494
Timm8a	Translocase of inner mitochondrial membrane 8 homolog	30	7	24	7	NM_013898
Csda	Cold shock domain protein A	50	10	30	9	AV216648
Idh3a	Isocitrate dehydrogenase 3 (NAD+) alpha	31	3	34	6	AK003393
Nedd4	Neural precursor cell expressed. Ubiquitination.	38	1	9	<1	NM_010890
Ptpn2	Protein tyrosine phosphatase, non-receptor type 2. Neg. reg. of inflam.	30	<1	24	1	NM_008977
BC035044	Hematopoietic-specific transcript	72	2	30	<1	BC035044
Transcription factors						
Myc	Myelocytomatosis proto-oncogene	102	2	65	11	BC006728
Ruvbl1	RuvB-like protein 1, Pontin52, Helicase, binds TBP, Myc, E2F, b-catenin	30	<1	14	4	NM_019685
Ruvbl2	RuvB-like protein 2, Reptin52, Helicase, transcription regulation	43	3	29	6	NM_011304
Myb	v-myb myeloblastosis viral oncogene homolog, transcript variant 1	78	3	52	<1	NM_010848
Mybl2	B-Myb, regulates cell cycle via p107, maintains ES cell stem-likeness	8	<1	14	<1	NM_008652
Gfi1	Growth factor independent 1. Zinc finger transcriptional repressor	33	8	41	<1	NM_010278
Nsbp1	Nucleosome binding protein 1, transactivation, embryonic expression	21	3	18	2	NM_016710
Hmgb3	High mobility group box 3. In hemopoietic stem cells, inhibits dif.	72	4	12	2	NM_008253
Rbbp4	Retinoblastoma binding protein 4	62	<1	36	10	BF011461
Tsc22d1	TSC22 domain family, member 1, Tgfb1i4, HLH transcription factor	49	1	96	9	AU016382
Downregulated in SCF Hoxb8-ER progenitors, but not expressed in GM-CSF Hoxb8 progenitors (earlier stem cell genes)						
Cd34	CD34 antigen, hemopoietic stem cells, adhesion	128	7	<1	<1	NM_133654
Flt3	Fms-related tyrosine kinase 3, early hemopoietic stem cells	23	<1	<1	<1	NM_010229
Crlrc	Calcitonin receptor-like receptor	40	1	<1	<1	AF209905
Gpr56	G-protein coupled recptor 56	48	<1	<1	<1	AK141886
Ptprcap	CD45-associated protein	21	<1	<1	<1	NM_016933
Kcna1	Potassium voltage-gated channel, shaker-related subfamily, member 3	14	<1	<1	<1	AI323624
C1qr1	Complement component 1, q subcomponent, receptor 1. AA4.1, Ly68	39	1	<1	<1	AF209905
Msi2	Musashi homolog 2	28	1	<1	<1	BB418489
Sox4	SRY-box containing gene 4, HMG protein, oncoprotein	32	<1	<1	<1	NM_009238
Hmgn1	High-mobility group nucleosome binding domain 1. Embryonic and stem	94	6	<1	<1	NM_008251
Hmga2	High mobility group AT-hook 2	87	2	<1	<1	NM_010441
Meis1	Meis1, myeloid ecotropic viral integration site 1 homolog. Stem cells	17	<1	<1	<1	NM_010789
Erg	Ets-related gene	16	1	<1	<1	AV329219
Nrip1	Nucelar receptor interacting protein 1, RIP140	22	<1	<1	<1	BB764550

Supplementary Table 5.3. Gene up-regulation in SCF Hoxb8-ER neutrophil progenitors and in GM-CSF Hoxb8-ER macrophage progenitors during terminal differentiation.

		SCF Hoxb8-ER Neut Prog		GM-CSF Hoxb8-ER Mac Prog		
Gene	**Comment**	**Prog**	**Diff**	**Prog**	**Diff**	**Genbank**
Early myeloidmarkers						
Fcgr2b	IgG Fc gamma receptor 2 beta, low affinity	32	34	34	52	BM224327
Fcgr3	IgG Fc gamma receptor 3, low affinity	38	38	32	58	NM_010188
Ccr2	Receptor for macrophage chemotactic protein (MCP1)	138	62	84	192	U47035
Fcer1g	IgE Fc receptor 1 gamma, high affinity	32	30	44	104	NM_010185
Cd33	Cd33 antigen	23	30	26	17	NM_021293
Neutrophil specific						
IL8rb	IL8 receptor beta, neutrophil chemokine receptor	<1	180	<1	<1	NM_009909
Il17r	IL17 Receptor	11	80	<1	2	NM_008359
C5r1	Complement component 5 receptor one	<1	58	4	5	NM_007577
Lfn	Lactoferrin	<1	190	<1	<1	NM_008522
Lrg1	LRG1, Leucine-rich alpha-2-glycoprotein	<1	120	2	1	NM_029796
Cd177	Cd177 antigen. NB-1, Prv-1, Increased in polycythemia rubra vera-I	<1	110	<1	<1	BC027283
Camp	Cathelicidin antimicrobial peptide	<1	440	<1	<1	NM_009921
Lcn2	Lipocalin 2. In granulocytic precursors and epithelia cells	3	240	3	5	X14607
Mmp9	Neutrophil gelatinase, Matrix metalloproteinase 9, Gelatinase B	<1	196	2	14	NM_013599
Pglyrp1	Peptidoglycan recognition protein, neutrophil granual protein	4	380	8	9	NM_009402
Stfa1	Stefin A1. Cystein proteinase inhibitor. Cathepsin, Stefin 3, Cystatin A	10	520	2	10	AW146083
Stfa2l1	stefin A2 like 1, Cystein proteinase inhibitor	4	460	1	17	BB667930
Itgb2l	Neutophil-specific Integrin beta 2-like	<1	240	<1	<1	NM_008405
Stfa3	Stefin A3, Cystein proteinase inhibitor	<1	340	<1	10	NM_025288
Ngp	Neutrophilic granual protein, Bectenecin, Cathelin- and Cystatin-homology	13	170	22	2	NM_008694
Chi3l3	Chitinase 3-like 3. YM1, Glycosidase	<1	720	<1	28	NM_009892
Chi3l4	Chitinase 3-like 4. YM2	3	243	<1	5	AY065557
Ifitm6	Interferon-induced transmembrane protein 6	<1	234	3	16	BB193024
Cyp4f18	Cytochrome P450, family 4, subfamily f, polypeptide 18	2	96	<1	<1	NM_024444
Map3k5	Mitogen activated protein kinase kinase kinase 5. Links TRAF6 to p38	7	57	<1	1	AV377656
Trem1	Triggering receptor on myeloid cells	1	48	<1	<1	NM_021406
Olfm4	Olfactomedian 4. Secreted neutrophil glycoprotein, pDP4. Regulated by Pu.1	<1	320	8	6	AV290148
Arg1	Arginase 1	<1	330	<1	<1	NM_007482
Ceacam1	CEA-related cell adhesion molecule 1	3	183	4	6	BC016891
Ceacam10	CEA-related cell adhesion molecule 2	<1	235	<1	1	NM_007675
Expi1	extracellular proteinase inhibitor, Wdnm1	2	173	15	11	AV006463
Sasp	Skin aspartyl protease	<1	122	1	8	AK004007
Retn1a	Resistin like alpha, Fizz1, cEBP epsilon-dependent	<1	200	1	1	NM_020509
Syne1	Synaptic nuclear envelope 1. Nesprin 1, Nuclear organization	<1	154	<1	<1	BI734306
Bcl6	Zn-finger transcriptional repressor	<1	76	<1	2	NM_009744
Rnf11	Ring finger protein 11, Ubiquitination specificity	8	110	4	7	BI150320
Rnf144	Ring finger protein 144, Ubiquitination specificity	16	102	<1	<1	BB125275
Pdi4	Pepdidyl arginine deiminase type IV, Histone H3-specific transrepression	<1	146	<1	<1	NM_011061
Septin5	CDCRel1, GTP-binding protein	3	96	10	4	AF033350
Trim 12	Tripartite motif protein 12	1	22	<1	<1	BM244351
Crispld2	Cysteine-rich secretory protein LCCL domain containing 2	<1	56	<1	<1	BB558800
Diap1	Diaphanous protein homolog 1. Rho effector, cell motility	<1	44	2	4	AW554652
Slc2a3	Facilitated glucose transporter	20	274	3	2	BB414515
Olfml2b	Olfactomedian-like 2b, photomedian 2	<1	72	<1	<1	BC025654
Mcpt2	Mast cell protease 2	<1	88	<1	<1	NM_008571
Mcpt5	Mast cell protease 5	4	412	<1	<1	NM_010780
Cd73	Cd73 antigen. Ecto-5'-nucleotidase	<1	30	<1	<1	AV273591
Tgm2	Transglutaminase 2, C polypeptide. Adhesion, NF-kB activation	1	34	1	6	AW321975
Hsd11b1	Hydroxysteroid 11-beta dehydrogenqase 1	<1	84	14	1	NM_008288
Unknown	216 aa, Protein ID BAE42230	<1	110	<1	<1	BG070087
Unknown	786 aa, Denn and Madd domains. Conserved to worm. Gene 1437121	2	42	<1	5	BB168293
Unknown	537 aa, conserved to worm, PL48,Up in neuts from HL60. Gene 1460555	8	66	2	2	BM242294

(Supplementary Table 5.3, continued)

Monocyte / Dendritic-Specific						
Mmp12	Macrophage elastase, Matrix metalloproteinase 12,	<1	5	56	300	NM_008605
Cd68	Cd68 antigen, Macrosialin, Class D scavenger receptor	6	5	26	120	BC021637
Msr1	Macrophage scavenger receptor 1 (SR-A)	<1	<1	2	30	NM_031195
Msr2	Macrophage scavenger receptor 2	<1	<1	<1	32	BC016551
Clec4n	C-type lectin domain family 4, member n. Inflammatory marker.	<1	<1	72	360	NM_020001
Itgax	Integrin alpha X, Dendritic marker, Cd11c	<1	5	14	117	NM_021334
Clec2i	C-type lectin domain family 2, member I. Unknown function	<1	<1	11	66	NM_025422
Clec4b	C-type lectin domain family 4, member b, Activating immunoreceptor	<1	<1	7	54	NM_027218
Mgl2	Macrophage galactose N-acetyl-galactosamine specific lectin	<1	7	12	132	AW494220
Ifi30	Interferon gamma inducible protein 30, Lysosomal thiol reductase	1	<1	28	76	NM_023065
Lpl	Lipoprotein Lipase, Secreted, Hydrolyzes VLDL	<1	27	140	250	NM_008509
Cd74	Cd74 antigen. Invariant polypeptide of MHC, class II, CLIP, DHLAG	<1	6	11	292	BC003476
Ccl17	CCR4 ligand, T cell chemokine produced by macrophages	<1	<1	5	48	NM_011332
Ccl22	CCR4 ligand, T cell chemokine produced by macrophages, aka MDC	<1	<1	<1	19	BC012658
H2-Ea	Histocompatibility 2, class II antigen E alpha	<1	<1	2	109	NM_010381
H2-Ab1	Histocompatibility 2, class II antigen A beta 1	<1	<1	5	95	BC008168
H2-Aa	Histocompatibility 2, class II antigen A, alpha	<1	20	9	164	AV018723
H2-Eb1	Histocompatibility 2, class II antigen E beta 1	<1	3	4	142	NM_010382
H2-DMb2	Histocompatibility 2, class II, locus DMb2	2	3	9	69	NM_010388
H2-DMa	Histocompatibility 2, class II, locus Dma	15	2	10	94	NM_010386
F7	Coagulation factor VII, produced by atherosclerotic macrophages	<1	14	166	250	NM_010172
Cxcl2	Chemokine (C-X-C motif) ligand 2, Macrophage inflammatory protein 2	<1	<1	<1	74	NM_009140
Lrp1	low density lipoprotein receptor-related protein 1	<1	1	8	30	NM_008512
Nov	Nephroblastoma overexpressed, angiogenesis inducer, CTGF related	<1	<1	22	54	X96585
Ccl9	chemokine (C-C motif) ligand 9, MIP1 gamma, Scya9/Scya10	107	12	130	150	NM_011338
Fcgrt	Fc receptor, IgG, alpha chain transporter	<1	2	34	60	NM_010189
BB559293	456 aa, Widely expressed, BB559293	<1	<1	24	44	NM_175172

(Supplementary Table 5.3, continued)

Myeloid differentiation markers upregulated in both neutrophils and monocytes						
Fpr1	Formyl peptide receptor 1	<1	280	<1	40	NM_013521
Fpr-rs2	Formyl peptide receptor-related sequence 2	1	392	4	104	NM_008039
Clec7A	C-type lectin domain family 7, member A. Fungal recognition	4	138	20	147	NM_020008
CD300lf	CD300 antigen like family member F, Pigr3, CLIM1	<1	260	5	35	NM_145634
Mrc1	Mannose receptor C1, macrophage/dendritic. Binds bacterial C-terminal mannose	<1	76	13	226	NM_008625
P2ry6	pyrimidinergic receptor P2Y, G-protein coupled, 6, activated by UDP	<1	18	<1	38	BC027331
Cd14	Cd14 antigen, TLR coreceptor	5	40	40	136	NM_009841
Itgam	Integrin alpha M, CD11b/CD18, Mac1	2	131	12	48	NM_008401
Fgr	Src-family myeloid tyrosine protein kinase	2	70	2	52	NM_010208
Mmp8	Matrix metalloproteinase 8	5	520	74	154	NM_008611
Lyzs	Lysozyme	19	350	190	250	AW208566
Gsn	Gelsolin, involved in podosome formation	5	180	90	92	NM_010354
Lgmn	Legumain, activates cathepsins B, H, L	<1	29	1	65	NM_011175
Atp6v0d2	ATPase, H+ transporting, lysosomal V0 subunit D2	<1	80	17	126	AV204216
Vti1b	Vesicle transport through interaction with t-SNAREs 1B homologs,exocytosis	<1	54	<1	26	AV002218
Sirpb1	Signal regulatory protein beta 1, promotes phagocytosis, filopodia & lamellipodia	<1	140	3	76	AI662854
Clec4d	C-type lectin domain family 4, member d, endocytic recptor	31	156	27	308	NM_010819
Tlr2	Toll-like receptor 2	<1	45	12	48	NM_011905
Lilrb4	leukocyte immunoglobulin-like receptor, subfamily B, member 4	2	150	70	210	U05264
Pira1	Paired-Ig-like receptor A1, activating, binds FcRgamma	<1	27	50	75	NM_011087
Pilra	Paired Ig-like type 2 receptor alpha, inhibitory	<1	220	16	48	BB775785
Pira6	Paired-Ig-like receptor A6, activating, binds FcRgamma	<1	102	44	86	NM_011093
Pilrb1	Paired-Ig-like type II receptor beta, activating, FDFACT	2	76	18	53	NM_133209
Pirb5	Paired-Ig-like receptor B5, inhibitory, dendritic/B cells	<1	58	14	34	U96693
Ccr1	Chemokine (C-C motif) receptor 1	<1	99	10	68	BC011092
Bst1	Marrow stromal cell antigen 1/Cd157/fMLP receptor. Adhesion & chemotaxisis.	<1	68	<1	34	NM_009763
C3aR1	Complement component 3a receptor 1	1	60	6	26	BC003728
Clec4a3	C-type lectin domain family 4, a3. DCIR3; Dendritic cell inhibitory receptor 3.	<1	43	8	92	AK014135
Clec4a2	DCIR; Dendritic cell immunoreceptor-inhibitory, Clecsf6	2	130	10	94	NM_011999
Gpnmb	Glycoprotein nmb, transmembrane, adhesion, binds RGD, osteoactivin	4	104	108	266	NM_053110
IL1r2	Interleukin 1 receptor, type II (pro-inflammatory)	3	40	12	42	NM_010555
Il1rl1	interleukin 1 receptor-like 1, negative feedback of pro-inflammation	44	212	2	32	D13695
Tnfrsf1b	Tumor necrosis factor receptor superfamily, member 1b, pro-inflammatory	9	20	12	128	M59378
Tgfbi	Transforming growth factor, beta induced. Binds integrin. ECM adhesion protein	16	50	<1	25	NM_009369
IL1b	Interleukin 1 beta	5	186	6	68	BC011437
Ccl6	CC chemokine ligand 6, Scya6, C10, macrophage chemokine	<1	58	99	340	NM_009139
Myadm	Myeloid-associated differentiation marker, unknown function	<1	64	9	73	NM_016969
Adam8	A disintegrin and metallopeptidase domain 8	<1	150	12	32	NM_007403
Hck	Src-family tyrosine protein kinase	12	90	2	24	NM_010407
Arg2	Arginase, type II (NO biosynthesis)	<1	72	<1	16	NM_009705
Sell	Selectin, lymphocyte, Mediates roling of leukocytes on endothelium	2	36	2	10	NM_011346
C3	Complement component C3	<1	256	10	70	K02782
Timp2	Tissue inhibitor of metalloproteinase 2	2	44	2	17	BF168458
Cd9	Cd9 antigen. Mobility related protein 1, tetraspanin protein	6	57	5	55	NM_007657
Gpr109a	G protein-coupled receptor 109A. Interferon-gamma inducible gene	<1	162	5	22	NM_030701
Ifitm6	interferon induced transmembrane protein 6	<1	66	4	19	BB193024
Cybb	Cytochrome b-245, beta polypeptide, gp91phox	<1	172	18	36	NM_007807
Stk17b	Serine/threonine kinase 17b (apoptosis-inducing)	13	140	8	47	NM_133810
Gpsm3	G-protein signaling modulator 3, regulates Gi alpha activation	4	280	18	52	NM_134116
S100a8	Mrp8; pro-inflammatory, activates endothelial cells, high in neutrophils	6	312	140	258	NM_013650
S100a9	Mrp14; pro-inflammatory, activates endothelial cells, high in neutrophils	4	368	42	48	NM_009114
Csf2ra	Colony-stimulating factor 2 receptor alpha, low-affinity, GM-CSFR alpha	9	108	54	78	NM_009970
Csf2rb1	Colony stimulating factor 2 receptor, beta 1, low-affinity, GM-CSFR beta1	14	52	38	134	NM_007780
Sema4a	Sema domain, immunoglobulin domain (Ig), transmembrane domain (TM) and short cytoplasmic domain, (semaphorin) 4A T cell costimulation	<1	32	20	34	BB114323
Ctss	Cathepsin S	7	217	108	457	NM_021281
Capg	Capping protein (actin filament), gelsolin-like. Receptor ruffling, phagocytosis	5	31	28	107	NM_007599
Dusp1	Dual specificity phosphatase 1. Ptpn16. Neg reg of JNK, cell cycle, inflammation	5	109	5	114	NM_013642
Ier5	Immediate early response 5. Unknown function	2	20	2	22	NM_010500
Spp1	Secreted phosphoprotein 1. Osteopontin, pro-inflammatory	6	96	202	148	NM_009263
Cd200r1	CD200 receptor 1. Ig superfamily, myeloid-restricted, neg reg of cell activation	5	10	4	52	NM_021325
Samhd1	SAM and phosphohydrolase domain 1. Unknown function	2	68	6	31	NM_018851
Lyst	Lysozomal trafficking regulator	5	88	7	12	BB463428
Zfp36	Zinc finger protein 36, mRNA stability	<1	36	9	64	X14678
Slc15a3	Solute carrier family 15, member 3, Histidine and dipeptide transporter	<1	31	2	24	NM_023044
C10orf54	308 amino acids	1	47	19	31	NM_028732
Unknown	Unclassifiable transcript, BC025215	5	160	106	216	AK018202

(Supplementary Table 5.3, continued)

Transcription factors						
Mxd1	Max dimerization protein	4	88	7	15	BB036846
Atf3	c-jun-related bZIP transcription factor	<1	31	3	56	NM_007498
JunB	Jun family member B, bZIP transcription factor	7	54	4	54	NM_008416
Fos	FBJ osteosarcoma proto-oncogene, bZIP transcription factor	8	72	12	214	NM_010234
Btg2	B-cell translocation gene 2, anti-proliferative, Tis21, Pc3	2	52	12	200	BG965405
Id2	Inhibitor of Helix-Loop-Helix DNA-binding proteins	1	56	5	98	NM_010496
Klf2	Krupple-like factor 2, activates p21WAF1/CIP1	2	37	7	14	NM_008452
Jun	bZIP transcription factor	2	15	2	12	BC002081
Klf6	Krupple-like factor 6	3	21	5	15	NM_011803
Jund1	Jun family member D, bZIP transcription factor	10	70	12	45	NM_010592
Ets1	E26 proto-oncogene	<1	8	7	<1	BB151715
Klf7	Krupple-like factor 7	2	30	3	6	BE851797
Cebpb	CCAAT/enhancer binding protein (C/EBP), beta	11	54	54	92	NM_009883
Pbxip1	Pre-B-cell leukemia transcription factor interacting protein 1	2	25	2	8	BC026838

Supplementary Table 5.4. Inflammatory response of GM-CSF Hoxb8-ER macrophages to LPS or BLP. "Basal" signifies transcript levels in unstimulated macrophages; "LPS" signifies transcript levels following 2 hours of stimulation by bacterial lipopolysaccaride; "BLP" signifies transcript levels following 2 hours of stimulation by bacterial lipoprotein; "Fold stim" indicates magnitude of transcript up-regulation evoked by LPS.

Gene	Comment	Genbank	Basal	LPS 2hr	BLP 2 hrs	Fold-stimulation
Secreted proteins/Ligands						
IL1a	Interleukin 1 alpha	BC003727	4	134	26	>30
Il6	Interleukin 6	NM_031168	<1	55	<1	>30
IL23a	Interleukin 23, alpha subunit p19	NM_031252	<1	50	1	>30
Lif	Leukemia inhibitory factor	BB235045	1	81	20	>30
Ccl5	Chemokine (C-C motif) ligand 5, RANTES, Scya5	NM_013653	<1	53	<1	>30
Cxcl10	Chemokine (C-X-C motif) ligand 10, IP10, Scyb10, T cell chemoattractant	NM_021274	<1	182	121	>30
Cxcl2	chemokine (C-X-C motif) ligand 2. MIP-2, scyb2	NM_009140	2	118	85	>30
Serpinb2	Serine (or cysteine) peptidase inhibitor, clade B, member 2. PAI-2	NM_011111	2	76	19	25
Tnfsf9	Tumor necrosis factor (ligand) superfamily, member 9, binds T cell 4-1BB receptor	NM_009404	<1	24	<1	25
Il12b	Interleukin 12b. Drives T helper cell differentiation	NM_008352	<1	19	<1	19
Serpinb9g	Serine (or cysteine) peptidase inhibitor, clade B, member 9g, Inhibits granzyme b	AF425083	5	94	40	19
Dmkn	Dermokine alpha/beta, secreted peptide, unknown function	BI452905	<1	18	12	18
Ifn1	Interferon beta 1	NM_010510	<1	16	<1	16
Ccrl2	Chemokine (C-C motif) receptor-like 2. Receptor for MCP-1	AJ318863	7	104	54	15
Hamp1	Hepcidin antimicrobial peptide 1	NM_032541	<1	14	<1	14
Inhba	inhibin beta-A. Dimer=activin. Negative regulation of inflammation	NM_008380	5	71	8	14
Il1b	Interleukin 1 beta	BC011437	18	215	86	12
Tnf	Tumor necrosis factor	NM_013693	30	320	145	11
Ccl7	Chemokine (C-C motif) ligand 7, MCP3, Scya7	AF128193	<1	11	2	11
Ccl2	Chemokine (C-C motif) ligand 2, Scya2, MCP1	AF065933	4	51	9	11
Cxcl11	Chemokine (C-X-C motif) ligand 11, T cell alpha chemoattractant	AF136449	2	18	3	10
Serpine1	Serine (or cysteine) peptidase inhibitor, clade E, member 1. PAI-1	NM_008871	11	110	23	10
Ccl3	Chemokine (C-C motif) ligand 3, MIP1alpha, Scya3	NM_011337	26	254	114	10
Dcip1	Dendritic cell inflammatory protein 1	BB829808	6	54	9	9
Icosl	Icos ligand. Costimulatory receptor ligand, binds B7-H2, coactivates T cells	NM_015790	4	28	11	7
Signaling regulators						
Isg15	Interferon-stimulated gene 15, covalently modifies protein	AK019325	<1	54	44	>30
Usp18	Ubiquitin specific protease 18. Hydrolyzes ISG15 from protein	NM_011909	<1	46	42	>30
Rtp4	Receptor transport protein 4, 28kDa IFN alpha responsive protein,	NM_023386	<1	51	48	>30
Gdf15	Growth differentiation factor 15. Macrophage inhibitory cytokine 1, TGF beta family	NM_011819	<1	80	58	>30
Tnfaip3	Tumor necrosis factor, alpha-induced protein 3. A20. Neg reg Toll/NF-kB signaling	NM_009397	2	42	17	21
Socs3	Cytokine-inducible SH2-containing protein 3, negative regulation	NM_007707	<1	21	10	21
Phlda1	Pleckstrin homology-like domain, family A, member 1. Promotes survival	NM_009344	4	60	24	13
Dusp2	Dual specificity phosphatase 2. PAC-1, Map kinase phosphatase	L11330	1	10	10	10
Dusp16	Dual specificity phosphatase 16. MKP-7. Targets Jun kinase.	NM_130447	3	20	4	6
Peli1	Pellino1. Required for NF-kB activation through IL1R	NM_023324	4	30	8	7
Pde4b	phosphodiesterase 4B, cAMP specific. Inflammatory cell activation	AF326555	4	26	10	6
Rnd3	Rho family GTPase 3. Ras homolog gene family, member E.	NM_028810	<1	6	<1	6
Tlr7	Toll-like receptor 7	NM_133211	6	30	22	5
Tnfrsf23	Tumor necrosis factor receptor super family member 23, TRAIL decoy receptor	NM_024290	<1	18	17	18

(Supplementary Table 5.4, continued)

Gene	Comment	Genbank	Basal	LPS 2hr	BLP 2 hrs	Fold-stimulation
Others						
Ptgs2	Prostaglandin-endoperoxide synthase 2, Cyclooxygenase 2	M88242	2	119	59	>30
Tgm2	Transglutaminase 2, C polypeptide	BC016492	2	74	62	>30
Gbp2	Guanylate nucleotide binding protein 2	NM_010260	<1	38	26	>30
Ifit2	Interferon-induced protein with tetratricopeptide repeats 2	NM_008332	<1	98	56	>30
Ifi204	Interferon-activated gene 204. Tanscriptional coactivator	NM_008329	<1	35	26	>30
Rsad2	radical S-adenosyl methionine domain containing 2. Anti-viral glycoprotein viperin	NM_021384	<1	118	84	>30
Tyki	Thymidylate kinase family LPS-inducibel member	NM_020557	<1	35	30	>30
Ifit3	Interferon-induced protein with tetratricopeptide repeats 3	NM_010501	<1	56	46	>30
Ifit1	Interferon-induced protein with tetratricopeptide repeats 1	NM_008331	<1	116	48	>30
Ifi205	Interferon-activated gene 205	AI481797	<1	48	28	>30
Mpa2l	Macrophage activation 2-like, G-protein	BM241485	2	52	32	>30
Bcl2a1a	B-cell leukemia/lymphoma 2 related protein A1a	AI326167	<1	8	4	15
Bcl2l11	BCL2-like 11 (apoptosis facilitator). Bim	AF032460	2	44	15	24
Trim30	Tripartite motif protein 30	BM241342	<1	22	21	22
Serpine 1	Serine (or cysteine) peptidase inhibitor, clade E, member 1. PAI-1	NM_008871	3	50	10	15
Irg1	Immunoresponsive gene 1, propionate catabolism	L38281	9	104	16	12
Icam1	Intracellular adhesion molecule 1. CD54	BC008626	2	28	10	12
Gm1960	Gene model 1960. Dedritic cell inflammatory protein 1	BB829808	4	54	8	12
Saa3	Serum amyloid A3	NM_011315	5	55	6	11
Myd116	Myeloid differentaition primary response gene 116. PP1 regulatory subunit 16	NM_008654	5	46	9	10
Il4i11	Interleukin 4-induced 1. Fig1	NM_010215	3	22	3	8
AdoRA2b	Adenosine A2b receptor. Inflammation regulation	NM_007413	6	50	17	8
Rdh11	Retinol dehydrogenase 11 (IL4-induced)	BC018261	3	22	5	7
Transcription factors/regulators of mRNA abundance						
Nfkb2	NF-κB2, Nuclear factor kappa B subunit p100		<1	54	28	>30
Nfkb1	NF-κB1, Nuclear factor kappa B subunit p105	L28118	20	100	44	5
Rel	c-Rel, required for LPS-induced transcription of IL12p40 subunit	NM_009044	3	28	10	9
RelB	Reticuloendotheliosis oncogene related B	NM_009046	9	52	40	5
I-kB alpha	NF-kB inhibitor alpha	NM_010907	8	210	165	24
I-kB beta	NF-kB inhibitor beta	NM_010908	2	54	29	27
I-kB epsilon	NF-kB inhibitor epsilon	AK011965	<1	36	24	>30
I-kB zeta	IkappaB zeta, negative regulator of nuclear NFKB	NM_030612	3	58	24	17
I-kBNS	Negative regulator of NF-kappa-B, related to IKBs	AW495632	10	122	72	12
I-kBke	Inhibitor of kappa B kinase epsilon	NM_019777	<1	52	24	>30
Fra2	Fos-like antigen 2	NM_008037	<1	32	15	>30
JunD1	bZIP transcription factor	NM_010592	38	250	220	7
Jundp2	Jun dimerization protein 2, inhibits AP1, promotes differentiation	NM_030887	7	45	8	6
Maf	bZIP transcription factor. Activates LPS-induced IL-10 transcription	BC022952	3	25	12	9
Stat1	Signal transducer and activator of transcription 1 (IFN signaling)	BB229853	<1	51	48	>30
Stat2	Signal transducer and activator of transcription 2 (IFN signaling)	AF088862	<1	38	32	>30
Six1	Sine oculis-related homeobox 1 homolog, development	BB137929	1	24	9	17
Nupr1	Nuclear protein 1. p8 transcription factor.	NM_019738	6	42	10	7
MALT1	Mucosa associated lymphoid tissue lymphoma translocation gene 1. NF-kB activation	BB296321	8	44	28	6
Egr1	Early growth response 1	NM_007913	10	38	26	4
Egr2	Early growth response 2, Krox20, Zinc-finger transcription factor	X06746	6	25	22	4

Chapter 6

Homeodomain transcription factors HOX and Meis1 in leukemia:

Conclusions and future directions

Homeodomain-containing transcription factor Hox family members and Meis1 play a pivotal role in normal hematopoiesis and the pathogenesis of human AML and MLL, two leukemia types showing very poor prognosis and high percentage of mortality (Armstrong et al., 2002). In most AML and MLL cases, the expression of a subset of *Hox* genes in addition with *Meis1* is generally aberrantly up regulated or maintained, a genetic aberration sufficient to cause rapid leukemia transformation. Therefore, understanding the functions of these homeodomain factors in hematopoietic system is not only important to dissect the mechanisms regulating the normal or malignant hematopoiesis, but also necessary to develop the specific therapeutic approaches for AML or MLL. These two issues remain largely unclear, and hence became our interests and goals.

The fundamental scientific questions in this field we asked were specifically: i) How is the expression of *Hox* genes and *Meis1* maintained or upregulated in AML or MLL patients, while their expression is usually quickly downregulated and eventually shut off during early progenitor differentiation? ii) What subpopulations in hematopoeitic system are targeted during AML transformation and then become the leukemia initiating cells, i.e. leukemia cancer stem cells? iii) As the transcription factors, how do Hox and Meis1 factors lead to transformation of hematopoietic progenitors? How do these factors cooperate with each other? What are the genetic pathways regulated by these factors? What biochemical and molecular properties are required for these factors to program transformation? Essentially, are they transcriptional activators or repressors? These questions represent different aspects of leukemogenesis induced by Hox and Meis1, and the answers to them were largely

unstudied or elusive. Previous studies done by Drs. Guy Sauvegeau, Keith Humphries and their colleagues have established a murine leukemia model for *Hox* genes (for example, *HoxA9* or *HoxB3*) and *Meis1* by using bone marrow transplantation experiments, in which the expression of *Hox* genes alone eventually caused leukemia only after a long latency (within 20~30 weeks), the expression of *Meis1* alone never induced any leukemia, however, the co-expression of both *Hox* gene and *Meis1* caused leukemia rapidly (within 8-10 weeks) (Thorsteinsdottir et al., 2001). Yet, the marrow transplantation leukemia models were not able to answer the questions we asked, because of the complexity of the *in vivo* disease model usually concurrent with many secondary genetic changes and mechanisms. Thus, we need to design alternative relevant approaches to understand these issues we raised above, which also provided me an excellent scientific topic and a training opportunity in Dr. Mark Kamps' lab.

1. Mechanism of leukemia transformation by Hox factors and Meis1.

Establishing a cellular model by identification of the leukemia initiating cells or leukemia cancer stem cells represents an efficient and powerful system to examine the leukemogenesis in relevant cellular contexts. Sufficient evidence supported that leukemia is essentially a disease that either targets hematopoietic stem cells (HSC) directly or transforms the committed progenitors into those with acquired properties of HSC (Passegue et al., 2003). More recently, such concept has also been proven correct at least in some of, if not all, the solid tumor types. For enough good reasons that stuck in Mark's minds, the approach we took in the beginning was to try to

establish a cellular model that would not only recapitulate the *in vivo* disease caused by *Hox* and *Meis1*, but also would facilitate the cellular and genetic analysis. Previous studies in our lab have found that HoxA9 alone was able to block cellular differentiation of GM-CSF dependent myeloid restricted progenitors and the co-expression of *Meis1* in such condition allowed the resistance to additional cellular differentiation signals such as G-CSF (Calvo et al., 2001). However, in both cases, such GM-CSF dependent progenitors lacked leukemogenic potentials *in vivo* (Unpublished observations by Drs. Katherine Calvo and Mark Kamps). Yet, it is known that HoxA9 alone promoted the expansion of hematopoietic stem cells (HSC) *in vitro* cultured in the presence of multiple cytokines, which eventually induced leukemia by itself or with co-expressed *Meis1* when transferred *in vivo* (Thorsteinsdottir et al., 2001; Thorsteinsdottir et al., 2002). Thus, a relevant cellular model of leukemia initiating progenitors with coexpression of *HoxA9* plus *Meis1* has not been set up and could not be established by using GM-CSF *in vitro*. The hints came out from previous studies done by a former graduate student Dr. David Sykes who established leukemia-initiating cells for E2A-PBX utilizing SCF with or without lineage promoting cytokines (IL-7 or IL-3) (Sykes and Kamps, 2004). Here, using the similar *in vitro* progenitor maintenance conditions (either SCF alone, or SCF plus IL-7 or IL-3) followed by *in vivo* evaluation by mouse injection experiment, I successfully established the AML-initiating cells (containing efficient AML cancer stem cells) when coexpressed with *HoxA9* plus *Meis1*, as well as the non-leukemogenic or inefficient leukemogenic progenitors when expressed with *HoxA9* alone. The progenitors expressed with *HoxA9* alone were 100% myeloid restricted,

and leukemia stem cells established by *HoxA9* plus *Meis1* were not fully committed to myeloid lineages, similar to those transformed by MLL fusion protein *in vitro*. With this cellular model, we found the cellular functions of Meis1 in terms of arresting cellular differentiation at earlier stages, promoting cellular proliferation in the presence of SCF, and establishing a unique progenitor phenotype in the supporting cytokines such as IL-7 or Flt3 ligand (FL), two cytokines essential for lymphoid progenitors and HSCs.

SCF-dependent cellular models also represented a powerful system to identify the leukemia stem cell signature genes that are regulated by Meis1 with coexpressed HoxA9. The comparison between leukemia stem cells (established by coexpression of *HoxA9* plus *Meis1*) and non-leukemogenic progenitors (established by expression of *HoxA9* alone) turned out to be a quite short list of differentially expressed genes, which included about thirty genes uniquely expressed in leukemia stem cells with *Meis1* expressed, therefore, we defined these genes as Meis1-related leukemia signature genes or Meis1-regulated target genes. Among them many are very interesting genes, including those uniquely expressed in HSC or other tissue specific stem cells (such as mouse stem cell antigen *Cd34,* receptor tyrosine kinase *Flt3,* RNA binding protein *Msi2h,* etc) and those already strongly linked to leukemia or cancer (such as *Flt3*, v-Est related transcription factor *Erg1*, HMG transcription factor *Sox4* and *Msi2h*). The activation mutations of *Flt3* receptor were found in about one third of human AML patients, the translocation of *Erg1* or *Msi2h* was found in human leukemia or sarcoma, and the transactivation of *Sox4* was identified as the common lesions in murine spontaneous leukemia induced by retroviral mutagenesis screening.

I established the functional relationship between the expression of *Meis1* and the upregulation of *Flt3* receptor in hematopoietic progenitors, which provided a molecular explanation of general *Flt3* upregulation in AML, i.e., the upregulation of *Meis1* precedes and establishes the expression and subsequent selection for mutation of *Flt3* receptor. I then established a novel FL-dependent hematopoietic progenitor transformation assay that is dependent on the intact functions of Meis1. I proved that Flt3 was a significant contributor for the leukemia induced by *HoxA9* plus *Meis1*. HoxA9, Meis1 and cofactor Pbx were recruited to the *Flt3* cis-elements within enhancer regions and the first intron region; *Flt3* knockout caused a dramatic lagging of the leukemia kinetics (Unpublished observation by Drs Gang Wang and Mark Kamps). Thus, we have established a genetic pathway in AML, i.e, *MLL or NSD1 fusion* $\rightarrow$ *HOX/Meis1* $\rightarrow$ *Flt3*. This pathway was further validated by a recent report identifying the function of wildtype Flt3 receptor on promoting the leukemogeneis induced by NUP98-HOX fusion proteins (Palmqvist et al., 2006). The relevance of other interesting targets (such as *Sox4*, *Erg1* and etc) is still unclear and remains as interesting topics for the future directions in the lab. For example, *Sox4* was also implicated involved in tumor metastasis of breast cancer cells into lung (Minn et al., 2005). In the proximal promoter of *Sox4*, there are a conserved Pbx:Hox binding site and a nearly Meis1 recognition site, which indicates a direct regulatory relationship of Meis1 and Hox:Pbx complexes on the *Sox4* gene expression in AML.

The biochemical properties of Meis1 that are required for leukemia transformation were also identified using this cellular model. In order to generate the FL-dependent progenitor transformation *in vitro* with coexpressed HoxA9, Meis1

required the intact DNA binding activity, the intact Pbx-interaction motif and the intact C-terminal transactivation domain (CTD). The same three functions of Meis1 were also required for inducing AML *in vivo*. The CTD domain of Meis1 harbored two essential hydrophobic motifs (amino acid MGGFM and WHYM. Mutations within either one of these two motifs, or even a single amino acid substitution W387A, dramatically interfered with the function of Meis1 on induction of the *Flt3* expression. The combined mutations on both motifs completely abolished the functions of Meis1 in the generation of Flt3+ transformed hematopoietic progenitors *in vitro* and the induction of AML *in vivo*. I hypothesize that these two motifs provide the interaction surface for recruiting unknown essential cofactor(s) that are required for leukemia transformation. Recently, Dr. Mark Featherstone and his colleagues observed strong transcriptional activation activities of the Meis1 CTD, when fusing to GAL4 DNA binding domain, and this activation was enhanced by cellular signals such as those induced by protein kinase A (PKA) (Huang et al., 2005). It is consistent to the high intrinsic transactivity of this domain in yeast (Unpublished observation by Drs Gang Wang and Mark Kamps) and our reports on the transactivation function of Vp16-Meis1:Pbx complex using a luciferase reporter containing tandem repeats of Meis1:Pbx recognition sites (Wang et al., 2006). In the the identification of the Meis1 CTD cofactors, yeast two hybrid screening of Meis1 CTD interacting cofactors was unsuccessful because of the intrinsic transactivation activity, and tandem affinity purification technology (TAP) and peptide affinity purification (wildtype CTD vs mutant CTD) represent alternative approaches in the future. Recently, Dr. Marc Montimony and his colleagues identified the Transducers of regulated CREB (TORC)

as a transcriptional coactivator that mediated gene activation upon activation of PKA (Conkright et al., 2003). There appeared a parallel similarity between Meis1 and TORC after PKA activation, and as a candidate approach, TORC may be involved in the transactivation mediated by the Meis1 CTD domain.

I also report tht transcriptional activation is the major required activity for Meis1 to induce AML. Previous studies showed that Meis1, HoxA9 and their cofactor Pbx could be either transcriptional activator or repressor in different cellular contexts. Translocation mutations of HoxA9 and PBX1 in in AML or pre-B cell leukemia generated the aberrant transcriptional activating forms of these two factors, NUP98-HOXA9 and E2A-PBX respectively, which indicated that transactivation is the major transforming activity by these two factors. In the thesis, I examined the transcriptional activity of Meis1 in AML using a genetic approach. I found that a dominant transcriptional activation form of Meis1 (Vp16-Meis1), with coexpressed *HoxA9*, accelerated progenitor transformation and leukemogenesis, while a dominant transcriptional repression form of Meis1 decelerated transformation. More interestingly, Vp16-Meis1 alone was able to transform the progenitors and induce leukemia or myeloproliferative disease, by mimicking the combined functions of HoxA9 plus Meis1. Similarly, Vp16-HoxA9 or Vp16-Pbx1 also transformed hematopoietic progenitors and induced leukemia (Unpublished observation by Drs Gang Wang and Mark Kamps). There are clear differences between these transcriptional activating forms of leukemia oncoproteins. First, the natural leukemia traslocation products E2A-PBX and NUP98-HoxA9 are always much more potent in leukemogenesis than artificial generated fusion proteins Vp16-Meis1 or Vp16-Pbx1.

This indicated that other than transcriptional activation which is mimicked by Vp16 fuison, additional functions (such as protein dimerization) might harbor in their fusion parter E2A (Bayly and LeBrun, 2000) or NUP98 (Kasper et al., 1999). Second, the leukemia phenotypes induced by these fusion oncoproteins differed. E2A-PBX induced AML (Sykes and Kamps, 2004), T cell leukemia (Feldman et al., 2000) and pre-B cell leukemia (Bijl et al., 2005). Vp16Meis1 induced AML and myeloid proliferative disease, a chronic myeloid leukemia like disease, suggenting a lack of tight differentiation arrest involved in Vp16Meis1 mediated transformation. Vp16-Pbx1 only caused about 50% of penetrance of transformation *in vivo*. Thus, although transcriptional activation plays a crucial role in programming leukemia induction by Meis1 and its cofactors, additional functions imparted by their translocation fusion partners contribute to aggressiveness, penetrance and phenotypes of disease.

The bonus from the studies of Vp16-Meis1 was the unexpected observation that this transactivation form of Meis1 transformed progenitors in the absence of the expression of endogenous *Hox* genes, which provided a system to examine the biology of Hox factors. Unexpectedly, we found that the genes regulated by HoxA9 or HoxA7 largely covered those regulated by Meis1 identified earlier. Initially, this observation was quite surprisingly, but it does make sense considering the fact that Meis1 target genes were actually identified from the progenitors with *Meis1* and *HoxA9* coexpressed. Using the transactivation form of Meis1, Vp16-Meis1, I also provided evidence supporting that Hox factors and Meis1 co-occupy on the same cellular promoters. In the context of dominant Meis1 transactivation, neither the CTD domain of Meis1 nor the N-terminal domain (NTD) of HoxA9 was required in terms

of progenitor transformation. The NTD domain of HoxA9 (amino acid 1 to 138) was essential for all known transforming functions involving HoxA9 when coexpressed with normal Meis1, however its essential function was compensated by a Vp16 transactivation domain fused on another protein Meis1, indicating that HoxA9 and Meis1 bind onto the same promoters. Further supporting evidence came from the ChIP analysis evidencing the physical co-existence of these factors onto *Flt3* promoters (maybe also *Sox4*) in addition to the domain swapping experiments, in which the swapping of HoxA9 NTD and Meis1 CTD domains did not interfere with the *in vitro* transforming potentials of these two proteins. It is also consistent to the previous reports on the protein-protein interactions and the colocalization of HoxA9, Meis1 and Pbx2 in myeloid progenitor cells (Shen et al., 1999).

Our observations together with others' established a common complex/common promoter model for the leukemogenic functions mediated by Hox factors and Meis1. In this model, Hox, Meis1 and Pbx proteins form stable transcriptional complexes on common cellular promoters through the protein-protein interactions and the protein-DNA interactions. Two domains, HoxA9 NTD and Meis1 CTD, cooperate to achieve the optimal gene activation, maybe through recruiting unknown transcriptional cofactors or mediators. I propose that it is a molecular and genetic basis of strong cooperation between Hox and Meis1 proteins found in human and murine AMLs.

Several issues still remain unsolved within this common complex/promoter model. (i) How do the HoxA9 NTD and Meis1 CTD domains lead to gene activation? By sequence alignment, I found conserved motifs within these two domains that are

required for progenitor immortalization *in vitro* (data not shown). I hypothesize that these two domains recruit some yet-to-identified crucial mediators/cofactors via these conserved motifs. It is a direct that the lab will pursue in the future. (ii) It is still unknown about the functional relevance of other Hox-Meis1 target genes such as *Sox4*, *Erg1, Msi2h* and etc. Whether or not they are direct targets of Hox and Meis1, and whether or not they are required for leukemogenesis, are not clear. ChIP analysis, EMSA assays, generation of knockout mouse models, or utilizing stably expressed siRNA (gene knockdown) in the leukemia stem cells, will tackle these questions. (iii) In addition to hematopoietic system, Meis1 was also implicated involved in the maintenance of tumor progenitors of Wilm's tumor (Dekel et al., 2006), a kidney embryonic cancer, and the neuroblastoma (Geerts et al., 2003). It is also known that different Hox proteins are expressed in these tissues (data not shown). Thus, Hox-Meis1 in these tissue-specific tumors may be functionally parellel to what we have observed in leukemia.

2. Epigenetic regulation of Hox genes.

During embryogenesis, the expression of *Hox* genes is tightly and precisely controlled, because each of these Hox factors determines a different segmental structure along anterior to posterior axis of the animals. In adult hematopoeisis, the expression of *Hox* genes is equally important because the loss or gain of the *Hox* gene expression causes either the hematopoietic defects or the malignant progenitor expansion. In human AML and MLL patients, the common feature is the upregulation of *Hox* genes as well as *Meis1*. Thus, in order to cure the leukemia with *Hox* gene

upregulation, understanding the mechanism of their upregulation is equally important to understanding the functions of Hox and Meis1 proteins.

The epigenetic regulation of *Hox* genes in leukemia was well studied in the case of *MLL*, whose translocations are responsible for up to 10% of human AML cases. Here, I reported another *Hox* gene upregulation mechanism responsible for around 5% of AML involving chromosomal translocation of histone methyltransferase NSD1, which generated a fusion protein NUP98-NSD1. I found that NUP98-NSD1 harbored the abilities to transform hematopoietic progenitor *in vitro* and to induce AML in murine models, both evidencing upregulation of a subset of *Hox-A* genes (*HoxA5, A7, A9, A10*) and *Meis1*. NUP98-NSD1 was directly recruited to *HoxA5* to *HoxA10* gene locus, and induced the histone modification changes that represented gene activation markers. I found that NUP98-NSD1 utilized its intrinsic H3K36 HMT activities, recruited HAT proteins CBP/p300 and antagonized the recruitment of HMT Ezh2 polycomb group proteins. The PHD finger region (PHD^{v}-CH) of NSD1 was responsible for tethering the fusion protein to the *Hox-A* locus. NUP98 fusion part and the NSD1 SET domain cooperated to achieve optimal gene activation. The leukemia transformation activities of NUP98-NSD1 required functions of the *Hox*-locus targeting domain (PHD^{v}-CH), the NUP98 FG repeats, and SET domain, indicating both the NUP98 fusion part and H3K36 HMT activity are involved in the *Hox-A* gene activation and leukemogenesis. Finally, I showed that the wildtype NSD1 is also a regulator of *Hox-A* genes. NSD1 represents a novel *Hox* locus transcriptional regulator, whose mutations are involved in stem cell biology and neurology.

Several issues are unclear in the functions of NUP98-NSD1. (i) How does PHD^{v}-CH domain tether the fusion protein or NSD1 to *Hox* locus? These motifs may be either involved in the recognition of specific DNA elements or specific histone markers (Li et al., 2006), or may be recruited by specific DNA binding factors. (ii) How does NUP98-NSD1 antagonize the binding of Ezh2 to *Hox* locus? Whether or not they compete for the common DNA binding site or the common recruiting factors remains as a very interesting question. Interestingly, Suzanne Strome and her colleagues found that *C. elegas* NSD1 homologue MES-4, as the major form of H3K36 histone methyltransferase in *C. elegas*, antagonized the function of MES-2, MES-3 and MES-6, which formed the *C. elegas* homologues of Ezh2 polycomb complex (Bender et al., 2006). (iii) How does the wildtype NSD1 regulate *Hox* gene expression? Like *MLL*, *NSD1* may also serve as a *Trithorax* group gene. In fly, there exists one single *NSD1* family gene and it would be interesting to examine whether or not the mutation of this gene in fly causes homoetic transformation phenotype. Also, how NSD1 affects the cellular differentiation and proliferation of hemtapoieitc progenitors is also an interesting question. To address this question, we are collaborating with Dr. Pierre Chambon whose group have recently generated a conditional knockout strain for *Nsd1* (Rayasam et al., 2003).

Taken together, I touched different layers of leukemogenesis induced by Hox and Meis1 proteins, from the upstream regulators responsible for their upregulation in AML, their biochemical properties, and their downstream target genes (Figure 6.1). In the future, the better therapeutic approaches for Hox-positive AML caese may be achieved through using the combined methods that include down-regulation of the

Hox genes, destabilization of the Hox-Meis1-Pbx complexes, and inhibition of their downstream effecters such as Flt3 receptor.

Figure 6.1. Model summarizing the AML leukemogenic pathways. 70~80% of human AML and almost all MLL cases exhibit upregulation of the *Hox-A* genes and *Meis1*. This diagram contains three layers of AML leukemogenic pathways.

(1) The upregulation of the *Hox-A* locus (maybe also for *Meis1* locus). The epigenetic modifying transcriptional factors, either mutated or dysregulated as the initial "first-hit" of AML, caused the dysregulation of epigenetic modification at histone tails that led to the upregulation of the *Hox-A* gene expression. The examples of this pathway include the MLL fusion protein, such as MLL-AF10 (CALM-AF10) that recruited the H3K79 HMT hDOT1 and MLL-CBP/p300 that harbored histone acetyltransferase activity, and also the NUP98-NSD1 fusion that brings histone acetyltrasferase activity and H3K36 HMT activity together.

(2) After Hox-A and Meis1 proteins were translated, they form the common transcriptional complex with cofactor PBX proteins. Protein-protein interactions (Meis1-PBX, Hox-PBX) and protein-DNA interactions (Meis1-DNA, Hox-DNA) are required for the complex formation. The Meis1 CTD and the Hox NTD domains harbor the transcriptional activation activities and cooperate to achieve the optimal activation of downstream target genes. Leukemia translocation products or artificial fusion protein, NUP98-HoxA9, E2a-PBX (or Vp16-PBX1) or Vp16-Meis1, mimicks the natural complex, hijacks downstream pathways and enforces the transformation.

(3) The downstream targets that are activated by Hox-A-Meis-PBX complex include *CD34, FLT3, Sox4, Erg1, Msh2h* and etc. These proteins play a role in either homing of the leukemia stem cells (LSC) (such as for CD34 or FLT3), survival and proliferation of the LSC (such as for FLT3), or maintanace of the transforming potentials. Mutation occurs usually as the secondary "hit" during leukemogenesis, such as the activating mutations of receptor FLT3 and the translocation of Erg1 or Msh2h.

(4) For the therapeutics, the methods should be designed to target all these steps in order to better the AML curation, which include the chemicals interfering with the activity of histone modifying enzymes, the compounds that disrupt the transcriptional complex formation on DNA, and the specific inhibitors for the downstream mediator proteins such as FLT3 receptor.

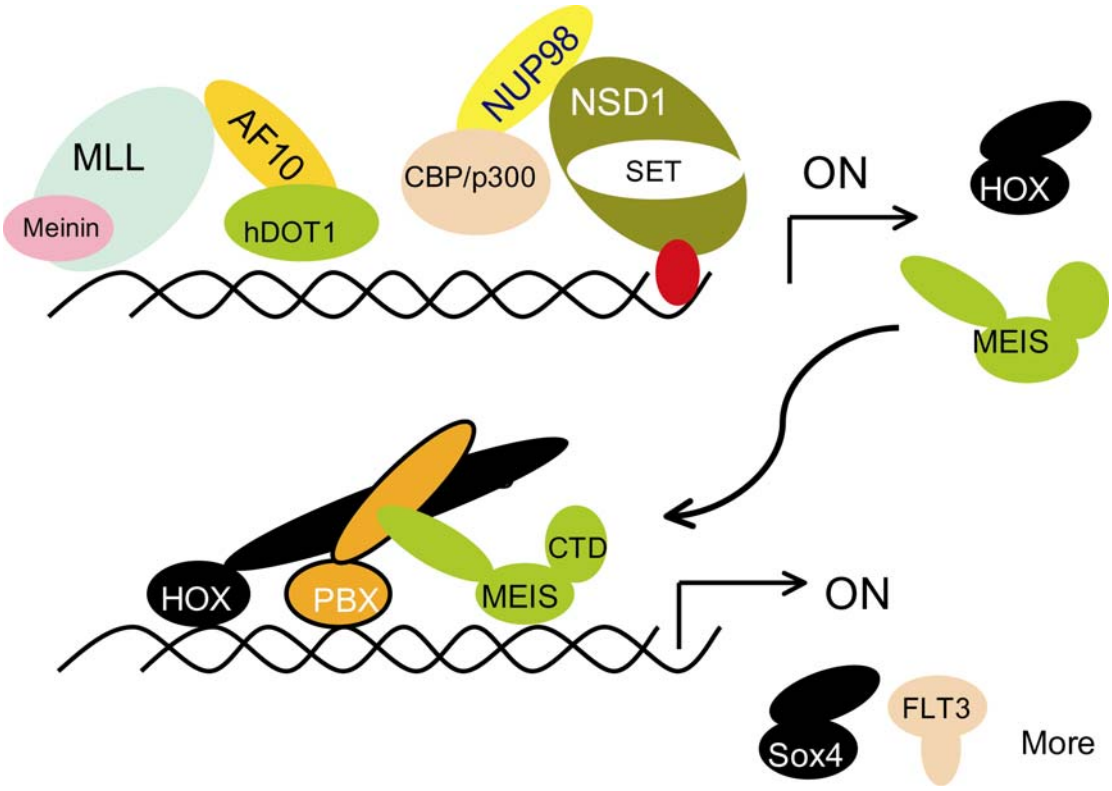
MLL
Meinin
AF10
hDOT1
NUP98
CBP/p300
NSD1
SET
ON
HOX
MEIS
CTD
HOX
PBX
MEIS
ON
Sox4
FLT3
More

Chapter 7

Reference

Afonja, O., Smith, J. E., Jr., Cheng, D. M., Goldenberg, A. S., Amorosi, E., Shimamoto, T., Nakamura, S., Ohyashiki, K., Ohyashiki, J., Toyama, K., and Takeshita, K. (2000). MEIS1 and HOXA7 genes in human acute myeloid leukemia. Leuk Res *24*, 849-855.

Angrand, P. O., Apiou, F., Stewart, A. F., Dutrillaux, B., Losson, R., and Chambon, P. (2001). NSD3, a new SET domain-containing gene, maps to 8p12 and is amplified in human breast cancer cell lines. Genomics *74*, 79-88.

Armstrong, S. A., Staunton, J. E., Silverman, L. B., Pieters, R., den Boer, M. L., Minden, M. D., Sallan, S. E., Lander, E. S., Golub, T. R., and Korsmeyer, S. J. (2002). MLL translocations specify a distinct gene expression profile that distinguishes a unique leukemia. Nat Genet *30*, 41-47.

Ayton, P. M., and Cleary, M. L. (2003). Transformation of myeloid progenitors by MLL oncoproteins is dependent on Hoxa7 and Hoxa9. Genes Dev *17*, 2298-2307.
Azcoitia, V., Aracil, M., Martinez, A. C., and Torres, M. (2005). The homeodomain protein Meis1 is essential for definitive hematopoiesis and vascular patterning in the mouse embryo. Dev Biol *280*, 307-320.

Bannister, A. J., Schneider, R., Myers, F. A., Thorne, A. W., Crane-Robinson, C., and Kouzarides, T. (2005). Spatial distribution of di- and tri-methyl lysine 36 of histone H3 at active genes. J Biol Chem *280*, 17732-17736.

Bayly, R., and LeBrun, D. P. (2000). Role for homodimerization in growth deregulation by E2a fusion proteins. Mol Cell Biol *20*, 5789-5796.

Bender, L. B., Suh, J., Carroll, C. R., Fong, Y., Fingerman, I. M., Briggs, S. D., Cao, R., Zhang, Y., Reinke, V., and Strome, S. (2006). MES-4: an autosome-associated histone methyltransferase that participates in silencing the X chromosomes in the C. elegans germ line. Development *133*, 3907-3917.

Bernstein, B. E., Kamal, M., Lindblad-Toh, K., Bekiranov, S., Bailey, D. K., Huebert, D. J., McMahon, S., Karlsson, E. K., Kulbokas, E. J., 3rd, Gingeras, T. R., *et al.* (2005). Genomic maps and comparative analysis of histone modifications in human and mouse. Cell *120*, 169-181.

Berthelsen, J., Kilstrup-Nielsen, C., Blasi, F., Mavilio, F., and Zappavigna, V. (1999). The subcellular localization of PBX1 and EXD proteins depends on nuclear import and export signals and is modulated by association with PREP1 and HTH. Genes Dev *13*, 946-953.

Berthelsen, J., Zappavigna, V., Mavilio, F., and Blasi, F. (1998). Prep1, a novel functional partner of Pbx proteins. Embo J *17*, 1423-1433.

Bijl, J., Sauvageau, M., Thompson, A., and Sauvageau, G. (2005). High incidence of proviral integrations in the Hoxa locus in a new model of E2a-PBX1-induced B-cell leukemia. Genes Dev *19*, 224-233.

Borrow, J., Shearman, A. M., Stanton, V. P., Jr., Becher, R., Collins, T., Williams, A. J., Dube, I., Katz, F., Kwong, Y. L., Morris, C., *et al.* (1996). The t(7;11)(p15;p15) translocation in acute myeloid leukaemia fuses the genes for nucleoporin NUP98 and class I homeoprotein HOXA9 [see comments]. Nat Genet *12*, 159-167.

Burglin, T. R. (1997). Analysis of TALE superclass homeobox genes (MEIS, PBC, KNOX, Iroquois, TGIF) reveals a novel domain conserved between plants and animals. Nucleic Acids Res *25*, 4173-4180.

Calvo, K. R., Knoepfler, P. S., Sykes, D. B., Pasillas, M. P., and Kamps, M. P. (2001). Meis1a suppresses differentiation by G-CSF and promotes proliferation by SCF: Potential mechanisms of cooperativity with Hoxa9 in myeloid leukemia. Proc Natl Acad Sci U S A *98*, 13120-13125.

Calvo, K. R., Sykes, D. B., Pasillas, M., and Kamps, M. P. (2000). Hoxa9 immortalizes a granulocyte-macrophage colony-stimulating factor- dependent promyelocyte capable of biphenotypic differentiation to neutrophils or macrophages, independent of enforced meis expression [In Process Citation]. Mol Cell Biol *20*, 3274-3285.

Cao, R., and Zhang, Y. (2004). SUZ12 is required for both the histone methyltransferase activity and the silencing function of the EED-EZH2 complex. Mol Cell *15*, 57-67.

Cecconi, M., Forzano, F., Milani, D., Cavani, S., Baldo, C., Selicorni, A., Pantaleoni, C., Silengo, M., Ferrero, G. B., Scarano, G., *et al.* (2005). Mutation analysis of the NSD1 gene in a group of 59 patients with congenital overgrowth. Am J Med Genet A *134*, 247-253.

Cerveira, N., Correia, C., Doria, S., Bizarro, S., Rocha, P., Gomes, P., Torres, L., Norton, L., Borges, B. S., Castedo, S., and Teixeira, M. R. (2003). Frequency of NUP98-NSD1 fusion transcript in childhood acute myeloid leukaemia. Leukemia *17*, 2244-2247.

Chang, C. P., Jacobs, Y., Nakamura, T., Jenkins, N. A., Copeland, N. G., and Cleary, M. L. (1997). Meis proteins are major in vivo DNA binding partners for wild-type but not chimeric Pbx proteins. Mol Cell Biol *17*, 5679-5687.

Chen, J., Kremer, C. S., and Bender, T. P. (2002). A Myb dependent pathway maintains Friend murine erythroleukemia cells in an immature and proliferating state. Oncogene *21*, 1859-1869.

Conkright, M. D., Canettieri, G., Screaton, R., Guzman, E., Miraglia, L., Hogenesch, J. B., and Montminy, M. (2003). TORCs: transducers of regulated CREB activity. Mol Cell *12*, 413-423.

Dekel, B., Metsuyanim, S., Schmidt-Ott, K. M., Fridman, E., Jacob-Hirsch, J., Simon, A., Pinthus, J., Mor, Y., Barasch, J., Amariglio, N., *et al.* (2006). Multiple imprinted and stemness genes provide a link between normal and tumor progenitor cells of the developing human kidney. Cancer Res *66*, 6040-6049.

Drabkin, H. A., Parsy, C., Ferguson, K., Guilhot, F., Lacotte, L., Roy, L., Zeng, C., Baron, A., Hunger, S. P., Varella-Garcia, M., *et al.* (2002). Quantitative HOX expression in chromosomally defined subsets of acute myelogenous leukemia. Leukemia *16*, 186-195.

Engelke, U., Wang, D. M., and Lipsick, J. S. (1997). Cells transformed by a v-Myb-estrogen receptor fusion differentiate into multinucleated giant cells. J Virol *71*, 3760-3766.

Feldman, B. J., Hampton, T., and Cleary, M. L. (2000). A carboxy-terminal deletion mutant of Notch1 accelerates lymphoid oncogenesis in E2A-PBX1 transgenic mice. Blood *96*, 1906-1913.

Ferrando, A. A., Armstrong, S. A., Neuberg, D. S., Sallan, S. E., Silverman, L. B., Korsmeyer, S. J., and Look, A. T. (2003). Gene expression signatures in MLL-rearranged T-lineage and B-precursor acute leukemias: dominance of HOX dysregulation. Blood *102*, 262-268.

Ferretti, E., Cambronero, F., Tumpel, S., Longobardi, E., Wiedemann, L. M., Blasi, F., and Krumlauf, R. (2005). Hoxb1 enhancer and control of rhombomere 4 expression: complex interplay between PREP1-PBX1-HOXB1 binding sites. Mol Cell Biol *25*, 8541-8552.

Ferretti, E., Schulz, H., Talarico, D., Blasi, F., and Berthelsen, J. (1999). The PBX-regulating protein PREP1 is present in different PBX-complexed forms in mouse. Mech Dev *83*, 53-64.

Ferretti, E., Villaescusa, J. C., Di Rosa, P., Fernandez-Diaz, L. C., Longobardi, E., Mazzieri, R., Miccio, A., Micali, N., Selleri, L., Ferrari, G., and Blasi, F. (2006). Hypomorphic mutation of the TALE gene Prep1 (pKnox1) causes a major reduction of Pbx and Meis proteins and a pleiotropic embryonic phenotype. Mol Cell Biol *26*, 5650-5662.

Fischbach, N. A., Rozenfeld, S., Shen, W., Fong, S., Chrobak, D., Ginzinger, D., Kogan, S. C., Radhakrishnan, A., Le Beau, M. M., Largman, C., and Lawrence, H. J. (2005). HOXB6 overexpression in murine bone marrow immortalizes a

myelomonocytic precursor in vitro and causes hematopoietic stem cell expansion and acute myeloid leukemia in vivo. Blood *105*, 1456-1466.

Fujino, T., Suzuki, A., Ito, Y., Ohyashiki, K., Hatano, Y., Miura, I., and Nakamura, T. (2002). Single-translocation and double-chimeric transcripts: detection of NUP98-HOXA9 in myeloid leukemias with HOXA11 or HOXA13 breaks of the chromosomal translocation t(7;11)(p15;p15). Blood *99*, 1428-1433.

Gaines, P., Chi, J., and Berliner, N. (2005). Heterogeneity of functional responses in differentiated myeloid cell lines reveals EPRO cells as a valid model of murine neutrophil functional activation. J Leukoc Biol *77*, 669-679.

Geerts, D., Schilderink, N., Jorritsma, G., and Versteeg, R. (2003). The role of the MEIS homeobox genes in neuroblastoma. Cancer Lett *197*, 87-92.

Golub, T. R., Slonim, D. K., Tamayo, P., Huard, C., Gaasenbeek, M., Mesirov, J. P., Coller, H., Loh, M. L., Downing, J. R., Caligiuri, M. A.*, et al.* (1999). Molecular classification of cancer: class discovery and class prediction by gene expression monitoring. Science *286*, 531-537.

Hacker, H., Redecke, V., Blagoev, B., Kratchmarova, I., Hsu, L. C., Wang, G. G., Kamps, M. P., Raz, E., Wagner, H., Hacker, G.*, et al.* (2006). Specificity in Toll-like receptor signalling through distinct effector functions of TRAF3 and TRAF6. Nature *439*, 204-207.

Hess, J. L. (2004). MLL: a histone methyltransferase disrupted in leukemia. Trends Mol Med *10*, 500-507.

Hisa, T., Spence, S. E., Rachel, R. A., Fujita, M., Nakamura, T., Ward, J. M., Devor-Henneman, D. E., Saiki, Y., Kutsuna, H., Tessarollo, L.*, et al.* (2004). Hematopoietic, angiogenic and eye defects in Meis1 mutant animals. Embo J *23*, 450-459.

Hock, H., Hamblen, M. J., Rooke, H. M., Traver, D., Bronson, R. T., Cameron, S., and Orkin, S. H. (2003). Intrinsic requirement for zinc finger transcription factor Gfi-1 in neutrophil differentiation. Immunity *18*, 109-120.

Huang, H., Rastegar, M., Bodner, C., Goh, S. L., Rambaldi, I., and Featherstone, M. (2005). MEIS C termini harbor transcriptional activation domains that respond to cell signaling. J Biol Chem *280*, 10119-10127.

Huang, N., vom Baur, E., Garnier, J. M., Lerouge, T., Vonesch, J. L., Lutz, Y., Chambon, P., and Losson, R. (1998). Two distinct nuclear receptor interaction domains in NSD1, a novel SET protein that exhibits characteristics of both corepressors and coactivators. Embo J *17*, 3398-3412.

Ida, K., Kitabayashi, I., Taki, T., Taniwaki, M., Noro, K., Yamamoto, M., Ohki, M., and Hayashi, Y. (1997). Adenoviral E1A-associated protein p300 is involved in acute myeloid leukemia with t(11;22)(q23;q13). Blood *90*, 4699-4704.

Jacobs, Y., Schnabel, C. A., and Cleary, M. L. (1999). Trimeric association of Hox and TALE homeodomain proteins mediates Hoxb2 hindbrain enhancer activity. Mol Cell Biol *19*, 5134-5142.

Jaju, R. J., Fidler, C., Haas, O. A., Strickson, A. J., Watkins, F., Clark, K., Cross, N. C., Cheng, J. F., Aplan, P. D., Kearney, L., *et al.* (2001). A novel gene, NSD1, is fused to NUP98 in the t(5;11)(q35;p15.5) in de novo childhood acute myeloid leukemia. Blood *98*, 1264-1267.

Kamps, M. P., and Baltimore, D. (1993). E2A-Pbx1, the t(1;19) translocation protein of human pre-B-cell acute lymphocytic leukemia, causes acute myeloid leukemia in mice. Mol Cell Biol *13*, 351-357.

Karin, M., and Greten, F. R. (2005). NF-kappaB: linking inflammation and immunity to cancer development and progression. Nat Rev Immunol *5*, 749-759.

Kasper, L. H., Brindle, P. K., Schnabel, C. A., Pritchard, C. E., Cleary, M. L., and van Deursen, J. M. (1999). CREB binding protein interacts with nucleoporin-specific FG repeats that activate transcription and mediate NUP98-HOXA9 oncogenicity. Mol Cell Biol *19*, 764-776.

Keats, J. J., Maxwell, C. A., Taylor, B. J., Hendzel, M. J., Chesi, M., Bergsagel, P. L., Larratt, L. M., Mant, M. J., Reiman, T., Belch, A. R., and Pilarski, L. M. (2005). Overexpression of transcripts originating from the MMSET locus characterizes all t(4;14)(p16;q32)-positive multiple myeloma patients. Blood *105*, 4060-4069.

Kharbanda, S., Nakamura, T., Stone, R., Hass, R., Bernstein, S., Datta, R., Sukhatme, V. P., and Kufe, D. (1991). Expression of the early growth response 1 and 2 zinc finger genes during induction of monocytic differentiation. J Clin Invest *88*, 571-577.

Knoepfler, P. S., Calvo, K. R., Chen, H., Antonarakis, S. E., and Kamps, M. P. (1997). Meis1 and pKnox1 bind DNA cooperatively with Pbx1 utilizing an interaction surface disrupted in oncoprotein E2a-Pbx1. Proc Natl Acad Sci U S A *94*, 14553-14558.

Knoepfler, P. S., Lu, Q., and Kamps, M. P. (1996). Pbx-1 Hox heterodimers bind DNA on inseparable half-sites that permit intrinsic DNA binding specificity of the Hox partner at nucleotides 3' to a TAAT motif. Nucleic Acids Res *24*, 2288-2294.

Knoepfler, P. S., Sykes, D. B., Pasillas, M., and Kamps, M. P. (2001). HoxB8 requires its Pbx-interaction motif to block differentiation of primary myeloid

progenitors and of most cell line models of myeloid differentiation. Oncogene *20*, 5440-5448.

Krishnaraju, K., Hoffman, B., and Liebermann, D. A. (1998). The zinc finger transcription factor Egr-1 activates macrophage differentiation in M1 myeloblastic leukemia cells. Blood *92*, 1957-1966.

Kroon, E., Krosl, J., Thorsteinsdottir, U., Baban, S., Buchberg, A. M., and Sauvageau, G. (1998). Hoxa9 transforms primary bone marrow cells through specific collaboration with Meis1a but not Pbx1b. Embo J *17*, 3714-3725.

Kumar, A., Lee, C. M., and Reddy, E. P. (2003). c-Myc is essential but not sufficient for c-Myb-mediated block of granulocytic differentiation. J Biol Chem *278*, 11480-11488.

Kurant, E., Eytan, D., and Salzberg, A. (2001). Mutational analysis of the Drosophila homothorax gene. Genetics *157*, 689-698.

La Starza, R., Gorello, P., Rosati, R., Riezzo, A., Veronese, A., Ferrazzi, E., Martelli, M. F., Negrini, M., and Mecucci, C. (2004). Cryptic insertion producing two NUP98/NSD1 chimeric transcripts in adult refractory anemia with an excess of blasts. Genes Chromosomes Cancer *41*, 395-399.

Lawrence, H. J., Christensen, J., Fong, S., Hu, Y. L., Weissman, I., Sauvageau, G., Humphries, R. K., and Largman, C. (2005). Loss of expression of the HOXA-9 homeobox gene impairs the proliferation and repopulating ability of hematopoietic stem cells. Blood.

Lawrence, H. J., Helgason, C. D., Sauvageau, G., Fong, S., Izon, D. J., Humphries, R. K., and Largman, C. (1997). Mice bearing a targeted interruption of the homeobox gene HOXA9 have defects in myeloid, erythroid, and lymphoid hematopoiesis. Blood *89*, 1922-1930.

Lawrence, H. J., Rozenfeld, S., Cruz, C., Matsukuma, K., Kwong, A., Komuves, L., Buchberg, A. M., and Largman, C. (1999). Frequent co-expression of the HOXA9 and MEIS1 homeobox genes in human myeloid leukemias. Leukemia *13*, 1993-1999.

Li, H., Ilin, S., Wang, W., Duncan, E. M., Wysocka, J., Allis, C. D., and Patel, D. J. (2006). Molecular basis for site-specific read-out of histone H3K4me3 by the BPTF PHD finger of NURF. Nature *442*, 91-95.

Li, M., Zhou, J. Y., Ge, Y., Matherly, L. H., and Wu, G. S. (2003). The phosphatase MKP1 is a transcriptional target of p53 involved in cell cycle regulation. J Biol Chem *278*, 41059-41068.

Liebermann, D. A., and Hoffman, B. (1994). Differentiation primary response genes and proto-oncogenes as positive and negative regulators of terminal hematopoietic cell differentiation. Stem Cells *12*, 352-369.

Lipsick, J. S., and Wang, D. M. (1999). Transformation by v-Myb. Oncogene *18*, 3047-3055.

Liu, H., Chen, B., Xiong, H., Huang, Q. H., Zhang, Q. H., Wang, Z. G., Li, B. L., Chen, Z., and Chen, S. J. (2004). Functional contribution of EEN to leukemogenic transformation by MLL-EEN fusion protein. Oncogene *23*, 3385-3394.

Lu, Q., and Kamps, M. P. (1996). Structural determinants within Pbx1 that mediate cooperative DNA binding with pentapeptide-containing Hox proteins: proposal for a model of a Pbx1-Hox-DNA complex. Mol Cell Biol *16*, 1632-1640.

Lyon, J. J., and Watson, R. J. (1995). Conditional inhibition of erythroid differentiation by c-Myb/oestrogen receptor fusion proteins. Differentiation *59*, 171-178.

Mann, R. S., and Affolter, M. (1998). Hox proteins meet more partners. Curr Opin Genet Dev *8*, 423-429.

Milne, T. A., Briggs, S. D., Brock, H. W., Martin, M. E., Gibbs, D., Allis, C. D., and Hess, J. L. (2002). MLL targets SET domain methyltransferase activity to Hox gene promoters. Mol Cell *10*, 1107-1117.

Minn, A. J., Gupta, G. P., Siegel, P. M., Bos, P. D., Shu, W., Giri, D. D., Viale, A., Olshen, A. B., Gerald, W. L., and Massague, J. (2005). Genes that mediate breast cancer metastasis to lung. Nature *436*, 518-524.

Moens, C. B., and Selleri, L. (2006). Hox cofactors in vertebrate development. Dev Biol *291*, 193-206.

Moskow, J. J., Bullrich, F., Huebner, K., Daar, I. O., and Buchberg, A. M. (1995). Meis1, a PBX1-related homeobox gene involved in myeloid leukemia in BXH-2 mice. Mol Cell Biol *15*, 5434-5443.

Nakamura, T. (2005). NUP98 fusion in human leukemia: dysregulation of the nuclear pore and homeodomain proteins. Int J Hematol *82*, 21-27.

Nakamura, T., Largaespada, D. A., Shaughnessy, J. D., Jr., Jenkins, N. A., and Copeland, N. G. (1996). Cooperative activation of Hoxa and Pbx1-related genes in murine myeloid leukaemias. Nat Genet *12*, 149-153.

Nakamura, T., Mori, T., Tada, S., Krajewski, W., Rozovskaia, T., Wassell, R., Dubois, G., Mazo, A., Croce, C. M., and Canaani, E. (2002). ALL-1 is a histone methyltransferase that assembles a supercomplex of proteins involved in transcriptional regulation. Mol Cell *10*, 1119-1128.

Nemeth, M. J., Cline, A. P., Anderson, S. M., Garrett-Beal, L. J., and Bodine, D. M. (2005). Hmgb3 deficiency deregulates proliferation and differentiation of common lymphoid and myeloid progenitors. Blood *105*, 627-634.

Okada, Y., Feng, Q., Lin, Y., Jiang, Q., Li, Y., Coffield, V. M., Su, L., Xu, G., and Zhang, Y. (2005). hDOT1L links histone methylation to leukemogenesis. Cell *121*, 167-178.

Okada, Y., Jiang, Q., Lemieux, M., Jeannotte, L., Su, L., and Zhang, Y. (2006). Leukaemic transformation by CALM-AF10 involves upregulation of Hoxa5 by hDOT1L. Nat Cell Biol *8*, 1017-1024.

Ono, R., Nosaka, T., and Hayashi, Y. (2005). Roles of a trithorax group gene, MLL, in hematopoiesis. Int J Hematol *81*, 288-293.

Owens, B. M., and Hawley, R. G. (2002). HOX and non-HOX homeobox genes in leukemic hematopoiesis. Stem Cells *20*, 364-379.

Palmqvist, L., Argiropoulos, B., Pineault, N., Abramovich, C., Sly, L. M., Krystal, G., Wan, A., and Humphries, R. K. (2006). The Flt3 receptor tyrosine kinase collaborates with NUP98-HOX fusions in acute myeloid leukemia. Blood *108*, 1030-1036.

Panagopoulos, I., Isaksson, M., Billstrom, R., Strombeck, B., Mitelman, F., and Johansson, B. (2003). Fusion of the NUP98 gene and the homeobox gene HOXC13 in acute myeloid leukemia with t(11;12)(p15;q13). Genes Chromosomes Cancer *36*, 107-112.

Park, J. M., Greten, F. R., Wong, A., Westrick, R. J., Arthur, J. S., Otsu, K., Hoffmann, A., Montminy, M., and Karin, M. (2005). Signaling pathways and genes that inhibit pathogen-induced macrophage apoptosis--CREB and NF-kappaB as key regulators. Immunity *23*, 319-329.

Passegue, E., Jamieson, C. H., Ailles, L. E., and Weissman, I. L. (2003). Normal and leukemic hematopoiesis: are leukemias a stem cell disorder or a reacquisition of stem cell characteristics? Proc Natl Acad Sci U S A *100 Suppl 1*, 11842-11849.

Passner, J. M., Ryoo, H. D., Shen, L., Mann, R. S., and Aggarwal, A. K. (1999). Structure of a DNA-bound Ultrabithorax-Extradenticle homeodomain complex. Nature *397*, 714-719.

Pearson, J. C., Lemons, D., and McGinnis, W. (2005). Modulating Hox gene functions during animal body patterning. Nat Rev Genet *6*, 893-904.

Pineault, N., Helgason, C. D., Lawrence, H. J., and Humphries, R. K. (2002). Differential expression of Hox, Meis1, and Pbx1 genes in primitive cells throughout murine hematopoietic ontogeny. Exp Hematol *30*, 49-57.

Piper, D. E., Batchelor, A. H., Chang, C. P., Cleary, M. L., and Wolberger, C. (1999). Structure of a HoxB1-Pbx1 heterodimer bound to DNA: role of the hexapeptide and a fourth homeodomain helix in complex formation. Cell *96*, 587-597.

Pokholok, D. K., Harbison, C. T., Levine, S., Cole, M., Hannett, N. M., Lee, T. I., Bell, G. W., Walker, K., Rolfe, P. A., Herbolsheimer, E., *et al.* (2005). Genome-wide map of nucleosome acetylation and methylation in yeast. Cell *122*, 517-527.

Rayasam, G. V., Wendling, O., Angrand, P. O., Mark, M., Niederreither, K., Song, L., Lerouge, T., Hager, G. L., Chambon, P., and Losson, R. (2003). NSD1 is essential for early post-implantation development and has a catalytically active SET domain. Embo J *22*, 3153-3163.

Rieckhof, G. E., Casares, F., Ryoo, H. D., Abu-Shaar, M., and Mann, R. S. (1997). Nuclear translocation of extradenticle requires homothorax, which encodes an extradenticle-related homeodomain protein. Cell *91*, 171-183.

Ringrose, L., and Paro, R. (2004). Epigenetic regulation of cellular memory by the Polycomb and Trithorax group proteins. Annu Rev Genet *38*, 413-443.

Rosati, R., La Starza, R., Veronese, A., Aventin, A., Schwienbacher, C., Vallespi, T., Negrini, M., Martelli, M. F., and Mecucci, C. (2002). NUP98 is fused to the NSD3 gene in acute myeloid leukemia associated with t(8;11)(p11.2;p15). Blood *99*, 3857-3860.

Sauvageau, G., Lansdorp, P. M., Eaves, C. J., Hogge, D. E., Dragowska, W. H., Reid, D. S., Largman, C., Lawrence, H. J., and Humphries, R. K. (1994). Differential expression of homeobox genes in functionally distinct CD34+ subpopulations of human bone marrow cells. Proc Natl Acad Sci U S A *91*, 12223-12227.

Schaft, D., Roguev, A., Kotovic, K. M., Shevchenko, A., Sarov, M., Neugebauer, K. M., and Stewart, A. F. (2003). The histone 3 lysine 36 methyltransferase, SET2, is involved in transcriptional elongation. Nucleic Acids Res *31*, 2475-2482.

Shen, W. F., Chang, C. P., Rozenfeld, S., Sauvageau, G., Humphries, R. K., Lu, M., Lawrence, H. J., Cleary, M. L., and Largman, C. (1996). Hox homeodomain proteins exhibit selective complex stabilities with Pbx and DNA. Nucleic Acids Res *24*, 898-906.

Shen, W. F., Montgomery, J. C., Rozenfeld, S., Moskow, J. J., Lawrence, H. J., Buchberg, A. M., and Largman, C. (1997). AbdB-like Hox proteins stabilize DNA binding by the Meis1 homeodomain proteins. Mol Cell Biol *17*, 6448-6458.

Shen, W. F., Rozenfeld, S., Kwong, A., Kom ves, L. G., Lawrence, H. J., and Largman, C. (1999). HOXA9 forms triple complexes with PBX2 and MEIS1 in myeloid cells. Mol Cell Biol *19*, 3051-3061.

Slany, R. K. (2005). When epigenetics kills: MLL fusion proteins in leukemia. Hematol Oncol *23*, 1-9.

So, C. W., Karsunky, H., Passegue, E., Cozzio, A., Weissman, I. L., and Cleary, M. L. (2003). MLL-GAS7 transforms multipotent hematopoietic progenitors and induces mixed lineage leukemias in mice. Cancer Cell *3*, 161-171.

Sykes, D. B., and Kamps, M. P. (2001). Estrogen-dependent E2a/Pbx1 myeloid cell lines exhibit conditional differentiation that can be arrested by other leukemic oncoproteins. Blood *98*, 2308-2318.

Sykes, D. B., and Kamps, M. P. (2003). Estrogen-regulated conditional oncoproteins: tools to address open questions in normal myeloid cell function, normal myeloid differentiation, and the genetic basis of differentiation arrest in myeloid leukemia. Leuk Lymphoma *44*, 1131-1139.

Sykes, D. B., and Kamps, M. P. (2004). E2a/Pbx1 induces the rapid proliferation of stem cell factor-dependent murine pro-T cells that cause acute T-lymphoid or myeloid leukemias in mice. Mol Cell Biol *24*, 1256-1269.

Taketani, T., Taki, T., Shibuya, N., Kikuchi, A., Hanada, R., and Hayashi, Y. (2002). Novel NUP98-HOXC11 fusion gene resulted from a chromosomal break within exon 1 of HOXC11 in acute myeloid leukemia with t(11;12)(p15;q13). Cancer Res *62*, 4571-4574.

Thorsteinsdottir, U., Kroon, E., Jerome, L., Blasi, F., and Sauvageau, G. (2001). Defining roles for HOX and MEIS1 genes in induction of acute myeloid leukemia. Mol Cell Biol *21*, 224-234.

Thorsteinsdottir, U., Mamo, A., Kroon, E., Jerome, L., Bijl, J., Lawrence, H. J., Humphries, K., and Sauvageau, G. (2002). Overexpression of the myeloid leukemia-associated Hoxa9 gene in bone marrow cells induces stem cell expansion. Blood *99*, 121-129.

Thorsteinsdottir, U., Sauvageau, G., and Humphries, R. K. (1997). Hox homeobox genes as regulators of normal and leukemic hematopoiesis. Hematol Oncol Clin North Am *11*, 1221-1237.

Wang, G. G., Pasillas, M. P., and Kamps, M. P. (2005). Meis1 programs transcription of FLT3 and cancer stem cell character, using a mechanism that requires interaction with Pbx and a novel function of the Meis1 C-terminus. Blood *106*, 254-264.

Wang, G. G., Pasillas, M. P., and Kamps, M. P. (2006). Persistent transactivation by meis1 replaces hox function in myeloid leukemogenesis models: evidence for co-occupancy of meis1-pbx and hox-pbx complexes on promoters of leukemia-associated genes. Mol Cell Biol *26*, 3902-3916.

Wang, J., Iwasaki, H., Krivtsov, A., Febbo, P. G., Thorner, A. R., Ernst, P., Anastasiadou, E., Kutok, J. L., Kogan, S. C., Zinkel, S. S., *et al.* (2005c). Conditional MLL-CBP targets GMP and models therapy-related myeloproliferative disease. Embo J *24*, 368-381.

Weisberg, S. P., McCann, D., Desai, M., Rosenbaum, M., Leibel, R. L., and Ferrante, A. W., Jr. (2003). Obesity is associated with macrophage accumulation in adipose tissue. J Clin Invest *112*, 1796-1808.

White, J. R., and Weston, K. (2000). Myb is required for self-renewal in a model system of early hematopoiesis. Oncogene *19*, 1196-1205.

Wood, M. A., McMahon, S. B., and Cole, M. D. (2000). An ATPase/helicase complex is an essential cofactor for oncogenic transformation by c-Myc. Mol Cell *5*, 321-330.

Wysocka, J., Swigut, T., Xiao, H., Milne, T. A., Kwon, S. Y., Landry, J., Kauer, M., Tackett, A. J., Chait, B. T., Badenhorst, P., *et al.* (2006). A PHD finger of NURF couples histone H3 lysine 4 trimethylation with chromatin remodelling. Nature *442*, 86-90.

Yang, A. H., Kaushal, D., Rehen, S. K., Kriedt, K., Kingsbury, M. A., McConnell, M. J., and Chun, J. (2003). Chromosome segregation defects contribute to aneuploidy in normal neural progenitor cells. J Neurosci *23*, 10454-10462.

Yu, B. D., Hanson, R. D., Hess, J. L., Horning, S. E., and Korsmeyer, S. J. (1998). MLL, a mammalian trithorax-group gene, functions as a transcriptional maintenance factor in morphogenesis. Proc Natl Acad Sci U S A *95*, 10632-10636.

Zeisig, B. B., Milne, T., Garcia-Cuellar, M. P., Schreiner, S., Martin, M. E., Fuchs, U., Borkhardt, A., Chanda, S. K., Walker, J., Soden, R., *et al.* (2004). Hoxa9 and Meis1 are key targets for MLL-ENL-mediated cellular immortalization. Mol Cell Biol *24*, 617-628.

Zhao, Z., Yu, Y., Meyer, D., Wu, C., and Shen, W. H. (2005). Prevention of early flowering by expression of FLOWERING LOCUS C requires methylation of histone H3 K36. Nat Cell Biol *7*, 1256-1260.